

Geological Society Memoir No. 33

# The Gregory Rift Valley and Neogene–Recent Volcanoes of Northern Tanzania

J. B. Dawson



Published by the Geological Society

The Gregory Rift Valley and Neogene–Recent  
Volcanoes of Northern Tanzania

Geological Society Memoirs  
The Geological Society of London  
**Books Editorial Committee**

**Chief Editor**

BOB PANKHURST (UK)

**Society Books Editors**

JOHN GREGORY (UK)

JIM GRIFFITHS (UK)

JOHN HOWE (UK)

PHIL LEAT (UK)

NICK ROBINS (UK)

JONATHAN TURNER (UK)

**Society Books Advisors**

MIKE BROWN (USA)

ERIC BUFFETAUT (FRANCE)

JONATHAN CRAIG (ITALY)

RETO GIERÉ (GERMANY)

TOM MCCANN (GERMANY)

DOUG STEAD (CANADA)

RANDELL STEPHENSON (NETHERLANDS)

**Geological Society books refereeing procedures**

The Society makes every effort to ensure that the scientific and production quality of its books matches that of its journals. Since 1997, all book proposals have been refereed by specialist reviewers as well as by the Society's Books Editorial Committee. If the referees identify weaknesses in the proposal, these must be addressed before the proposal is accepted.

Once the book is accepted, the Society Book Editors ensure that the volume editors follow strict guidelines on refereeing and quality control. We insist that individual papers can only be accepted after satisfactory review by two independent referees. The questions on the review forms are similar to those for *Journal of the Geological Society*. The referees' forms and comments must be available to the Society's Book Editors on request.

Although many of the books result from meetings, the editors are expected to commission papers that were not presented at the meeting to ensure that the book provides a balanced coverage of the subject. Being accepted for presentation at the meeting does not guarantee inclusion in the book.

More information about submitting a proposal and producing a book for the Society can be found on its web site: [www.geolsoc.org.uk](http://www.geolsoc.org.uk).

It is recommended that reference to all or part of this book should be made in the following way:

*From:* DAWSON, J. B. 2008. *The Gregory Rift Valley and Neogene–Recent Volcanoes of Northern Tanzania*. Geological Society, London, Memoirs, **33**.

GEOLOGICAL SOCIETY MEMOIR NO. 33

The Gregory Rift Valley and Neogene–Recent  
Volcanoes of Northern Tanzania

BY

J. B. DAWSON  
University of Edinburgh, UK

2008  
Published by  
The Geological Society  
London

## THE GEOLOGICAL SOCIETY

The Geological Society of London (GSL) was founded in 1807. It is the oldest national geological society in the world and the largest in Europe. It was incorporated under Royal Charter in 1825 and is Registered Charity 210161.

The Society is the UK national learned and professional society for geology with a worldwide Fellowship (FGS) of over 9000. The Society has the power to confer Chartered status on suitably qualified Fellows, and about 2000 of the Fellowship carry the title (CGeol). Chartered Geologists may also obtain the equivalent European title, European Geologist (EurGeol). One fifth of the Society's fellowship resides outside the UK. To find out more about the Society, log on to [www.geolsoc.org.uk](http://www.geolsoc.org.uk).

**The Geological Society Publishing House** (Bath, UK) produces the Society's international journals and books, and acts as European distributor for selected publications of the American Association of Petroleum Geologists (AAPG), the Indonesian Petroleum Association (IPA), the Geological Society of America (GSA), the Society for Sedimentary Geology (SEPM) and the Geologists' Association (GA). Joint marketing agreements ensure that GSL Fellows may purchase these societies' publications at a discount. The Society's online bookshop (accessible from [www.geolsoc.org.uk](http://www.geolsoc.org.uk)) offers secure book purchasing with your credit or debit card.

To find out about joining the Society and benefiting from substantial discounts on publications of GSL and other societies worldwide, consult [www.geolsoc.org.uk](http://www.geolsoc.org.uk), or contact the Fellowship Department at: The Geological Society, Burlington House, Piccadilly, London W1J 0BG; Tel. +44 (0)20 7434 9944; Fax +44 (0)20 7439 8975; E-mail: [enquiries@geolsoc.org.uk](mailto:enquiries@geolsoc.org.uk).

For information about the Society's meetings, consult *Events* on [www.geolsoc.org.uk](http://www.geolsoc.org.uk). To find out more about the Society's Corporate Affiliates Scheme, write to [enquiries@geolsoc.org.uk](mailto:enquiries@geolsoc.org.uk)

Published by The Geological Society from:

The Geological Society Publishing House, Unit 7, Brassmill Enterprise Centre, Brassmill Lane, Bath BA1 3JN, UK

(Orders: Tel. +44 (0)1225 445046, Fax +44 (0)1225 442836)

Online bookshop: [www.geolsoc.org.uk/bookshop](http://www.geolsoc.org.uk/bookshop)

The publishers make no representation, express or implied, with regard to the accuracy of the information contained in this book and cannot accept any legal responsibility for any errors or omissions that may be made.

© The Geological Society of London 2008. All rights reserved. No reproduction, copy or transmission of this publication may be made without written permission. No paragraph of this publication may be reproduced, copied or transmitted save with the provisions of the Copyright Licensing Agency, 90 Tottenham Court Road, London W1P 9HE. Users registered with the Copyright Clearance Center, 27 Congress Street, Salem, MA 01970, USA: the item-fee code for this publication is 0435-4052/08/\$15.00.

### British Library Cataloguing in Publication Data

A catalogue record for this book is available from the British Library.

ISBN 978-1-86239-267-0

Typeset by Techset Composition Ltd., Salisbury, UK

Printed by Antony Rowe Ltd, Chippenham, UK

### Distributors

#### North America

For trade and institutional orders:

The Geological Society, c/o AIDC, 82 Winter Sport Lane, Williston, VT 05495, USA

Orders: Tel. +1 800-972-9892

Fax +1 802-864-7626

E-mail [gsl.orders@aidcvt.com](mailto:gsl.orders@aidcvt.com)

For individual and corporate orders:

AAPG Bookstore, PO Box 979, Tulsa, OK 74101-0979, USA

Orders: Tel. +1 918-584-2555

Fax +1 918-560-2652

E-mail [bookstore@aapg.org](mailto:bookstore@aapg.org)

Website <http://bookstore.aapg.org>

#### India

Affiliated East-West Press Private Ltd, Marketing Division, G-1/16 Ansari Road, Darya Ganj, New Delhi 110 002, India

Orders: Tel. +91 11 2327-9113/2326-4180

Fax +91 11 2326-0538

E-mail [affiliat@vsnl.com](mailto:affiliat@vsnl.com)

## Acknowledgements

My first encounter with East African geology was as a geologist with the Tanganyika Geological Survey in 1960. My late wife Christine was a wonderful companion in the bush in the early days before family commitments kept her reluctantly at home. Amongst other things, before the arrival of the official Ordnance Survey 1:50 000 sheets, she made me topographic maps from aerial photographs that enabled mapping of the Oldoinyo Lengai and Monduli areas. I was well served by my Tanganyika field staff, particularly my assistant Salum Kichwa, and I had the stalwart company of my Survey colleague Ray Pickering during my first descent into the crater of Oldoinyo Lengai. The rigours of fieldwork in Maasailand were much eased by Francis and Helen Townsend, John Stephenson and Joe Fourie of the Maasai District Headquarters in Monduli. At Survey headquarters in Dodoma I learned much from discussion with Dan Harkin, Alec McKinlay, Eddie Haldemann, Trevor James and John Whittingham, and I was taught the rudiments of Up-Country Kiswahili by Giovanni Balletto (of 'No Picnic On Mt Kenya' fame).

In later work in Tanzania, I enjoyed the company of Thure Sahama, Colin Clark, Magnus Garson, Miroslav Krs, Harry Pinkerton, Gill Norton, Dave Pyle, Celia Nyamweru, Cassi Paslick, Dodie James, Aloyce Tesha, Roger Mitchell, Valerie Dennison, Tony Mariano and Barbara Scott Smith. On several expeditions, the logistics were expertly managed by Mike, Dave and Thad Peterson of Dorobo Safaris, Arusha, and their staff, especially Alex, Peter and Lomnyak.

Projects on Tanzanian rocks, in particular, have involved Joe Smith and Ian Steele at the University of Chicago; others involved were Dave Powell, Joy Baldwin, Tom Frisch, Peter Bowden, Bob Hutchinson, Noel Gale, Mitch Macintyre, Keith Bell, Colin Donaldson, Richard Batchelor, Ray Kanaris-Sotiriou, Adrian Jones, Arch Reid, Ian Ridley, Mike Rhodes, Mike Henderson, Jeff Cooper, Roy Cohen, Keith O'Nions, Tony Fallick, Peter Hill, John Craven, Richard Hinton, Cassi Paslick, Alex Halliday, Kevin Burton and Roger Mitchell.

On aspects of Tanzanian and East African geology, I have benefited from discussions and correspondence with Ray Macdonald, Laurie Williams, Basil King, Glyn Isaac, Jörg Keller, Charles Downie, Peter Wilkinson, Dick Hay, Roberta Rudnick, Andy

Nyblade, Gail Ashley, Sue Brantley, Alan Woolley, Peter Wyllie, Cindy Ebinger, Adrian Foster, Sally Gibson and Martin Roberts. I also thank the people who kindly sent me reprints of their work and I am particularly grateful to Magnus Garson who provided data on Kwaraha and Hanang. I am grateful to Colin Bristow, Mikko Punkari and Dean Polley for providing the photographs for Figures 7.7, 7.15, 7.16 and 7.19.

The technical and secretarial staff in the Earth sciences departments in the universities of St Andrews, Sheffield, Edinburgh and Chicago are particularly thanked for their cheerful and unstinting support. The Natural Environment Research Council and NATO are thanked for several research grants, and the Carnegie Trust for the Universities of Scotland, the Institute of Mining and Metallurgy, and the Royal Society also provided support for fieldwork in Tanzania.

During the preparation of this memoir, Yvonne Cooper and Gerry White helped with photography and drafting respectively, and John Wexler and Marie Cope of the Graphics and Multimedia Resource Centre, University of Edinburgh, are thanked for assistance with image processing. The staff of the National Library of Scotland and the Special Collection of the Edinburgh University Library were of great help in accessing some of the older literature. I am grateful to Ray Macdonald, Martin Smith and Nick Rodgers for undertaking the task of reviewing the original manuscript and for their encouraging and constructive comments. Phil Leat was responsible for the overall editing and Sally Oberst and Angharad Hills gave much welcome advice during the production stage.

Finally, I would not have become involved in African geology without the influence of W. Q. Kennedy, former Professor of Geology at the University of Leeds. He established the Research Institute of African Geology in Leeds in 1956, and I was sent with my postgraduate colleague Pete Nixon to Basutoland in 1957 to study kimberlites. Tom Clifford, Magnus Garson, John Hepworth and John Vail, some of whose work is cited in this volume, were amongst the other members of the Institute. During our research, Kennedy engendered in us the enthusiasm for Africa that he himself had developed when, as a student at the University of Glasgow, he had been taught and inspired by J. W. Gregory.

## **Dedication**

This volume is dedicated to Christine, Sarah, Michael and Rebecca

## Contents

<b>Acknowledgements</b>	<b>vii</b>	The Yaida Basin	35
<b>Chapter 1 Introduction</b>	<b>1</b>	The Olduvai Basin and Laetoli	35
		Amboseli	37
<b>Chapter 2 Discovery of the African rift valleys: early work on the Gregory Rift Valley and volcanoes in Northern Tanzania</b>	<b>3</b>	Summary of the rift valley basins	37
Discovery of the African rift valleys	3		
Early geological work in northern Tanzania	5		
<b>Chapter 3 Regional geology</b>	<b>9</b>		
<b>Chapter 4 Geophysical evidence for the structure of the crust and upper mantle of the Tanzania Craton and the Gregory Rift Valley</b>	<b>13</b>	<b>Chapter 7 The Neogene–Recent volcanic rocks</b>	<b>39</b>
Gravity studies	13	Rock nomenclature	39
Seismic experiments	13	Descriptions of individual volcanoes or volcanic areas	39
An integrated model and possible constraints	13	The Older Extrusives	40
Teleseismic results and inferences	14	Shombole	40
Seismicity	15	Oldoinyo Sambu	40
Heat flow	16	Mosonik	41
Magnetic data	17	Gelai	41
Magnetotelluric data	17	Ketumbeine	42
Lithosphere strength	17	The Crater Highlands	42
Crustal extension and its causes	18	Elanairobi/Embagai (Empakai)	42
Summary of geophysical work	18	Un-named mountain	42
		Olmoti	43
<b>Chapter 5 Tectonic development of the rift structures</b>	<b>21</b>	Loolmalasin	43
Early rift structure	21	Ngorongoro	44
The northern Tanzania late Tertiary depression	21	Lemagrut	44
Eruption of the first set of volcanoes: the Older Extrusives	23	Sadiman	50
Plio-Pleistocene faulting	23	Oldeani	50
Late Pliocene faulting	23	Angata Salei–Serengeti plains	50
Major Pleistocene faulting	23	The Engaruka–Manyara area	50
The Natron Basin boundary fault system	23	Essimingor (also known as Losimingori)	51
Manyara Basin boundary fault system	26	Tarosero	51
The Mbulu Plateau and the Maasai Block	26	Monduli	52
Faulting of the volcanoes in the Crater Highlands	27	Kilimanjaro	54
The Eyasi half graben faulting	29	The Younger Extrusives	57
The Kibangaini grid-faulted area	29	Oldoinyo Lengai	57
Upper Pleistocene–Recent faulting	29	Kerimasi	64
Faulting: broader issues	29	Natron–Engaruka tuff-cone area	66
Single-stage or continuous faulting?	29	Burko	67
Style of faulting	29	Meru	68
Southern extension of the Gregory Rift?	29	Monduli–Arusha–Oljoro volcanic field	70
Relationship of the rift valley faults to structural elements in the underlying basement rocks	29	Basotu maars	70
		Kwaraha (sometimes referred to as (Ufiome)	71
		Hanang	71
		Igwisi Hills	72
		Hot springs	73
<b>Chapter 6 Rift-associated sedimentary basins</b>	<b>33</b>	<b>Chapter 8 Regional comparisons, petrochemistry and petrogenesis</b>	<b>79</b>
The Natron Basin	33	Comparative contemporary volcanism in south Kenya and north Tanzania	79
The Engaruka Basin	34	Petrochemistry	79
The Manyara Basin	34	The Northern Tanzania upper mantle	79
The Monduli area basins	35	Evidence from mantle xenoliths for mantle heterogeneity	79
The Balangida and Balangida Lelu basins	35	Xenolith isotope variations	80
The Eyasi Basin	35	The Labait Fe-rich peridotites	81
		Lava compositions	81
		Effects of crustal contamination and fractional crystallization	83

Petrogenesis	84	<b>Chapter 9 Future work</b>	<b>91</b>
Basalt-trachyte volcanoes	84		
Tarosero trachytes and comendites	86	<b>Appendix 1</b>	<b>93</b>
The Younger Extrusives: Oldoinyo Lengai as a model	86	<b>Appendix 2</b>	<b>97</b>
Parent magma(s) of the Younger Extrusives	86		
The Younger Extrusives paradox, and replenishment of the Tanzanian mantle	87	<b>Index</b>	<b>99</b>

# Chapter 1

## Introduction

There are only a few areas on Earth where continental plate break-up and the attendant magmatism are taking place at the present day. In this context, the East African Rift system takes pride of place as it is the most extensive, presently active, continental extension zone, the extension being accompanied

by seismicity, crustal thinning and, in some sectors, magmatism. The reason for this spectacular fracturing of the African Plate has been the subject of much debate but there is general consensus that it is due, at least in part, to the presence of rising thermal plumes in the mantle beneath Africa. The extension is now held

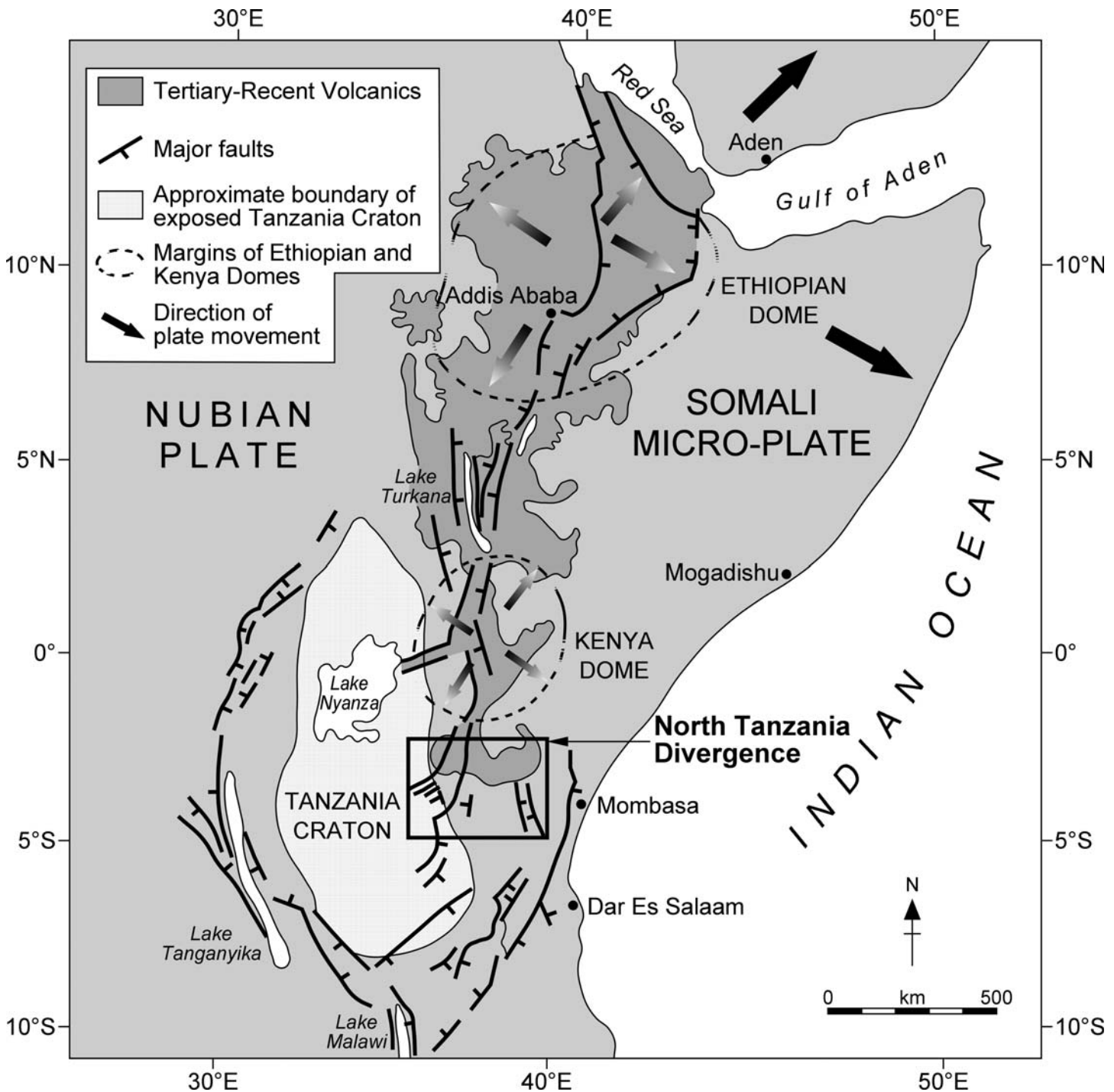


**Fig. 1.1.** Map of East Africa, showing the plate tectonic position of the North Tanzania Divergence relative to the Red Sea spreading centre, and the main structural units of the Ethiopian and Kenya domes and the Tanzania Craton.

J. B. Dawson, University of Edinburgh ([jbdawson@glg.ed.ac.uk](mailto:jbdawson@glg.ed.ac.uk))

From: DAWSON, J. B. 2008. *The Gregory Rift Valley and Neogene–Recent Volcanoes of Northern Tanzania*. Geological Society, London, Memoirs, **33**, 1–2. 0435-4052/08/\$15.00 © The Geological Society of London 2008. DOI: 10.1144/M33.1

to be due to the incipient separation caused by the plume-related eastward drift of the Somalia microplate away from the more stationary Nubian Plate (Fig. 1.1). The attendant fracturing extends from the Afar triple junction in the Red Sea in the north to at least the Zambezi River in the south. It splits into two branches around the Tanzania Craton which forms the topographic high of the East Africa Plateau, which itself is part of the larger highland area that covers much of southern Africa, referred to as the African Superswell (Nyblade & Robinson 1994).

The eastern branch of the fracture system, stretching from the Gulf of Aden, through Ethiopia and Kenya to northern Tanzania, mainly follows the north–south trend of the Mozambique Fold Belt and passes over the localized uplifts of the Ethiopia and Kenya Domes where the sub-parallel rift structures are best developed. The extension is greatest in the north, in the Afar area of Ethiopia, but reduces to little more than a few kilometres in northern Tanzania where the rifting stalls against the Tanzania Craton and splays out into what has been termed the North Tanzania Divergence.

Compared with the western branch of the system, this Eastern or Gregory Rift Valley is characterized by a greater amount of magmatism and, within this branch, the initiation of rift-associated volcanism has moved southwards over time. It began in Ethiopia, where magmatism started c. 30 Ma ago; commenced later in Kenya and was only initiated in northern Tanzania around 8 Ma. As a result northern Tanzania holds a special position in that there are examples of the volcanic rocks extruded at the onset of mantle melting. Further north, in Ethiopia and Kenya, where the rifting and volcanism are relatively mature, the products of early melting are largely buried by the larger volumes of volcanic rocks resulting from more extensive mantle melting.

The Tertiary–Recent volcanic area in northern Tanzania is a small appendage to the larger volcanic massifs in Ethiopia and Kenya to the north, but this belies the wealth of volcanic features and magma types to be found within this relatively small province. It contains features such as snow-capped Kilimanjaro, the highest mountain on the African continent; Ngorongoro, one of the largest calderas on Earth; and the active volcano Oldoinyo Lengai, which is unique for its extrusion of alkali carbonatite. Moreover, this young volcanic area contains an extraordinarily wide variety of volcanic rock types, ranging from ultramafic lavas through alkali basalts, peralkaline trachytes, phonolites and comendites to volcanic carbonatites. There is an ongoing investigation into the origin and evolution of this compositionally wide range of rocks which has been advanced by study of the upper-mantle xenoliths that provide insights into the nature of the upper mantle beneath the Gregory Rift. Xenolith-bearing volcanic rocks occur at a greater number of localities in northern Tanzania than in any other sector of the Gregory Rift Valley, and the chemical and isotopic compositions of the xenoliths have provided evidence for a complex mantle history which is partly reflected in the range in chemistry of the volcanic rocks referred to above.

In addition to the magmatism, a further significant consequence of the extension-related fracturing was the formation of elongate basins now filled with volcanic rocks, sediments, and fresh and saline lakes. The chronology of these basins has been a major

tool in understanding the history of the rifting and, in the context of anthropology and human evolution, these basins have been of prime importance. Once again, Tanzania figures prominently. The discovery of remains of an ancient hominid, *Zinjanthropus boisei* ('Nutcracker Man'), in the basin sediments of the Olduvai Gorge stimulated further anthropological studies in the rift basins of Kenya and Ethiopia, and has resulted in East Africa being acknowledged as 'the Cradle of Mankind'.

The volcanic areas in Ethiopia and, particularly Kenya, have been more thoroughly studied and described than those in northern Tanzania. In its areal relationship between the rift faulting and volcanic activity, northern Tanzania broadly resembles Kenya and Ethiopia but, although the rifting and volcanicity form a geographical continuum with those in southern Kenya, there are significant differences with respect to the overall rift structure, the relatively young age of the volcanicity in Tanzania, and in contemporaneous magma types. These were reviewed briefly by Dawson (1992) and, in the following account, commentary will be made on the differences in the regional geology and geophysics.

The monograph begins with an account of observations of the East African landscape made during explorations in the mid- to late- 1800s; observations that ultimately led to the recognition of the fracture system that we now refer to as 'the rift valleys' (Chapter 2). The following section is a short review of the pre-1960 geological studies in the part of East Africa that is now known as Tanzania. Chapter 3 places the Gregory Rift Valley within its regional geological setting, and is followed by an account of the geophysical advances made during the past two decades. These advances, together with our knowledge of the regional distribution of rock units, have led to an integrated picture of the deeper structural setting of the rifting and magmatism (Chapter 4). Chapter 5 details the progressive development of the rift structures, particularly in the context of the influence of pre-existing structural elements, and this is followed by descriptions of the sedimentary basins that formed as the result of the rifting and the relevance of their sedimentary deposits for dating the rifting (Chapter 6). Descriptions of the northern Tanzania volcanoes form the next, most extensive section (Chapter 7), and the petrogenesis of the volcanic rocks is interpreted in the context of the known composition of mantle beneath the rift valley and the processes that impact on magmas whilst *en route* to the surface (Chapter 8).

Overall, it is the objective of this monograph to give a summary of the present knowledge of the interplay between the break-up of the northern Tanzania segment of the African Plate and its associated magmatism

## References

- DAWSON, J. B. 1992. Neogene tectonics and volcanicity in the North Tanzania sector of the Gregory Rift Valley: contrasts with the Kenya sector. *Tectonophysics*, **204**, 81–92.
- NYBLADE, A. A. & ROBINSON, S. W. 1994. The African Superswell. *Geophysical Research Letters*, **21**, 765–768.

## Chapter 2

### Discovery of the African rift valleys: early work on the Gregory Rift Valley and volcanoes in Northern Tanzania

#### Discovery of the African rift valleys

The Austrian geomorphologist Eduard Suess was the first to recognize the importance of the African rift valleys. However, Suess never visited Africa, and he would never have been able to make his perceptive recognition of this aspect of the geomorphology of the African continent had it not been for earlier field explorers.

The discovery of the African rift valleys can be traced back to the middle part of the nineteenth century. At the time, little was known about the interior of much of Africa, partly because, due to uplift of the continental rim, easy access to much of the interior of Central Africa was precluded by major cataract systems near the mouths of many of the larger rivers (Congo, Niger, Zambesi).

The mainspring for the exploration of East Africa came from a largely unacknowledged source, the missionary community on the East African coast. In 1846, the Church Missionary Society of London established a mission station at Kisuludini in the Rabai Hills on the mainland across from Mombasa Island. The mission was started by Johann Krapf, who was soon joined by Johann Erhardt and Johann Rebmann. All three were Lutherans, trained at Basel; apparently the Society had difficulties recruiting British missionaries for the arduous mission life in East Africa (Oliver 1952). In addition to their pastoral duties, the missionaries travelled inland in attempts to find suitable sites for further mission stations and, during these journeys, they made observations on the geographical features they encountered. It was on such journeys that Rebmann first saw the snow on Kilimanjaro on 11 May 1848, and Krapf saw the snow-capped Mt Kenya in May 1849. In an attempt to find more information about possible routes to the interior, the missionaries (Erhardt in particular) questioned Arab traders who had ventured into the interior in search of slaves and ivory (Krapf 1860). This resulted in the production in 1855 of a map of the interior of East Africa drawn 'in true accordance with information received from natives'. This map is in the possession of the Royal Geographical Society in London, and is catalogued 'Tanzania General 16'. Amongst other features, the map shows three 'Snow Mountains': Kilimanjaro, 'Kignea' and Ndonyo Engai, the 'snow' on the last being in reality a capping of white carbonatite. Oldoinyo Lengai was specifically identified as an active volcano in a later account of Arab trade routes (Wakefield 1870).

At the time, little was known of the area beyond the coastal fringe, and the 1855 map became the stimulus to European exploration of the interior of East Africa that was the domain of the Sultan of Zanzibar. Victorian Britain, from its bases in South Africa and Egypt, had colonial interests in Central Africa and a particular interest in the source of the Nile. The 1855 map shows, well into the interior, a vast area of water termed the Sea of Unyamwezi, a large round body with a thin tail pointing to the south, the shape leading the map to be referred to colloquially as the 'Slug Map'. In retrospect, the body of the slug proved to be Lake Victoria/Nyanza, and the tail to be lakes Tanganyika and Nyasa/Malawi. The possibility that this body of water might be the long sought-after source of the Nile was not lost on the Royal Geographical Society of London which, under the presidency of the geologist Sir Roderick Murchison, sponsored Richard Burton and John Hanning Speke to explore what later became known as the Lake Regions.

Leaving Zanzibar on 16 June 1857, Burton and Speke followed the Arab caravan route from Bagamoyo on the coast and crossed the central plateau of Tanzania, arriving, via Tabora, at Ujiji on Lake Tanganyika on 13 February 1858 (Fig. 2.1). Burton noted the steep descent from the plateau to the lake and, during a journey to the north end of Lake Tanganyika was impressed by the length but narrowness of the lake (Burton 1860). This morphology was further confirmed for the southern part of the lake when it was circumnavigated by Henry Stanley in 1876 (Stanley 1878). On their return journey to the coast, Speke temporarily left a sick Burton with Arab hosts at Tabora to make a side-journey to the north where he discovered the Sea of Unyamwezi, i.e. Lake Nyanza which he named 'Victoria' and which subsequently did indeed prove to be the source of the Nile.

Further south, in 1859 David Livingstone travelled up the Zambesi and Shire rivers with a party that included his brother Charles and John Kirk (later to become the British Consul in Zanzibar). On 16 September 1859, they set eyes on Lake Nyasa and Livingstone noted 'at this point, the valley is about twelve miles wide' (Livingstone & Livingstone 1865, p.108). It subsequently transpired that the lake is as long and narrow as Lake Tanganyika. Then, in May 1864, Samuel Baker, having travelled south up the Nile from the Sudan, discovered Lake Albert Nyanza (Baker 1866), the narrow and elongate form of which became apparent after its circumnavigation in 1876 by Romolo Gessi, one of General Gordon's lieutenants operating from Khartoum (Gessi 1892). Thus, from the heart of Africa, a pattern of long, narrow lakes with a dominantly north-south trend was beginning to emerge.

Meanwhile, exploration into Kenya had not proceeded so rapidly, mainly due to the deterrent effect of the warlike Maasai. A proposal by the Scottish geographer Alexander Keith Johnston to explore Maasailand was agreed by the African Committee of the Royal Geographical Society, but the remit of the expedition in 1879-1880 was re-directed towards exploration of the country between the northern end of Lake Nyasa and the southern end of Lake Tanganyika. A member of the expedition was Joseph Thomson, who had studied geology at the University of Edinburgh under Archibald Geikie (J. B. Thomson 1896), and it fell to Thomson to assume leadership of the expedition after the death from dysentery of its leader, Johnston, and to record the results of the expedition (Thomson 1880, 1881). Thomson's 1880 paper, the first with any significant geological observations pertaining to the African rift valleys, contains geological cross-sections across the area, and records sheared and crushed rocks at the southern end of Lake Tanganyika. From this Thomson deduced 'such a condition indicates the existence of a great fault'. He also recorded the presence of the Rungwe volcanics at the northern end of Lake Nyasa which he tentatively, but mistakenly, correlated with the Stormberg volcanics of South Africa.

In addition to the interest in East Africa shown by Britain, France and Italy, by the 1880s, there had also been several German expeditions, both scientific and commercial, into what is now Tanzania. Chronologically and territorially some of these overlapped with British expeditions. One example is the journey by Count von der Decken who, in 1862, visited Kilimanjaro and Lake Jipe and, on a second visit, climbed Kilimanjaro to 14 000 feet and surveyed Mt Meru (Decken 1869).

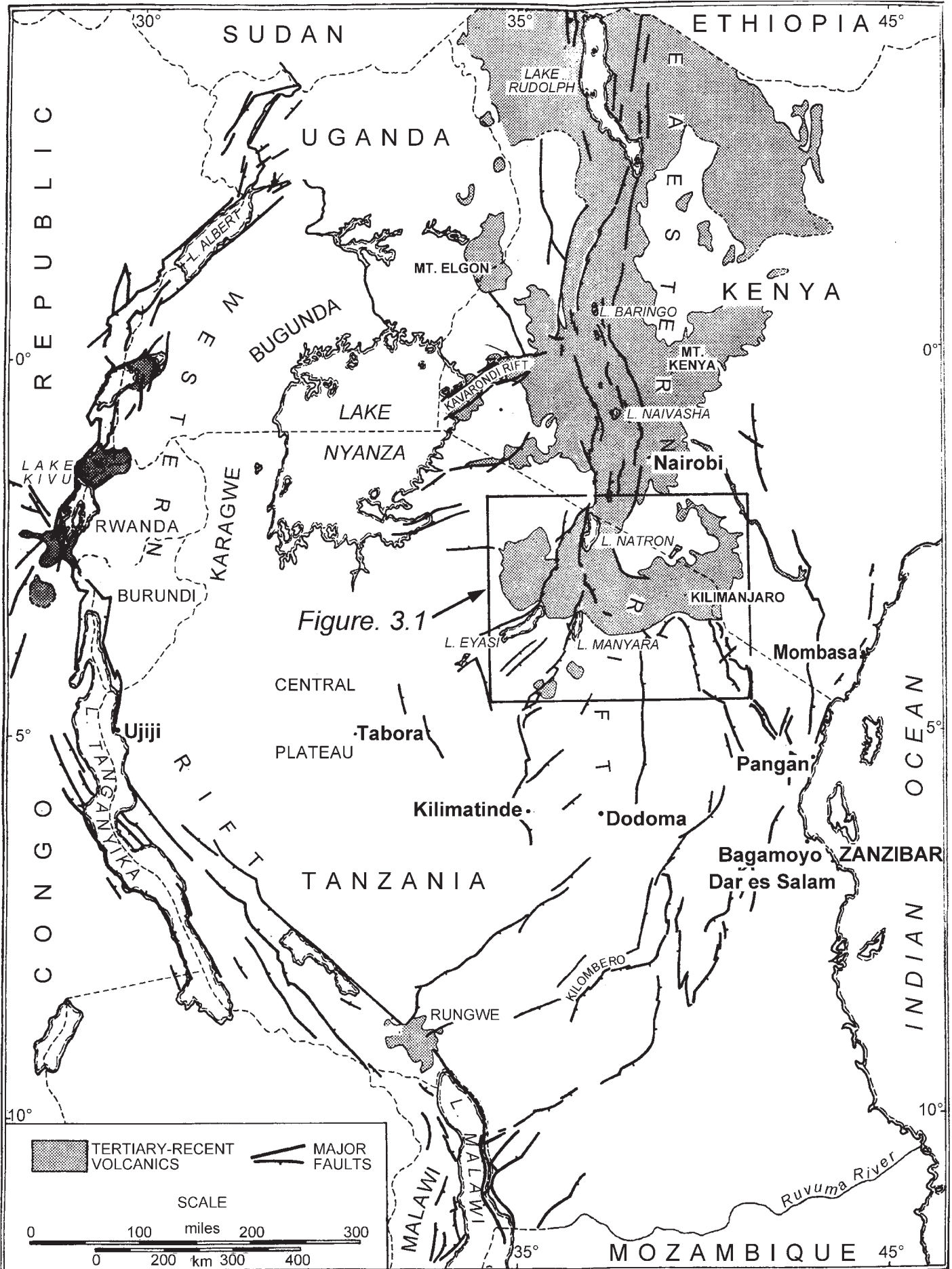


Fig. 2.1. Map of East Africa showing the rift system and localities mainly referred to in Chapter 2 (modified after King 1970).

Subsequent to his travels to Lakes Nyasa and Tanganyika, in 1883 Thomson at last obtained sponsorship from the Royal Geographical Society to explore Maasailand. His plan was to follow an Arab trade route, infrequently travelled because of the predations of the Maasai, to Lake Baringo, a body of water previously unseen by Europeans but whose surrounding country was fabled by the Arabs as a source of much ivory (Farler 1882). Leaving from Mombasa, near Kilimanjaro he had difficulties with the Maasai as the result of resentment caused by a battle between the Maasai and an earlier, large German expedition led by Gustav Fischer, which had then proceeded westwards towards Lake Manyara (referred to below). After placating the Maasai, Thomson's onward journey took him further north than the route taken by Fischer; he descended into the rift valley near Mt Longonot, continued to Lake Naivasha (the furthest point of the Fischer expedition) and, eventually reached Lake Baringo. *En route* he visited Lakes Elmenteita and Nakuru and noted that all the lakes lie within the elongate depression that we now recognize as the rift valley. After visiting the lower western slopes of Mount Kenya, where his hopes of climbing the mountain were dashed by hostile Maasai, he reached Lake Baringo on 10 November 1883. Thomson's description of the setting of the lake from the edge of the Laikipia Plateau is the first description of rift valley geomorphology: 'suddenly emerging from the dense forest... at the edge of the meridional trough... there was the mysterious Lake Baringo several thousand feet below... Imagine if you can a trough or depression 3300 feet above the sea-level, and twenty miles broad, the mountains rising with a very great abruptness on both sides to a height of 9000 feet. In the centre of this depression lies a dazzling expanse of water. Round the lake... a remarkable assemblage of straight lines, wall-like extensions and angular lines produces an impressive and quite unique landscape. It speaks eloquently, however, of igneous disturbances; for there you observe numerous earth movements, faults crossing each other at right angles, and other features, which are clearly not modelled by surface agents, all of them so recent in origin as to remain comparatively untouched by the hand of time, which seems to abhor anything approaching a straight line' (Thomson 1887, 228–230). Later on this journey, Thomson travelled west to Lake Nyanza, and then returned to Baringo via Mt Elgon, noting *en route* the major fault escarpments on the western side of the rift valley.

Between 1887 and 1888 the Hungarian, Count Samuel Teleki, accompanied by the Austrian Ludwig von Höhnel, travelled on a hunting and natural history expedition from Pangani on the East African coast across central Kenya to the southern borders of Ethiopia. It was von Höhnel who kept the records and made maps of the terrain crossed by the expedition (Höhnel 1890, 1894). In southern Ethiopia, the expedition discovered two large lakes, Basso Narok and Basso Ebor, which Teleki renamed respectively lakes Rudolph and Stephanie after the Prince Regent of the Austro-Hungarian Empire and his consort. Like lakes Tanganyika and Nyasa, Lake Rudolph in particular proved to be long and narrow, and von Höhnel had the perception to link the Rudolph depression with Thomson's 'meridional trough' in Kenya to the south. Von Höhnel was a friend of Eduard Suess who had been plotting the shapes of the various lakes as they were discovered; sitting in Vienna, he had never set foot in Africa. Drawing on the cumulative information from the early explorers, and with the collaboration of von Höhnel after his return to Vienna, Suess (1891) proposed, in a compendium on the geology of East Africa (Höhnel *et al.* 1891), that the chains of ribbon-like lakes lie in sunken valleys, which he termed 'grabens', resulting from major fractures running across the African continent from the Red Sea to the Zambesi. Later, in a more extended work, he proposed that these fractures linked northwards via the Red Sea to the Dead Sea depression (Suess 1885–1909). This has indeed proved to be the case, but the nature of the fracturing and the geological events attending it in

East Africa had to await the observations made by J. W. Gregory during two journeys into central Kenya in 1893 and 1919 (Gregory 1894, 1896, 1921). Gregory made several fundamental observations about the Quaternary of East Africa, published in his classic *The Great Rift Valley* (Gregory 1896); these included observations on the former extension of glaciers on Mt Kenya, the former existence of great lake systems in areas that are now arid, and the subsidence of East African Plateau on the site of Lake Nyanza and the consequent interruption of major river systems. But it was in his earlier 1894 account that Gregory introduced the term 'rift valley', for which he will be remembered, defining it as 'a linear valley with parallel and almost vertical sides, which has fallen owing to a series of parallel faults'.

### Early geological work in northern Tanzania

As noted earlier, it was not only Britain that was showing an interest in East Africa in the latter part of the nineteenth century. Following the virtual annexation of part of the East African mainland by the Company for German Colonization under Carl Peters in 1884, a joint boundary commission under the direction of Kirk, the British Consul in Zanzibar, was set up in 1885, and in October 1890, apart from a thin coastal strip ten miles wide, the former mainland domains of the Sultan of Zanzibar were partitioned into British and German spheres of influence, with the boundary running from the coast south of Mombasa northwestwards towards Lake Nyanza/Victoria (Kirk 1887; Smith 1894).

Pakenham (1991) details the attendant and subsequent political and commercial manoeuvrings, but suffice to say that, even before the partitioning, and beginning in the 1860s, there had been an increasing number of German expeditions into what is now Tanzania. It is due to these expeditions that we have the first accounts of the Tanzania sector of the rift valley and many of the volcanoes of northern Tanzania. The visits of von der Decken to Kilimanjaro and Meru were mentioned earlier. In 1882–1883, Gustav Fischer, in what turned out to be a rival expedition to that of Thomson, travelled from Pangani to Kilimanjaro and Arusha, but then west to Lake Manyara and north up the rift valley, arriving at Lake Naivasha in Kenya before Thomson. In Njorowa Gorge, on the southern shore of Lake Naivasha, stands a pinnacle of peralkaline rhyolite. Its name, 'Fischer's Tower', perpetuated to the present day, commemorates his visit. Also during his northwards journey from Lake Manyara he became the first European to see the active volcano Oldoinyo Lengai (Fischer 1884–1885).

Other notable expeditions were those of Baumann in 1892–1893 (Baumann 1894); of Meyer, who went as far as the Western Rift Valley and discovered the Kivu volcanic province, and who also was the first European to reach the summit of Kilimanjaro in 1889 (Meyer 1893, 1900); and of Schöller, who crossed Maasailand to reach Uganda (Schöller 1901–1904). Although rocks collected on the Fischer, Baumann and Schöller expeditions were later described by Mügge (1886), Lenk (1894) and Kunzli (1901), respectively, as were rocks from Kilimanjaro by Finckh (1903, 1906), these expeditions were mainly concerned with the geography of the area. An exception was the first geophysical fieldwork that took place in 1899 and 1900, when Ernst Kohlschütter (the German astronomer who had been attached to the survey that had carried out the earlier boundary commission) made the first pendulum gravity readings across the Tanganyika Plateau and the Gregory Rift Valley (Kohlschütter 1901). His data were incorporated into a later synthesis of East African geology by Krenkel (1922).

More detailed geological observation arose in 1904 when Carl Uhlig led an expedition which surveyed the Manyara–Natron sector of the rift valley more thoroughly than had Fischer; Uhlig was the first to note the asymmetry of this sector of the rift

(Uhlig 1905, 1907a, b). During the expedition, Fritz Jaeger made the first recorded ascents of Meru and Oldoinyo Lengai in 1904 and also explored the Crater Highlands to the west of the rift valley (Jaeger 1911, 1913). Rocks collected by Jaeger were described by Finckh (1911). Oldoinyo Lengai continued to hold a fascination for the German geologists, and was climbed again by Uhlig and F. Th. Müller in 1910 (Uhlig & Jaeger 1942), by Hans Reck in 1911 (Reck 1914c, 1923) and by Shulze in 1915 (Reck & Shulze 1921).

In 1913, Reck made the earliest stratigraphic studies of the Olduvai Gorge to the west of the Crater Highlands (Reck 1914a, b), during which he collected many mammalian fossils that he took to Berlin. These fossils subsequently turned out to have important implications for East African anthropology. Geological fieldwork in German East Africa was interrupted by the 1914–1918 war but publications arising from pre-war work continued for some time afterwards, notable contributions being Reck's collection of photographs of Oldoinyo Lengai (Reck 1924), Erdmannsdorfer's descriptions of wollastonite-bearing igneous rocks from Oldoinyo Lengai (Erdmannsdorfer 1935), and a detailed volume on the Manyara–Natron area (Uhlig & Jaeger 1942).

Following the 1914–1918 war, the former German East Africa became Tanganyika Territory under a mandate from the League of Nations. Under the new British administration, the Tanganyika Geological Survey was established in Dodoma. Initially, because of their relatively low economic potential, the areas around the Gregory Rift Valley and the Neogene volcanoes had a low priority within the regional-geology mapping programme. This was redressed in the 1950s and early 1960s and maps of most of these areas have now been published on a scale of 1:125 000. The individual maps, which are referred to in the appropriate places later in this volume, contain brief explanations of the geology.

In addition to the efforts of the Survey staff, geologists and geophysicists from academic institutions have carried out detailed studies, particularly in more recent years. These are mainly referred to later, but three significant contributions made prior to 1960 are mentioned here:

(1) In 1928 the anthropologist L. S. B. Leakey visited Berlin and, despite Reck's scepticism, recognized artefacts amongst the material gathered by Reck at Olduvai Gorge in 1913. This recognition resulted in a series of expeditions, beginning in the 1930s, to collect new material. The work arising from these expeditions has led to Olduvai being recognized as a world-famous hominid locality and, via Leakey's connection with the Coryndon Museum in Nairobi (now the National Museum of Kenya), was the impetus for anthropological research in Kenya and Ethiopia, as well as other parts of Tanganyika. In addition, *en route* to Olduvai on the 1934–1935 expedition, P. E. Kent recognized and later described the lake beds at Lake Manyara, and, on the same expedition, carried out the first mapping of the Laetoli Beds to the south of Olduvai. The dating of volcanic components in the strata at both Olduvai and Laetoli, in connection with elucidating the chronology of hominid evolution, has led to a clearer knowledge of the eruption history of some of the northern Tanzania volcanoes.

(2) Between 1930 and 1935, Bailey Willis, of the Carnegie Institute of Washington, travelled extensively in both the Western and Gregory Rifts, and a monograph detailing his observations contains the most exhaustive analysis to that date of the roles of extension v. compression in the formation of the rift valleys (Willis 1936). In contrast to Gregory, and on the basis of metamorphic rocks apparently overlying younger volcanic rocks on the west shore of Lake Natron, he concluded that thrusting and compression are the causes of the rift valley depression. It later transpired that the igneous rocks are intrusive into the schists.

(3) As part of the regional mapping programme, in 1953 and 1957 joint expeditions of the Tanganyika Geological Survey and

the Department of Geology at the University of Sheffield, carried out geological and glaciological surveys of Kilimanjaro. The geological account (Downie & Wilkinson 1972) is one of the most comprehensive reports pertaining to a single African volcano, and the glaciological data (Downie 1964) provide a yardstick against which to measure glacier retreat over the past half-century.

On 9 December 1961, Tanganyika became independent and the highest point on Kilimanjaro, formerly known as Kaiser Wilhelm Point, was renamed Uhuru (Freedom) Peak on that date. After its unification with Zanzibar, on 29 October 1964 the name of Tanganyika merged with that of Zanzibar to become Tanzania.

## References

- BAKER, S. W. 1866. *Albert N'Yanza, Great Basin of the Nile*. MacMillan, London, 2 volumes.
- BAUMANN, B. 1894. *Durch Masailand zur Nilquelle*. Reimer, Berlin.
- BURTON, R. F. 1860. *The Lake Regions of Central Africa*. Longman, Green, Longman & Roberts, London, 2 volumes.
- DECKEN, C. C. & VON DER, 1869. *Reisen in Ost Afrika* (referred to in Thomson (1887, p.4) and Gregory (1921, p.53)).
- DOWNIE, C. 1964. Glaciations of Mount Kilimanjaro, Northeast Tanganyika. *Bulletin of the Geological Society of America*, **75**, 1–16.
- DOWNIE, C. & WILKINSON, P. 1972. *The Geology of Kilimanjaro*. University of Sheffield, Sheffield.
- ERDMANNSDORFER, O. 1935. Über wollastoniturtit und die Entstehungsweisen von alkaligesteiner. *Sitzungsberichte der Heidelberg Akademie für Wissenschaften, Mathematik und Naturgeschichte*, **K 1.2**, 1–23.
- FARLER, J. P. 1882. Native routes in East Africa from Pangani to the Masai country and the Victoria Nyanza. *Proceedings of the Royal Geographical Society, New Series*, **4**, 730–753.
- FINCKH, L. 1903. Die trachydolerite des Kibo (Kilimandscharo) und die kenyte des Kenya. *Zeitschrift der Deutsches Geologische Gesellschaft*, **55**, Monatsbericht 1–14.
- FINCKH, L. 1906. Die rhomberporphyre des Kilimandscharo. In: *Festschrift zum siebsigsten Geburtstag von Harry Rosenbusch*. Stuttgart, 372–398.
- FINCKH, L. 1911. Die von F. Jaeger in Deutsch-Ostafrika gesammelten Gesteine. In: JAEGER, F. (ed.) *Das Hochland der Riesenkrater und die umliegender Hochländer Deutsch Ostafrika*, Part 1. *Mitteilungen aus den Deutsches Schutzgebieten, Ergänzungsheft*, **4**, 71–85.
- FISCHER, G. A. 1884–1885. Reise in das Masailand. *Mitteilungen der Geographisches Gesellschaft Hamburg*, Pt 1 (1884), 36–99, Pts 2 and 3 (1885) 189–237 and 238–279.
- GISSI, R. 1892. *Seven Years in the Sudan*. Sampson Low, Marston & Co., London.
- GREGORY, J. W. 1894. Contributions to the physical geography of British East Africa. *Geographical Journal*, **4**, 290–315, 408–424, 505–514.
- GREGORY, J. W. 1896. *The Great Rift Valley*. John Murray, London.
- GREGORY, J. W. 1921. *The Rift Valleys and Geology of East Africa*. Seeley, Service, London.
- HÖHNEL, L. R. VON, 1890. Ost-Äquatorial Afrika zwischen Pangani und dem neuentdecken Rudolf-See. *Petermann's Mitteilungen Ergänzungsheft*, **99**, 1–44.
- HÖHNEL, L. R. VON, 1894. The Discovery of Lakes Rudolf and Stefanie. A narrative of Count Teleki's exploring and hunting expedition in Eastern Equatorial Africa in 1887–1888. Longmans, Green, London, 2 volumes. Abridged from the German edition of 1892.
- HÖHNEL, L. R., VON, ROSIHAL, A., TOULA, F. & SUESS, E. 1891. Beiträge zur geologischen Kenntniss der östlichen Afrika. *Denkschriften der Königlich Akademie für Wissenschaften Wien, Math-Naturwissenschaften Klasse*, **58**, 447–584.
- JAEGER, F. 1911. Das Hochland der Riesenkrater and die umliegender Hochländer Deutsch Ostafrika, Part 1. *Mitteilungen aus den Deutsches Schutzgebieten, Ergänzungsheft*, **4**, 1–133.
- JAEGER, F. 1913. Das Hochland der Riesenkrater and die umliegender Hochländer Deutsch Ostafrika, Part 2. *Mitteilungen aus den Deutsches Schutzgebieten, Ergänzungsheft*, **8**, 1–213.

- KING, B. C. 1970. Volcanicity and rift tectonics in East Africa. In: CLIFFORD, T. N. & GASS, I. G. (eds) *African Magmatism and Tectonics*. Oliver & Boyd, Edinburgh, 263–283.
- KIRK, J. 1887. Britain and Germany in East Africa; note. In: THOMSON, J. *Through Masailand: a Journey of Exploration among the Snow-clad Volcanic Mountains and Strange Tribes of Eastern Equatorial Africa*. Sampson Low, Marston, Searle & Rivington, London. 357–359.
- KOHLSCHÜTTER, E. 1901. Über den Bau der Erdkrust in Deutsch-Ostafrika. *Vorläufige Mitteilungen, Nachrichten der Königlichen Gesellschaft der Wissenschaften zu Göttingen*, **1901**, 1–40.
- KRAPF, J. L. 1860. *Travels, Researches and Missionary Labours during an Eighteen Years' Residence in Eastern Africa*. Trübner & Co., London.
- KRENKEL, E. 1922. *Die Bruchzonen Ostafrikas: Tektonik, Vulkanismus, Erdbeben and Schwereanomalien*. Bornträger, Berlin.
- KUNZLI, E. 1901. Die petrographische Ausbeute der Schoellerschen Expedition in Äquatorial Ostafrika. (Masailand). *Vierteljahrsheft der Naturforschenden Gesellschaft Zürich*, **46**, 128–172.
- LENK, H. 1894. Über Gesteine aus Deutsch Ostafrika. In: BAUMANN, B. *Durch Masailand zur Nilquelle*. Reimer, Berlin. 263–294.
- LIVINGSTONE, D. & LIVINGSTONE, C. 1865. *Narrative of an Expedition to the Zambesi and its Tributaries, and the Discovery of Lakes Shirwa and Nyasa 1858–1864*. John Murray, London.
- MEYER, H. 1893. Die grossen Bruchspalten und Vulkane in Äquatorial-Afrika. *Deutsche Geographische Blätter*, **16**, 105–127.
- MEYER, H. 1900. *Der Kilimandjaro*. Reimer, Berlin.
- MÜGGE, O. 1886. Untersuchungen der von Dr. G. A. Fischer gesammelten gesteine des Masailand. *Neues Jahrbuch für Mineralogie*, **4**, 238–264.
- OLIVER, R. 1952. *The Missionary Factor in East Africa*. Longman, Green & Co, London.
- PAKENHAM, T. 1991. *The Scramble for Africa*. Weidenfeld & Nicolson, London.
- RECK, H. 1914a. Erste vorläufige Mitteilungen über den Fund eines fossil Menschenskelets aus Zentralafrika. *Sitzungsberichten der Gesellschaft Naturforschender Freunde*, **3**, 81–95.
- RECK, H. 1914b. Zweite vorläufige Mitteilungen über fossile Tier- und Menschenfunde aus Oldoway in Zentralafrika. *Sitzungsberichten der Gesellschaft Naturforschender Freunde*, **3**, 305–318.
- RECK, H. 1914c. Oldoinyo Lengai, ein tätiger Vulkan in Gebiet der Deutschostafrikanischen Bruchstufe. *Branca Festschrift*, **7**, 373–409.
- RECK, H. 1923. Über der Ausbruch des Oldoinyo Lengai in Deutschostafrika in Jahre 1917. *Zeitschrift für Vulkanologie*, **7**, 55–56.
- RECK, H. 1924. L'Engai Bilder. *Zeitschrift für Vulkanologie*, **8**, 172–174.
- RECK, H. & SCHULZE, G. 1921. Ein Beitrag zur Kenntnis des Baues an der jüngsten Veränderung des l'Engai-Vulkanes im nordlichen Deutsch-Ostafrika. *Zeitschrift für Vulkanologie*, **6**, 47–71.
- SCHÖLLER, M. 1901–1904. *Mitteilungen über meine Reise nach Äquatorial-Ostafrika und Uganda, 1897–97*. Reimer, Berlin, Pt I (1901), Pt II (1904), Pt III 16 maps (1901).
- SMITH, C. S. 1894. The Anglo-German boundary in East Equatorial Africa. Proceedings of the British Commission. *Geographical Journal*, **4**, 424–439.
- STANLEY, H. M. 1878. *Through the Dark Continent*. Sampson Low, Marston, Searle & Rivington, London.
- Suess, E. 1891. Die Brüche des östlichen Afrika. Chapter 4. In: HÖHNEL, L. R. VON ET AL. *Denkschrift der Königlich Akademie für Wissenschaften Wien, Math-Naturwissenschaften Klasse*, **58**, 555–584.
- Suess, E. 1885–1909. *Das Antlitz der Erde (The Face of the Earth)*. Translated by H. Sollas & W. J. Sollas, 1904–1909). Clarendon Press, Oxford, 3 volumes.
- THOMSON, J. 1880. Notes on the geology of East–Central Africa. *Nature*, **28**, 102–104.
- THOMSON, J. 1881. *To the Central African Lakes and Back: the Narrative of the Royal Geographical Society's Central African Expedition 1879–80*. Sampson Low, Marston, Searle & Rivington, London, 2 volumes.
- THOMSON, J. 1887. *Through Masailand: a Journey of Exploration among the Snow-clad Volcanic Mountains and Strange Tribes of Eastern Equatorial Africa*. Sampson Low, Marston, Searle & Rivington, London. (New and revised edition of the original 1884 version).
- THOMSON, J. B. 1896. *Joseph Thomson – African Explorer*. Sampson Low, Marston & Co., London.
- UHLIG, C. 1905. Bericht über die Expedition der Otto-Winter Stiftung nach dem Umgebungen des Meru. *Zeitschrift der Gesellschaft für Erdkunde*, **1905**, 120–123.
- UHLIG, C. 1907a. Vom Kilimandscharo zum Meru. *Zeitschrift der Gesellschaft für Erdkunde*, **1907**, 627–650.
- UHLIG, C. 1907b. Der sogenannte grosse Ostafrikanische Graben zwischen Magad (Natron See) und Lawa ya Mweri (Manyara See). *Geographisches Zeitung*, **15**, 478–505.
- UHLIG, C. & JAEGER, F. 1942. Die Ostafrikanische Bruchstufe and die angrenzenden Gebiete zwischen die Seen Magad und Lawa ja Mweri sowie den Westfuss des Meru. *Deutsches Institut für Länderkunde, Wissenschaften Veröffentlichungen, New Series* **10**.
- WAKEFIELD, T. 1870. Routes of native caravans from the coast to the interior of Eastern Africa, chiefly from information given by Sadi Bin Ahedi, a native of a district near Gazi, in Udigo, a little north of Zanzibar. *Journal of the Royal Geographical Society*, **40**, 303–339.
- WILLIS, B. 1936. *East African Plateaus and Rift Valleys*. Carnegie Institution of Washington, Washington D.C.

## Chapter 3

### Regional geology

The present-day Gregory Rift Valley in northern Tanzania is an elongate north–south half graben flanked on its western side by a high, eastwards-facing escarpment; this differs from Kenya where there are also major faults on the eastern side of the rift valley. The words ‘present-day’ are used advisedly, as the present morphology is imposed upon an earlier, wider, volcano-infilled tectonic depression. As in Kenya, within and to either side of the rift valley there are extensive areas of Neogene and Quaternary volcanic rocks (Fig. 3.1). To the SW of the main volcanic area is the Eyasi half graben and, to the SE, the Pangani graben; these major features are infilled by volcanoes at their northeastern and northern ends, respectively.

The northern Tanzania volcanic province is younger overall than the Ethiopian, where magmatism was initiated at around 40 Ma, and Kenya provinces (Baker *et al.* 1972; George *et al.* 1998) suggesting that more recent mantle perturbations are responsible for the intra-plate magmatism and crustal fracturing in this part of Africa.

The province stands astride the surface interface between the Archaean rocks of the Tanzania Craton and the north–south-trending Mozambique orogenic fold belt (Fig. 3.1). The rocks of the craton have been divided into three major formations, the Dodoman (oldest), the Nyanzian and the Kavirondian (Quennell *et al.* 1956; Schlüter 1997) but, in brief, the craton is an amalgamation of several terranes comprising Archaean metasediments, including the so-called greenstone belts (some as old as >3 Ga), that were intruded by granites and migmatized during three short tectono-metamorphic events at around 2.9, 2.7 and 2.4 Ga (Pinna *et al.* 1996). A minor phase of granite intrusion was the latest event to affect this stable block at 1.85 Ga (Cahen *et al.* 1984).

The age, make-up and terminology of the ‘Mozambique Belt’ require some explanation. With the exception of Hanang, the most southerly of the northern Tanzanian volcanoes, which overlies cratonic rocks, the Tanzania Geological Survey maps show the volcanic province to be surrounded and underlain by metamorphic rocks assigned to the ‘Usagaran’, a major subduction-related, tectono-thermal event dated at around 2 Ga at the type locality in the Usagara Mountains at the southeastern margin of the Tanzania Craton (Quennell *et al.* 1956). Such rocks extend part-way across the Serengeti Plains to the west of the volcanic province, and over part of the Maasai Block to the east. However, metamorphic rocks in the Pare Mountains further to the east are dated at  $645 \pm 10$  Ma (Muhongo & Lenoir 1994).

The term ‘Mozambique orogenic belt’ was originally used by Holmes (1951) to describe the north–south-trending fold belt stretching from Ethiopia to Mozambique, partly bounded on the west by the Tanzania Craton, and this fold belt was later included by Kennedy (1964) in the series of Africa-wide fold belts affected by the so-called ‘Pan-African orogenic event’ at around 650 Ma. Specifically in northern Tanzania, Möller *et al.* (1995, 1998) suggested that, whereas the Usagaran metamorphic event is still recognizable at the type locality, the effects of the Usagaran metamorphism were largely erased in northern Tanzania during the Pan-African event due to large-scale thrusting of fold belt metamorphic rocks westward over the eastern margin of the Tanzania Craton (Shackleton 1986). Hepworth (1972) had earlier advocated that the complex metamorphism and structure of a large tract of terrain, to the east of the mapped craton boundary but to the west of the Pare Mountains, should be assigned to an event

earlier than the Pan-African, and Cahen *et al.* (1984) agreed that ‘ancient assemblages are involved in the Mozambique Belt along its western margin and are recognizable over some distance into the belt’. This has been further confirmed by recent work that shows the Mozambique Belt in Central Tanzania to consist of reworked, ancient crust of Archaean (2970–2500 Ma) or Palaeoproterozoic (2124–1837 Ma) age (Sommer *et al.* 2003). Hence, the reality is that, with the Tanzania Craton acting as a foreland, the Mozambique Belt is a polycyclic orogenic complex involving basement and cover rocks of more than one orogenic event, with the last taking place around 650 Ma. Similarly, Key *et al.* (1989), Mosley (1993) and Hauenberger *et al.* (2007) provide evidence for the polycyclic nature of the Mozambique Belt in Kenya.

Petrographically, the Usagaran has been divided into two major series: (i) the lower Masasi Series comprising mainly quartzofeldspathic gneisses, charnockites and hornblende–biotite gneisses; and (ii) the higher Crystalline Limestone Series, comprising quartzites, dolomitic marbles, graphitic marble, graphite schists, mica schists, kyanite gneisses and rarer metabasites (Quennell *et al.* 1956). Both series are extensively veined by pegmatites. Particularly interesting units in the Crystalline Limestone Series are the tanzanite-bearing marbles of the Leletema Hills (south of Kilimanjaro), ruby corundum–Cr zoisite amphibolite in the Longido area (Game 1954), and the rocks of Mautia Hill [6°8’S 36°29’E], the type locality for yoderite ( $[\text{MgAl}]_8 \text{SiO}_4[\text{O},\text{OH}]_{20}$ ) (McKie & Redford 1959), where yoderite–kyanite–talc schists are accompanied by piedmontite marbles.

The metamorphic grade of the Usagaran rocks ranges from biotite facies to upper amphibolite facies, whereas the Pan-African age rocks of the Pare Mountains are of granulite facies. However, granulite-facies granite (charnockite) and anorthosite also occur as the cores of mantled gneiss domes within the dominantly Usagaran metamorphic rocks at Loliondo and Longido near the Kenya border to the west and east of the rift valley, respectively.

As noted above, the northern Tanzania volcanic province stands astride the surface interface between the Archaean rocks of the Tanzania Craton and the north–south-trending Mozambique orogenic fold belt. Thus, on the basis of surface geology alone, it might appear that the volcanism and the rift structures are located within a tectonic crustal suture regime where there are mechanical and thermal contrasts between thick, cold, rigid Archaean lithosphere and thinner, anisotropic mobile-belt lithosphere. However, Smith (1994) and Smith & Mosley (1993) proposed that, in southern Kenya, due to the westward overthrusting by the Mozambique Belt rocks, the buried margin of the craton lies some 100 km to the east of the surface contact between the craton and the fold belt metamorphics. In support of this is a 1 km thick low-velocity P-wave layer, extending for 120 km westwards from the rift valley at Lake Magadi; the layer is interpreted as highly fractured and sheared Mozambique Belt rocks overlying the Tanzania Craton (Birt *et al.* 1997). In northern Tanzania, granulites dated at 2.0 Ga (Cohen *et al.* 1984) occur as xenoliths at the Lashaine volcano (see Dawson 2008, fig. 5.8) again some 100 km east of the mapped contact between the craton and the mobile belt. The age of the Lashaine granulites has not been reset due to tectonic downgrading, which suggests a stable, underlying structure i.e. the craton. Further, the suggestion of Archaean lithosphere below a thin layer of Proterozoic nappes is supported by heat flow values that, in central and northeastern Tanzania, are

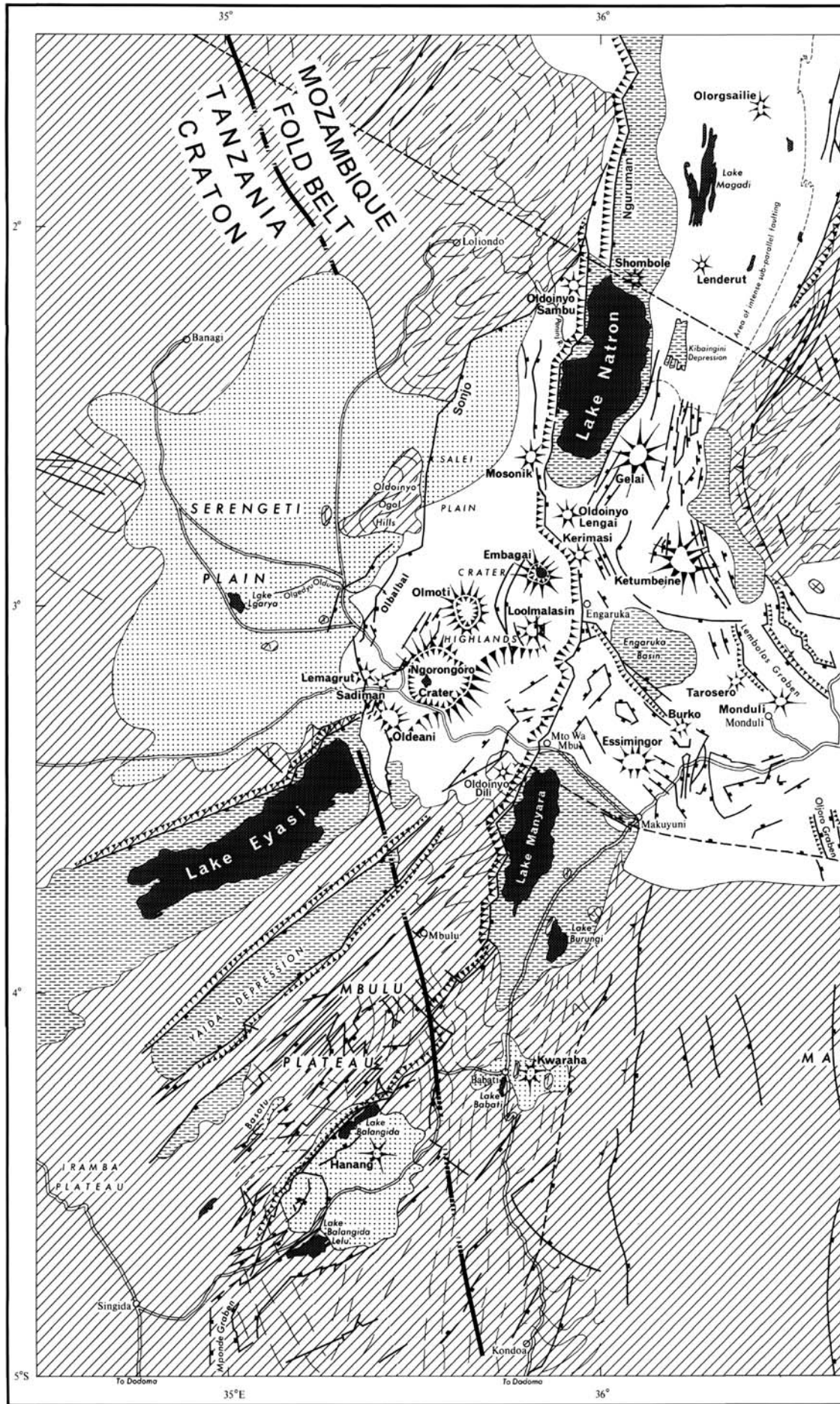
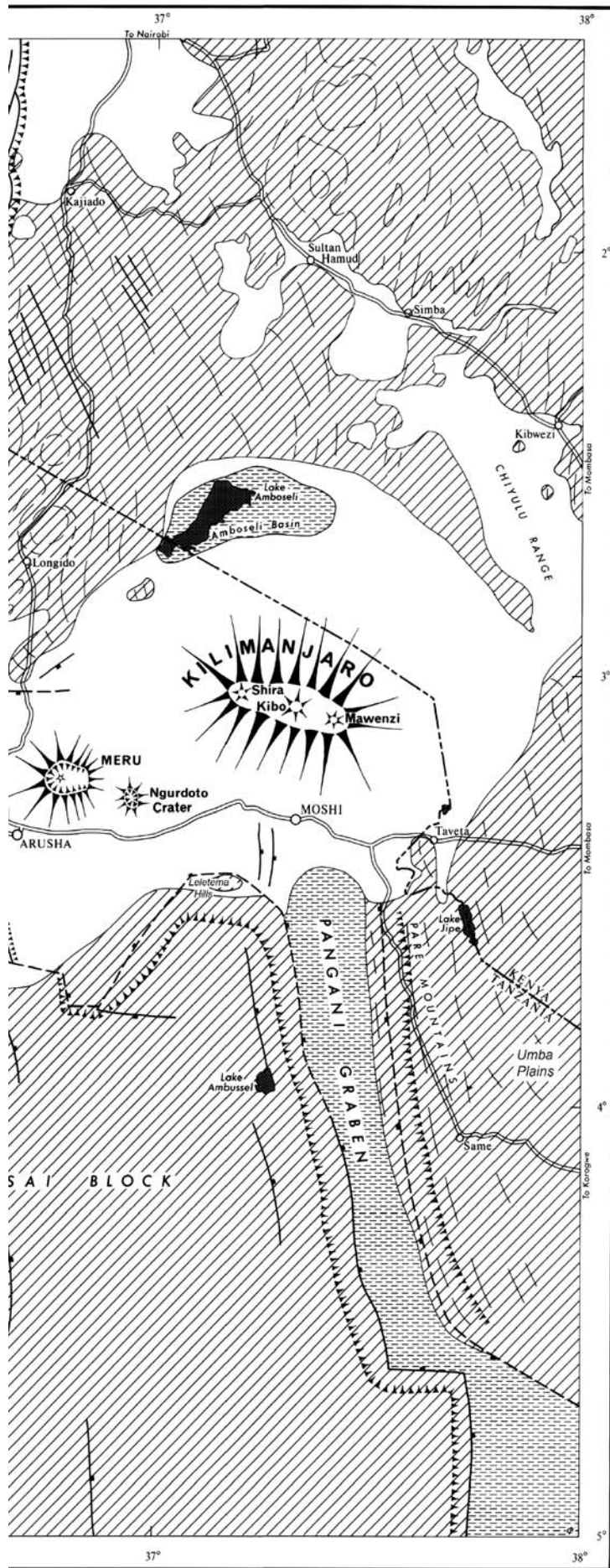
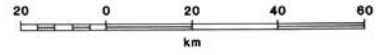


Fig. 3.1. Distribution of Neogene–Recent faults and volcanic rocks in northern Tanzania and adjoining parts of southern Kenya.



DISTRIBUTION OF NEOGENE FAULTS & VOLCANIC ROCKS IN NORTHERN TANZANIA & ADJOINING PARTS OF KENYA



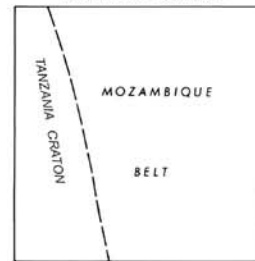
EXPLANATION OF SYMBOLS

- Modern alluvium and/or detritus
- Neogene Tuffs
- Neogene Lavas
- Basement
- Geological boundary
- Tertiary warp
- Inclination of Mid-Tertiary land surface
- Trend in Basement
- Fault, with downthrow
- Fault, inferred, with downthrow
- Volcanic cone
- Escarpment
- Main road
- Secondary road
- Town or village
- International boundary

COMPILATION NOTE

TOPOGRAPHY - Compiled from SK 57 1:1M Survey of Kenya, 1967 and Series 1301 1:1M D.O.S. 1969.  
 GEOLOGY - Compiled from Quarter Degree Geological Maps of the Tanzania and Kenya Geological Surveys 1:100000 by J.B. Dawson

BASEMENT GEOLOGY



LOCATION MAP

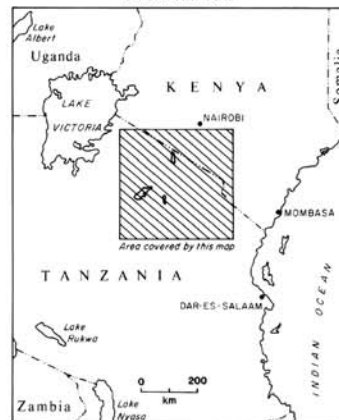


Fig. 3.1. (Continued)

those typical of a craton (see Chapter 4, Dawson 2008). Thus, it can be reasonably inferred that many of the Tanzanian volcanoes have erupted through Archaean cratonic lithosphere that is overlain by only a thin veneer of relatively young fold belt rocks. In the context of potential crustal contamination, this implication is important when considering the composition and isotope systematics of the volcanic rocks.

## References

- BAKER, B. H., MOHR, P. A. & WILLIAMS, L. A. J. 1972. *Geology of the Eastern Rift System of Africa*. Geological Society of America, Special Publications, **36**.
- BIRT, C. S., MAGUIRE, P. K. H., KHAN, M. A., THYBO, H., KELLER, G. R. & PATEL, J. 1997. The influence on pre-existing structures on the evolution of the southern Kenya Rift Valley – evidence from seismic and gravity studies. *Tectonophysics*, **278**, 211–242.
- CAHEN, L., SNELLING, N. J., DELHAL, J. & VAIL, J. R. 1984. *The Geochronology and Evolution of Africa*. Clarendon Press, Oxford.
- COHEN, R. S., O'NIONS, R. K. & DAWSON, J. B. 1984. Isotope geochemistry of xenoliths from East Africa: implications for the development of mantle reservoirs and their interaction. *Earth and Planetary Science Letters*, **68**, 209–220.
- DAWSON, J. B. 2008. *The Gregory Rift Valley and Neogene–Recent Volcanoes of Northern Tanzania*. Geological Society, London, Memoirs, **33**.
- GAME, P. M. 1954. Zoisite-amphibolite with corundum from Tanganyika. *Mineralogical Magazine*, **30**, 458–466.
- GEORGE, R. M., ROGERS, N. W. & KELLEY, S. 1998. Earliest magmatism in Ethiopia: evidence for two mantle plumes in one flood basalt province. *Geology*, **26**, 923–926.
- HAUZENBERGER, C. H., SOMMER, H., FRITZ, H., BAUERNHOFER, A., KRÖNER, A., HOINKES, G., WALLBRECHER, E. & THÖNI, M. 2007. SHRIMP U–Pb zircon and Sm–Nd garnet ages from the granulite-facies basement of SE Kenya: evidence for Neoproterozoic polycyclic assembly of the Mozambique Belt. *Journal of the Geological Society, London*, **164**, 189–201.
- HEPWORTH, J. V. 1972. The Mozambique orogenic belt and its foreland in northeast Tanzania: a photogeologically-based study. *Journal of the Geological Society, London*, **128**, 461–500.
- HOLMES, A. 1951. The sequence of pre-Cambrian orogenic belts in south and central Africa. *Proceedings of the 18<sup>th</sup> International Geological Congress, 1948*, **14**, 254–269.
- KENNEDY, W. Q. 1964. The structural differentiation of Africa in the Pan-Africa ( $500 \pm$  m.y.) tectonic episode. *8<sup>th</sup> Annual Report of the Research Institute of African Geology, University of Leeds, Session 1962–63*, **8**, 48–49.
- KEY, R. M., CHARLESLEY, T. J., HACKMAN, B. D., WILKINSON, A. F. & RUNDLE, C. C. 1989. Superimposed Upper Proterozoic collision-controlled orogenies in the Mozambique orogenic belt of Kenya. *Precambrian Research*, **44**, 197–225.
- MCKIE, D. & REDFORD, A. J. 1959. Yoderite, a new hydrous magnesium iron aluminosilicate from Mautia Hill, Tanganyika. *Mineralogical Magazine*, **32**, 282–307.
- MÖLLER, A., APPEL, P., MEZGER, K. & SCHENK, V. 1995. Evidence for a 2 Ga subduction zone: eclogites in the Usagaran belt of Tanzania. *Geology*, **23**, 1067–1070.
- MÖLLER, A., MEZGER, K. & SCHENK, V. 1998. Crustal age domains and the evolution of the continental crust in the Mozambique Belt of Tanzania: a combined Sm–Nd, Rb–Sr and Pb–Pb evidence. *Journal of Petrology*, **39**, 749–783.
- MOSLEY, P. N. 1993. Geological evolution of the late Proterozoic ‘Mozambique Belt’ of Kenya. *Tectonophysics*, **221**, 223–250.
- MUHONGO, S. & LENOIR, J.-L. 1994. Pan-African granulite-facies metamorphism in the Mozambique Belt of Tanzania: U–Pb geochronology. *Journal of the Geological Society of London*, **151**, 343–347.
- PINNA, P., COCHERIE, A., THIEBLEMONT, D., FEYBESSE, J.-L. & LAGNY, P. 1996. Évolution géodynamique du craton Est-Africain et déterminisme géologique. *Chronique de la Recherche Minière*, **525**, 33–43.
- QUENNEL, A. M., MCKINLAY, A. C. M. & AITKEN, W. G. 1956. *Summary of the Geology of Tanganyika. Part 1. Introduction and stratigraphy*. Government Printer, Dar es Salaam.
- SCHLÜTER, T. 1997. *Geology of East Africa*. Borntraeger, Berlin.
- SHACKLETON, R. M. 1986. Precambrian collision tectonics in Africa. In: COWARD, M. P. & RIES, A. C. (eds) *Collision Tectonics*. Geological Society, London, Special Publications, **19**, 329–349.
- SMITH, M. 1994. Stratigraphic and structural constraints on mechanisms of active rifting in the Gregory Rift, Kenya. *Tectonophysics*, **236**, 3–22.
- SMITH, M. & MOSLEY, P. 1993. Crustal heterogeneities and basement influence on the development of the Kenya Rift, East Africa. *Tectonics*, **12**, 591–606.
- SOMMER, H., KRÖNER, A., HAUZENBERGER, C., MUHONGO, S. & WINGATE, T. D. 2003. Metamorphic petrology and zircon geochronology of high-grade rocks from the central Mozambique Belt of Tanzania: crustal recycling of Archaean and Palaeoproterozoic material during the Pan-African orogeny. *Journal of Metamorphic Petrology*, **21**, 915–934.

## Chapter 4

### Geophysical evidence for the structure of the crust and upper mantle of the Tanzania Craton and the Gregory Rift Valley

The past three decades have seen an upsurge in geophysical fieldwork across the East African Rift Valley in Kenya (KRISP: the Kenya Rift International Seismic Project; Prodehl *et al.* 1994; Fuchs *et al.* 1997) and in Ethiopia (Project EAGLE: the Ethiopia Afar Geophysical Lithosphere Experiment; Yirgu *et al.* 2006). In northern Tanzania, in 1994, A. A. Nyblade and co-workers established an array of broadband receivers in northern Tanzania, the Tanzania Broadband Seismic Experiment, TBSE (Nyblade *et al.* 1996) that, together with interpretation of earlier commercially acquired data, have provided new insights into the present-day structure of the Tanzania Craton and the Mozambique belt. Although in many experiments data have also been acquired for the Western Rift, attention will be confined in the following section to observations on the northern Tanzania and southern Kenya sectors of the Gregory Rift Valley.

The interpretation of gravity data alone does not give a unique solution because Bouguer anomalies can reflect lateral changes in: (i) the density of the crust; (ii) the density of the upper mantle; (iii) the depth to the crust/mantle interface, the Moho; or (iv) a combination of these possible variables. Gravity measurements can, when combined with data from seismic experiments and measured rock densities, lead to integrated models for the structure of the crust and upper mantle, but it is relevant to discuss here the results obtained by individual disciplines.

#### Gravity studies

Northern Tanzania lies on the southern margin of a broad, regional, negative Bouguer anomaly around  $350 \pm 50$  km wide and with an amplitude of 800 g.u. relative to a background value of  $-1200$  g.u. (Fig. 4.1). The anomaly, which is highest in Kenya and decreases southwestwards, lies slightly to the west of the present-day rift valley, strikes NNE and is superimposed on a wider 1000 km negative area (Fairhead 1976). This zone is isostatically compensated with respect to adjacent lithosphere, resulting in plateau uplift and high topographic relief. This is particularly apparent where the domal uplift in Kenya coincides with the most negative gravity values. The overall, regional, negative gravity anomaly has been interpreted as reflecting a zone of hot, low-density asthenosphere which has risen due to thinning of the lithosphere.

Along the axis of the rift valley in Kenya is a thin, positive (high-density) anomaly that has been attributed to either the injection of a single 10 km wide dyke (Fairhead 1976), or to a zone of dyke injection, the zone having a density ( $\rho$ : density in  $\text{kg m}^{-3}$ ) of  $2750 \text{ kg m}^{-3}$ , compared with normal basement density of  $2700 \text{ kg m}^{-3}$ ; the depth of the injection zone has been modelled as extending down to 22 km (Swain 1992).

In northern Tanzania, an elongate gravity low is almost continuous to the east and south side of the Sonjo–Eyasi fault (Fig. 4.1) and is interpreted as due to large thicknesses of low-density lavas that ponded against the fault escarpment (Fairhead 1976). Other large gravity lows occur in the Kitingiri Basin, to the west of the Eyasi Basin, and in the Mponde graben, south of Lake Balangida Lelu (Ebinger *et al.* 1997). Less intense, elongate gravity lows occur over the Natron and Manyara basins and at the north end of the Pangani graben. After removal of the regional negative Bouguer anomaly associated with the Kenya Dome, negative anomalies are associated with many of the individual

volcanoes; as an example, the volcanic chain running from Burko to Meru, coincides with low density ( $\rho$   $2100 \text{ kg m}^{-3}$ ) surface volcanics overlying Precambrian basement with  $\rho$   $2670 \text{ kg m}^{-3}$ . Within this, the Meru anomaly can be modelled as being due to a dense volcanic plug, 2 km in diameter with  $\rho$   $2900 \text{ kg m}^{-3}$  extending to within 0.5 km of the surface (Fairhead 1980).

#### Seismic experiments

During the late 1980s and early 1990s, seismic refraction profiles were obtained by the Kenya Rift International Seismic Project (KRISP) to investigate the crustal structure in Kenya, the main results having been reported by Prodehl *et al.* (1994) and Fuchs *et al.* (1997). Their results have been complemented in Tanzania by data from the Tanzania Broadband Seismic Experiment (TBSE) reported by Nyblade *et al.* (1996), Last *et al.* (1997), Ritsema *et al.* (1998) and Brazier *et al.* (2000). The following account draws largely on a review of these results by Nyblade (2002).

KRISP found that, along the rift axis, the depth to the Moho is 35 km in southern Kenya but shallows to 20 km northwards. Away from the rift, crustal thickness is 35–42 km for the Mozambique Belt, and 34–40 km for the Tanzania Craton. The KRISP results for the upper mantle give low Pn velocities of  $7.5\text{--}7.8 \text{ km s}^{-1}$  under the rift axis, compared with  $8.1\text{--}8.3 \text{ km s}^{-1}$  under the unrifted Mozambique Belt and Tanzania Craton. The change from low to high velocities is abrupt and coincides with the main border faults, indicating that thermal modification of the uppermost mantle in Kenya is confined to the rift. However, teleseismic results indicate a broader zone of thermal modification in the deeper parts of the mantle (Green *et al.* 1991; Slack *et al.* 1994).

For northern Tanzania, the TBSE results give depths to Moho of 36–39 km for the Mozambique Belt, and 37–42 km for the Tanzania Craton; mean crustal shear velocities are  $3.74$  and  $3.79 \text{ km s}^{-1}$ , respectively (Last *et al.* 1997). Further, Brazier *et al.* (2000) found Pn velocities of  $8.3\text{--}8.35 \text{ km s}^{-1}$  beneath the Mozambique Belt and  $8.4\text{--}8.45 \text{ km s}^{-1}$  beneath the Tanzania Craton down to depths of *c.* 200 km. Compared with Pn velocities in the range  $8.0\text{--}8.6 \text{ km s}^{-1}$  in the upper mantle beneath other Archaean terranes (e.g. Finland and western Russia, King & Calcagnile 1976; the Canadian shield, Le Fevre & Helmberger 1989; the Kaapvaal craton, Simon *et al.* 2003), these velocities are at the high end of the range, suggesting denser (?colder) mantle.

#### An integrated model and possible constraints

Most early models of the regional Bouguer anomaly lacked collaborative data for seismically determined crustal thicknesses or measured densities for crustal and mantle rocks from the region. Simiyu & Keller (1997) give an integrated seismic/gravity/rock-density model involving measured densities for non-volcanic crustal rocks. Gravity and seismic data suggest that, in southern Kenya away from the rift, the crust, with density  $2850 \text{ kg m}^{-3}$  and a thickness of *c.* 35 km, overlies mantle lithosphere with density  $3260 \text{ kg m}^{-3}$ . For the anomaly within the rift, Simiyu & Keller (1997) proposed low, anomalous mantle densities of  $3170\text{--}3120 \text{ kg m}^{-3}$  which are lower than the  $3220 \text{ kg m}^{-3}$  of

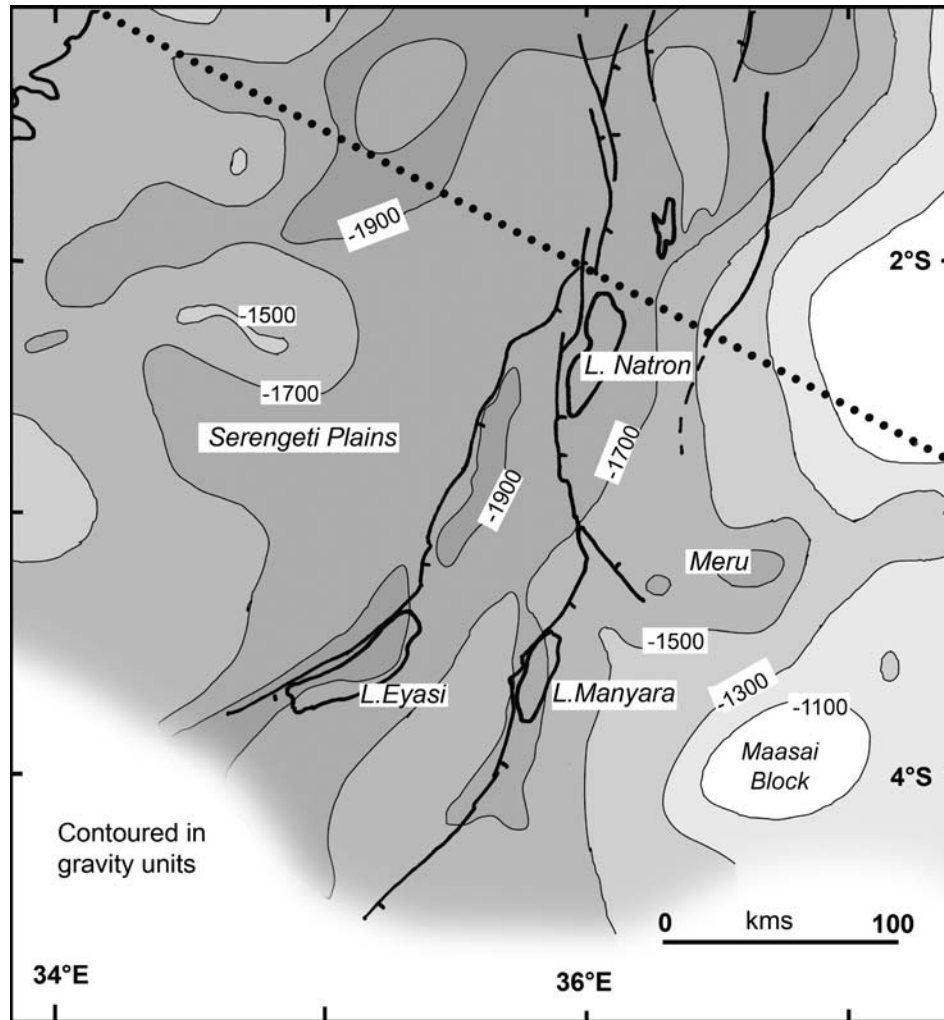


Fig. 4.1 Bouguer anomaly map of northern Tanzania, contoured at 100 g.u. intervals (modified after Fairhead 1976).

Fairhead (1976). A north–south gravity profile from Lake Turkana to southern Tanzania (Simiyu & Keller 1997), shows that anomalous mantle is at a depth of around 35 km (i.e. at the depth of the Moho) from Lake Turkana to Nairobi but, further south, the depth to the anomaly increases rapidly from around 35 km at Lake Magadi to around 90 km south of Lake Manyara, whence it persists southwards. Moreover, this model requires that, south of Lake Magadi, the anomalous mantle underlies a wedge of normal mantle with density  $3200 \text{ kg m}^{-3}$ . This change in mantle structure just south of Lake Magadi coincides with the changes in tectonic style and contemporaneous magmatism noted by Dawson (1992), who also proposed thickening of the crust across a suture between the Tanzania Craton and the mobile belt, coincident with the rift valley.

Geophysical models must be assessed within possible geological and geochemical constraints. First, as discussed above, beneath a thin veneer of Mozambique Belt nappes, the Tanzania Craton most probably extends at depth some distance to the east of its surface contact with the mobile belt; thus the rift structures in southern Kenya and northern Tanzania do not coincide with the craton margin, as assumed in some gravity models (Tesha *et al.* 1997; Simiyu & Keller 1997). Second, an alternative interpretation to the proposed anomalously-light asthenosphere wedge is provided by xenoliths of metasomatized and veined mantle peridotite in the Pello Hill tuff cone just south of Lake Natron (Dawson & Smith 1988). In these lithosphere xenoliths, veins rich in mica and amphibole have metasomatized adjacent peridotite wall rock, and density varies from  $3150 \text{ kg m}^{-3}$  (vein) to  $3280 \text{ kg m}^{-3}$  (metasomatized peridotite) and  $3350 \text{ kg m}^{-3}$  for

unmodified peridotite; mixtures of these three lithosphere densities can give the ‘asthenosphere’ density of  $3220 \text{ kg m}^{-3}$  required by the gravity models. In addition, Lee *et al.* (1999) give density  $3280\text{--}3350 \text{ kg m}^{-3}$  for peridotite xenoliths from Labait. The measured density of  $3350 \text{ kg m}^{-3}$  for both sets of unmodified peridotite is closer to the  $3290 \text{ kg m}^{-3}$  of Fairhead (1976) than to the  $3220 \text{ kg m}^{-3}$  of the Simiyu & Keller (1997) model.

The geochemical signature of basaltic rocks in the Magadi area of Kenya is another factor apparently at variance with some geophysical models. The rock compositions require them to have been derived by variable degrees of melting within the mantle garnet peridotite stability field (Le Roex *et al.* 2001). The inference is that the lavas must have formed within the lithosphere, rather than in the ambient asthenosphere or within a rising mantle plume. Hence, it is concluded that, in contrast to most gravity models, the lithospheric mantle must extend to at least 75 km beneath the axial part of the rift. However, this constraint is compatible with the gravity model of Byrne *et al.* (1997) who, having noted the continuity of two strong reflectors beneath the rift valley, argued that, although the lithosphere in the region has been thinned and stretched, it has not been disrupted or replaced by asthenosphere upwelling to depths as shallow as the Moho.

#### Teleseismic results and inferences

Although the Pn wave data suggest no regional thermal anomalies in the craton and Mozambique Belt for the deeper parts of the

mantle, broadband teleseismic experiments (utilizing major source regions for teleseismic earthquakes in the Hindu Kush/Pamir region and the Fiji/Tonga subduction zone) indicate mantle S-wave velocity variations on the 410 km and 660 km discontinuities in Tanzania (Ritsema *et al.* 1998; Nyblade *et al.* 2000; Nyblade 2002). The S-velocity variations derive from travel-time tomography. Higher-than-average velocities exist beneath the Tanzania Craton, whereas a low-velocity zone, with a vertical extent to depths of >400 km and laterally over a region *c.* 300 km, is found under the Mozambique Belt. As defined by the faster S-velocities, the lithospheric keel beneath the Tanzania Craton extends to a depth of *c.* 250 km (Priestley *et al.* 2006) which is in broad agreement with minimum depths of derivation of 180 km for peridotite xenoliths from the Lashaine, Labait and Igwisi Hills volcanoes (Chapter 8, Dawson 2008). In general, the 410 km and 660 km discontinuities are interpreted as being due to the transitions in (MgFe)SiO<sub>4</sub> (olivine being the dominant upper mantle phase at higher levels) from first the  $\alpha$ - to the  $\beta$ -form and second, at greater pressures, from  $\gamma$ -(MgFe)SiO<sub>4</sub> to perovskite + magnesiowustite. The slopes of equilibrium phase boundaries indicate that, in regions of higher temperature, the 410 km discontinuity should be deflected downwards and the 660 km discontinuity should deflect upwards. In Tanzania, along a 4.5°S profile, where the rifting is in the Tanzania Craton, the 410 km discontinuity is depressed by 30–40 km over a zone 200–400 km wide, whereas the 660 km discontinuity is relatively flat. The topography of these discontinuities indicates that the lower-than-average velocities under this section of the rift result from elevated temperature, with the thinning of the zone between the two discontinuities corresponding to a temperature increase of 200–300 °C. The coincidence of the depressed 410 km discontinuity with the low-velocity zone indicates that the differences in the S-wave velocities between the craton and the Mozambique Belt are due to elevated temperature. Although on the basis of the S-wave parameters the thermal anomaly does not appear to extend beyond depths of 500–600 km, Rayleigh and Love wave tomography indicates the presence of a large thermal anomaly that can be interpreted as the presence of a plume head beneath the craton (Weeraratne *et al.* 2003; Sebai *et al.* 2006). The anomaly becomes diffuse at around 280 km depth suggesting that the Tanzania cratonic keel is a shallower structure than the West Africa, Congo and Kalahari cratons (Sebai *et al.* 2006).

In a review of seismic anisotropy beneath continental interiors in general, Fouch & Rondenay (2006) report evidence for multiple layers of seismic anisotropy in the area around the Tanzania Craton, which they attribute to structural complexity. Around the edges of the craton, shear waves have fast polarization directions that mimic both the shape of the craton and the seismically detected lithospheric keel, whilst beneath the craton itself there is more complexity in splitting behaviour. Lithospheric anisotropy is clearly present, and the complexity in some areas suggests a component of sub-lithospheric anisotropy. Kendall *et al.* (2006) suggested that, at least in Ethiopia, there is a coincidence between zones of seismic anisotropy and melt migration.

## Seismicity

The distribution of earthquake epicentres in East Africa shows that they are largely confined to the present-day rift valleys or their immediate surroundings, but there are more large-magnitude earthquakes in the Western Rift than in the Gregory Rift (Wohlenberg 1969; Kebede & Kulhanek 1991).

Báth (1975) lists 319 earthquakes of magnitude >5 in the region bounded by latitudes 2°N and 12°S and 28°E and 40°E during the period December 1910 to December 1973. In the area covering the Gregory Rift Valley and its surrounding area in

northern Tanzania (2–5°S and 34–38°E), there were 51 earthquakes of magnitude >5, two being of magnitude 6.0 and 5.9 (Fig. 4.2). Another, of magnitude 7.2 on 7 May 1964, caused damage and casualties in the Mbulu area, and resulted in a change in the shape of Lake Babati, though no surface ruptures were observed (Whittingham 1964). Five seismological studies analysing this event (summarized by Nyblade & Langston 1995) largely agreed that the best estimate for the focal depth of this earthquake was  $31 \pm 3$  km and that the focal mechanism indicated strike-slip faulting, unusual in an area of predominantly normal faulting. Many smaller earthquakes testify to continuous movement in the crust beneath the Gregory Rift. Rykounov *et al.* (1972) reported up to 30 events per day during 1968–69, all between magnitude 0.5 and 3.5 and all originating in the crust. Seismicity was relatively high around Ngorongoro, Oldoinyo Lengai and the southern end of Lake Manyara. Nyblade *et al.* (1996) reported some 2000 events in northeastern Tanzania between June 1994 and June 1995; most nucleated in the upper crust but several occurred at lower crustal depths of >15–20 km. The events were mainly concentrated in two swarms, one in the rifted area near the south end of Lake Manyara, and another, shallower swarm, to the south of Kondoia in an area with no significant surface expressions of rifting; the Kondoia area data are interpreted as reflecting southward propagation of the rift. More recent tremors in June and July 2007, with magnitudes varying between 4.0 and 5.94, had their centres in the area immediately to the east of Gelai and Ketumbeine, SE of Lake Natron (U.S.G.S. Earthquakes Hazards Program, Denver).

Foster & Jackson (1998) have analysed data for two Tanzanian earthquakes occurring in May 1990. Both had focal depths of *c.* 5 km and have epicentres just west of the Manyara basin boundary-escarpment, and were most probably related to the rifting. The east-dipping nodal plane of one event (900515a—magnitude 5.6) strikes north–south and is interpreted as the fault plane. The nodal plane of the second event (900515b) is east–west, not parallel to faults exposed at the surface but rather to the Archaean trend. On a continental scale, slip vectors analysed by Foster & Jackson (1998) for 84 major seismic events in eastern Africa broadly agree with a best-fit plate model that predicts an overall east–west extension between the Nubian and Somalia plates (Jestin *et al.* 1994) (see Dawson 2008, fig. 1.1), but the analysis shows that, on a regional scale, the extension is more NE–SW in Kenya and Tanzania, compared with NW–SE in Malawi and southern Africa. This concurs with NE–SW extension derived from analysis of fault directions in northern Tanzania (Dawson 1964; Ring *et al.* 2005).

For earthquakes generated below 20 km, Nyblade & Langston (1995) conclude that, to be brittle enough to deform seismogenically, the lower crust in East Africa must be cooler than predicted by some earlier models. The inference is that this is due to lower abundances of radiogenic elements, and hence the lithology must be of mafic composition, as predicted by Shudovsky *et al.* (1987). Although it is established that seismicity occurs throughout both the lower and upper crust, Foster & Jackson (1998) showed that: (i) parts of the East African crust have a seismogenic thickness of up to 35 km; and (ii) heat flow calculations suggest temperatures of *c.* 325–475 °C at 35 km depth, again requiring that the lower crust must have an anhydrous, mafic bulk composition. The corollary is that significantly more heat production must come from the upper crust, and it also raises the question of the formation of a mafic lower crust. Although magmatic underplating is a possible explanation (as suggested by Shudovsky *et al.* 1987), it is open to question whether this transfer of mafic material was achieved during the Cenozoic magmatism when the underplating might have been more closely restricted to the volcanogenic zones, or whether it was during earlier more widespread magmatism associated with the Proterozoic dyke swarms of the Mbulu Plateau (Nyblade & Langston 1995). Some geological constraint is provided by deep crustal granulite xenoliths in the Lashaine

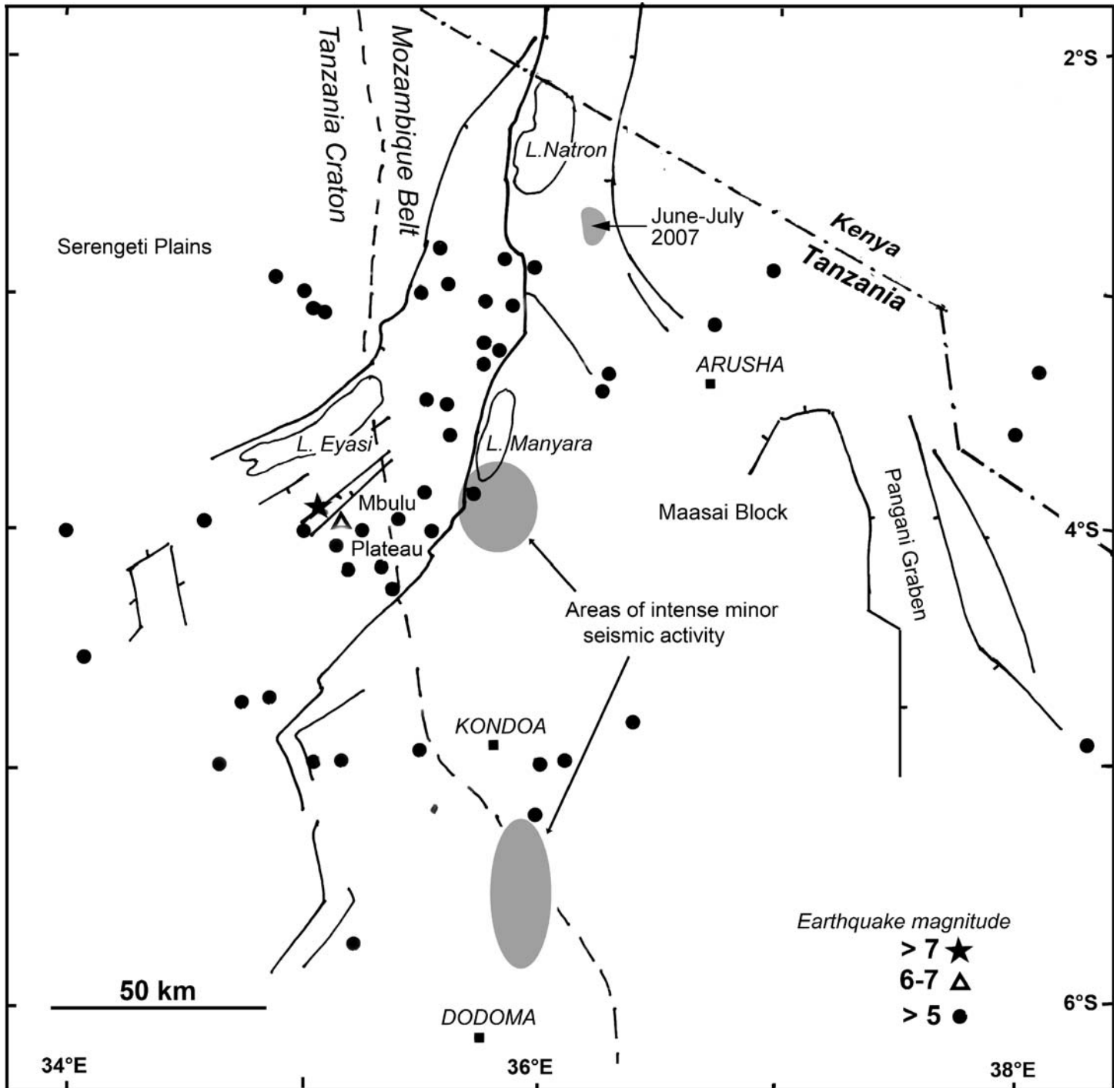


Fig. 4.2 Epicentres of major (>5 magnitude) earthquakes in northern Tanzania between 1951 and 1965 (data from Båth 1975). Locations of the two swarms of minor earthquakes, occurring between 1994 and 1996, are from Nyblade *et al.* (1996).

tuff cone (Dawson 1964; Jones *et al.* 1983) which are of mafic to intermediate bulk composition (Dawson 1977); if they originated by underplating, their age of 2.0 Ga (Cohen *et al.* 1984) would favour a Palaeoproterozoic event.

Nyblade *et al.* (1996) drew attention to the fact that, in contrast to the large number of earthquakes in the Eyasi and Manyara areas, there are few events associated with the Pangani graben. One, in May 1989, in the Pare Mountains on the east side of the Pangani graben, had a source depth of 28 km and the focal mechanism for a normal fault with a WNW–ESE or east–west fault plane, neither nodal plane coinciding with the NNW orientation of the graben boundary faults. Le Gall *et al.* (2004), citing some seismic activity and an alleged small tuff eruption in the Pare

Mountains in 1998, suggested that the Pangani graben is still tectonically active. However, in the context of possible directions for the further propagation of the Gregory Rift (i.e. southwestwards into the Tanzania Craton, southwards along the craton/mobile belt suture, or southeastwards via the Pangani graben to link up with the Davie Fracture zone offshore (Mougenot *et al.* 1986), the relatively sparse seismic activity appears to relegate the Pangani Rift to a minor role.

#### Heat flow

In Kenya, heat flow on the western and eastern flanks of the rift (the latter in the Mozambique Belt) is 40–50 and

40–60 mWm<sup>-2</sup> respectively, whereas on the rift floor values range between 50 and 100 mWm<sup>-2</sup> (Wheildon *et al.* 1994).

In northern Tanzania, the average of eight heat flow measurements on the Tanzania craton is 34 mWm<sup>-2</sup> (range 21–47) (Nyblade *et al.* 1990), and a further measurement on the craton, south of Lake Nyanza, gave a heat flow of 33 mWm<sup>-2</sup> (Nyblade 1997), close to the average. Nyblade *et al.* (1990) give an average value of 47 mWm<sup>-2</sup> (range 39–62) for five measurements in the Mozambique Belt, these values being very similar to those for eastern Kenya. Although sites at Basotu (on the Mbulu Plateau), and Arkatan (near Makuyuni), are close to major faults associated with the most recent rifting, the heat flow recorded at these sites is none the less lower than values of between 51 and 87 mWm<sup>-2</sup> recorded on the Tanzanian offshore islands of Pemba and Zanzibar, which are generally held to be close to the eastern rifted margin of East Africa. Only one measurement of 62 mWm<sup>-2</sup>, at Holili near Moshi, lies within the coastal heat flow range; this figure also distorts the average value for the Mozambique Belt. In detail, the heat flow at some sites in the mobile belt (e.g. Longido 44, Arkatan 39, and Olboloti (near Kondo) 41 mWm<sup>-2</sup>, respectively) is similar to, or even lower than, some sites on the craton (Basotu 46, and Kizaga 47 mWm<sup>-2</sup>). In view of the probability that much of the western margin of the Mozambique Belt is underlain at quite shallow depths by cratonic rocks (Chapter 2), this convergence is perhaps not surprising. The data for world-wide Archaean cratons and adjacent Proterozoic terrains that have not been affected by later tectonism show low heat flow of around 41 mW m<sup>-2</sup> (Nyblade & Pollack 1993), comparable to that for the Tanzania Craton and fold belt. This comparison suggests that the absence of a broad, heat flow anomaly in Tanzania and also in Kenya away from the rift (which is also in agreement with the seismic evidence) indicating that the crust and uppermost mantle have not been subject to significant thermal modification during the Tertiary–Recent tectonism.

Moreover, geothermobarometric estimates of upper mantle garnet lherzolite xenoliths from Igwisi (40 mWm<sup>-2</sup>; Dawson 1994) on the Tanzania Craton and at Lashaine (c. 45 mWm<sup>-2</sup>; Henjes-Kunst & Altherr 1992) lie on a typical cratonic geothermal gradient, whereas xenoliths from the contemporaneous Labait volcano (c. 55 mW m<sup>-2</sup>; Dawson *et al.* 1997), just south of Hanang and also lying on the craton, derive from hotter lithosphere. The Labait data suggest that a thermal anomaly, not yet expressed in surface heat flow, is present in the upper mantle beneath the southerly-propagating tip of the rift (Dawson *et al.* 1997; Dawson 1997).

The ambient thermal state of the sub-Tanzania mantle is exemplified by the peridotite xenoliths from Lashaine that mainly document temperatures of 1045 ± 50 °C at a pressure of 40 ± 4 GPa, plotting along a c. 45 mWm<sup>-2</sup> model geotherm. In contrast, xenoliths from the Chyulu Hills (50 km north of Kilimanjaro and of approximately the same age as Lashaine) plot along a 60 mWm<sup>-2</sup> geotherm (Henjes-Kunst & Altherr 1992). This points to differences in the thermal state of the upper mantle between southern Kenya and northern Tanzania, again underlining the structural and petrological differences between the two areas (Dawson 1992).

## Magnetic data

Aeromagnetic anomaly data give higher resolution images of shallow crustal structure than those provided by gravity data. Recent surveys show, across the Archaean area of the Mbulu Plateau, narrow NE- and NNW trending anomalies or broad east–west anomalies that correspond to dyke swarms and greenstone belts, respectively. In contrast, the Maasai Block is characterized by NE and north–south magnetic lineaments that, together

with a relatively positive Bouguer anomaly, suggest that it is a discrete structural unit (Ebinger *et al.* 1997).

Magnetic signals are masked or subdued in the rift valley basins and on the Serengeti, indicating that the magnetic basement lies deeper. Using the 3D Euler deconvolution technique, which provides a means of estimating the depth and orientation of magnetic sources, Ebinger *et al.* (1997) found that shallow Euler solutions correspond to greenstone belts, lithological contacts and shear zones on the exposed basement, whereas deeper solutions (>3 km) occur over basin gravity highs or areas of steep magnetic gradients. Intermediate solutions (1–3 km) correlate with the subsurface projection of Neogene normal faults bounding the rift valley basins, and also some basement structures. Analysis of clusters of Euler solutions indicate the following: (i) circular clusters of solutions up to 3 km deep correspond to most of the Neogene volcanoes (Lemagrut, Sadiman, Ngorongoro, Loolmalasin, Kerimasi, Oldoinyo Lengai, Essimigor, Tarosero, Meru & Hanang); however, Gelai and Kwaraha have no magnetic sources; (ii) a cluster of solutions coincides with a gravity high that separates the east and west Eyasi basins; depth to the magnetic basement in the east Eyasi basin is <2 km; (iii) the most continuous solution clusters in the Natron–Manyara–Balangida basins are at the subsurface projections of the southern Natron, central Manyara and Mponde graben border faults. Other aligned solutions correlate with the Engaruka Basin fault at its intersection with the Natron boundary fault, and also along faults on the east side of Lake Natron. Euler solution alignments also suggest east–west structures cross-cutting the rift beneath Lake Manyara, these solutions coinciding with a zone of high seismicity (Nyblade *et al.* 1996) and the inferred southern boundary of the late Tertiary tectonic depression (see Chapter 3, Dawson 2008); (iv) in the Eyasi basin, which overlies the mapped interface between the Tanzania Craton and the Mozambique Belt metamorphic rocks, there is no correlation with Euler solutions, which argues against a steep contact between the two units and against differences in magnetic properties between the two tectonic units; and (v) maximum depths for the rift valley basins from Euler deconvolution are: W. Eyasi 3.5 km, E. Eyasi <2 km, Natron 3.3 km. Manyara 2.9 km, Balangida <1 km.

## Magnetotelluric data

Magnetotelluric data collected in southern Kenya, along a west–east profile from Lake Nyanza via Lake Magadi to the Chyulu Hills, show a sharp break from low conductivity on the western flank of the rift valley to high conductivity in the rift valley immediately to the east of the Nguruman escarpment. This is interpreted as due to the high conductivity of sediments within the rift. In the area to the east of Lake Magadi, an eastward change towards lower conductivity is gradual, coinciding with the more gentle step faulting (Simpson *et al.* 1997). The magnetotelluric evidence does not support the hypothesis, derived from seismic data, that melts are present in the upper mantle beneath the rift (Simpson 2000). To date, no magnetotelluric data are available for the rift valley in northern Tanzania.

## Lithosphere strength

Estimates of the effective plate thickness ( $T_e$ ) can place some constraint on models of crust and upper mantle structure derived from gravity studies. Using a mean crustal density of 2800 kg m<sup>-3</sup> and 3200 kg m<sup>-3</sup> for the mantle, Ebinger *et al.* (1997) derived the following  $T_e$ : for craton lithosphere: 64 ± 5 km; for Mozambique mobile belt lithosphere: 30 ± 3 km; for lithosphere beneath the Natron–Manyara–Balangida section of the rift: 23 km; and beneath the Eyasi rift: >30 km. The estimates for the craton and

mobile belt are typical of Precambrian lithosphere, and are in agreement with the gravity and heat flow data for unmodified lithosphere away from the rift, but for perturbed lithosphere beneath the rift itself.

### Crustal extension and its causes

The East African rifting is generally accepted as a reflection of perturbation in the upper mantle and it is a matter for debate whether this perturbation, manifest in the more recent Tanzania magmatism and giving rise to a southerly-propagating lithosphere fracture system, might be linked to easterly movement of the Somalia microplate relative to the larger Nubian Plate or whether the African Plate as a whole is drifting north over a mantle plume, the buoyancy of which may have caused crustal stretching. Domal uplift, a potential cause of lithosphere extension, is small in northern Tanzania compared with that in Kenya and Ethiopia. Contrasting with the generally held view that the underlying cause for the extension arises in the mantle, Coblenz & Sandiford (1994) suggested that large extensional stresses in the elevated regions of Ethiopia and Kenya arise from lithospheric density variations; however, they did not address the fundamental question of why these regions are in fact elevated, an explanation for which is given in the African Superswell model of Nyblade & Robinson (1994).

Implicit in the concept of rifting is the belief that there must be horizontal extension, and various models have arrived at differing estimates. Plate tectonic modelling, based on poles of rotation and angular separation of the Red Sea and the Gulf of Aden gave estimates of crustal separation in Kenya of 30 km (McKenzie *et al.* 1970) whereas Royer *et al.* (2006), again using poles of rotation, proposed that eastward drift of the Somalia Plate has caused  $129 \pm 62$  km extension at the northern tip of the eastern African Rift over the past 11 Ma. Calais *et al.* (2006), using both earthquake slip vector data and GPS (Global Positioning Systems) data and, assuming constant rates of extension since initiation, estimated extension in the Western Rift of 30 km over *c.* 7 Ma and of 8 to 0 km (varying from north to south) in the Eastern Rift over 5 Ma. These estimates compare with 15 km extension for the Western Rift calculated from surface fault geometries (Morley 1988), and 15 km for the Eastern Rift in Kenya (based on a width of 10 km for the width of dense intrusion obtained from interpretation of the gravity high, plus lateral extension of *c.* 5 km due to normal faulting (Baker & Wohlenberg 1971; Fairhead 1976). Although there is disparity in these estimates, there is consensus that extension is greatest at the northern end of the rift valley system and that the extension, at least in the case of Kenya, is too large to be entirely due to domal uplift (Baker & Wohlenberg 1971). Moreover, domal uplift is minimal in northern Tanzania compared with that in Kenya and Ethiopia.

In the specific case of northern Tanzania, inclusions of metasomatized granitic and basic crustal rocks (fenites) in the ejectamenta from the Oldoinyo Lengai volcano (Dawson 1962) show that crustal rocks still underlie the median axis of the rifted area, but the presence of dykes and veins in peridotite blocks from Pello Hill, just south of Lake Natron (Dawson & Smith 1988) provides evidence for brittle-fracture extension at mantle depths.

### Summary of geophysical work

On a regional scale, gravity and seismic studies in northern Tanzania show that, away from the rifted zones, the thickness of the crust of the Tanzania Craton and the Mozambique mobile belt is similar, with depths to Moho of 37–42 and 36–39 km, respectively. Mean crustal shear velocities are 3.74 and 3.79 km s<sup>-1</sup> respectively. The depth to the base of the lithosphere

beneath the Tanzania Craton is 150–200 km and, combined with evidence that the effective elastic strength and heat flow is similar to Precambrian terrains world-wide, the inference is that, unlike the case in Kenya, the lithosphere has not been substantially thinned during Neogene tectono-thermal events. However, there is seismic evidence for an upper mantle thermal anomaly beneath the Tanzania Craton which, if plume-related, is a possible explanation for the isostatic uplift of the East African Plateau (Birt *et al.* 1995); this itself is part of the anomalously high plateau area extending over much of southern Africa, the African Superswell (Nyblade & Robinson 1994), which is attributed to upwelling mantle flow from the core–mantle boundary (Lithgow-Bertelloni & Silver 1998).

In the immediate vicinity of the rift, gravity lows coincide with volcanic centres and thick sediments in half graben basins. Seismicity is most pronounced in connection with faults cutting the Tanzania Craton, and minor earthquake swarms and centres to the south of the present rift structure indicate southwards propagation of the rift. Earthquake depths suggest that their epicentres are located in both the lower and the upper crust, and that the lower crust must be of anhydrous mafic composition. Some exceptionally deep events originate in the mantle which, by inference, must be atypically cold and brittle. Although heat flow measurements along the rift are not exceptionally high, there are numerous hot springs in the Natron, Manyara and Eyasi basins, and in the area to the south of the main rifting.

### References

- BAKER, B. H. & WOHLBERG, J. 1971. Structure and evolution of the Kenya Rift Valley. *Nature*, **229**, 538–542.
- BÅTH, M. 1975. Seismicity of the Tanzania region. *Tectonophysics*, **27**, 358–379.
- BIRT, C. S., MAGUIRE, P. H. K., KHAN, M. A. & THYBO, H. 1995. A combined interpretation of the KRISP 94 seismic and gravity data; Evidence for a mantle plume beneath the East African plateau. *EOS, Transactions of the American Geophysical Union* (abstracts), **76**, F 607–608.
- BRAZIER, N. A., NYBLADE, A. A., LANGSTON, C. A. & OWENS, T. J. 2000. Pn wave velocities beneath the Tanzania craton and adjacent mobile belts, East Africa. *Geophysical Research Letters*, **27**, 2365–2368.
- BYRNE, G. F., JACOB, A. W. B., MECHE, J. & DINDI, E. 1997. Seismic structure of the upper mantle beneath the southern Kenya Rift from wide-angle data. *Tectonophysics*, **238**, 243–260.
- CALAIS, E., EBINGER, C., HARTNADY, C. & NOCQUET, J. M. 2006. Kinematics of the East African Rift from GPS and earthquake slip vector data. In: YIRGU, G., EBINGER, C. Y. & MAGUIRE, K. H. (eds) *The Afar Volcanic Province within the East African Rift System*. Geological Society, London, Special Publications, **259**, 9–22.
- COBLENTZ, D. D. & SANDIFORD, M. 1994. Tectonic stresses in the African plate: Constraints on the ambient lithospheric stress state. *Geology*, **22**, 831–834.
- COHEN, R. S., O'NIONS, R. K. & DAWSON, J. B. 1984. Isotope geochemistry of xenoliths from East Africa: implications for the development of mantle reservoirs and their interaction. *Earth and Planetary Science Letters*, **68**, 209–220.
- DAWSON, J. B. 1962. The geology of Oldoinyo Lengai. *Bulletin Volcanologique*, **24**, 349–387.
- DAWSON, J. B. 1964. *Monduli*. Tanzania Geological Survey, Quarter Degree Sheet **54**.
- DAWSON, J. B. 1977. Sub-cratonic and upper mantle models based on xenolith suites in kimberlite and nephelinitic diatremes. *Journal of the Geological Society, London*, **134**, 173–184.
- DAWSON, J. B. 1992. Neogene tectonics and volcanicity in the North Tanzania sector of the Gregory Rift Valley: contrasts with the Kenya sector. *Tectonophysics*, **204**, 81–92.
- DAWSON, J. B. 1994. Quaternary kimberlitic volcanism on the Tanzania craton. *Contributions to Mineralogy and Petrology*, **116**, 473–485.

- DAWSON, J. B. 1997. A thermal anomaly in the upper mantle beneath the southerly-propagating tip of the East African rift valley: evidence from mantle xenoliths in northern Tanzania. *In: JACOB, A. W. B., DELVAUX, D. & KHAN, M. A. (eds) Lithospheric Structure, Evolution and Sedimentation in Continental Rifts*. Communications of the Dublin Institute for Advanced Studies, Ser.D., Geophysical Bulletin, **48**, 29–31.
- DAWSON, J. B. 2008. *The Gregory Rift Valley and Neogene–Recent Volcanoes of Northern Tanzania*. Geological Society, London, Memoirs, **33**.
- DAWSON, J. B. & SMITH, J. V. 1988. Veined and metasomatized peridotites from Pello Hill, Tanzania: evidence for anomalously light mantle beneath the Tanzania sector of the eastern Rift Valley. *Contributions to Mineralogy and Petrology*, **100**, 510–527.
- DAWSON, J. B., JAMES, D., PASLICK, C. & HALLIDAY, A. M. 1997. Ultrabasic potassic low-volume magmatism and continental rifting in north–central Tanzania: association with enhanced heat flow. *Russian Geology and Geophysics*, **38**, 69–81.
- EBINGER, C., POUJOM DJOMANI, Y., MBEDE, E., FOSTER, A. & DAWSON, J. B. 1997. Rifting Archaean lithosphere: the Eyasi–Manyara–Natron rifts, East Africa. *Journal of the Geological Society, London*, **154**, 947–960.
- FAIRHEAD, J. D. 1976. The structure of the lithosphere beneath the eastern rift, East Africa, deduced from gravity studies. *Tectonophysics*, **30**, 269–298.
- FAIRHEAD, J. D. 1980. The structure of the cross-cutting volcanic chain of northern Tanzania and its relation to the East African rift system. *Tectonophysics*, **65**, 193–208.
- FOSTER, A. & JACKSON, J. J. 1998. Source parameters of large African earthquakes: implications for crustal rheology and regional kinematics. *Geophysical Journal International*, **134**, 422–448.
- FOUCH, M. J. & RONDENAY, S. 2006. Seismic anisotropy beneath stable continental interiors. *Physics of the Earth and Planetary Interiors*, **158**, 292–320.
- FUCHS, K., ALTHERR, R., MULLER, S. & PRODEHL, C. (eds) 1997. Structure and dynamic processes in the lithosphere of the Afro–Arabian rift system. *Tectonophysics*, **278**, 1–352.
- GREEN, W. V., ACHAUER, U. & MEYER, R. P. 1991. A three-dimensional seismic image of the crust and upper mantle beneath the Kenya rift. *Nature*, **354**, 199–203.
- HENJES-KUNST, F. & ALTHERR, R. 1992. Metamorphic petrology of xenoliths from Kenya and northern Tanzania and implications for geotherms and lithospheric structures. *Journal of Petrology*, **33**, 1125–1156.
- JESTIN, F., HUCHON, P. & GAULIER, J. M. 1994. The Somali plate and the East African rift system: present day kinematics. *Geophysical Journal International*, **116**, 637–654.
- JONES, A. P., SMITH, J. V., DAWSON, J. B. & HANSEN, E. C. 1983. Metamorphism, partial melting and K-metasomatism of garnet–scapolite–kyanite granulite xenoliths from Lashaine, Tanzania. *Journal of Geology*, **91**, 143–165.
- KEBEDE, F. & KULHANEK, O. 1991. Recent seismicity of the East African Rift system and its implications. *Physics of the Earth and Planetary Interiors*, **68**, 259–273.
- KENDALL, J. M., PILIDOU, S., KEIR, D., BASTOW, I. D., STUART, G. W. & AYELE, A. 2006. Mantle upwellings, melt migration and the rifting of Africa: insights from seismic anisotropy. *In: YIRGU, G., EBINGER, C. Y. & MAGUIRE, K. H. (eds) The Afar Volcanic Province within the East African Rift System*. Geological Society, London, Special Publications, **259**, 55–72.
- KING, D. W. & CALCAGNILE, G. 1976. P-wave velocities in the upper mantle beneath Fennoscandia and western Russia. *Journal of Geophysical Research of the Royal Astronomical Society*, **46**, 407–432.
- LAST, R. J., NYBLADE, A. A., LANGSTON, C. A. & OWENS, T. J. 1997. Crustal structure of the East African Plateau from receiver functions and Rayleigh wave phase velocities. *Journal of Geophysical Research*, **102**, 24469–24483.
- LE GALL, B., GERNIGON, L. ET AL. 2004. Neogene–Holocene rift propagation in central Tanzania: morphostructural and aeromagnetic evidence from the Kilombero area. *Geological Society of America, Bulletin*, **83**, 490–510.
- LE ROEX, A. P., SPÁTH, A. & ZARTMAN, R. E. 2001. Lithospheric thickness beneath the southern Kenya Rift: implications from basalt geochemistry. *Contributions to Mineralogy and Petrology*, **142**, 89–106.
- LEE, C. T. & RUDNICK, R. L. 1999. Compositionally-stratified cratonic lithosphere: petrology and geochemistry of peridotite xenoliths from the Labait volcano, Tanzania. *In: GURNEY, J. J., GURNEY, J. L., PASCOE, M. D. & RICHARDSON, S. H. (eds) Proceedings of the 7th International Kimberlite Conference, Cape Town, 1998*, Vol. 2, 503–521.
- LE FEVRE, L. V. & HELMBERGER, D. V. 1989. Upper mantle P-velocity of the Canadian Shield. *Journal of Geophysical Research*, **94**, 17749–17765.
- LITHGOW-BERTELLONI, C. & SILVER, P. S. 1998. Dynamic topography, plate driving forces and the African superswell. *Nature*, **395**, 269–272.
- MCKENZIE, D. O., DAVIES, D. & MOLNAR, P. 1970. Plate tectonics of the Red Sea and East Africa. *Nature*, **226**, 243–248.
- MORLEY, C. K. 1988. Variable extension in Lake Tanganyika. *Tectonics*, **7**, 785–801.
- MOUGENOT, D., RECQ, M., VIRLOGEUX, P. & LEPVRIER, C. 1986. Seaward extension of the East African rift. *Nature*, **321**, 599–603.
- NYBLADE, A. A. 1997. Heat flow across the East African Plateau. *Geophysical Research Letters*, **24**, 2083–2086.
- NYBLADE, A. A. 2002. Crust and upper mantle structure in East Africa: implications for the origin of Cenozoic rifting and volcanism and the formation of magmatic rifted margins. *In: MENZIES, M., KLEMPERER, S. L., EBINGER, C. J. & BAKER, J. (eds) Volcanic Rifted Margins*. Geological Society of America, Special Papers, **362**, 15–26.
- NYBLADE, A. A. & LANGSTON, C. A. 1995. East African earthquakes below 20 km and their implications. *Geophysical Journal International*, **121**, 49–62.
- NYBLADE, A. A. & POLLACK, H. N. 1993. A global analysis of heat flow from Precambrian terrains: implications for the thermal structure of Archean and Proterozoic lithosphere. *Journal of Geophysical Research*, **98**, 12207–12218.
- NYBLADE, A. A. & ROBINSON, S. W. 1994. The African Superswell. *Geophysical Research Letters*, **21**, 765–768.
- NYBLADE, A. A., POLLACK, H. N., JONES, D. L., PODMORE, F. & MUSHAYANDEBVU, M. 1990. Terrestrial heat-flow in east and southern Africa. *Journal of Geophysical Research*, **95**, 17371–17384.
- NYBLADE, A. A., BURT, C., LANGSTON, C. A., OWENS, T. J. & LAST, R. J. 1996. Seismic experiment reveals rifting of craton in Tanzania. *EOS, Transactions of the American Geophysical Union*, **77**, 519–521.
- NYBLADE, A. A., OWENS, T. J., GURROLA, H., RITSEMA, J. & LANGSTON, C. A. 2000. Seismic evidence for a deep upper mantle anomaly beneath East Africa. *Geology*, **28**, 599–602.
- PRIESTLEY, K., MCKENZIE, D. O. & DEBAYLE, E. 2006. The state of the upper mantle beneath southern Africa. *Tectonophysics*, **416**, 101–112.
- PRODEHL, C., KELLER, G. R. & KHAN, M. A. 1994. Crustal and upper mantle structure of the Kenya Rift. *Tectonophysics*, **236**, 1–483.
- RING, U., SCHWARTZ, H. L., BROMAGE, T. G. & SANAANE, C. 2005. Kinematic and sedimentological evolution of the Manyara Rift in northern Tanzania, East Africa. *Geological Magazine*, **142**, 355–368.
- RITSEMA, J., NYBLADE, A. A., OWENS, T. J. & LANGSTON, C. A. 1998. Upper mantle seismic velocity structure beneath Tanzania, East Africa: implications for the stability of cratonic lithosphere. *Journal of Geophysical Research*, **103**, 21210–21213.
- ROYER, J. Y., GORDON, R. G. & HORNER-JOHNSON, B. C. 2006. Motion of Nubia relative to Antarctica since 11 Ma: Implications for the Nubia–Somalia, Pacific–North America and Indi–Eurasia motion. *Geology*, **34**, 501–504.
- RYKOUNOV, L. N., SEDOV, V. V., SAVRINA, L. A. & BOURMIN, V. J. 1972. Study of micro-earthquakes in the rift zones of East Africa. *Tectonophysics*, **15**, 123–130.
- SEBAI, A., STUTZMAN, E., MONTAGNER, J. P., SICILIA, D. & BEUCLER, E. 2006. Anisotropic structure of the African upper

- mantle from Rayleigh and Love wave tomography. *Physics of the Earth and Planetary Interiors*, **155**, 48–62.
- SHUDOFKY, G. N., CLOETINGH, S., STEIN, S. & WORREL, R. 1987. Unusually deep earthquakes in East Africa constraints on the thermo-mechanical structure of a continental rift system. *Geophysical Research Letters*, **14**, 741–744.
- SIMIYU, S. M. & KELLER, G. R. 1997. An integrated analysis of lithospheric structure across the East African plateau based on gravity anomalies and recent seismic studies. *Tectonophysics*, **278**, 291–313.
- SIMON, R. E., WRIGHT, C., KWADIBA, M. T. O. & KGASWANE, E. M. 2003. Mantle structure and composition to 800-km depth beneath southern Africa and surrounding oceans from broadband body waves. *Lithos*, **71**, 353–367.
- SIMPSON, F. 2000. A three-dimensional electromagnetic model of the southern Kenya Rift: Departure from two dimensionality as a possible consequence of a rotating stress field. *Journal of Geophysical Research*, **105**, 19 321–19 334.
- SIMPSON, F., HAAK, V., KHAN, M. A., SAKKAS, V. & MEJU, M. 1997. The KRISP magnetotelluric survey of 1995: first results. *Tectonophysics*, **278**, 261–271.
- SLACK, P. D. & DAVIES, P. M. & the KRISP Teleseismic Working Group 1994. Attenuation and velocity of P-waves in the mantle beneath the East African rift, Kenya. *Tectonophysics*, **236**, 331–358.
- SWAIN, C. J. 1992. The Kenya rift axial high: a re-interpretation. *Tectonophysics*, **204**, 59–70.
- TESHA, A. L., NYBLADE, A. A., KELLER, R. A. & DOSER, D. I. 1997. Rift localization in suture-thickened crust: evidence from Bouguer gravity anomalies in north-eastern Tanzania, East Africa. *Tectonophysics*, **278**, 315–328.
- WEERARATNE, D. S., FORSYTH, D. W., FISCHER, K. M. & NYBLADE, A. A. 2003. Evidence for an upper mantle plume beneath the Tanzanian craton from Rayleigh wave tomography. *Journal of Geophysical Research*, **108** (B9), 2427, doi: 10.1029/2002JB002273.
- WHEILDON, J., MORGAN, P., WILLIAMSON, K. H., EVANS, T. R. & SWANBERG, C. A. 1994. Heat flow in the Kenya rift zone. *Tectonophysics*, **236**, 131–149.
- WHITTINGHAM, J. K. 1964. Report on the earth tremor of 7 May 1964. *Geological Survey of Tanzania, Unpublished Report JKW/ 34*.
- WOHLENBERG, G. J. 1969. Some remarks on the seismicity of East Africa between 4°N–12°S and 23°E–40°E. *Tectonophysics*, **8**, 562–577.
- YIRGU, G., EBINGER, C. Y. & MAGUIRE, K. H. (eds) 2006. *The Afar Volcanic Province within the East African Rift System*. Geological Society, London, Special Publications, **259**.

## Chapter 5

### Tectonic development of the rift structures

During the Neogene–Recent there have been two major phases of crustal deformation in northern Tanzania. Each deformation event has been followed by a major pulse of volcanism arising from instabilities in the mantle.

The chronology of the development of the rift faulting has been made possible by the dating of volcanic rocks that erupted before and after particular episodes of faulting. Appendix 1 (Dawson 2008) lists the current dating results for the volcanic rocks. However, most of the dates were obtained many years ago by the K–Ar method and more refined stratigraphy will doubtless arise from Ar/Ar dating in the future.

#### Early rift structure

Whereas in Kenya, there is evidence for an elongate pre-rift depression in which the earliest volcanics were deposited (Baker 1986), there is at present only sparse evidence for the presence of pre-volcanic sedimentary basins in northern Tanzania. The limited evidence comes from an exposure at the base of the rift escarpment at the north end of Lake Manyara, where a sedimentary formation, termed the Manyara Group, comprises a boulder conglomerate unconformably overlying metamorphic basement rocks. The conglomerate itself is overlain by siltstones, sandstones, waterlain tuffs and ashes with an intercalated basalt that has been dated at  $4.86 \pm 0.24$  Ma. This is taken to indicate that, in this area, limited basin subsidence (? related to faulting) and basaltic volcanism had begun by around 4.9 Ma (Foster 1997; Foster *et al.* 1997). This shallow-basin formation follows the oldest volcanism in the area, the eruption of Essimngor lying 25 km to the east which has rocks dated between 8.1 and 3.2 Ma. In some respects this is analogous to western Kenya, where Miocene basin formation was preceded by the eruption of highly explosive volcanoes such as Mt Elgon and Napak (Baker *et al.* 1972).

The main evidence for the earliest phase of Tertiary crustal deformation in East Africa derives from studies of the shape and altitude of a widespread erosion surface of sub-Miocene age (Saggerson & Baker 1965; Baker *et al.* 1972). In Kenya this warped land surface rises to an elliptical dome >1500 m above sea level (a.s.l.) in the Mau and Aberdare Ranges (Fig. 5.1). This symmetrical dome is bisected by the narrow graben of the present-day rift valley. In northern Tanzania, due to the effect of the Tanzania Craton, the shape of the deformed land surface is less regular. The surface is at 1500 m a.s.l. around Longido and decreases in elevation both westwards towards the rift valley and southeastwards towards Kilimanjaro and the coast. On the Maasai Block, it is around 1200 m but decreases in height westward towards the rift valley, and also northwards and eastwards. The eastern margin of the Maasai Block is still at around 900 m where it forms the western side of the Pangani graben and the northerly drop, together with decrease in height from Longido, have combined to form the ‘Kilimanjaro Depression’ (Downie & Wilkinson 1972). The surface on the Pare Mountains, to the east of the Pangani graben, is at >1800 m above the steep, west-facing escarpment and decreases gently eastwards towards the Umba Plains (McConnell 1972). At the eastern margin of the Mbulu plateau, the surface is at >1800 m but it decreases in height northwestwards to 1200 m at Lake Eyasi. On the upthrow-side of the Eyasi scarp it is again at >1800 m, as further north in the Loliondo area; this section of the surface then slopes

decreasingly in height westwards across the Serengeti Plains towards Lake Nyanza.

#### The northern Tanzania late Tertiary depression

The earliest faulting in East Africa follows the deformation of the sub-Miocene land-surface. In Kenya, following a period of downwarping, the first effect was a southerly extension of a pre-existing fault (the Turkwell fault) to create an asymmetric graben, faulted on its western side, running from Lake Turkana to Lake Eyasi (Baker *et al.* 1972). Later faulting created the trough-shaped graben around 60 km wide that cuts across the updomed land surface in Kenya. In northern Tanzania, due to the effects of the Tanzania Craton, there is a wider area of faulting, termed the North Tanzania Divergence (Baker *et al.* 1972). Dawson (1992) has proposed that the earliest post-Miocene faulting gave rise to a wide, tectonic depression, bounded by faults or by downwarps of the sub-Miocene land-surface (Fig. 5.2). The depression is bounded to the south by the Maasai (or Kondo) Block around which the area of tectonic disturbance bifurcates continuing to the SW as the NE-trending Eyasi half graben, and to the SE as the NNW-trending Pangani graben. The structure of the north-eastern margin of the depression is a downwarp with minor faulting, that has given rise to a series of benches, the highest coinciding with the unfaulted but tilted peneplain. The breaks between the benches are old, eroded fault escarpments first noted by Uhlig (1907*a, b*) and remarked upon by Willis (1936). The structure of the northern margin is speculative (?faulted or downwarped) as the structure is obscured by the later Meru and Kilimanjaro volcanics.

The north-western margin, cutting across the eastern edge of the Serengeti Plains, comprises the Sonjo–Eyasi fault, that runs NE to join up with a major fault that runs *en échelon* with the Nguruman fault north of the present-day Lake Natron (Dawson 2008, fig. 3.1); the Nguruman fault had formed by 7 Ma, creating a half graben (Baker 1986). An elongate gravity low, that is almost continuous to the east and south side of the Sonjo–Eyasi fault (Dawson 2008, fig. 4.1), has been interpreted as due to large thicknesses of low-density lavas that ponded along the foot of the escarpment (Fairhead 1976). The southwestern segment of this system is the fault giving rise to the escarpment on the north side of the Eyasi half graben that loses height westwards until it fades out in the Wembere basin; some minor NW-throwing opposing faults are present at the NE end of the Eyasi basin. To the SE of the Eyasi half graben is the Yaida graben that consists of two opposing, almost parallel faults between 8 and 5 km apart. This lies where the sub-Miocene land surface is descending from the Mbulu Plateau into the Eyasi half graben, and results from fracturing of the hinge of the Eyasi downwarp.

The continuity and age of the Sonjo–Eyasi fault, as proposed by Baker *et al.* (1972), Dawson (1992) and Manega (1993), have been questioned, so it is necessary to consider the arguments and counter-arguments. Foster *et al.* (1997) propose that the age of the Eyasi section of the fault is possibly the same as that of the main rift escarpment faulting at around 1.2 Ma. To support this, they cite: (1) the steep, immature morphology of the Eyasi escarpment; and (2) that the fault cuts 3.1 Ma ankaramites from Lemagrut (and hence must be younger than 3.1 Ma). Counter-arguments are that: (a) the northeastern end of the Eyasi half graben is buried beneath the Crater Highland volcanoes which predate 1.2 Ma; (b) the upper part of the Eyasi escarpment is strongly eroded (Pickering 1961),

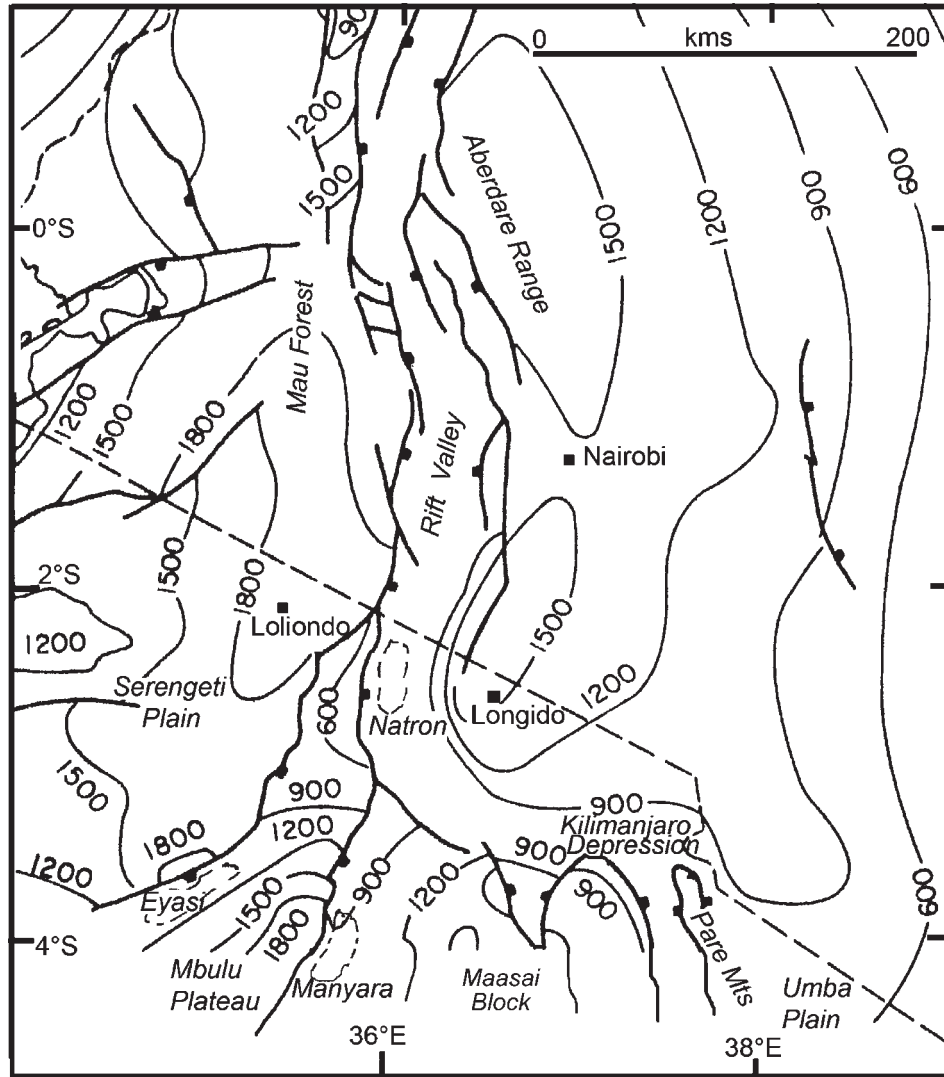


Fig. 5.1. Isobases of the sub-Miocene erosion surface in southern Kenya and northern Tanzania (modified after Baker *et al.* 1972).

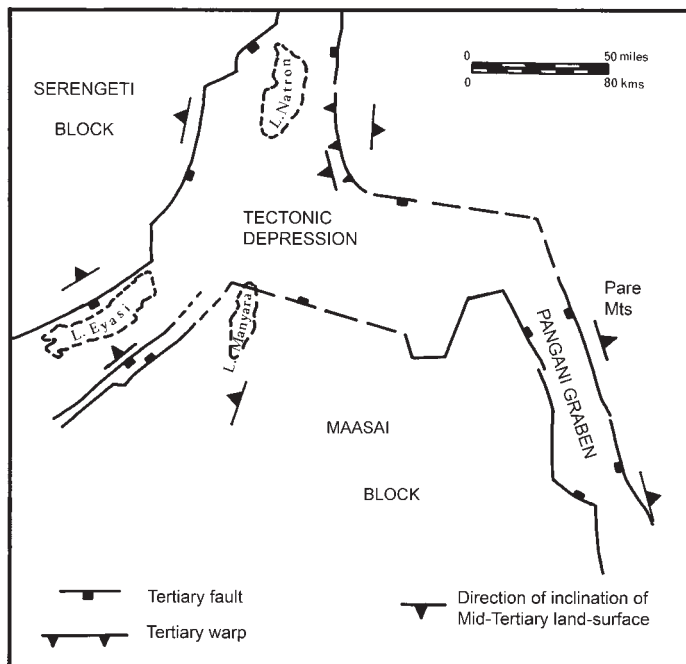


Fig. 5.2. The late Tertiary northern Tanzania tectonic depression. The positions of some of the large present-day lakes are shown for reference.

indicating more than one movement on the fault; and (c) the faulting that cuts the Lemagrut volcanics is of much less magnitude than the Eyasi fault. The collective field evidence points to at least two phases of movement on the fault (a possibility not discussed by Foster *et al.* 1997), with post-3.1 Ma reactivation along the Lemagrut section. Foster *et al.* (1997) also questioned the continuity of the Sonjo-Eyasi fault, claiming that the fault could not be traced south of the Oldoinyo Ogot Hills, and that such a fault would have impeded deposition of easterly-derived volcanoclastic sediments into the Olduvai Basin. The Tanganyika Geological Survey Quarter Degree Sheets 38 (Oldoinyo Ogot; Pickering 1958) and 52 (Endulen; Pickering 1964) show a line of minor escarpments (in this area not unreasonably interpreted as resulting from faults) continuing from the south side of the Oldoinyo Ogot Hills along the west side of the Olbalbal depression, to join up with faults cutting across the Lemagrut volcano; these eventually link up with the Eyasi fault. The Ogot Hills are a group of inselbergs rising above the flat peneplain of the Serengeti, and the apparent relatively minor displacement of the fault in the area immediately south of the Ogot Hills can be interpreted as due to topographic unevenness of the basement land-surface across which the fault cuts. Regarding the second point, some upper flows from the Crater Highlands volcanoes have ages of up to 3.8 Ma (Appendix 1, Dawson 2008). Volcanic rocks deeper in the sequences are currently unexposed, but must have been extruded before 3.8 Ma. The depositional history in the Olduvai Basin only begins at *c.* 2 Ma (Hay 1976; Walter *et al.*

1991) and thus there would have been ample time (a minimum of 1.8 Ma) for a fault-bounded depression to the east of the Olduvai Basin to have been infilled by volcanic flows and sediments from the Crater Highlands before the boundary scarp was overstepped. An analogy can be made with the Sonjo section of the fault further north, where lavas from Oldoinyo Sambu have infilled the depression to the east of the fault, and eventually overstepped onto the foot wall (Dundas & Awadalla, unpublished).

The southern margin of the post-Miocene depression can be inferred from both geophysical and field evidence. First, the direction of the contours on the regional Bouguer anomaly changes abruptly from a NNE direction in the area to the south of Lake Manyara and on the Masai Block, to east–west in the area to the east and north of Lake Manyara. The contours then trend eastwards on the south side of the chain of volcanoes running from Essimngor to Meru (see Dawson 2008, fig. 4.1); for greater detail see Fairhead (1976). Second, the geological evidence is that, at the western end of the inferred depression, the present-day *c.* 350 m high rift scarp on the western side of Lake Manyara exposes a major, abrupt break in lithology between Neogene basalts to the north of the Msasa River, and Precambrian gneisses to the south. This break is best explained by a fault with a downthrow of at least 350 m with a northerly component, although its strike is not apparent. East of the Manyara Basin, at a latitude of *c.* 3°35'S, discontinuous outcrops show successions of Neogene basalt to the north in faulted contact with Maasai Block gneisses to the south, the faults trending east–west or WNW–ESE (Jones 1967). The faults run parallel to the contours on the regional Bouguer anomaly map. To the south of this line of faults, discontinuous thin lava flows overlie the undulose gneiss terrain. Further east, in the Shambarai area (to the south of Arusha), Guest (1953), quoting data from the Tanganyika Water Development Department, reported that, just to the north of basement outcrops, a borehole (B.H. 6/48) 'penetrated lava to a depth of 1065 feet ... (which) ... estimates a downthrow of the basement of between, 1100 to 1300 feet'. Finally, the eastern end is well documented where the northern edge of the Maasai Block is downfaulted into the Kilimanjaro depression (Downie & Wilkinson 1972; Grainger 1968). Hence, despite burial by Pleistocene sediments in the Lake Manyara basin, and being obscured further east by overstepping Pleistocene lava flows, it is possible to infer a major pre-Pleistocene fault with a dominantly east–west or WNW–ESE trend along a latitude of approximately 3°35'S. North of this line, the basalt terrain is extensively faulted, indicative of a low-strength, brittle lithology; in the gneiss terrain to the south, the comparatively few faults are long (30–80 km). In the area between the well documented eastern end and the inferred western end, the inferred east–west-trending fault has suffered minor disruption by Pleistocene north–south faults of the Oljoro graben, SW of Arusha.

### **Eruption of the first set of volcanoes: the Older Extrusives**

Volcanoes erupted within the late Tertiary tectonic depression, infilling the depression until, at various points around the margins of the depression, lavas overstepped the boundary faults (Fig. 5.3). These volcanoes are described more fully in Chapter 6 (Dawson 2008). Sedimentary successions accumulated at various points within the depression.

### **Plio-Pleistocene faulting**

#### *Late Pliocene faulting*

Minor faulting in the Upper Pliocene–Lower Pleistocene formed the Lembolos graben (Fig. 5.4), and affected the trachyte–phonolite volcanics on the Tarosero volcano, where faults cutting lavas on the lower slopes, dated at *c.* 2.2 Ma, are buried by later 1.98 Ma lavas in the summit area (MacIntyre *et al.* 1974).

In the Lake Natron area, the Peninj Group sediments were deposited in the shallow, faulted depression of proto-Lake Natron (Dundas & Awadalla, unpublished). Feldspar in the basal tuff of the group has given an age of 1.7 Ma (Manega 1993) which is the minimum age for the pre-sedimentation faulting.

An erosion bevel on the main rift escarpment on the west side of Lake Manyara, together with a corresponding nick-point on the Endabash River, has been interpreted as due to early, relatively minor faulting on the main Manyara Basin boundary fault (Orridge 1965). A distinct erosion bevel at the top of the otherwise sharp fault escarpment between Lake Manyara and Engaruka (Dawson personal observation) may also be due to pre-1.2 Ma faulting.

#### *Major Pleistocene faulting*

A major episode of faulting at *c.* 1.0 ± 0.2 Ma has given rise to what is geomorphologically the present-day rift valley. The age of this faulting, based on dates obtained on the highest lavas in faulted lava sequences and also on extrusions up the main fault in the sector north of Lake Manyara (see Appendix 1, Dawson 2008), is between 1.2 and 0.9 Ma (MacIntyre *et al.* 1974; Foster *et al.* 1997). This age equates with the major faulting episode in the Kirikiti–Lengitoto area in Kenya in the period 1.3 to 0.9 Ma (Fairhead *et al.* 1972). This faulting has been superimposed on the volcanic and sedimentary successions previously extruded and deposited within, and around the margins of, the late Tertiary tectonic depression (Fig. 5.5). A reversal in the drainage in the Olduvai Basin took place at this time (*c.* 1.15 Ma; Hay 1976).

The main manifestation of this major faulting event is the high east-facing escarpment that runs from Lake Natron southwards to Lake Balangida Lelu (Fig. 5.6). In the north, the faulting exposes the volcanic rocks forming the eastern flanks of Oldoinyo Sambu and the volcanoes of the Crater Highlands and, further south, exposes basement rocks of the Mozambique fold belt and the Tanzania Craton.

Between the Kenya border and Lake Manyara the trend of the fault escarpment is generally north–south, but south of Manyara, it swings gradually westwards until at Lake Balangida the trend is NW–SE (Fig. 3.1). It forms an asymmetric half graben, having no major, eastern equivalent (unlike the rift valley in Kenya to the north), and the eastern margin of the present-day rift depression is formed by a series of small faults and downwarps that are the southern continuation of the Ngong–Turoka fault in Kenya.

A significant feature of the faulting was a disruption of older drainage directions, and the formation of a series of enclosed sedimentation basins at the foot of the main escarpment, these being, from north to south, the Natron, Engaruka, Manyara, Balangida and Balangida Lelu basins; of these, the Natron, Balangida and Balangida Lelu basins have small opposed faults facing the main escarpment. Before the onset of the Pleistocene drying-out event the Natron Basin most probably linked up with the Magadi Basin in Kenya and, prior to the eruption of Oldoinyo Lengai and Kerimasi, which form a topographic high, the Natron and Engaruka basins may have been continuous. To the west of the main rift, the asymmetric older Eyasi Basin lies at the foot of the SE-facing Eyasi escarpment.

#### *The Natron Basin boundary fault system*

The boundary fault trends approximately north–south and, between the Kenya border and the south end of Lake Natron, the system is segmented (Fig. 5.7). The main Sambu segment extends from the border to the Peninj delta (where there are some east–west offsets), followed to the south by the Binini,

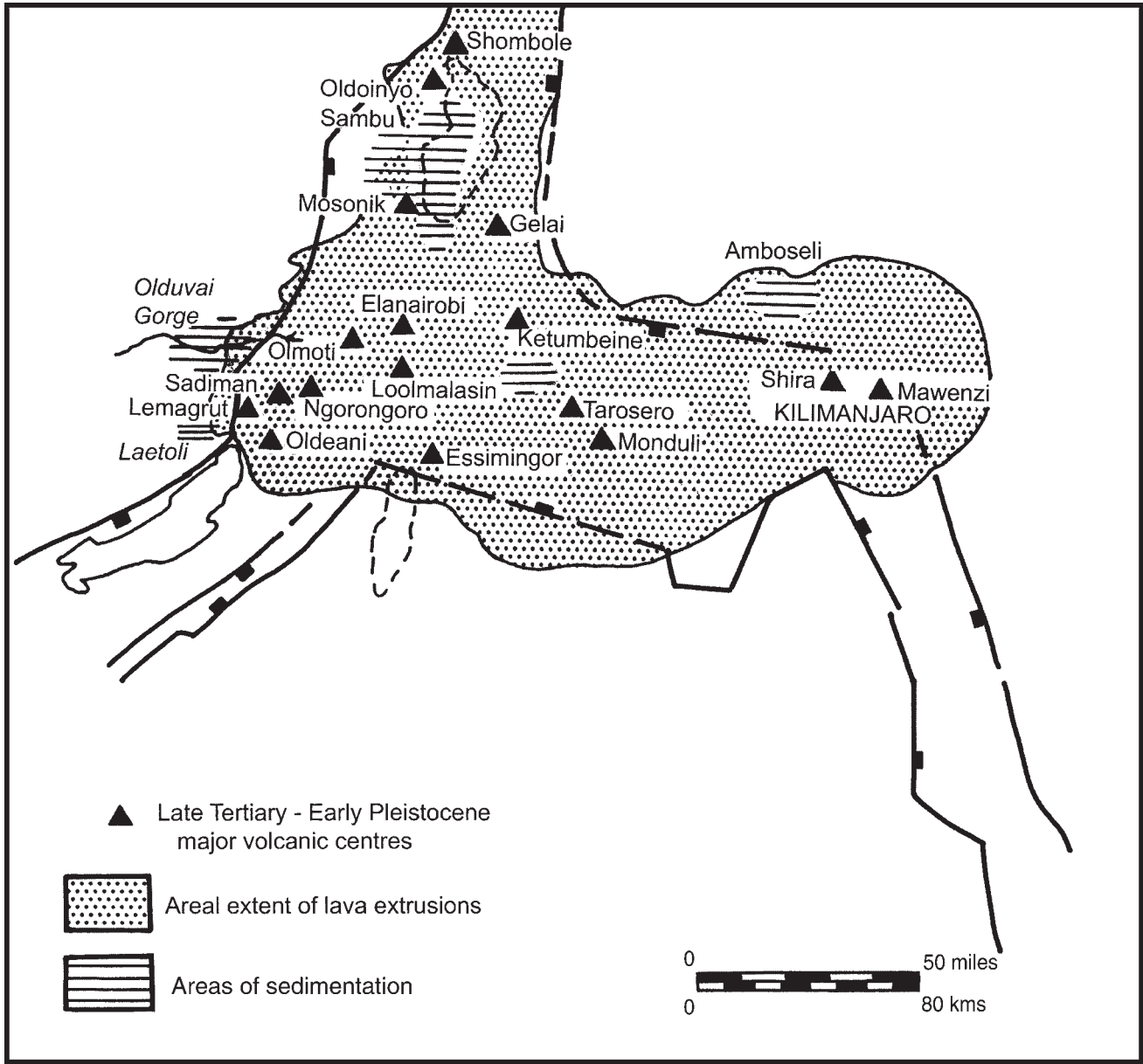


Fig. 5.3. Distribution of the Older Extrusive volcanic centres, and areas of Plio-Pleistocene sedimentation.



Fig. 5.4. The Matunginini fault escarpment, looking across the Lembolos graben from the SW (see Fig. 5.8). It forms the eastern boundary of the graben and exposes 250 m of horizontal basalts, the youngest of which is dated at 2.0 Ma.

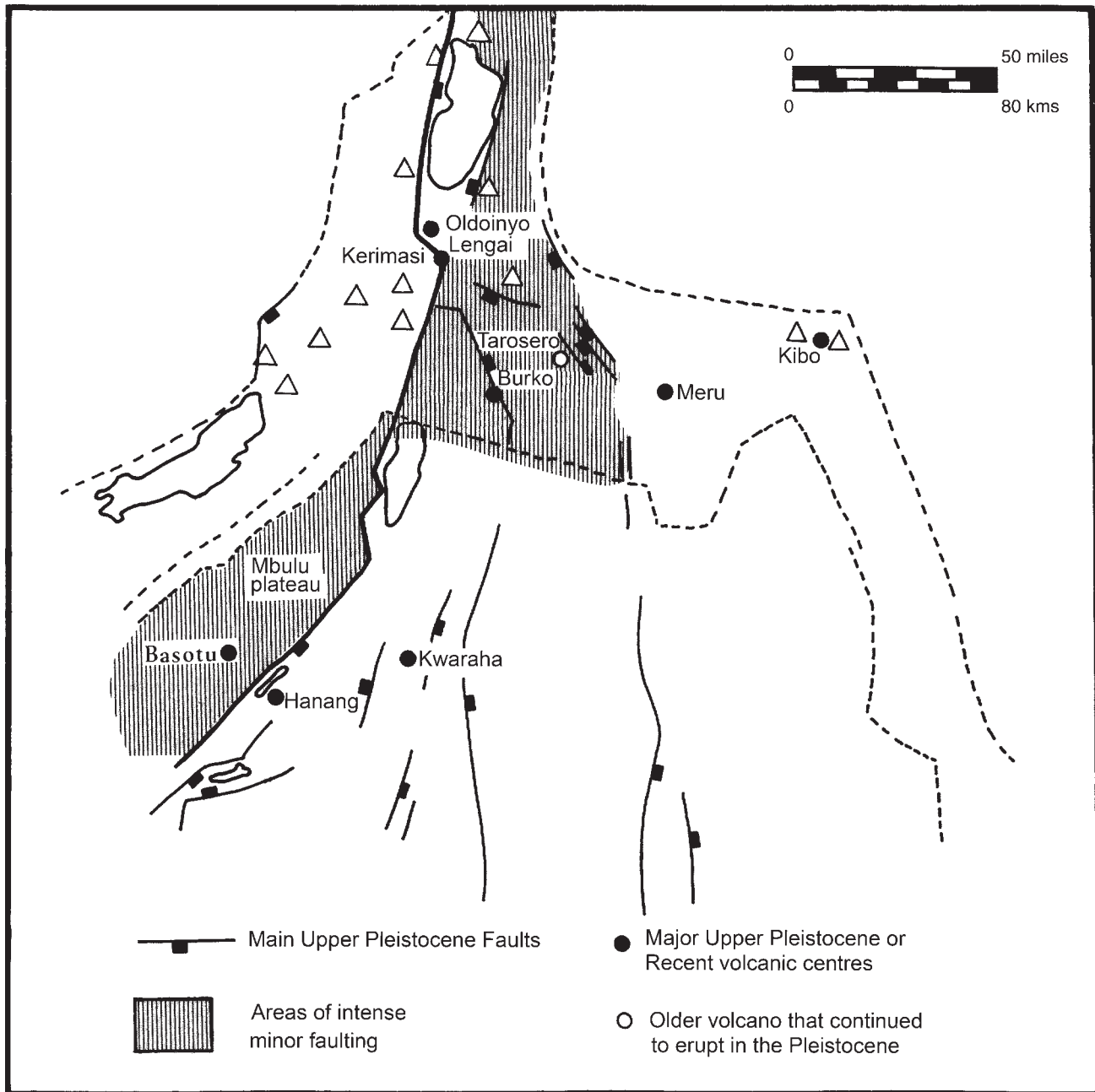


Fig. 5.5. Distribution of the main Upper Pleistocene faults and Younger Extrusive volcanoes.

Ngongolo, Mto wa Mbagai, and Sanjan fault segments. The height of the escarpment varies from 1200 m at Oldoinyo Sambu to zero where the Engaruka–Loliondo dirt road crosses the line of the escarpment, whence the height increases again southwards. The Sanjan Fault is the most westerly of these segments, and between it and the other segments is the Moinik valley, in which are extensive outcrops of sediments deposited in the proto-Lake Natron (see above). South of Lake Natron, the fault, with an escarpment 600 m high, runs north–south to a point just south of Oldoinyo Lengai, where a small SE-trending sector occurs before the fault is blanketed beneath the Kerimasi volcano. The fault reappears running north–south of Kerimasi, having been offset some 8 km to the east relative to its line between Lake Natron and Oldoinyo Lengai. It is not possible to ascertain whether this offset results from a continuity of the short visible SE-trending sector beneath Kerimasi, or whether the fault is segmented at this point. The escarpment height at Engaruka is *c.* 550 m.

South of Engaruka, the throw of the main rift fault is taken up by two fault systems: the main boundary fault of the Manyara Basin that continues southwards, and a diverging, lesser SE-trending fault, the Engaruka Basin fault, that forms the southwestern boundary of the Engaruka Basin (Fig. 5.8). The triangular block of terrain between these two faults, the Engaruka Block, is back-tilted southwestwards towards the Manyara boundary fault. This block itself, which is broken by many minor faults, decreases in height from its highest elevation (1220 m a.s.l.) just south of Engaruka southwards towards Lake Manyara (945 m a.s.l.).

Further to the SE, the Engaruka Basin fault is replaced by several closely spaced faults that form a SE-trending zone of parallel, elongate horsts and grabens (Fig. 5.8). Several faults on the Engaruka Block trend in this same dominant direction, and similar faults occur prominently in the area between and south of the Essimigor and Burko volcanoes. Also in this area, numerous small faults trending north–south or NNW–ESE combine with the SE-trending faults to form grabens, horsts and fault blocks,



**Fig. 5.6.** The Manyara Basin boundary fault escarpment, north of Lake Manyara (see Fig. 5.8). The escarpment exposes the eastern flanks of some Crater Highland volcanoes, and varies in height from *c.* 250 m at Manyara to 600 m at its northern end near Engaruka.

the last being tilted to the west or SW. The NNW–SSE trend is also apparent south of Meru in faults forming the Oljoro graben. Lavas in the wall of this graben have been dated at 2.49–2.3 Ma (Wilkinson *et al.* 1986).

The pronounced NW–SE fault direction is also found in the area NW of Meru, where SE-trending faulting cuts both the lower northern slopes of the Tarosero volcano, and is also the trend of the Tarosero, Matunginini and Matisiwi faults that form the Lembolos graben. The ages of these faults are *c.* 2.0 Ma, based on faulted basalt and trachyte (2.4–2.04) and fault-blanketing phonolite (1.98 Ma) on Tarosero, and also on a date of 2.0 Ma on the highest faulted basalt flow on the Matunginini escarpment (MacIntyre *et al.* 1974). Further, the Lembolos graben is buried beneath extrusive rocks from Meru, the oldest lavas of which are 1.5 Ma.

A minor fault direction in this area is WNW–ESE or east–west, shown by faults cutting across the southern slopes of Ketumbeine, by faults forming the southern boundary of the Ardai Basin, and a possible fault on the south side of the Monduli volcano. This trend is that of the inferred southern boundary of the late Tertiary tectonic depression.

Analyses of the fault directions in the Engaruka–Arusha area indicate that the dominant direction is NW–SE, with a minor one at NNW–SSE, indicating maximum extension was *c.* N50°E (Dawson 1964; Ring *et al.* 2005). This compares with a dominant NNE–WSW direction with maximum extension at *c.* N100°E in the Magadi area (Atmaoui & Hollnack 2003) which again emphasizes structural differences between southern Kenya and northern Tanzania.

In the area between Engaruka and Lake Manyara, and to the north and south of the main road between Makuyuni and Arusha, many of these relatively minor faults are the eruption sites of small flows and scoria cones (see Fig. 5.8). Most of these minor faults (e.g. Yayai and Elunata) have escarpments of <100 m.

#### *Manyara Basin boundary fault system*

South of Engaruka, the Manyara Basin boundary fault has a SSW trend, though with minor indentations caused by small north–south sectors near Kitete and Mto wa Mbu (Fig. 5.8). The escarpment exposes layered lava flows derived from the Crater Highland

volcanoes to the west, and continuity of these horizontal flows suggests no segmentation of the fault as far south as Mto wa Mbu, where a thin ramp between two sectors enables the Makuyuni–Ngorongoro road to ascend the escarpment. To the north of Lake Manyara itself, a minor basin at Erumkoko is the result of back-tilting of a small fault block westwards towards the main boundary fault.

Just south of Mto wa Mbu, at the gorge of the Msasa River, the lithology exposed in the entire escarpment changes abruptly from Neogene lavas to the north to basement gneisses further south. The highly variable height of the escarpment south from this point, the undulating topography of the gneiss terrain of the footwall, and the absence of horizontal formations, makes it difficult to ascertain whether the boundary fault is segmented but south of Lake Manyara the trace of the fault becomes saw-toothed due to SW-oriented sections being increasingly interspersed with north- or NW-trending sections. This pattern continues to around 4°15'S, where the SW-trend becomes dominant and continues well to the SW past Hanang (Dawson 2008, fig. 3.1). This change of pattern coincides with exposure in the fault escarpment of Archaean rocks, that also occupy the floor of the depression (Selby & Thomas 1966). This area, comprising the Balangida and Balangida Lelu basins, is still bounded on its northwestern side by the continuation of the Manyara boundary fault, but a variation here is that small, opposing, SW-trending faults form the southeastern margin of both basins.

Along its length, the height of this continuous boundary fault escarpment decreases from 500–600 m at Lake Manyara to no more than 200 m at Balangida Lelu. SW of Lake Balangida Lelu the fault escarpments fade out in the relatively subdued topography (escarpments of up to 100 m) of the north–south-trending Mponde graben (Fozzard 1958). Further south, minor scarps and an area of seismicity are interpreted to be the expressions of incipient faulting (Nyblade *et al.* 1996; Le Gall *et al.* 2004).

#### *The Mbulu Plateau and the Maasai Block*

The plateau to the west of the Manyara and Balangida basins is cut by numerous SW-trending faults mainly showing only minor topographic expression. The age of most cannot be determined, though some at the northeastern end of the plateau cut lavas from the

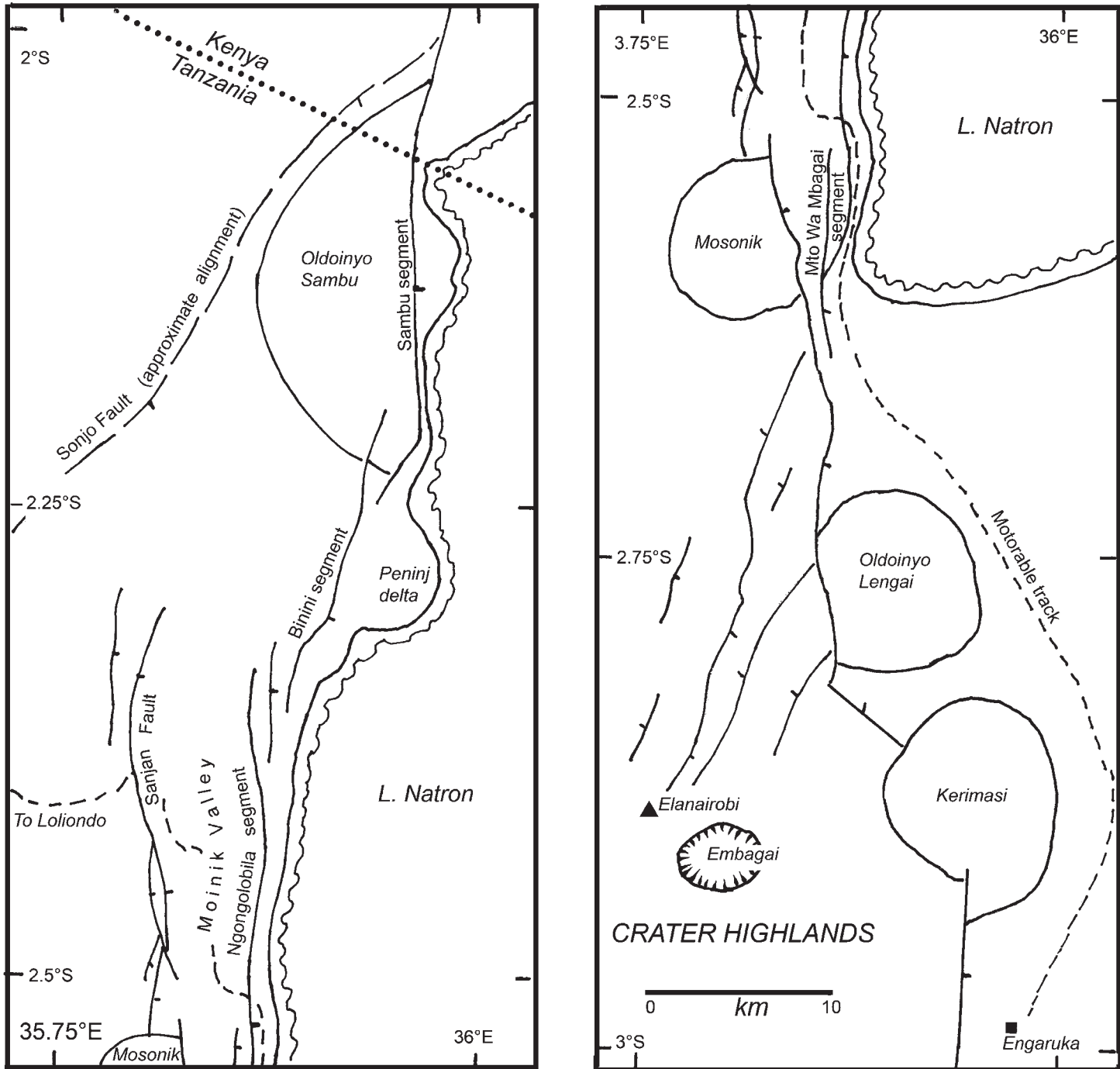


Fig. 5.7. The Natron Basin boundary fault system, showing segmentation particularly in the area immediately west of Lake Natron.

Crater Highland volcanoes and could thus be attributed to the post-1.2 Ma faulting episode, or to reactivation at that time.

To the east of the Manyara Basin, the Maasai Block (Fig 5.2) is cut by several north-south or NNW-SSE faults; the more westerly are the boundaries of large west-dipping fault blocks.

#### *Faulting of the volcanoes in the Crater Highlands*

Between Lake Natron and Oldoinyo Lengai, several faults branch away from the Natron boundary fault to run SSW or SW across the northern slopes of Elanairobi (Fig. 5.7). They run parallel to, or are a continuation of, faults running in the same direction across the Crater Highlands, including one cutting across the northwestern rim of the Ngorongoro crater (Dawson 2008, fig. 7.5). Foster (1997) also identified a linear SW-trending

feature along the western side of the Crater Highlands, based on a marked contrast in the drainage to the east and west of the feature. He proposed that this is the surface expression of a major west-dipping fault which he termed the Angata Salei Fault. Minor faults, related to reactivation of the Eyasi section of the Sonjo-Eyasi fault, cut north-south across Lemagrut and the western flank of Oldeani. Other north-south faults cut the eastern slopes of Oldeani, then link up with minor NE-trending faults on the south side of Lake Eyasi. Many minor faults on the lower slopes of the Ngorongoro and Olmoti volcanoes were formed at the time of the deepening of the Olbalbal depression in the late Pleistocene (Hay 1976). Numerous small faults occur on the footwall of the Manyara Basin boundary fault in the area between Mto wa Mbu and Karatu (Dawson 2008, fig. 7.5). These are exposed in deforested areas, and their apparent absence in contiguous areas to the north may be due to obscuring by forest.



### *The Eyasi half graben faulting*

As noted earlier, faulting occurred in the late Pliocene to form the half graben. Following the extrusion of the Crater Highlands volcanoes that filled the NE end of the graben, reactivation caused minor faults that cross Lemagrut and Oldeani to link up with faults in the Olbalbal graben. The reactivated part of the fault escarpment above Lake Eyasi created by this faulting is sharp and *c.* 500 m high. The maximum height on the escarpment is around 900 m (Kent 1941).

### *The Kibangaini grid-faulted area*

The area between the northern flanks of the Gelai volcano and the Kenya border, around Lake Natron (Dawson 2008, fig. 3.1) is characterized by a style of faulting unlike that described above. The term 'grid-faulting' was introduced by Gregory (1921) to describe 'that condition by which the valley floor is divided into narrow strips which rise to different elevations and are bounded by near vertical walls' with the vertical displacement of the strips being no more than 20–30 m. The term was first used to describe this style of faulting in the Magadi area of Kenya, of which the Kibangaini area is a southerly continuation. An inference of the sharpness of the fault scarps, combined with their small throw, is that they must be of Recent age.

### **Upper Pleistocene–Recent faulting**

In addition to the Recent faulting in the Kibangaini area, the pyroclastics of Kerimasi were faulted at *c.* 0.37 Ma prior to the initial eruption of Oldoinyo Lengai, the youngest major centre (MacIntyre *et al.* 1974).

### **Faulting: broader issues**

#### *Single-stage or continuous faulting?*

Whereas the overall geochronology of the lava sequences indicates a major faulting episode at 1.0–1.2 Ma, it is open to question whether the whole throw on the faults results from a single event or whether the overall displacement is the accumulation of a number of smaller movements. Hay (1976) suggested that episodic faulting may be more apparent than real, citing the sediments of the Olduvai Gorge basin that have been faulted several times between 2.0 and 0.4 Ma. Some support for sporadic, cumulative faulting is also found in the southern part of the Kenya Rift just north of the Tanzanian border, where Isaac (1968) documented faulting during much of the deposition of the mid-Pleistocene Ologesaile Formation. Recent dating of trachytes in the Magadi area also showed that faulting on the floor of the rift valley took place sporadically between 2.25 and 0.36 Ma (Dunningham 2005).

#### *Style of faulting*

There is no evidence for reverse faults. Petroleum industry seismic traverses have shown that listric faults form the boundaries to many half grabens in the Western Rift and in many of the rift-valley basins in Kenya (references in Morley 1999a).

No similar traverses have been made across the main Tanzania half graben. Although intuitively it might be expected that listric faults also bound the Tanzania basins, Birt *et al.* (1997) found no evidence in southernmost Kenya for the good reflections that should arise from major listric faults. In the case of minor faults on the western side of the Engaruka Basin (Fig. 5.8), one at least is pivotal, suggesting that it is vertical.

### *Southern extension of the Gregory Rift?*

Until recently, there was only limited evidence that Neogene–Recent rifting was propagating further south than the Mponde graben (Dawson 2008, fig. 3.1). There are no Pleistocene volcanoes south of Hanang, but the swarms of minor earthquakes in the Kondoa area are mentioned above. In the Kilimatinde area (Dawson 2008, fig. 2.1), linking with the Mponde graben, are escarpments which Fozzard (1958) links to the Pleistocene faulting further north, noting that they follow shear- and shatter-zones in the basement migmatites.

Further south in Tanzania are older half graben structures, mainly bounded by NE–SW-trending faults and infilled with Karoo (Upper Carboniferous and Triassic) sediments. These have been recognized for many years (e.g. Haughton 1963) and in the Kilombero area (Dawson 2008, fig. 2.1), where uplifted basement blocks are associated with major half grabens, Whittingham (1963) documented fault movements in late Neogene times. More recently, Le Gall *et al.* (2004) proposed that, in agreement with seismicity associated with the faults, there is Neogene–Recent extensional overprinting of the older, Karoo-age fault zone along both rift-parallel and transverse faults in the Kilombero area. They further suggested that the Kilombero rift zone connects northward to the Manyara rift zone by way of an active transverse fault zone which cuts NW across the Tanzania Craton. Further south, they envisaged the rifting continuing via the Karoo-age Ruhuhu graben to the Tanganyika–Rukwa–Malawi rift, thereby linking the eastern and western arms of the overall East African rift system.

### *Relationship of the rift valley faults to structural elements in the underlying basement rocks*

There is a long-standing tenet that the rift valleys in central and eastern Africa follow the trends of the Pan-African orogens that wrap round the ancient cratons. First proposed by Holmes (1951), and followed by others such as Dixey (1956) and McConnell (1972), this thesis is broadly correct for the western branch of the African rift system that follows the Kibaride and Ubendian fold belts round the western margin of the Tanzania Craton, and round the Zambian Craton (Clifford 1970; Morley 1999b). There is also some linearity in the Kenya sector of the Mozambique fold belt, though many departures from the general north–south trend have been noted (Baker *et al.* 1972). However, nowhere in the East African rift system is there such a departure from the overall trend of the fold belts as in the North Tanzania Divergence (Dawson 2008, fig. 1.1). Dawson (1992) and Nyblade & Brazier (2002) have proposed a key role for the rigid Tanzania Craton, against which the eastern branch of the rift has stalled.

The most critical analysis of the structure of the Tanzania Craton and Mozambique Belt in northern Tanzania (Hepworth 1972) recognizes different structural trends that are possibly relevant to the interpretation of the Tertiary–Recent rift fractures.

On the craton, Hepworth (1972) recognizes:

1. A strong, straight NE–SW trend which is followed by the present day Eyasi half graben, and thus termed the Eyasi trend. The underlying trend is that of a prominent Archaean dyke-swarm around 400 km long and 300 km wide, dated at 2.2 to 2.6 Ga (Vail 1970). Although Halls *et al.* (1987) claimed that this dyke swarm terminates at the mapped craton-Mozambique fold belt boundary, aeromagnetic data show faint NE–SW magnetic lineaments across (?beneath) the Mozambique Belt (Ebinger *et al.* 1997); the trend is unrelated to the Mozambique Belt.
2. A straight NW–SE trend, developed as shear-belts (the Bubu cataclases) in the Archaean granite basement. This is the same trend as the Kondoa (see below) and may have been

superimposed on the craton during a later orogenesis in the Mozambique Belt.

3. A WNW–ESE trend characteristic of the Dodoman Archaean fold belt. Unlike the two other trends, it is gently curving and is perpetuated by trends in the Mozambique Belt.

Within the Mozambique fold belt are:

4. The most prominent trend, referred to as the Kondoan trend which is WNW–ESE or NW–SE, and oblique to the trend of the orogenic belt as a whole. This is the same direction as two important late-Proterozoic (635–550 Ma) mylonite and cataclastic shear zones, the Aswa–Nandi–Loita and Nyangea–Athi–Ikutha shear zones, that cut across the Mozambique Belt in central Kenya (Smith & Mosley 1993). On a continental scale, this trend coincides with the northern termination of the western rift valley (Morley 1999b) and, more locally, is the trend of the northwestern arm of Lake Magadi.
5. A less prominent NE–SW or NNE–SSW trend, termed the Parangan, which is dominant on the Mbulu Plateau and on the northern part of the Maasai Block; this is the same direction as the Eyasi trend.
6. Large, closed folds to the west of the Pare Mountains, perhaps due to the combined effects of NE–SW and NW–SE folds.
7. A NNW–SSE trend now picked out by the boundary faults of the Pangani graben.

In the case of the faults forming the late Tertiary depression, the Eyasi Basin and Yaida graben, the faults parallel the cratonic Eyasi trend. Some sectors of the Sonjo Fault, particularly those to NW of Lake Natron, follow the Eyasi trend but are interspersed with sectors running north–south, a direction also followed by the boundary fault continuing southwards from Kenya on the eastern side of the depression. The postulated southern boundary fault of the depression trends east–west. It lies along the northern edge of the Maasai Block which, on geophysical grounds, appears to be a distinct structural terrane.

In the case of the Pleistocene faults, most on the Mbulu Plateau, and those cutting across the Crater Highlands follow the Eyasi trend. The north–south sectors of the Natron and Manyara boundary fault systems follow the same trend as some cutting the Maasai Block which are a continuum of the main north–south trend in Kenya. As noted earlier, the group of faults in the Engaruka–Manyara–Arusha area are dominantly NW–SE. In Kenya, where this trend has also been recognized in induction transfer functions during the KRISP-94 magnetotelluric survey (Simpson *et al.* 1997), it has been linked to the continental-scale Proterozoic Aswa shear zone (Smith & Mosley 1993). In Tanzania this is the Bubu and Kondoan trend, although to suggest such an influence on the Pleistocene faults is at odds with the absence of such an influence on the orientation of the earlier late-Pliocene faulting. The orientation of these faults (Dawson 1964; Ring *et al.* 2005) is consistent with NE–SW extension rather than to basement structure control.

The linearity of the chain of volcanoes that trends west–east across the Tanzania volcanic province from Essimngor to Meru and Kilimanjaro has given rise to speculation as to their being either due a transform fault running normal to the rift trend (Fairhead 1980) or, in the case of the more easterly volcanoes of both Kenya and Tanzania (the so-called ‘off-rift’ volcanoes), to eruption up listric faults (Bosworth 1987). Analysis of the distribution of the northern Tanzania volcanoes, particularly with regard to distribution during each of the two main episodes of eruption during the evolution of the North Tanzania Divergence (Dawson 1992), does not support these suggestions. Some groups of volcanoes undoubtedly have a well-defined linearity, the best being the volcanoes of the Crater Highlands that follow the NE Eyasi trend, as do the explosion craters and maars of Basotu on the Mbulu Plateau. Another is the NW–SE line

formed by the coeval Gelai–Kitumbeine–Tarosero–Monduli group, parallel to the downwarped eastern margin of the late Tertiary depression. Alternative explanations to Fairhead’s (1980) Burko–Monduli–Meru Line are that Burko erupted along the line of the Engaruka Basin fault swarm, that Meru formed close to the junction of the Lembolos and Oljoro grabens, and that Kilimanjaro (an extension of the line) grew at the intersection of the Pangani graben with the late Tertiary depression.

To summarize, whereas there is evidence that the faulting and chains of volcanoes to the west of the main Natron–Manyara–Balangida boundary fault reflect the dominant Eyasi trend in the Archaean basement, to the east of the main fault the linkage of both faulting and volcanicity to structures in the basement is more tenuous. In this context, the deeper structure of the Maasai Block, that has the geophysical properties of a small discrete terrane (Ebinger *et al.* 1997), is still unknown.

## References

- ATMAOUI, N. & HOLLNACK, D. 2003. Neotectonics and extension direction of the southern Kenya Rift, Lake Magadi area. *Tectonophysics*, **364**, 71–83.
- BAKER, B. H. 1986. Tectonics and volcanism in the southern Kenya Rift Valley and its influence on rift sedimentation. In: FROSTICK, L. E., RENAULT, R. W., REID, I. & TIERCELIN, J. J. (eds) *Sedimentation in the African Rifts*. Geological Society, London, Special Publications, **25**, 45–57.
- BAKER, B. H., MOHR, P. A. & WILLIAMS, L. A. J. 1972. *Geology of the Eastern Rift System of Africa*. Geological Society of America, Special Publications, **36**.
- BOSWORTH, W. 1987. Off-axis volcanism in the Gregory rift, east Africa: Implications for models of continental rifting. *Geology*, **15**, 397–400.
- BIRT, C. S., MAGUIRE, P. K. H., KHAN, M. A., THYBO, H., KELLER, G. R. & PATEL, J. 1997. The influence on pre-existing structures on the evolution of the southern Kenya Rift Valley – evidence from seismic and gravity studies. *Tectonophysics*, **278**, 211–242.
- CLIFFORD, T. N. 1970. The structural framework of Africa. In: CLIFFORD, T. N. & GASS, I. G. (eds) *African magmatism and tectonics*. Oliver & Boyd, Edinburgh, 1–26.
- DAWSON, J. B. 1964. *Monduli*. Tanzania Geological Survey. Quarter Degree Sheet **54**.
- DAWSON, J. B. 1992. Neogene tectonics and volcanicity in the North Tanzania sector of the Gregory Rift Valley: contrasts with the Kenya sector. *Tectonophysics*, **204**, 81–92.
- DAWSON, J. B. 2008. *The Gregory Rift Valley and Neogene–Recent Volcanoes of Northern Tanzania*. Geological Society, London, Memoirs, **33**.
- DIXEY, F. 1956. The East African Rift System. *Colonial Geology and Mineral Resources, Supplement Series, Bulletin Supplement 1*. H M Stationery Office, London.
- DOWNIE, C. & WILKINSON, P. 1972. *The Geology of Kilimanjaro*. University of Sheffield, Sheffield.
- DUNDAS, D. L. & AWADALLA, G. W. (unpublished). *Loliondo*. Unpublished report and map of Quarter Degree Sheet 16 and 27. Tanzania Geological Survey. Mapped 1966.
- DUNNINGHAM, J. P. 2005. *Long-term Evolution of Normal Fault Systems: Controls on the Development and Evolution of Extensional Structures in the Neotectonic Kenyan Rift, East Africa*. PhD thesis, University of Edinburgh.
- EBINGER, C., POUJOM DJOMANI, Y., MBEDE, E., FOSTER, A. & DAWSON, J. B. 1997. Rifting Archaean lithosphere: the Eyasi–Manyara–Natron rifts, East Africa. *Journal of the Geological Society, London*, **154**, 947–60.
- EVANS, A. L., FAIRHEAD, J. D. & MITCHELL, J. G. 1971. Potassium–argon ages from the volcanic province of northern Tanzania. *Nature*, **229**, 19–20.
- FAIRHEAD, J. D. 1976. The structure of the lithosphere beneath the eastern rift, East Africa, deduced from gravity studies. *Tectonophysics*, **30**, 269–98.

- FAIRHEAD, J. D. 1980. The structure of the cross-cutting volcanic chain of northern Tanzania and its relation to the East African rift system. *Tectonophysics*, **65**, 193–208.
- FAIRHEAD, J. D., MITCHELL, J. G. & WILLIAMS, L. A. J. 1972. New K/Ar determinations on Rift volcanics of S. Kenya and their bearing on the age of Rift faulting. *Nature*, **238**, 66–9.
- FOSTER, A. 1997. *The Seismicity and Tectonics of Africa*. PhD thesis, University of Cambridge.
- FOSTER, A., EBINGER, C., MBEDE, E. & REX, D. 1997. Tectonic development of the northern sector of the East African Rift System. *Journal of the Geological Society, London*, **154**, 689–700.
- FOZZARD, P. M. H. 1958. The Mponde river area, Singida District: Quarter Degree Sheet 41 NW. *Records of the Geological Survey of Tanganyika*, **VIII**, 1–5.
- GRAINGER, D. J. 1968. *Shambarai*. Tanzania Mineral Resources Division, Quarter Degree Sheet **71**.
- GREGORY, J. W. 1921. *The Rift Valleys and Geology of East Africa*. Seeley, Service, London.
- GUEST, N. J. 1953. *The Geology of Part of Northern Tanganyika Territory*. PhD thesis, University of Sheffield.
- HALLS, H. C., BURNS, K. G., BULLOCK, S. J. & BATTERHAM, P. M. 1987. Mafic dyke swarms of Tanzania interpreted from aeromagnetic data. In: HALLS, H. C. & FAHRIG, W. (eds) *Mafic Dyke Swarms*. Geological Association of Canada, Special Papers, **34**, 173–218.
- HAUGHTON, S. H. 1963. *The Stratigraphic History of Africa South of the Sahara*. Oliver & Boyd, Edinburgh.
- HAY, R. L. 1976. *Geology of the Olduvai Gorge*. University of California Press, Berkeley.
- HEPWORTH, J. V. 1972. The Mozambique orogenic belt and its foreland in northeast Tanzania: a photogeologically-based study. *Journal of the Geological Society, London*, **128**, 461–500.
- HOLMES, A. 1951. The sequence of pre-Cambrian orogenic belts in south and central Africa. *Proceedings of the 18<sup>th</sup> International Geological Congress, 1948*, **14**, 254–269.
- ISAAC, G. L. 1968. *The Acheulian Site Complex at Olorgesailie, Kenya: A Contribution to the Interpretation of Middle Pleistocene Culture in East Africa*. PhD thesis, University of Cambridge.
- JONES, H. 1967. *Makuyuni*. Tanzania Mineral Resources Division, Quarter Degree Sheet **70**.
- KENT, P. E. 1941. The Recent history and Pleistocene deposits of the plateau north of Lake Eyasi, Tanganyika. *Geological Magazine*, **78**, 173–184.
- LE GALL, B., GERNIGON, L., ET AL. 2004. Neogene–Holocene rift propagation in central Tanzania: morphostructural and aeromagnetic evidence from the Kilombero area. *Geological Society of America, Bulletin*, **83**, 490–510.
- MACINTYRE, R. M., MITCHELL, J. G. & DAWSON, J. B. 1974. Age of the fault movements in the Tanzanian sector of the East African rift system. *Nature*, **247**, 354–356.
- MANEGA, P. C. 1993. *Geochronology, Geochemistry and Isotope Study of the Plio-Pleistocene Hominid Sites and the Ngorongoro Volcanic Highlands in Northern Tanzania*. PhD thesis, University of Colorado.
- MCCONNELL, R. B. 1972. Geological development of the rift system of eastern Africa. *Bulletin of the Geological Society of America*, **83**, 2549–2572.
- MORLEY, C. K. (ed.) 1999a. *Geoscience of Rift Systems – Evolution of East Africa*. American Association of Petroleum Geologists, Studies in Geology, **44**.
- MORLEY, C. K. 1999b. Influence of pre-existing fabric on rift structure. In: MORLEY, C. K. (ed.) *Geoscience of Rift Systems – Evolution of East Africa*. American Association of Petroleum Geologists, Studies in Geology, **44**, 151–160.
- MOUGENOT, D., RECQ, M., VIRLOGEUX, P. & LEPVRIER, C. 1986. Seaward extension of the East African rift. *Nature*, **321**, 599–603.
- NYBLADE, A. A. & BRAZIER, R. A. 2002. Precambrian lithospheric controls on the development of the East African rift system. *Geology*, **30**, 755–758.
- NYBLADE, A. A., BURT, C., LANGSTON, C. A., OWENS, T. J. & LAST, R. J. 1996. Seismic experiment reveals rifting of craton in Tanzania. *EOS, Transactions of the American Geophysical Union*, **77**, 519–521.
- ORRIDGE, G. R. 1965. *Mbulu*. Tanzania Mineral Resources Division, Quarter Degree Sheet **69**.
- PICKERING, R. 1958. *Oldoinyo Ogoi*. Tanganyika Geological Survey, Quarter Degree Sheet **38**.
- PICKERING, R. 1961. The geology of the country round Endulen. *Records of the Geological Survey of Tanganyika*, **XI**, 1–9.
- PICKERING, R. 1964. *Endulen*. Tanzania Geological Survey, Quarter Degree Sheet **52**.
- RING, U., SCHWARTZ, H. L., BROMAGE, T. G. & SANAANE, C. 2005. Kinematic and sedimentological evolution of the Manyara Rift in northern Tanzania, East Africa. *Geological Magazine*, **142**, 355–368.
- SAGGERSON, E. P. & BAKER, B. H. 1965. Post-Jurassic erosion surfaces of East Africa and their deformation in relation to rift structure. *Journal of the Geological Society, London*, **121**, 51–72.
- SELBY, J. & THOMAS, C. M. 1966. *Balangida Lelu*. Tanzania Mineral Resources Division, Quarter Degree Sheet **103**.
- SIMPSON, F., HAAK, V., KHAN, M. A., SAKKAS, V. & MEJU, M. 1997. The KRISP magnetotelluric survey of 1995: first results. *Tectonophysics*, **278**, 261–271.
- SMITH, M. & MOSLEY, P. 1993. Crustal heterogeneities and basement influence on the development of the Kenya Rift, East Africa. *Tectonics*, **12**, 591–606.
- UHLIG, C. 1907a. Vom Kilimandscharo zum Meru. *Zeitschrift der Gesellschaft für Erdkunde*, **1907**, 627–650.
- UHLIG, C. 1907b. Der sogenannte grosse Ostafrikanische Graben zwischen Magad (Natron See) und Lawa ya Mweri (Manyara See). *Geographisches Zeitung*, **15**, 478–505.
- VAIL, J. R. 1970. Tectonic controls of dykes and related irruptive rocks in eastern Africa. In: CLIFFORD, T. N. & GASS, I. G. (eds) *African Magmatism and Tectonics*. Oliver & Boyd, Edinburgh, 337–354.
- WALTER, R. C., MANEGA, P. C., HAY, R. L., DRAKE, R. E. & CURTIS, G. H. 1991. Laser fusion <sup>40</sup>Ar/<sup>39</sup>Ar dating of Bed I, Olduvai Gorge, Tanzania. *Nature*, **354**, 145–149.
- WHITTINGHAM, J. K. 1963. The geological environment of the Kilombero valley. *Records of the Geological Survey of Tanganyika*, **X**, 17–27.
- WILKINSON, P., MITCHELL, J. G., CATTERMOLE, P. J. & DOWNIE, C. 1986. Volcanic chronology of the Meru–Kilimanjaro region, Northern Tanzania. *Journal of the Geological Society of London*, **143**, 601–605.
- WILLIS, B. 1936. *East African Plateaus and Rift Valleys*. Carnegie Institution of Washington, Washington D.C.
- YIRGU, G., EBINGER, C. Y. & MAGUIRE, K. H. (eds) 2006. *The Afar Volcanic Province within the East African Rift System*. Geological Society, London, Special Publications, **259**.

## Chapter 6

### Rift-associated sedimentary basins

The warping of the mid-Tertiary land surface and the subsequent faulting gave rise to a series of half grabens. Due to the disruption of earlier river systems, inland drainage basins formed within the half grabens and, in these basins, lake sediments were deposited, often intercalated with lava flows and ash-fall deposits, the thickest sedimentary successions forming in depocentres immediately adjacent to the boundary faults.

The most prominent of the basins are along the foot of the east-facing Pleistocene escarpment, being, from north to south, Natron, Engaruka, Manyara, Balangida and Balangida Lelu (Fig. 6.1). Unlike the half graben rift basins in Lake Tangayika (Rosendahl 1987) and in parts of Kenya, the northern Tanzania basins are not enclosed within opposed faults, nor are they linked by accommodation zones. These basins, together with the Eyasi half graben basin, now contain saline lakes. Other sedimentation basins are those of Olduvai/Laetoli and Amboseli, and some small ones in the Monduli area.

#### The Natron Basin

The Natron Basin in its early stages was probably joined to the Magadi Basin to the north. The maximum depth of the basin, estimated from Euler deconvolution (Ebinger *et al.* 1997), is around 3.3 km, which is similar to the 3.5 km depth to the basement derived from seismic refraction data for the Magadi Basin (Birt *et al.* 1997). Much of the basin is underlain by the Sambu volcanics and the Peninj Beds which were deposited in the palaeo-Lake Natron until *c.* 1.2 Ma when the sedimentation was ended by the Natron boundary faulting.

*Palaeo-Lake Natron.* Sedimentation in the Natron Basin began at *c.* 1.7 Ma in a shallow, depression that may have been fault-generated. A succession of basalts and nephelinites from Oldoinyo Sambu and Mosonik, dated at 3.5–1.77 Ma (Isaac & Curtis 1974), is overlain by the sediments of the Peninj Group, from which they are separated by a thin layer of sediment and a weathered lava (the Hajaró lava) collectively termed the Pre-Peninj Beds. The Peninj Group, named after the Peninj River where they are best exposed between the Sanjan and Natron faults immediately to the west of the present-day Lake Natron, is a 100 m succession of sediments with interbedded lavas. The sediments contain hominid remains and artefacts (Leakey & Leakey 1964; Isaac 1965; Howell 1972; Dundas & Awadalla, unpublished). The group comprises the lower Humbu Formation, formed of deltaic freshwater beds deposited in a shallow depression. The sediments are sands with clays and reworked tuffs with one thin limestone horizon. The palaeomagnetism of the tuffs record the Matuyama Epoch, including the Olduvai reversal at 1.87–1.67 Ma (Thouveny & Taieb 1986). The overlying, more widespread, Moinik Formation was deposited in a saline lake that extended westwards across the Salei Plains towards the Oldoinyo Ogot escarpment (Isaac 1965; Dundas & Awadalla, unpublished). The sediments contrast strongly with those of the underlying Humbu Formation, the conditions probably being like those of the modern Lake Natron, with deposition of fine clays, laminated trachytic tuffs and evaporites. Cherts derived from the clays are widespread, and

a chert nodule and a bedded chert with trona moulds have  $\delta^{18}\text{O}$  values of 40.3 and 36.6‰, respectively (O'Neil & Hay 1973). The overall Peninj Group was deposited between 1.7 and 1.2 Ma (Dawson 2008, Appendix 1). From the tectonic aspect, the Peninj area provides important evidence for: (a) the formation of an internal drainage basin due to pre-Pleistocene faulting; and (b) an age of <1.2 Ma for the faulting that terminated the Peninj Group sedimentation and formed the Natron Basin boundary fault.

*Present-day Lake Natron.* This is surrounded by, and sits below, the High Natron Beds, a 7 m section of zeolitized clays and tuffs with irregular nodules of chert, some rimmed by magadiite  $[\text{NaSi}_7\text{O}_{13}(\text{OH})_3 \cdot 3\text{H}_2\text{O}]$  and kenyaite  $[\text{Na}_2\text{Si}_{22}\text{O}_{41}(\text{OH})_8 \cdot 6\text{H}_2\text{O}]$ . Chert nodules and magadiite have  $\delta^{18}\text{O}$  values of 32.4 to 34.6‰ (O'Neil & Hay 1973). The High Natron Beds are probably correlatable with the High Magadi Beds surrounding Lake Magadi, which were deposited during a lake highstand at around 9 ka (Butzer *et al.* 1972). There was an earlier highstand at around 130 ka during which freshwater stromatolite growth took place (Hilaire-Marcel *et al.* 1986).

The modern lake lies at an average height of 610 m a.s.l., is 22–35 km wide and 75 km long, with a present surface area of around 1059 km<sup>2</sup>. The lake is shallow (only 3–4 m depth), and the evaporation rate is high, up to 20 mm per day. Its saline waters are rich in sodium carbonate/bicarbonate, NaCl and silica, and its pH is >9.5 (Howell 1972). The lake is fed by four permanent rivers, being from north to south: (1) the Engare Nyiro that flows south into the lake from Kenya; (2) the Peninj; (3) the Moinik rivers that enter the west side of the lake; and (4) the Engare Sero which enters the SW corner. All rise in the highlands to the west of the Natron Basin boundary fault. As well as volcanic detritus, the first three rivers contribute metamorphic debris from the basement hills to the west of the Nguruman and Sambu escarpments, as well as volcanic detritus, whereas the Engare Sero transports only volcanic debris from the Crater Highlands. Brackish lagoons exist where the rivers enter the lake and, in addition to these permanent rivers, there are many brackish or salt springs on the western and eastern shores of the lake. When the lake waters reach a high salinity, proliferation of brine shrimps result in the surface layer having a bright-red coloration.

Much of the lake surface is covered by a surface layer of trona, thermonatrite and halite, similar layers below the surface being interbedded with black organic clays to depths up to 6 m (Guest & Stevens 1951). The clays result from input of volcanic dust into the lake which, combined with organic material from detritus and algal blooms, forms the organic-rich bottom sediments, which also contain gaylussite and pirssonite and up to 10% authigenic analcime (Hay 1966). Although most of the carbonate salts have been leached out of the sodium-rich volcanic rocks surrounding the lake, there has been some direct volcanic input into the lake during natrocarbonatite eruptions of Oldoinyo Lengai. Magnesite has been deposited around one of the springs on the east side of the lake below Gelai. Guest (1951) suggests it was deposited when spring water rich in leached  $\text{Mg}_2\text{SO}_4$  reacted with saline lake waters, an origin supported by the intergrowth of the magnesite with hectorite ( $\text{Na}_{0.33}[\text{Mg},\text{Ca}]_3\text{Si}_4\text{O}_{10}[\text{OH}]_2$ ) (McKie 1956). A point of non-geological interest is that the salt-flats on the lake are now the only breeding place for Lesser Flamingo in the rift valley (Brown 1959).

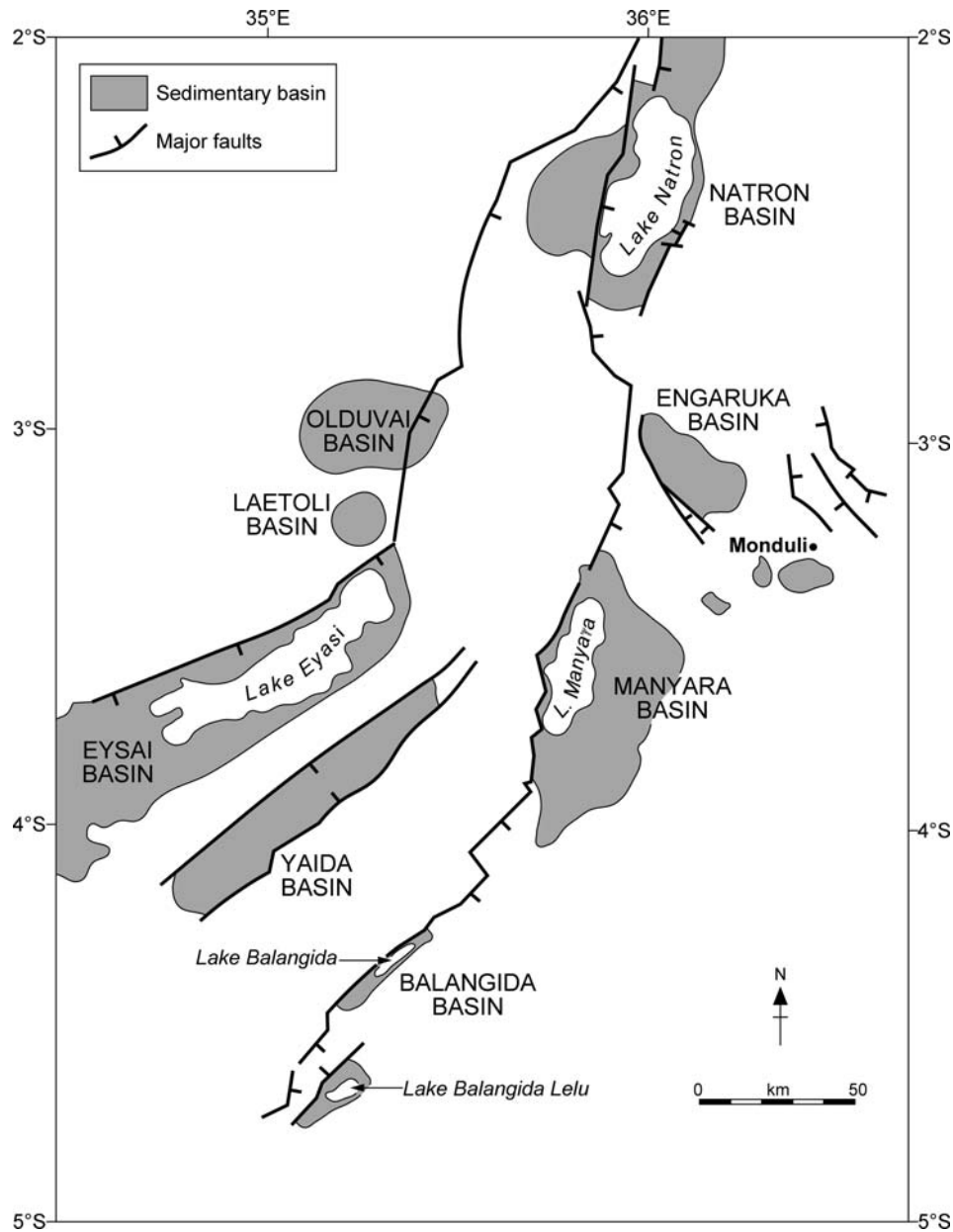


Fig. 6.1. Location of the rift-associated sedimentary basins relative to the major faults.

### The Engaruka Basin

The Engaruka Basin is separated from the Natron Basin by the topographic highs of the Oldoinyo Lengai and Kerimasi volcanoes, and from the Manyara Basin by the Engaruka Block (Fig. 5.8). It contains a shallow, seasonal lake fed by the perennial Engaruka River, draining from the Crater Highlands to the west, and smaller seasonal rivers rising on the volcanoes to the east, north and south of the basin. The sediments are poorly exposed, the main exposures being in the gorge of the Emugur Oretati (the river draining westwards between the Ketumbeine and Tarosero volcanoes), and in the gorge of the Engaibataat river that drains into the basin from the SW. These rivers expose tuffs and water-reworked tuffs, the age of which is not precisely known. However, their intercalation with flows of olivine basalt that have baked and reddened the sediments (Dawson 1964a) indicates some deposition during at least the later stages of the activity of Ketumbeine and/or Tarosero. On the northeastern margin of the basin are exposures of calcite-rich crystal tuffs from Kerimasi.

### The Manyara Basin

The only evidence for the presence of pre-volcanic sedimentary basins in northern Tanzania derives from an exposure at the base of the rift escarpment at the north end of Lake Manyara, where the Manyara Group comprises a boulder conglomerate unconformably overlying metamorphic basement rocks; the conglomerate is overlain by siltstones, sandstones, waterlain tuffs and ashes with an intercalated basalt that has been dated at  $4.86 \pm 0.24$  Ma. This succession has been interpreted as indicating some basin subsidence (possibly related to faulting) by around 4.9 Ma (Foster 1997; Foster *et al.* 1997). However, before the formation of the present-day basin at around 1.0 to 1.2 Ma, there was the intervening period of Older Extrusive magmatism.

The modern Manyara Basin, the maximum depth of which has been calculated from Euler deconvolution as being *c.* 2.9 km (Ebinger *et al.* 1997), is one of contrasts. Beneath the veneer of Pleistocene–Recent sediments, the basin at its northern end is underlain at shallow depths by volcanic rocks from the Crater

Highlands volcanoes and from Essimngor, whereas the southern part is underlain solely by Proterozoic metamorphic rocks. Also, the southern part of the basin is characterized by much minor seismic activity, whereas the northern part is relatively quiet seismically.

The present-day Lake Manyara occupies only the western part of a formerly more extensive Pleistocene basin that extended to the east of present-day Lake Burungi (also known as Sereri) that, like Manyara, is another remnant of the former Pleistocene lake (Dawson 2008, fig. 3.1). The eastern margin of the palaeo-lake is at least 40 km east of the present shoreline, suggesting an areal extent of *c.* 1800 km<sup>2</sup> compared with the current 480 km<sup>2</sup>. It is debatable whether the westerly migration of the lake to its present position below the rift escarpment is connected with the general onset of aridity in Africa during the Pleistocene or due to a deepening of the western part of the basin following a series of minor movements on the main boundary fault, or both. The highest level of the former lake, as deduced from guano deposit around a former island of Precambrian quartzite at Minjingu, is around 100 m above the present-day lake (Orridge 1965). The eastern shore of the ancient lake is delineated by a series of at least five terrace-like shoreline features, one of which is characterized by the presence of chert nodules, pisolitic limestones and stromatolites. Some stromatolites show several stages of spongy and oncolitic development (Loftus 1985). However, Casanova (1986) has pointed out that there are no examples of stromatolites currently forming in the sodium carbonate/bicarbonate lakes but, in common with other rift valley lakes where there are fossil stromatolites (Bogoria, Magadi, Natron), their presence is evidence of freshwater palaeolakes containing significant dissolved calcium carbonate.

The fossil lake beds, best exposed around Makuyuni, were first identified as such by Kent (1942) who, from fossil fish and mammals, suggested correlation with Bed II of the Olduvai Gorge succession *i.e.* Early or Middle Pleistocene. Ring *et al.* (2005) divide the Manyara Beds into lower and upper members, both of which contain much tuffaceous material. The lower member is a lacustrine sequence comprising basal conglomerate overlain by sandstones, marls and thin tuffs. These have yielded fossil mammals, including a hominin skull fragment and a tooth that, together with suid teeth, give a rough age of <1.7 to 0.7 Ma, corresponding to the Middle and Upper Bed II and Lower Bed III of Olduvai. The upper member represents an abrupt change from lacustrine to terrestrial sedimentation due to westward migration of the eastern shoreline. It is a dominantly terrestrial facies and consists of mudstones (some showing salt pseudomorphs and desiccation cracks), siltstones and tuffaceous conglomerates and breccias that represent flood-plain, channel-fill and debris flow facies. Mammal fossils suggest correlation with Olduvai Bed III (*c.* 0.7–0.4 Ma, late Pleistocene).

The average depth of the present lake is only around 3 m. In the dry season, the surface of the lake is covered with trona deposits and in times of drought the lake may almost dry up. There are a few freshwater lagoons along the western edge of the lake, where perennial rivers descend from the escarpment, and where water from springs along the foot of the escarpment enters the lake.

Phosphate-bearing horizons in sediments are mined around a former island of basement quartzites at Minjingu. Cormorant skeletons in the beds give grounds for suggesting that the phosphate originated as guano.

#### *The Monduli area basins*

In the area to the west of Monduli are three small sedimentary basins, the Yayai, Elunata and Ar dai basins (Dawson 2008, fig. 5.8), formed by minor fault-scarps damming streams draining southwards off the Essimngor, Burko, Tarosero and Monduli

volcanoes (Dawson 1964*a*). The basins are drained by minor rivers that have cut overflow channels through the escarpments to drain via the Engorika and Loilera rivers into Lake Manyara. Exposure in the basins is poor; olivine-rich tuffs from the Lashaine cone are exposed in a minor river draining southwards across the Ar dai Basin.

#### *The Balangida and Balangida Lelu basins*

These basins lie at the foot of the same boundary-fault escarpment as the Manyara Basin, but are separated from it by a topographic high of metamorphic rocks. Both basins are underlain by Archaean rocks of the Tanzania Craton. They contain lakes that are seasonally saline, and the surrounding areas are covered with superficial alluvial and aeolian sands and silts. The eastern part of the Balangida Basin is occupied by the Hanang volcano which, on its northwestern side, sheds fanglomerates into the basin. Both basins are believed to be shallow, with the maximum depth of the Balangida Basin, estimated from Euler deconvolution, being <1 km (Ebinger *et al.* 1997).

#### **The Eyasi Basin**

The Eyasi Basin lies within the Eyasi half graben and is bounded to the NW by the Eyasi escarpment; very minor NW-throwing faults form the southern edge of the basin. The basin is occupied by Lake Eyasi, a shallow seasonal lake which, on drying out, leaves mud, trona and halite. The superficial sediments around the lake are of sand-clay size, and are frequently wind-eroded and covered by small dunes. Deeper material is not exposed. The regional Bouguer anomaly map (Dawson 2008, fig. 4.1) shows a low anomaly beneath the east end of the basin; this is separated from a larger anomaly to the west (beneath the Wembere steppe) by a shallow ridge lying beneath the west end of Lake Eyasi. Euler deconvolution indicates the depth to the magnetic basement beneath the East Eyasi basin to be <1 km, compared with 3.5 km beneath the Wembere (W. Eyasi) Basin (Ebinger *et al.* 1997).

#### **The Yaida Basin**

The Yaida Basin occupies what is possibly the best example of a graben in East Africa. Earlier called the Hohenlohe graben (Jaeger 1913), it lies between two opposing NE-trending, 100 km long fault scarps that are almost parallel. The northern escarpment has a maximum height of 300 m, the southern of 400 m. The width between the escarpments varies from 10 to 16 km, widening from NE–SW. Nothing is recorded of the sediments within the graben.

#### **The Olduvai Basin and Laetoli**

The Olduvai Basin is a shallow, rift-platform basin situated on the Serengeti Plain to the west of the Crater Highlands. Its sedimentary rocks, exposed in the Olduvai Gorge and some minor tributaries, are justifiably famous for their hominid and Plio-Pleistocene mammalian fossils. The dating of individual formations in connection with anthropological studies at both Olduvai and Laetoli, and the correlation of some of these dated formations with volcanic activity to the east, has been of considerable benefit to volcanic chronology in the Crater Highlands.

The first fossil finds at Olduvai were made by a German entomologist, a Professor Kattwinkel, whilst collecting butterflies in 1911. His small collection aroused interest when he returned to Berlin, and resulted in an expedition to Olduvai in 1913 led by Hans Reck, who made the first systematic ordering of the

lithological units from Beds I to V (Reck 1914*a, b*). In 1928, L. S. B. Leakey visited Berlin and recognized artefacts amongst the material gathered in 1913, and led to a series of expeditions to collect new material. The history of investigations into the fossils of Olduvai from 1911 to 1975 is reviewed by M. Leakey (1978).

The first attempt to set the fossil finds in their geological context at Olduvai was made by Reck (1914*a*) and various stratigraphic refinements were made up to the 1960s. The most systematic sedimentological work began in 1962 and culminated in the monograph of Hay (1976), from which the following account is mainly drawn. Ashley & Hay (2002) later analysed lateral variations across the basin that elucidate the palaeoenvironment during an early stage of deposition and, more recently, Ashley (2007) has identified five episodes of lake expansion and contraction that may be linked to variations in insolation which, in turn, result from variations in global precession; the lake episodes are thus suggested as being connected to astronomical forcing.

The Olduvai Beds were deposited in a basin that was *c.* 50 km in diameter through much of the Pleistocene. A shallow saline lake some 15–20 km in diameter occupied the axial area of the basin during the early history of the basin. The maximum thickness of the beds is *c.* 140 m, with the greatest thickness in the eastern part of the basin. Above underlying basalt (possibly erupted from Olmoti), the beds are subdivided into seven formations: Beds I–IV, the Masek Beds, the Ndotu Beds and the Naisiusiu Beds; Beds I to IV cover the interval between *c.* 2.1 and 0.6 Ma (Curtis & Hay 1972; Walter *et al.* 1991; and see Appendix 1). In addition, Holocene sediments are present in the gorge and on the surrounding Serengeti Plains.

The earliest deposits (Beds I and II) were derived by airfall, *nuée ardente* and fluvial input from the east or south. Bed I (the thickest formation, up to 62 m thick, 2.0–1.7 Ma) comprises airfall tuffs, reworked tuffs, ignimbrites and olivine basalt flows into a saline lake, the flows being of local derivation compared with the tuffs and ignimbrites that were derived from the Crater Highlands. The reworked pyroclastic rocks originated in a pyroclastic fan complex on the eastern and southern shores of the lake. Bed II (20–30 m thick) spans the period 1.7 to *c.* 1.15 Ma. The lower part lithologically resembles the tuffs and saline lake deposits of Bed I but, above a disconformity (which marks the onset of widespread faulting and folding in the central part of the basin) the upper part of Bed II records a decrease in the size of the saline lake which disappeared just before the end of Bed II deposition. The disconformity marks a faunal change from swamp- and water-dwelling forms to a predominance of forms favouring open savannah and riverine conditions. Further, Bed II is important from the viewpoint of Palaeolithic industry sites, with Oldowan sites in the lower part, and developed Oldowan and Acheulian sites in the middle and upper sections of the bed. Similarly there is a difference in hominid remains, with remains of *Homo habilis* below the disconformity and *Homo erectus* above the break; remains of *Australopithecus* (*Zinjanthropus*) *boisii* occur both high and low in Bed II (Fig. 6.2). Chert nodules in Bed II have  $\delta^{18}\text{O}$  values of 31.1 to 38.7‰ (O'Neil & Hay 1973).

A widespread episode of faulting at around 1.15 Ma caused erosion of Bed II and partly changed the direction of sediment provenance. Beds III (7–9 m thick) and IV (*c.* 2 m thick) were deposited on alluvial plains that received metamorphic debris from the north and west, in addition to volcanic debris from the south and east. The sediments are mainly claystones and sandstones containing smectite and illite (Hay & Kyser 2001). The Masek Beds (12 m thick) disconformably overlie Beds III and IV and were the last to be deposited before the erosion that cut the Olduvai Gorge. They comprise wind-worked tephra erupted from Kerimasi to the NE and detrital sediments that occasionally infill channels in the underlying sediments.



Fig. 6.2. Interbedded tuffaceous sandstones and siltstones of Bed II, Olduvai Gorge. The plinth by the standing figure marks the site of the first discovery of *Australopithecus cf. boisei* ('Nutcracker Man').

The Masek Beds were followed by deposition of the Ndotu Beds (up to 18 m thick) during a period of faulting, erosion and partial infilling of the gorge. The lower Ndotu Beds are small patches of sand, conglomerate and tuffs deposited at various levels on the eroded side of the gorge. Deposition of the lower clastic sediments spanned 400 000 to 60 000 year BP, whereas the upper parts of the Ndotu Beds were deposited between 60 000 and 32 000 year BP from early eruptions of Oldoinyo Lengai. The Ndotu Beds also form a thin layer of tuff on the plains around the gorge. The Naisiusiu Beds (*c.* 8 m thick) were deposited after erosion of the Ndotu Beds, and consist of aeolian tuffs that cover the sides of the gorge and the surrounding plains. The beds consist of tephra derived from Oldoinyo Lengai, and are dated at 22 000 to 15 000 year BP.

Calcretes occur in Bed IV and in the Masek, Ndotu and Naisiusiu Beds. Formerly interpreted as surface limestones, they are now recognized as derived from carbonate-rich tephra from Kerimasi and Oldoinyo Lengai (Dawson 1964*b*). The calcretes, often overlie zeolite-rich horizons (Hay 1963); the zeolites arising by breakdown of nepheline and glass within the tephra due to interaction with natrocarbonatite ash; the zeolites are analcime, natrolite, phillipsite and chabazite, and they occur together with calcite, rare dolomite and locally-common dawsonite ( $\text{NaAl}[\text{OH}]_2\text{CO}_3$ ) (Hay & Reeder 1978).

During the lifetime of the basin, the location of the drainage sump migrated eastwards with the Ndotu Beds now confined to the Olbalbal depression following faulting along the most easterly of the faults affecting the basin. The basin was deformed almost continuously from Bed I to the present, with most faults trending NE–SW, mainly parallel to the Olbalbal fault. The eastern margin of the Bed I basin was downwarped and locally faulted, and this continued during the deposition of Bed II. Beds III and IV record movements along new faults that may be correlated with major movements on the Natron–Manyara boundary fault to the east at *c.* 1.0–1.2 Ma; the reversal of drainage and changes in the type of sediment input caused by this episode of faulting is noted above. Several new faults occurred during the deposition of the Masek Beds. The Ndotu Beds record an intense phase of deformation at around 0.4–0.03 Ma when the Olbalbal depression subsided, with southeastwards tilting of the basin. Numerous faults cutting the slopes of the Ngorongoro and Olmoti volcanoes to the east were also active at this time.

Laetoli lies to the south of Olduvai and its stratigraphy, hominid and other mammalian fossils have been studied by the same group of investigators as at Olduvai. The Laetoli Beds are Pliocene

air-fall and wind-reworked tuffs that are interbedded with lavas on the lower western and southern slopes of the Lemagrut volcano (Dawson 2008, fig. 3.1). The beds, originally called the Vogel River Series, were first mapped by Kent (1941) and divided into the lower Laetoli Beds and the overlying Ngaloba Beds. Importantly, he recognized the volcanoclastic nature of the beds and that the fossils (e.g. elephants, giraffes) represent only terrestrial fauna, contrasting with the swamp- and lake-dwelling fauna at Olduvai. Fossil eggs of francolin, guinea fowl and ostriches (Harrison 2005; Harrison & Msuya 2005) confirm Kent's (1941) interpretation of the environment as savannah or open grassland.

The discovery of fossil hominids (Leakey *et al.* 1978) stimulated more research, including refinement of the stratigraphy and dating. The beds are now known to dip under (and are therefore older than) the Olduvai Beds but overlie lavas from Lemagrut (Hay in Howell 1972). Hay (1987) recognized a lower unit (c. 64 m thick) consisting mainly of wind-worked nephelinite tephra, with thin conglomerates and breccias; it is poorly fossiliferous. An upper unit 44–59 m thick consists mainly of wind-worked tuffs, some containing fragments of ijolite and nephelinite, and also minor air-fall tuffs. These tuffs are of phonolitic composition, and several horizons contain calcite, devitrified glass, pyroxene, garnet, melilite and biotite mainly derived from the Sadiman volcano 15 km to the east (Hay 1978). From carbon and oxygen isotope data the calcite was formerly believed to be secondary after original carbonatite alkali-carbonates (Hay & O'Neil 1983) but, on both textural and calcite composition grounds, Barker & Milliken (2008) propose that the cementing calcite is diagenetic, resulting from interaction of glass with groundwater.

Apart from other fossils, these calcite-rich horizons preserve the footprints of a group of hominids (Hay & Leakey 1982), and also delicate bird footprints and insects (Hay 1986). Very rapid cementation by diagenetic calcite, Fe-natronite and phillipsite is suggested as the cause of the preservation of these delicate prints (Barker & Milliken 2008).

Dates of 3.7 and 3.49 Ma have been obtained on biotites from the lower and upper tuffs, and a vogesite lava from one of a small group of vents to the south, SW and west of Lemagrut (the Ogol lavas), overlying the beds, is dated at 2.41 Ma (Drake & Curtis 1987). Dating of Lemagrut lavas from other localities has given ages ranging from 4.3 to 2.7 Ma, (Appendix 1, Dawson 2008) so both the superposition of the Sadiman-derived tuffs on the lower slopes of Lemagrut lavas at Laetoli, and the bracketing of the radiometric ages of Sadiman by those from Lemagrut, provide evidence for contemporaneous volcanic activity at the two volcanoes.

## Amboseli

Although not strictly comparable with the other fault-bounded rift valley basins nor with Olduvai and Laetoli, the Amboseli Basin owes its origin to the same epoch of crustal deformation and subsequent volcanicity. The Amboseli Basin was created when the eruption of Kilimanjaro interrupted the regional eastwards slope of the deformed sub-Miocene land surface to form a dam, allowing the Amboseli Beds to accumulate (Pickford 1986). The lake itself is c. 250 km<sup>2</sup> in extent at maximum and considerably less in the dry season. Most of the lake and its larger basin lie in Kenya where Williams (1967) recorded marls, clay limestones, clays and siltstones (the Oltukai Beds, Amboseli Clays and Sinya Beds) overlying basal conglomerates, gravels and sands. In the southern extension of the Amboseli Clays into Tanzania, meerscham (sepiolite-hydrous magnesium silicate, used for the manufacture of tobacco pipes and ornamental carvings) occurs as banded cavity fillings in dolomitic limestone cropping out near the southern end of the lake (Harris 1961).

## Summary of the rift valley basins

The initiation of the basins in the rift valley took place during the late Pliocene and early Pleistocene by faulting of the sub-Miocene land surface. During later faulting, a series of lakes formed in the present-day basins at the base of the Natron–Balangida boundary fault when mid-Pleistocene faulting resulted in the disruption of earlier drainage systems. All are now inland drainage systems and have seasonal evaporite deposition. The basins show a consistent pattern in that both the age and depth of the basins decrease from north to south, i.e. from the Natron Basin to the Balangida Lelu Basin. Such a pattern is consistent with a north–south propagation of the main boundary fault responsible for the half graben holding the basins. Similarly, the major fault on the northwestern side of the Eyasi Basin decreases in height to the SW, but the depth of the basin does not show a consistent concomitant decrease.

The lakes in the Natron and Manyara basins are less extensive now than they were in the Pleistocene. Whereas the reason for this in the Manyara Basin is ambiguous (?onset of Pleistocene desiccation or due to tectonic activity), the shrinkage of Lake Natron can be linked to similar decreases in level of some of the lakes in southern Kenya, for which there is evidence of its having been a response to climate change.

## References

- ASHLEY, G. M. 2007. Orbital rhythms, monsoons and playa lake response, Olduvai Basin, equatorial East Africa (ca 1.85–1.74 Ma). *Geology*, **35**, 1091–1094.
- ASHLEY, G. M. & HAY, R. L. 2002. Sedimentation patterns in a Plio-Pleistocene volcanoclastic rift-platform basin, Olduvai Gorge, Tanzania. In: RENAUT, R. W. & ASHLEY, G. M. (eds) *Sedimentation in Continental Rifts*. Society for Sedimentary Geology, Special Publications, **73**, 197–222.
- BARKER, D. & MILLIKEN, K. L. 2008. Cementation of the Footprint Tuff, Laetoli, Tanzania. *Canadian Mineralogist* (in press).
- BIRT, C. S., MAGUIRE, P. K. H., KHAN, M. A., THYBO, H., KELLER, G. R. & PATEL, J. 1997. The influence on pre-existing structures on the evolution of the southern Kenya Rift Valley – evidence from seismic and gravity studies. *Tectonophysics*, **278**, 211–242.
- BROWN, L. 1959. *The Mystery of the Flamingos*. Country Life, London.
- BUTZER, K. W., ISAAC, G. L., RICHARDSON, J. L. & WASHBOURN-KAMAU, C. 1972. Radiocarbon dating of East African lake levels. *Science*, **175**, 1069–1076.
- CASANOVA, J. 1986. East African stromatolites. In: FROSTICK, L. E., RENAUT, R. W., REID, I. & TIERCELIN, J. J. (eds) *Sedimentation in the African Rifts*. Geological Society, London, Special Publications, **25**, 201–210.
- CURTIS, G. H. & HAY, R. L. 1972. Further geological studies and K–Ar dating at Olduvai Gorge and Ngorongoro crater. In: BISHOP, W. W. & MILLER, J. W. (eds) *Calibration of Hominoid Evolution*. Scottish Academic Press, Edinburgh, 107–134.
- DAWSON, J. B. 1964a. *Monduli*. Tanzania Geological Survey Quarter Degree Sheet **54**.
- DAWSON, J. B. 1964b. Carbonatitic volcanic ashes in northern Tanganyika. *Bulletin Volcanologique*, **27**, 81–92.
- DAWSON, J. B. 2008. *The Gregory Rift Valley and Neogene–Recent Volcanoes of Northern Tanzania*. Geological Society, London, Memoirs, **33**.
- DRAKE, P. & CURTIS, G. H. 1987. K–Ar geochronology of the Laetoli fossil localities. In: LEAKEY, M. D. & HARRIS, J. M. (eds) *Laetoli, a Pliocene site in Northern Tanzania*. Clarendon Press, Oxford, 48–52.
- DUNDAS, D. L. & AWADALLA, G. W. (unpublished) *Loliondo*. Unpublished report and map of Quarter Degree Sheet 16 and 27, Tanzania Geological Survey, Mapped 1966.
- EBINGER, C., POUJOM DJOMANI, Y., MBEDE, E., FOSTER, A. & DAWSON, J. B. 1997. Rifting Archaean lithosphere: the Eyasi–Manyara–Natron rifts, East Africa. *Journal of the Geological Society, London*, **154**, 947–60.

- FOSTER, A. 1997. *The Seismicity and Tectonics of Africa*. PhD thesis, University of Cambridge.
- FOSTER, A., EBINGER, C., MBEDE, E. & REX, D. 1997. Tectonic development of the northern sector of the East African Rift System. *Journal of the Geological Society, London*, **154**, 689–700.
- GUEST, N. J. 1951. *Gelai magnesite*. Tanganyika Geological Survey, Mineral Resources Pamphlet **52**.
- GUEST, N. J. & STEVENS, J. A. 1951. *Lake Natron, its Springs, Rivers, Brines and Visible Saline Reserves*. Tanganyika Geological Survey, Mineral Resources Pamphlet **58**.
- HARRIS, J. F. 1961. *Summary of the Geology of Tanganyika. Memoir 1, Part IV: Economic geology*. Government Printer, Dar es Salaam, 102–103.
- HARRISON, T. 2005. Fossil bird eggs from the Pliocene of Laetoli, Tanzania: Their taxonomic and palaeoecological relationships. *Journal of African Earth Sciences*, **41**, 289–302.
- HARRISON, T. & MSUYA, C. P. 2005. Fossil struthionid shells from Laetoli, Tanzania: Taxonomic and biostratigraphic significance. *Journal of African Earth Sciences*, **41**, 303–315.
- HAY, R. L. 1963. Zeolitic weathering in Olduvai Gorge, Tanganyika. *Bulletin of the Geological Society of America*, **74**, 1281–1286.
- HAY, R. L. 1966. *Zeolites and Zeolitic Reactions in Sedimentary Rocks*. Geological Society of America, Special Publications, **85**, 39–44.
- HAY, R. L. 1976. *Geology of the Olduvai Gorge*. University of California Press, Berkeley.
- HAY, R. L. 1978. Melilitite–carbonatite tuffs in the Laetoli Beds of Tanzania. *Contributions to Mineralogy and Petrology*, **67**, 357–367.
- HAY, R. L. 1986. Role of tephra in the preservation of fossils in Cenozoic deposits in East Africa. In: FROSTICK, L. E., RENAULT, R. W., REID, I. & TIERCELIN, J. J. (eds) *Sedimentation in the African Rifts*. Geological Society, London, Special Publications, **25**, 339–344.
- HAY, R. L. 1987. Geology of the Laetoli area. In: LEAKEY, M. D. & HARRIS, J. M. (eds) *Laetoli: a Pliocene Site in Northern Tanzania*. Clarendon Press, Oxford, 23–47.
- HAY, R. L. & LEAKEY, M. D. 1982. The fossil footprints of Laetoli. *Scientific American*, **246**, 50–57.
- HAY, R. L. & O'NEILL, J. R. 1983. Carbonatite tuffs in the Laetoli Beds of Tanzania and the Kaiserstuhl in Germany. *Contributions to Mineralogy and Petrology*, **82**, 403–406.
- HAY, R. L. & KYSER, T. K. 2001. Chemical sedimentology and palaeoenvironmental history of Lake Olduvai, a Pliocene lake in northern Tanzania. *Bulletin of the Geological Society of America*, **113**, 1505–1521.
- HAY, R. L. & REEDER, R. J. 1978. Calcretes of the Olduvai Gorge and Ndolanya Beds of northern Tanzania. *Sedimentology*, **25**, 649–673.
- HILAIRE-MARCEL, C., CARRO, O. & CASANOVA, J. 1986. <sup>14</sup>C and Th/U dating of Pleistocene and Holocene stromatolites from East African palaeo-lakes. *Quaternary Research*, **25**, 312–329.
- HOWELL, F. C. 1972. Pliocene/Pleistocene hominidae in eastern Africa: absolute and relative ages. In: BISHOP, W. W. & MILLER, J. A. (eds) *Calibration of Hominoid Evolution*. Scottish Academic Press, Edinburgh, 331–368.
- ISAAC, G. L. 1965. The stratigraphy of the Peninj Beds and the provenance of the Natron Australopithecine mandible. *Quaternaria*, **7**, 101–130.
- ISAAC, G. L. & CURTIS, G. H. 1974. Age of the Acheulian industries from the Peninj Group, Tanzania. *Nature*, **249**, 624–627.
- JAEGER, F. 1913. Das Hochland der Riesenkrater und die umliegender Hochländer Deutsch Ostafrika, Part 2. *Mitteilungen aus den Deutsches Schutzgebieten, Ergänzungsheft*, **8**, 1–213.
- KENT, P. E. 1941. The Recent history and Pleistocene deposits of the plateau north of Lake Eyasi, Tanganyika. *Geological Magazine*, **78**, 173–184.
- KENT, P. E. 1942. A note on Pleistocene deposits near Lake Manyara, Tanganyika. *Geological Magazine*, **79**, 72–77.
- LEAKEY, L. S. B. & LEAKEY, M. D. 1964. Recent discoveries of fossil hominids at Olduvai and near Lake Natron. *Nature*, **209**, 3–9.
- LEAKEY, M. D. 1978. Olduvai Gorge 1911–75: a history of the investigations. In: BISHOP, W. W. (ed.) *Geological Background to Fossil Man*. Scottish Academic Press, Edinburgh, 151–155.
- LEAKEY, M. D., HAY, R. L., CURTIS, G. H., DRAKE, R. E., JACKES, M. K. & WHITE, T. D. 1978. Fossil hominids from the Laetoli Beds, Tanzania. In: BISHOP, W. W. (ed.) *Geological Background to Fossil Man*. Scottish Academic Press, Edinburgh, 157–170.
- LOFTUS, G. W. F. 1985. *Petrology and depositional environment of the Dinantian Burdiehouse Limestone formation of Scotland: their relevance to the accumulation of the Oil-Shale Group*. PhD thesis, University College, London.
- MCKIE, D. 1956. Mineralogical notes. *Records of the Geological Survey of Tanganyika*, **VI**, 87–93.
- O'NEIL, J. R. & HAY, R. L. 1973. <sup>18</sup>O/<sup>16</sup>O ratios in cherts associated with the saline lake deposits of East Africa. *Earth and Planetary Science Letters*, **19**, 257–266.
- ORRIDGE, G. R. 1965. *Mbulu*. Tanzania Mineral Resources Division Quarter Degree Sheet **69**.
- PICKFORD, M. 1986. Sedimentation and fossil preservation in the Nyanza Rift System, Kenya. In: FROSTICK, L. E., RENAULT, R. W., REID, I. & TIERCELIN, J. J. (eds) *Sedimentation in the African Rifts*. Geological Society, London, Special Publications, **25**, 345–362.
- RECK, H. 1914a. Erste vorläufige Mitteilungen über den Fund eines fossil Menschen skelets aus Zentralafrika. *Sitzungsberichten der Gesellschaft Naturforschender Freunde*, **3**, 81–95.
- RECK, H. 1914b. Zweite vorläufige Mitteilungen über fossile Tier- und Menschenfunde aus Oldoway in Zentralafrika. *Sitzungsberichten der Gesellschaft Naturforschender Freunde*, **3**, 305–318.
- RING, U., SCHWARTZ, H. L., BROMAGE, T. G. & SANAANE, C. 2005. Kinematic and sedimentological evolution of the Manyara Rift in northern Tanzania, East Africa. *Geological Magazine*, **142**, 355–68.
- ROSENDAHL, B. R. 1987. Architecture of continental rifts with special reference to East Africa. *Annual Reviews of Earth and Planetary Sciences*, **15**, 445–503.
- THOUVENY, N. & TAIEB, M. 1986. Preliminary magnetostratigraphic record of Pleistocene deposits, Lake Natron basin, Tanzania. In: FROSTICK, L. E., RENAULT, R. W., REID, I. & TIERCELIN, J. J. (eds) *Sedimentation in the African Rifts*. Geological Society, London, Special Publications, **25**, 331–336.
- WALTER, R. C., MANEGA, P. C., HAY, R. L., DRAKE, R. E. & CURTIS, G. H. 1991. Laser fusion <sup>40</sup>Ar/<sup>39</sup>Ar dating of Bed I, Olduvai Gorge, Tanzania. *Nature*, **354**, 145–149.
- WILLIAMS, L. A. J. 1967. *Geology of the Amboseli area*. PhD thesis, University of East Africa.

## Chapter 7

### The Neogene–Recent volcanic rocks

The late Tertiary–Recent volcanoes are largely confined to the area of the late Tertiary depression, the exceptions being the most southerly volcanoes of Hanang and Kwaraha, and the Basotu explosion craters of the Mbulu Plateau (Dawson 2008, fig. 3.1).

The first systematic attempt to classify the volcanoes was that of Guest (1953) who, mainly on the basis of rock type, divided them into the Older Extrusives (volcanoes characterized by extrusion of basalt) and the Younger Extrusives (formed by more alkaline rock types). Guest's classification is broadly correct, but modifications to the scheme have resulted from later regional mapping by the Tanzania Geological Survey, together with radiometric dating of rocks from individual centres. This has resulted in a more refined stratigraphy, particularly with respect to the timing of the volcanicity relative to the regional tectonics. For example, some peralkaline volcanoes, formerly included with the Younger Extrusives, are older than, or contemporaneous with, some Older Extrusive basaltic centres. The term 'peralkaline volcano' is used here to indicate that the structure is formed dominantly of peralkaline rocks i.e. those for which whole-rock chemical analyses show  $(\text{Na} + \text{K})/\text{Al} > 1$ .

Following the faulting that formed the late Tertiary tectonic depression, a group of major volcanoes erupted within the depression, the lavas largely infilling the depression and eventually overstepping the boundary fault-scarps at several points. In the SW, volcanoes erupting in the Crater Highlands infilled the northeastern end of the Eyasi half graben, and in the east, lavas from the Kilimanjaro massif filled the depression to the north of the Pangani graben.

The earliest date of eruption is poorly constrained since, even in the major fault escarpments, the first extrusive rocks of most of the volcanoes are not exposed. The only exposure of volcanic rocks in contact with the underlying basement rocks within the depression is in the extreme north, immediately south of the Kenya border, where basaltic lavas from Oldoinyo Sambu overlies Usagaran basement quartzites in the escarpment on the west shores of Lake Natron (Dundas & Awadalla, unpublished). One of these basalts has a K–Ar age of  $7.7 \pm 0.8$  Ma (Appendix 1). Although these are the oldest extrusions exposed in the escarpment on the eastern side of Oldoinyo Sambu, Dundas & Awadalla (unpublished) state that the oldest lavas from this volcano are melanephelinites and melilitites of the Bast Hills and Birera, to the west of the main volcano. These, as with early lavas from some other centres, are high-alkali, silica-undersaturated types. Like Oldoinyo Sambu, activity at Lemagrut also started with extrusions of nephelinite and subsequently produced abundant alkali basalt lavas.

Major extrusions of the alkali basalt–trachyte–phonolite association typify the activity at many of the large shield volcanoes (Elanairobi, Olmoti, Loolmalasin, Ngorongoro, Oldeani, Gelai, Ketumbeine, Tarosero, Monduli and the Shira and Mawenzi centres of Kilimanjaro). Some of these basaltic volcanoes, Ngorongoro, Olmoti, Elanairobi (collectively termed the Crater Highlands) and Ketumbeine, developed calderas in connection with trachytic eruptions during their later stages.

However, there are exceptions to this dominantly basaltic magmatism. The oldest dated rock within the province is an 8.1 Ma nephelinite from Essimngor (Appendix 1, Dawson 2008), but here undersaturated magmatism persisted with no later basaltic extrusions. In addition to Essimngor, Shombole, Mosonik and Sadiman are nephelinite–phonolite pyroclastic stratovolcanoes, thus contrasting with the basaltic lava-dominated shield

volcanoes. Hence, during the Older Extrusive episode, there was an overlap between peralkaline undersaturated magmatism and the more voluminous basaltic magmatism. For example, at Essimngor peralkaline magmatism was the sole type of activity and preceded the dominantly basaltic regional magmatism; it preceded but was then followed by basaltic activity at some centres such as Oldoinyo Sambu and Lemagrut; or it was contemporaneous with some of the basaltic volcanoes (Shombole, Mosonik and Sadiman).

The overall age range of this older phase of magmatism is from 8.1 Ma to around 1.2 Ma. The ages of these older volcanics overlap those of the Kirikiti and Ologesaile basalts immediately north in Kenya, extruded at 5.0 to 1.0 Ma (Baker *et al.* 1972; Fairhead *et al.* 1972) but there is no equivalent in northern Tanzania of the earlier Kenyan flood phonolites, dated at c. 13 Ma (Bishop *et al.* 1969).

The exact timing of the end of activity, and the length of the activity, at most of these older centres is not known. However, lava extrusions at several centres, such as at the Kibo cone on Kilimanjaro, and at Tarosero, continued into the Pleistocene, and lavas from the Crater Highlands and, possibly, Oldoinyo Sambu, are known in the Pleistocene sedimentary successions at Olduvai and Peninj.

#### Rock nomenclature

Most of the rock names given hereafter are made on the basis of thin-section examination by the referenced authors. For example, basaltic rocks containing plagioclase more sodic than labradorite are often referred to as 'trachybasalt'; only when chemical analyses are available can they be more correctly identified as mugearite or benmoreite. In naming rocks on the basis of their chemistry, the TAS (total alkalis–silica) system recommended by Le Maitre (1989) has been followed, except in the case of the 'foidite' grouping where, if possible, petrographic observation has allowed a more specific name to be given e.g. nephelinite, melilitite. In the case of olivine- and augite-phyric feldspathoidal lavas, especially from the Essimngor volcano, the broad thin-section criteria in Table 7.1 have been applied.

Some of the most modern geochemical work on volcanic rocks from the area is that of Paslick *et al.* (1995, 1996) who provide major, minor, trace element and Sr, Nd and Pb isotope data. To avoid unnecessary repetition, these analyses are referred to below as 'complete analyses'. In the case of some rock names given by Paslick *et al.* (1995, 1996), these were based on either earlier identifications by the petrographic laboratory of the Tanzania Geological Survey, or on whole-rock chemistry e.g. 'foidite' (as defined on a TAS diagram). Petrographic re-examination by the author in connection with this account has resulted in the renaming of some rocks.

Lava collections from some of the volcanoes have formed the basis for MSc and PhD theses. Space constraints make it impossible to give all the results presented in these theses, but data are summarized to give the interested reader some concept of the content of these valuable data sources.

#### Descriptions of individual volcanoes or volcanic areas

When not otherwise referenced, statements pertaining to the occurrence and identification of specific rock-types are based on

**Table 7.1.** Rock names based on thin section criteria

Rock name	Phenocrysts	Feldspathoid in groundmass
Limburgite	Mainly olivine + minor Ti-augite	Nepheline, analcime or sodalite
Ankaramite	50% olivine + 50% Ti-augite	Nepheline, analcime or sodalite
Augitite	< 10% olivine, mainly Ti-augite	Nepheline, analcime or sodalite

the author's fieldwork and thin section examination of rocks in his personal collection, now housed in the Natural History Museum, London (Oldoinyo Lengai specimens) and in the Harker Collection at the Sedgwick Museum, University of Cambridge (other Tanzanian samples). The colour plates, illustrate some of the features unique to the volcanoes of northern Tanzania.

Note: In the following accounts of the individual volcanic centres, the abbreviation QDS stands for 'Quarter Degree Sheet'.

## The Older Extrusives

### Shombole

*Type:* stratovolcano; *Lat/Long:* 2°09'S 36°06'E; *Elevation:* 1570 m; *Relief:* c. 1000 m; *Diameter:* 9.5 km; *Eruptive history:* Pliocene; *Crater diameter:* 2 × 2.5 km; *Composition:* nephelinite/carbonatite; *QDS* (Quarter Degree Sheet): 28 Kibangaini (Mineral Resources Division, Tanzania) and Report 61 (Geological Survey of Kenya).

Straddling the border between Kenya and Tanzania, Shombole lies mainly within Kenya. It is situated on the floor of the rift valley between the Magadi and Natron basins. The volcano is deeply eroded (Fig. 7.1), with exposure of its dominantly pyroclastic rocks in radial ravines and in north–south-trending fault escarpments that cut across the lower eastern slopes (Baker 1963). Fairhead *et al.* (1972) gave two K–Ar dates of  $1.96 \pm 0.07$  and  $2.00 \pm 0.05$  Ma on 'Shombole volcanics'. Kjaarsgaard & Peterson (1991) concluded a 2 Ma age from geological data, namely Quaternary trachytic lavas overlapping the eastern edge of the Shombole volcanics, and dating of trachytic lavas in the area (Crossley 1979).

The most recent and complete description of the volcano is by Peterson (1989a). A central vent is the main source of tuffs and agglomerates that are intercalated with the dominantly nephelinite lavas; ijolite blocks occur in the agglomerates (L. A. J. Williams



**Fig. 7.1.** Aerial view of Shombole from the SW. The dominantly pyroclastic deposits are reflected in the deeply-dissected topography. Trona deposits in Lake Natron appear in the foreground.

pers. comm.). A caldera-forming event filled the central vent with flat-lying pyroclastics and minor flows, which on the outer flanks dip radially at 10–15°. Carbonatite tuffs are exposed low on the eastern slopes, but the main early lava type is perovskite nephelinite, succeeded by titanite nephelinite and later phonolitic nephelinite. Kjaarsgaard & Peterson (1991) suggested that the carbonatites and nephelinites are linked by liquid immiscibility. Carbonatite-cemented breccia occurs on the lower SW slopes and carbonate replaces wollastonite in some caldera nephelinites. Phonolites, of which three petrographically different types are recognized, occur as minor extrusions and are interpreted, on isotopic grounds, as resulting from the interaction of nephelinite magma with lower crustal granulites (Bell & Peterson 1991).

### Oldoinyo Sambu

*Type:* shield volcano; *Lat/Long:* 2.15°S 35.93°E *Elevation:* 2043 m; *Relief:* 1400 m (east side), 700 m (west side); *Diameter:* 42 km; *Eruptive history:* Upper Pliocene to Middle Pleistocene; *Composition:* mainly olivine basalt; *QDS:* 16 and 17 Loliondo.

Oldoinyo Sambu is one of the most northerly of the Tanzanian volcanoes, with its northern slopes descending into Kenya. From the west and east it appears a broad dome. On its western side it rises gradually from the Salei Plain, but its eastern slopes are bisected, and exposed, by the main north–SE-facing 1200 m escarpment of the Natron Basin boundary fault (Fig. 7.2). There is no summit crater and most of the eastern half of the original volcano now lies beneath Lake Natron, though a small hill of basalt, poking up through recent sediments on the western shores of the lake, may have formed part of the summit prior to the faulting.

The volcano is composed mainly of flows of olivine basalt, with phenocrysts of augite, olivine and labradorite, and subordinate trachybasalt and phonolite. Just to the south of the Kenya border, the lowest lavas rest upon basement quartzite (Dundas & Awadalla unpublished); these basal lavas are dated as  $7.7 \pm 0.8$  Ma. Lenses of tuff and agglomerate are locally interbedded with



**Fig. 7.2.** Aerial view of Oldoinyo Sambu from the south. The volcano is bisected by the Natron basin boundary fault. Lake Natron (foreground) is covered with trona deposits and part of the Peninj delta appears in the left foreground.

basalts in the rift escarpment 4–6 km north of the Peninj delta, and deltaic and lacustrine sediments are intercalated with the basalts about 200 m below the top of the lava sequence in the gorge of the Peninj river on the southern lower slopes. A basalt just above these sediments gave a K–Ar age of 2.02 Ma. The lavas at the top of the succession were extruded before the end of the last reversed-polarity episode at 0.7 Ma. Thus, it appears that lavas were extruded for a period of around 5.5 million years.

Small outcrops of nephelinite and olivine nephelinite occur in the Bast Hills and in the Birera and Losanya areas to the west and SW of Oldoinyo Sambu. Their extrusion age is not known precisely, though those in the Bast Hills are overlain by Oldoinyo Sambu basalts. On the lower northern slopes of Oldoinyo Sambu, just over the border in Kenya, are flows of olivine basalt and small outcrops of biotite–olivine nephelinite (ankaratrite) (Saggerson 1966).

Krenkel (1922), quoting Finckh (1903 p.501), refers to, and gives an analysis of, a trachydolerite from Oldoinyo Sambu, which he compares with similar rocks from the Mawenzi peak on Kilimanjaro; compositionally (Appendix 2, Dawson 2008) the rock is a mugearite. Paslick *et al.* (1995) give complete rock analyses for basanites, nephelinites and picro-basalts in the rift escarpment at the south end of Lake Natron; however, it is not clear whether these flows are from Oldoinyo Sambu or from Elanairobi.

### Mosonik

*Type:* stratovolcano; *Lat/Long:* 2.61°S 35.80°E; *Elevation:* 1702 m; *Relief:* 480 m; *Volcano diameter:* 7.5 km; *Eruptive history:* Pliocene; *Composition:* nephelinite, phonolite, carbonatite; *QDS:* 39 Angata Salei.

Mosonik stands on the upthrown side of the Natron Basin boundary escarpment near the southern end of Lake Natron, and the cone is faulted on its northern side by the north–south-trending Sanjan Fault. Like Shombole and Essimingor, the volcano is unusual amongst the older volcanoes in being a nephelinitic stratovolcano, rather than a basaltic shield. Reflecting its dominantly pyroclastic make-up, it is strongly dissected, with deep radial valleys and steep intervening ridges (Fig. 7.3). There is now no evidence for a summit crater. Biotite from a nephelinite lava has yielded a date of 3.12 Ma (Isaac & Curtis 1974).

The Quarter Degree Sheet No. 39 (Angata Salei; Guest *et al.* 1961) shows that the cone consists mainly of nephelinitic–phonolitic tuffs and agglomerates, together with a lava lobe that extends east from the cone; the lava lobe may have issued from a breached crater. The flows comprising the lobe are of nephelinite and



**Fig. 7.3.** Aerial view of Mosonik from the SW. The well-dissected nature of the pyroclastic volcano is apparent. The Sanjan fault (left) and the Natron Basin boundary fault (see Fig. 5.7) appear to the north of the volcano.

nephelinitic phonolite, and are cut by a minor fault that parallels the main escarpment. Paslick *et al.* (1995, 1996) give complete rock analyses of a basanite and three nephelinites from the lava lobe, together with analyses of nepheline, clinopyroxene, perovskite, Ti-magnetite and titanite. James (1966) cited the presence of sodalite nephelinite (Rosenbusch 1907) and aegirine sövite (Brögger 1921). The Geological Survey map also shows a small plug of carbonatite intruding the volcanics in a valley on the north side of the mountain. M. S. Garson (pers. comm.) reports that a United Nations geological survey was unable to find this plug but found small arcuate dykes and areas of carbonatite breccia in an area south of the plug locality.

J. B. Dawson, A. N. Mariano and R. H. Mitchell visited the volcano in September 2005 and provide the following additional information: (i) carbonate-cemented tuffs and lapilli tuffs blanket the lower northern and western slopes of the mountain, and form an extensive cover on the plains to the west; (ii) within the pyroclastic rocks, fragmented nepheline- and pyroxene-phyric lava is the commonest material but true nephelinite is rare, as most samples have some feldspar in their groundmass and are hence transitional to phonolite. Feldspar-phyric phonolite is present but in relatively small amounts. Phlogopite, titanite and melanite are accessory phases in some lavas; (iii) blocks of mica pyroxenite, ijolite-mantled pyroxenite, ijolite and syenite and xenoliths of biotite quartzite and biotite schist occur in the agglomerates; and (iv) traverses into the valleys on the northern and western sides of the volcano, including the valley where the carbonatite is shown to be located on the QDS map, found no samples of carbonatite, either *in situ* or as detritus. However, in September 2007, Dawson & Mitchell found rare blocks of sövite in the gorge of the Leshuta River that drains eastwards from the volcano into Lake Natron, together with abundant consolidated, Mosonik-derived debris in the walls of the gorge.

### Gelai

*Type:* shield volcano; *Lat/Long:* 2.60°S 36.11°E; *Elevation:* 2942 m; *Relief:* 1720 m; *Volcano diameter:* 20 × 36 km *Crater diameter:* none; *Eruptive history:* Pliocene *Composition:* alkali basalt–trachyte; *QDS:* 28 Kibangaini and 40 Gelai and Ketumbeine.

Gelai is a broad, elongate NNE–SSW-trending shield without a summit crater. The lower slopes consist mainly of alkali olivine basalt or basanite, and Guest (1953) noted some that contain ‘enclaves of granular green olivine’ (? peridotite xenoliths). On the upper slopes and in the well-forested summit area are scattered outcrops of peralkaline trachyte. Numerous minor scoria- and tuff-cones occur on the lower northeastern and southwestern slopes, often following the trend of numerous, small faults trending NNE–SSW (Guest & Pickering 1966*a, b*); Those on the southwestern lower slopes are later than the main cone flows, and include peridotite xenolith-bearing tuff cones at Pello Hill and Eledoi (Dawson & Powell 1969; and see ‘Natron–Engaruka tuff-cone area’ below). The apparent absence of small faults and cones on the upper slopes of the volcano may be due to poor exposure, but could also be due to later extrusion of lavas in the summit area (as on Tarosero). An age for the basalts on the lower northern and eastern slopes is given by their being cut by small faults, which are a continuation of a fault swarm in southern Kenya that has been dated at around 1–1.5 Ma. Hence, at least the lower basalts of Gelai predate the faulting event.

Guest (1953) gave analyses of a barkevikite- and anorthoclase-phyric nepheline benmoreite from the lower SW flank of the mountain and Paslick *et al.* (1996) gave complete analyses of two basanites from the volcano, together with olivine and Ti-magnetite in one of the basanites.

To the north of Gelai is a low-lying, grid-faulted area, Kibangaini, that contains abundant trachytes similar to those in the



**Fig. 7.4.** Ketumbeine from the west. The volcano stands 1800 m above the Engaruka Basin (foreground). Note the break in slope due to higher viscosity lavas on the higher slopes and the flat summit area due to caldera collapse.

Magadi area immediately to the north. Some Kibangaini rocks contain riebeckite and kataphorite; analyses of two trachytes were given by Guest (1953) (Appendix 2, Dawson 2008).

#### *Ketumbeine*

*Type:* shield volcano; *Lat/Long:* 2.89°S 36.22°E; *Elevation:* 2658 m; *Relief:* 1800 m; *Volcano diameter:* 26 km; *Crater diameter:* 3 × 2 km; *Eruptive history:* Pliocene; *Composition:* alkali olivine basalt and trachyte; *QDS:* 40 Gelai and Ketumbeine.

Ketumbeine is a broad, almost circular, shield volcano. The lower slopes consist mainly of low-angle basalt flows but there is a distinct steepening of the slopes in the summit area due to the extrusion of more viscous lavas (Fig. 7.4). Unlike Gelai, there is a poorly exposed, elongate (north–south-trending) crater on the summit (Guest & Pickering 1966b). There are small cones and faults on the lower slopes and Guest (1953) reported that most rocks on the lower flanks are ‘basic andesite’ and on the upper slopes are trachyandesite and trachyte. A basalt from the lower southeastern slopes contains phlogopite as an intergranular and vesicle-filling phase. (Dawson personal observation). Guest (1953) recorded nephelinite from Lolgurdolgonja, a small late parasitic cone on the lower western slopes of the main volcano.

Paslick *et al.* (1995, 1996) gave complete analyses of four olivine basalts and basanites, with mineral analyses of olivine and clinopyroxene in one specimen and of feldspar and Ti-magnetite in another.

#### **The Crater Highlands**

This major group of dominantly basaltic shield volcanoes runs NE–SW from the Eyasi half graben for a distance of around 90 km and is bounded to the east by the steep, east-facing Natron Basin boundary fault escarpment (Fig. 7.5). The massif slopes down to the Salei Plain and the Olbalbal depression to the west and infills the Eyasi half graben at the southwestern end of the chain. As indicated by the name, some of the volcanoes (Ngorongoro, Olmoti and Elanairobi) have large craters, but several others, including the highest of this group of volcanoes, Loolmalasin, have no summit crater. Because of the thick soil and, particularly, the vegetation cover on the wetter, eastern and southern sides of the Highlands, exposure is not sufficient to establish the relative stratigraphy and age of the individual eruptive centres. It is possible that lavas from some centres are contemporaneous and intercalated.

Thick sequences of lavas presumed to originate from the more easterly centres of Elanairobi, Loolmalasin and Ngorongoro are exposed in the 800–1000 m escarpment between Lake Manyara and Lake Natron. The flows exposed in the escarpment between Oldoinyo Lengai and Lake Natron are distal flows of basanite, olivine basalt, mugearite, benmoreite and nephelinite, possibly from Elanairobi, and phonolitic nephelinites from Mosonik. Some are possibly interdigitated with distal, low-angle flows from Oldoinyo Sambu to the north. The faulted lava plateau on the floor of the rift valley between lakes Natron and Manyara is made up of flows from the Crater Highlands and distal flows from the Ketumbeine, Gelai and ?Tarosero volcanoes to the east.

#### *Elanairobi/Embagai (Empakai)*

*Type:* shield volcano; *Lat/Long:* 2.92°S 35.83°E; *Elevation:* 3235 m *Relief:* 2000 m above the Salei Plains to the west; *Diameter:* 30 km; *Eruptive history:* Pliocene; *Crater diameter:* 6.3 × 7.8 km; *Composition:* limburgite, trachybasalt, nephelinite, peralkaline phonolite; *QDS:* 39 Angata Salei.

Elanairobi is the most northerly of the Crater Highlands volcanoes. It is a broad shield, rising to 3222 m at its highest point, the Jaeger summit, and lies on a long NE–SW ridge that is bounded on its eastern side by faults that trend in the same direction. On the southern and south-eastern side of the mountain is the spectacular elliptical caldera of Embagai (Plate 1); this measures 6.3 × 7.8 km (the longer axis being east–west) and it has a maximum depth of 980 m. The eastern part of the crater is occupied by a circular lake 3.5 km in diameter, the level of which stands at 2209 m a.s.l. Recent lake-bottom sediments obtained in two boreholes have been deposited at *c.* 30 cm/ka during the late Pleistocene/early Holocene (Muzuka *et al.* 2004).

Trachybasalt flows form the lower parts, and nephelinite and aegirine phonolite the upper parts, of the Embagai crater walls, and limburgite flows occur at the base of the crater walls. Small parasitic cones on the crater floor have covered the crater floor and parts of the crater wall with trachybasalt tuffs, and tuffs crop out on the western and northeastern outer slopes and across the Jaeger summit. On the lower northern slopes, trachybasaltic tuffs overlie flows of basanite, nephelinite and olivine basalt in the gorge of the Engare Sero (Guest *et al.* 1961).

#### *Un-named mountain*

*Type:* unknown; *Lat/Long:* 2.98°S 35.89°E; *Elevation:* 2624 m; *Relief:* 600 m above the land to the west, 300 m above the top of the rift escarpment to the east; *Diameter:* *c.* 8 km; *QDS:* 39 Angata Salei.

This relatively small, un-named, remote mountain lies between Loolmalasin and the village of Kapenjiro. It slopes down gradually to the Embulbul Depression to the west, and more steeply to the top of the rift escarpment immediately west of Engaruka. It is deeply dissected and has the form of steep, heavily forested ridges incised by ravines that drain eastwards into the Engaruka Basin. Its topography suggests that it is a dissected stratovolcano, similar to Mosonik. The mountain is cut off from the nearest driveable track (that from Nainokanoka to Kapenjiro) by deep ravines.

The Lorngabolobolo River, drains the eastern part of the mountain into the Engaruka Basin some 3 km north of Engaruka. In addition to basalt boulders derived from the escarpment, there are boulders of agglomerate (containing basalt and abundant pyroxenite clasts and mica), nephelinite and nepheline-phyric phonolite; the river-bed sand contains abundant grains of mica, black pyroxene and an opaque phase (Dawson & Mitchell personal observation, September 2007). These lithologies are similar to those occurring at Mosonik.



Loolmalasin is the highest of the Crater Highlands volcanoes; 6 km to the west is the subsidiary peak of Olsirwa (3150 m), separated from Loolmalasin by a low col. The mountain is a broad shield and the slopes rise gently from Ngorongoro to the SW and the col between it and Olmoti to the west. The southeastern and eastern slopes, descending to the rift escarpment, are steep, forest-covered, and incised by deep ravines. The summit area, which has no crater, and that of Olsirwa are broken by small north–south fault escarpments.

Exposure is good only in the summit areas of both Loolmalasin and Olsirwa. Basalt and trachyte are the dominant rock-types, with agglomerate in both summit areas. Basalt, trachybasalt and ankaramite of the eastern slopes are exposed in the rift escarpment above Engaruka (Pickering 1965) and, together with mugearite (Paslick *et al.* 1995), are also found as boulders in steams flowing eastwards off the Crater Highlands. In addition, picrobasalt (Paslick *et al.* 1995), basanite and nephelinite (Dawson personal observation), are exposed in small fault-scarps in the area between Engaruka and Mto Wa Mbu.

### Ngorongoro

*Type:* shield volcano with caldera; *Lat/Long:* 3.40°S 36.00°E; *Elevation:* 2380 m; *Relief:* 1400 m above the rift valley; *Diameter:* 35 km; *Eruptive history:* Pliocene; *Crater diameter:* 19 × 22 km; *Composition:* olivine basalt, trachybasalt, trachyte; *QDS:* 53 Ngorongoro.

Ngorongoro is a broad, deeply eroded volcano that has a thick cover of rain forest on its southern and eastern slopes. It has a major summit caldera that is justifiably famous as one of Africa's finest wildlife sanctuaries. The crater (Plate 3) measures 19 × 22 km, the longer axis being east–west, and its area of c. 370 km<sup>2</sup> ranks it amongst the world's largest calderas. The crater floor is at an elevation of around 1700 m a.s.l., and the rim varies between 2100–2400 m. Prior to the collapse that formed the caldera, the volcano may have had an elevation of around 4500–5000 m. A series of small NE-trending faults cut across the northwestern slopes of the volcano, with one on the lower slopes forming the eastern side of the Olbalbal graben (Fig. 7.5).

On the crater floor and at the base of the walls are freshwater springs that are the water supplies for the numerous animals that inhabit the crater. The caldera has no stream outlet and an alkaline seasonal lake (Lake Magad) occurs on the crater floor; it is partly fed by the Munge River that descends from the Olmoti volcano to the north. On the southern and eastern shores of the lake are low eroded bluffs of lacustrine clay, ostracod-bearing clayey limestone and tuffs. These give <sup>14</sup>C ages of 27990 ± 500 BP to 24 400 ± 690 BP (Hay 1976), providing evidence for a lake highstand at around 24 000 BP, but there is no evidence for a highstand at around 9000 BP when many other East African lakes were much more extensive than at present. Flows of basalt and trachyte have welled out at the base of the crater walls, probably from ring fractures, though much of the crater floor appears to be underlain by tuffs. A gravity survey across the caldera (Searle 1971) showed a negative Bouguer anomaly, attributed to both low-density rocks forming the volcano itself and to sediments on the crater floor. There are several small scoria cones on the floor of the crater, one of which, Engitati Hill, is of basaltic composition, and has a vitroclastic texture suggesting that it was formed during a subaqueous eruption (Pickering 1965).

The volcano comprises mainly lavas of basaltic and trachytic composition, but ignimbrites predominate among the later eruptives. Exposures in the crater walls can be seen on the descent track from the western rim (the Windy Gap track) and on the ascent track to the southern rim (the Lerai track). The following account is abbreviated from Hay (1976). 'On the western track

are exposures of trachytic welded tuffs, interbedded with grey trachytic lava. Exposed on the southern track are 340 m of interbedded lavas and pyroclastic rocks; coarsely porphyritic plagioclase–augite–olivine–phyric trachyandesite lavas predominate in the lower part of the section, with slightly porphyritic trachyandesite and olivine basalt in the upper part. Ashes in the lower part of the succession represent voluminous ash eruptions that were erupted before the caldera collapse.' Twelve K–Ar dates range from 2.1 to 2.8 Ma, with a mean of seven dates of 2.46 Ma for a tuff in the lower part of the section, and a mean of five dates of 2.41 Ma for a trachyte 170 m higher in the section (Curtis & Hay 1972). The lower and upper lavas in this section are normally- and reverse-magnetized respectively, with the reversal being dated at 2.45 Ma, corresponding to the boundary between the Gauss normal epoch and the Matuyama reversed epoch (Grommé *et al.* 1970).

On the northwestern slopes of the volcano, stream sections expose trachyte and trachyandesites, together with thin flows of olivine–phyric basalt that overlie red trachytic ignimbrite. A succession of olivine basalt overlying green trachytic ignimbrite, derived from Ngorongoro, is exposed on the fault scarp on the west side of the Olbalbal graben north of Lemagrut (Hay 1976). Anorthoclase from the ignimbrite yielded an age of 2.1 ± 0.1 Ma (Curtis & Hay 1972).

Considering the size of the volcano, there are relatively few chemical data for the lavas. Paslick *et al.* (1995, 1996) gave complete analyses of a basanite and a trachyte, together with analyses of feldspar and Ti-magnetite in the basanite and olivine, clinopyroxene and anorthoclase in the trachyte. Wood (1968) gave analyses of basanite, tephrite, mugearite and phono-tephrite, mainly from the southern rim of the caldera (Appendix 2, Dawson 2008).

Trachytic ignimbrites and tuffs and olivine basalt flows, some interpreted as originating from Ngorongoro and ranging in age from 2.01 to 1.71 Ma, are exposed in the Olduvai Gorge 25 km to the NW. The basal lava in the succession is dated at 2.0 ± 0.1 Ma. (Curtis & Hay 1972). The most distal flow from the volcano is an ignimbrite at Naabi Hill on the Serengeti Plain some 80 km to the NW of Ngorongoro (Hay 1976). Basaltic lavas exposed in the rift escarpment 25 km east of Ngorongoro range in age from 3.8 Ma at the base of the escarpment to 1.4 Ma at the top (Bagdasaryan *et al.* 1973) (Appendix 1, Dawson 2008). However, it is not clear whether the lavas derive from Ngorongoro, the nearby Loolmalasin volcano, or both.

### Lemagrut

*Type:* shield volcano; *Lat/Long:* 3.17°S 35.39°E; *Elevation:* 3135 m; *Relief:* 1300 m above the Serengeti Plains to the west, and about 1000 m on the south side above the pass between Lemagrut and the Oldeani volcano; *Diameter:* 20 km; *Eruptive history:* ?Pliocene; *Crater diameter:* no crater; *Composition:* olivine basalt, nephelinite; *QDS:* 52 Endulen.

Lemagrut is a broad craterless dome standing adjacent to, and west of, Ngorongoro. Radial river valleys incise the northern and northwestern slopes in particular. The northern and western lower slopes are cut by small, east-facing escarpments that result from minor faulting associated with reactivation of the major Sonjo–Eyasi Fault.

The first stage in the formation of the volcano was the eruption of tuffs and agglomerates that occur mainly on the southwestern lower slopes and on the plains to the SW. The tuffs are lithic or crystal tuffs of olivine nephelinite composition; these are interbedded with agglomerates containing pebbles of nephelinite, basalt and jacupirangite, and with rare flows of nephelinite (Pickering 1964). The second stage of activity that formed the main part of the volcano was dominated by the extrusion of olivine basalt and trachybasalt.



**Plate 1.** Aerial view (from 11 000 m) from the east of the Embagai caldera and its lake. The caldera is approximately 7.5 km in diameter and has a maximum depth (to lake level) of 950 m.



**Plate 2.** Aerial view from the east of the circular, 6.5 km wide, Olmoti caldera. Objects in the foreground are Maasai cattle pens. Photograph by M. Punkari.



**Plate 3.** Aerial view (from the east at 11 000 m) of the Ngorongoro caldera; the crater measures  $19 \times 22$  km in diameter. Lake Magad is visible on the caldera floor and the Lemagrut volcano appears in the far distance. The dark area in the foreground, going up to the caldera rim, is forest.



**Plate 4.** The Kibo cone of Kilimanjaro from the south. The summit, the highest point in Africa, stands 5000 m above the surrounding plains. The snowfields are less extensive now than in 1960 when the photograph was taken.



**Plate 5.** Mawenzi from the SW, rising 900 m above The Saddle, the col separating it from Kibo. The serrated appearance is due to weathering-out of a radial dyke swarm.



**Plate 6.** Photograph from the air of the Kibo caldera, from the NE. Uhuru Peak (5895 m), the highest point on the African continent, stands on the far ridge.



**Plate 7.** Aerial view of Oldoinyo Lengai, from the NE, showing the Eastern Chasm debris-flow scar. The white material is altered natrocarbonatite, possibly the residue of lava overspill in the early part of the twentieth century. The main pyroclastic deposits are piled against the Natron Basin boundary escarpment that appears in the background. Photograph by M. Punkari.



**Plate 8.** The northern crater of Oldoinyo Lengai (October 1988) looking north from the summit towards Lake Natron in the distance. The crater is dominated by the cone surrounding the black active lava pool. Lava is flowing from the pool into the depression in the foreground. The scale is given by the tents (bottom right).



**Plate 9.** Photograph from the air of the northern crater of Oldoinyo Lengai from the NE (April 2006) showing hornito and collapsed lava cone within the crater, and whitened natrocarbonatite lava flows spilling over from the crater down the eastern and northwestern outer slopes. Compare with Figures 7.9 and 7.10. Photograph by Dean Polley.



**Plate 10.** Photomicrograph of wollastonite nephelinite BD3955 (Oldoinyo Lengai), in which unstable wollastonite (Wo) is surrounded by a fringe of replacing, metasomatic combeite (Co). Horizontal field width 2.2 mm; plane-polarized light. Ne, nepheline.

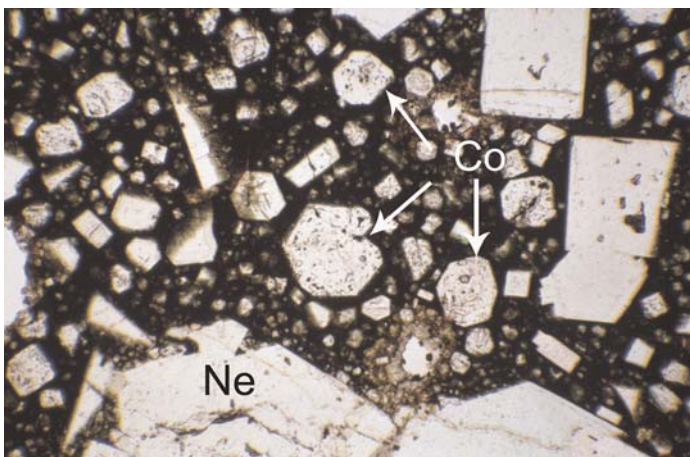


**Plate 11.** Photomicrograph of nephelinite BD3955 (from Oldoinyo Lengai), showing microphenocrysts of magmatic combeite (Co). Horizontal field width 2.2 mm; plane-polarized light. Ne, nepheline.

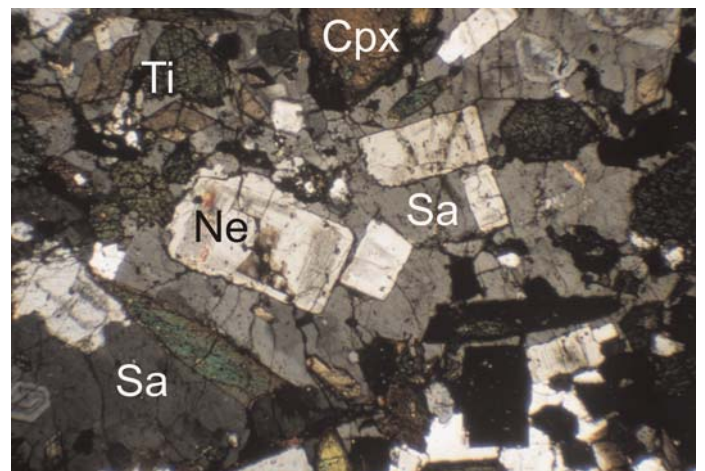


**Plate 12.** Photomicrograph of nepheline syenite BD59 (Oldoinyo Lengai). Phenocrysts of nepheline (Ne), clinopyroxene (Cpx) and titanite (Ti) are surrounded by poikilitic sanidine (Sa). Horizontal field width 5.4 mm; crossed polarizers.

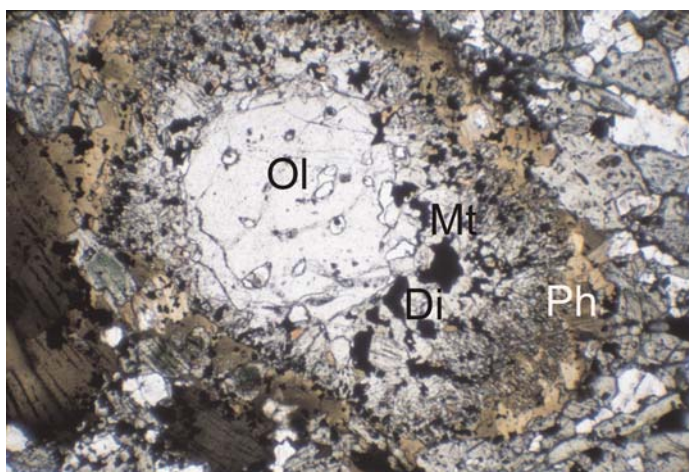


**Plate 13.** Photomicrograph of xenocrystic olivine (Ol) surrounded by a reaction rim of diopside (Di), magnetite (Mt) and phlogopite (Ph) in ijolite BD122 (Oldoinyo Lengai). Horizontal field width 5.4 mm; plane-polarized light.

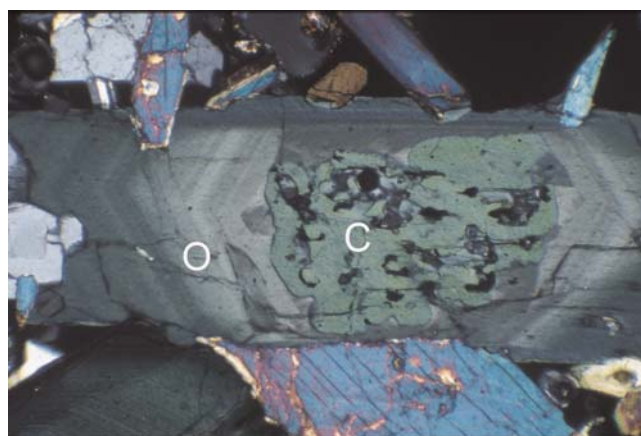


**Plate 14.** Photomicrograph of clinopyroxene in ijolite BD343 (Oldoinyo Lengai). A corroded core (C) is surrounded by complexly-zoned overgrowth (O). Horizontal field width 2.2 mm; crossed polarizers.

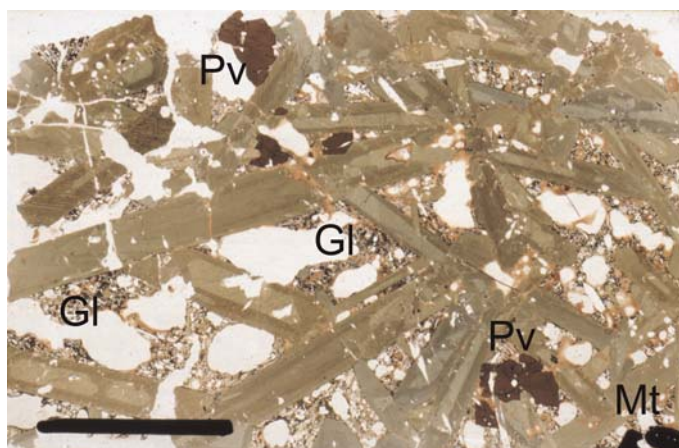


**Plate 15.** Photomicrograph of zoned green clinopyroxene, perovskite (Pv) and magnetite (Mt) cemented by vesiculated glass (Gl) in pyroxenite BD878 (Oldoinyo Lengai); white areas are voids. Scale bar is 10 mm; plane-polarized light.

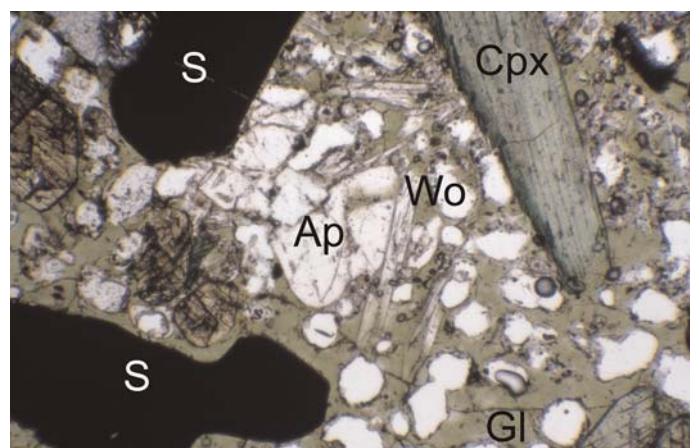


**Plate 16.** Photomicrograph of green vesiculated glass cementing phenocrysts of zoned clinopyroxene (Cpx) and sulphide (S) in ijolite BD127 (Oldoinyo Lengai). Acicular wollastonite (Wo) and apatite (Ap) have precipitated from the glass (Gl). Horizontal field width 2.2 mm; plane-polarized light.



**Plate 17.** Block of acicular wollastonite, with minor nepheline from Oldoinyo Lengai. The crystals are cemented by vesiculated glass. The texture was formed by rapid crystallization of a compositionally unusual magma that was supersaturated in wollastonite. Wollastonite occurs only rarely as an igneous mineral.

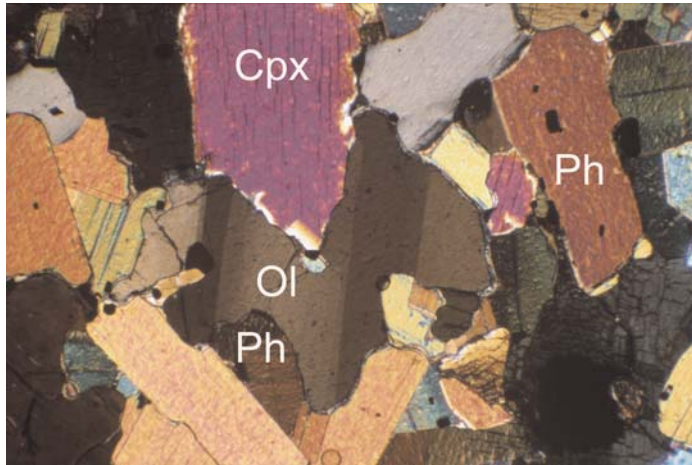


**Plate 18.** Photomicrograph of an olivine–mica pyroxenite BD93 (Oldoinyo Lengai), interpreted as an upper mantle metasomite. Strained and kinked olivine (Ol) is partly replaced by clinopyroxene (Cpx) and phlogopite (Ph). This is a more extreme example of metasomatic replacement of olivine than that shown in Plate 12. The radiogenic strontium and neodymium values for this sample plot to the ‘north’ of EMI on Figure 7.12. Horizontal field width 2.2 mm; crossed polarizers.

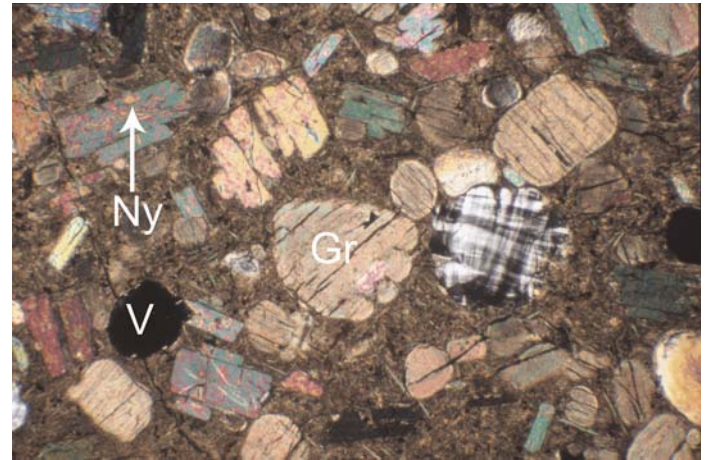


**Plate 19.** Photomicrograph of natrocarbonatite from Oldoinyo Lengai, showing phenocrysts of the complex alkali carbonates nyerereite (Ny, euhedral elongate grains) and gregoryite (Gr, rounded grains, with one basal section showing low-order colour polysynthetic twinning). V, vesicle. Horizontal field width is 5.4 mm; crossed polarizers.

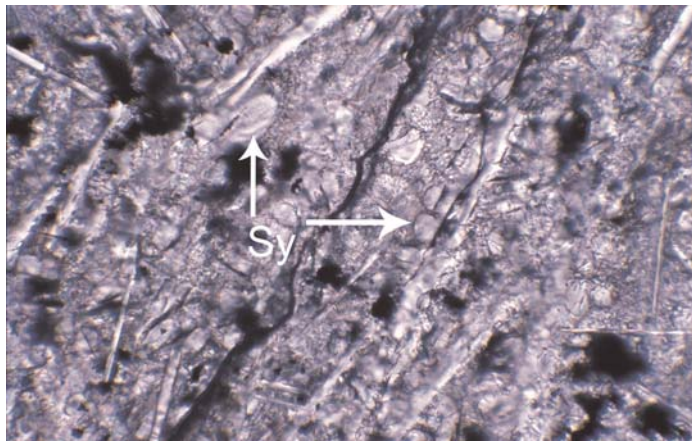


**Plate 20.** Photomicrograph of the groundmass of natrocarbonatite lava, showing rounded microphenocrysts of sylvite (Sy) and slender, elongate microphenocrysts of nyerereite. The rest of the groundmass comprises fine-grained crystals of a complex CaMgSrNaKLa carbonate, apatite, fluorite and opaque sulphides. Horizontal field width 0.5 mm; plane-polarized light.

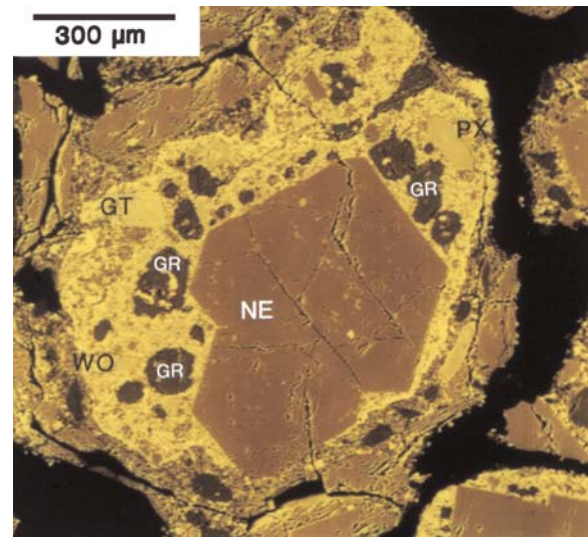


**Plate 21.** Back-scattered, false-colour, image of a lapillus from the 1993 eruption of Oldoinyo Lengai. The silicate lapillus (bright yellow) is encased in less bright natrocarbonatite. The silicate matrix contains a phenocryst of euhedral nepheline (NE) and microphenocrystic wollastonite (WO), garnet (GT) and pyroxene (PX). Set in the silicate matrix are rounded, exsolving globules of natrocarbonatite (GR); see Plate 22.

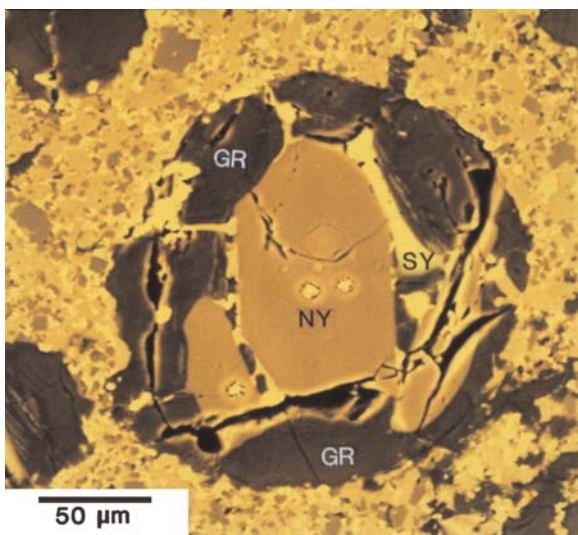


**Plate 22.** Back-scattered, false-colour image of a natrocarbonatite globule in the silicate groundmass of a lapillus from the 1993 eruption (see Plate 21). The globule contains the typical natrocarbonatite minerals gregoryite (GR), nyerereite (NY) and sylvite (SY). The globule is exsolving within the silicate lapillus and is unrelated to the natrocarbonatite surrounding the lapillus.

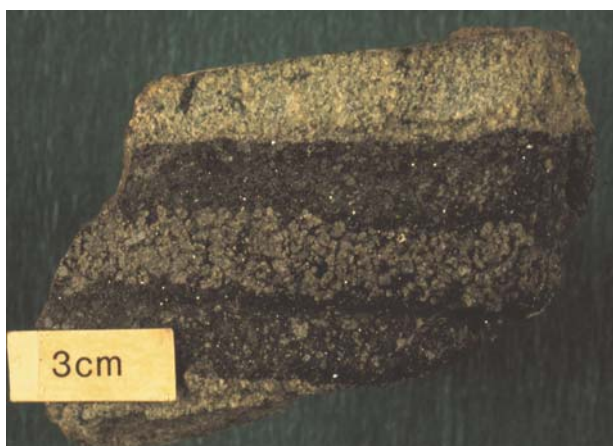


**Plate 23.** An upper mantle xenolith from the Pello Hill tuff cone (for location see Fig. 7. 18). The peridotite wall rock (light green) is cut by a brown vein consisting of mica, amphibole and ilmenite. The vein contains a median slice of altered peridotite that, due to Fe-metasomatism, is now browner than the original. The xenolith bears testimony to brittle fracture in the upper mantle beneath the rift valley.

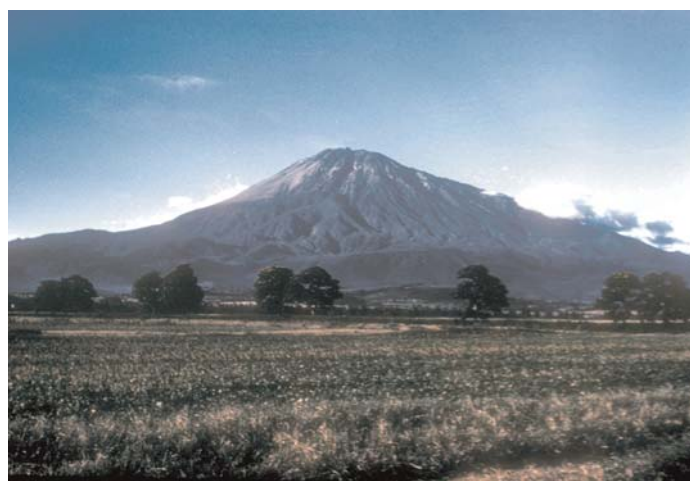


**Plate 24.** Meru from the west, showing classic stratovolcano cone shape and deep radial ravines on the upper slopes that may have been initiated by former glaciation. The summit of the volcano stands some 3000 m above the plains in the foreground.

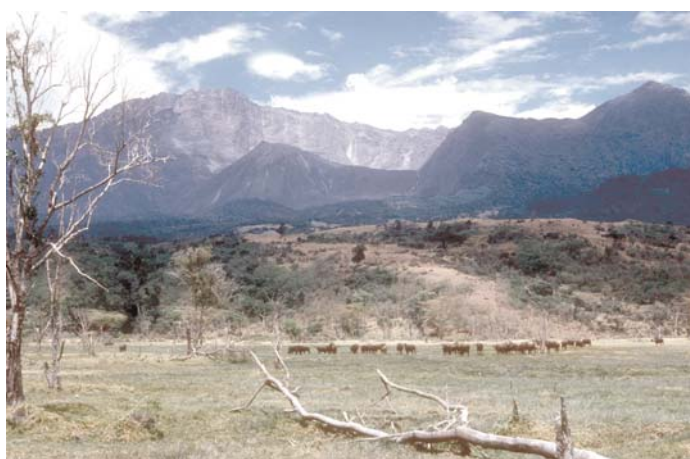


**Plate 25.** Meru from the east, looking into the crater which has been breached with a resulting immense debris avalanche. The recent, central ash cone is visible within the breached crater.

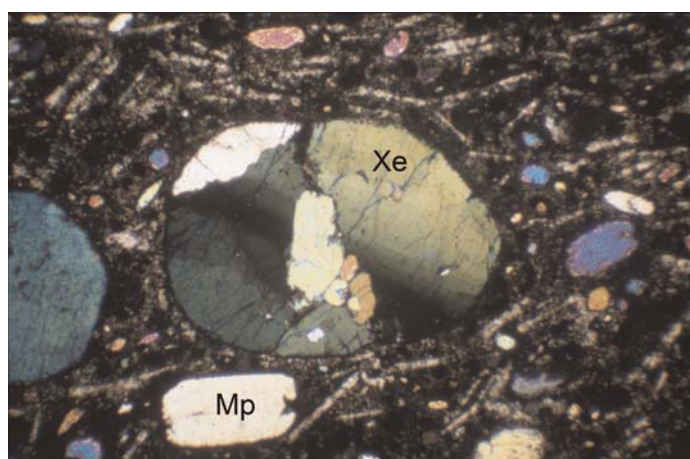


**Plate 26.** Photomicrograph of the kimberlite lava flow at the Igwisi Hills (see Fig. 7.25). A round microxenolith of strained and partly-recrystallized olivine (Xe), and a euhedral microphenocryst of magmatic olivine (Mp), are set in a matrix of dark serpentine and flow-aligned calcite laths. Horizontal field width 5.4 mm; crossed polarizers.

From stream channels on the north side of the volcano, Hay (1976) recorded abundant clasts of trachyandesite and plagioclase–olivine–augite–phyric basalt, and rare trachyte. In the Olduvai Side Gorge are similar clasts, plus clasts of nepheline–pyroxene–titanite–phyric nephelinite, and melilitite tuff containing melilitite, nepheline, pyroxene, perovskite, biotite, melanite and titanite.

On the lower southeastern slopes [ $3^{\circ}11'S$   $35^{\circ}22.5'E$ ], nepheline–phyric phonolite, containing groundmass sodalite, underlies a flow of olivine–barkevikite mugearite (Dawson personal observation). Paslick *et al.* (1995, 1996) provide complete analyses of this phonolite (and its nepheline and clinopyroxene), and of the mugearite (and of olivine, clinopyroxene, feldspar and Ti-magnetite therein).

On the western slopes of the volcano the fossiliferous Laetoli beds (see Dawson 2008, Chapter 5) are overlain by the Ogol lavas that erupted from small, local cones. The lavas, dated at 2.41 Ma, have been called vogesite (Drake & Curtis 1987) but Wirth & Adelsberger (2002) recorded them as being of primitive ( $mg\# > 0.6$ ) alkali olivine basalt (where  $mg\# = Mg/(Mg + Fe)$ ).

Stratigraphic relationships at Laetoli indicate that Lemagrut and Sadiman (below) were active at the same time.

### Sadiman

*Type:* stratovolcano; *Lat/Long:*  $3.20^{\circ}S$   $35.42^{\circ}E$ ; *Elevation:* 2870 m; *Relief:* 500 m; *Diameter:* 6 km; *Eruptive history:* Pliocene; *Crater diameter:* none; *Composition:* nephelinite, phonolite, melilitite, carbonatite; *QDS:* 52 Endulen.

Sadiman is a small, well-forested cone situated between Lemagrut and the Ngorongoro caldera. It is formed mainly of tuffs and agglomerates, containing clasts of nephelinite and melilitite, with subsidiary flows of nephelinite and phonolite (Pickering 1964). From stream channels on the north side of the volcano, Hay (1976) reported rare clasts of ijolite together with abundant clasts of nepheline–anorthoclase–pyroxene–phyric nephelinite and phonolite, in which microphenocrysts of titanite are common.

Nepheline–phyric phonolitic nephelinites containing abundant titanite (some strongly zoned) form the summit ridge (Dawson personal observation). A complete rock analysis, and analyses of nepheline and titanite from one of these nephelinites are given by Paslick *et al.* (1995, 1996). James (1966) described a 'nephelinite boss', which he refers to as 'Malanja'. As Sadiman stands above the Malanja depression and is surrounded by the lavas of Lemagrut, as described by James (1966), it seems probable that they are the same. He gave a whole-rock analysis of a nephelinite (Appendix 2, Dawson 2008) that, in its lower  $SiO_2$  content, differs from the phonolitic nephelinite of Paslick *et al.* (1995).

A lava sample from the volcano has given a K–Ar age of 3.7 Ma, which is indirectly confirmed by the presence of clasts of Sadiman lava in the lowest part of Bed I of the Olduvai succession (Hay 1976), indicating that the volcano is older than 2.1 Ma. The volcano is also believed to be the source of the phonolitic and melilititic ash of the fossiliferous Laetoli Beds 15 km to the west (Dawson 2008, Chapter 6).

### Oldeani

*Type:* shield volcano; *Lat/Long:*  $3.29^{\circ}S$   $35.44^{\circ}E$ ; *Elevation:* 3219 m; *Relief:* 2000 m above Lake Eyasi to the SW, 780 m above the rim of the Ngorongoro caldera to the east; *Diameter:* 20 km; *Eruptive history:* Pliocene; *Crater diameter:* 5 km; *Composition:* olivine basalt, basalt, ankaramite, trachybasalt, trachyte; *QDS:* 52 Endulen.

Oldeani is a broad dome that stands astride and infills the Eyasi half graben. The summit crater is breached to the west, and the

lower northwestern slopes are cut by small east-facing escarpments that result from minor faulting associated with reactivation of the major Sonjo–Eyasi fault.

Outcrop is poor, the eastern and southern slopes being covered with dense forest, and there is thick bamboo forest in the summit area. Flows of basalt occur on the western slopes, and of trachybasalt and trachyte in the summit area. Small basalt scoria cones are associated with minor faulting on the lower southeastern slopes (Pickering 1964).

Trachytic ignimbrite, and red soils derived from weathered ignimbrite, interpreted as deriving from Oldeani, are widespread on the Mbulu Plateau for distances up to 30 km to the south of Oldeani (Orridge 1965).

### Angata Salei–Serengeti plains

A large area to the west of the Crater Highlands, including much of the Salei and Serengeti plains, is covered with a brown calcareous tuff that, in places, drapes basement hills (Pickering 1958). This tuff thins and becomes more calcitic westwards towards Lake Nyanza, and in the Olduvai Gorge area it commonly overlies nephelinitic or trachytic tuffs from which it is separated by zones of zeolite. These calcareous tuffs were originally interpreted as calcrete (Pickering 1958; Hay 1963), but Dawson (1964a) suggested that the tuffs and, possibly, earlier 'calcretes' in the aeolian horizons in the upper Olduvai Beds might be the result of deposition and recrystallization of carbonatite tephra from the Kerimasi and Oldoinyo Lengai volcanoes that lie upwind of the Serengeti and thus ideally situated as tephra sources, a suggestion endorsed by Hay (1964). Subsequent detailed work (Hay 1976) correlates the Masek Beds exposed in the Olduvai Gorge (age 0.6 and *c.* 0.4 Ma) with eruptions of Kerimasi, and the more extensive Ndotu (60 000 to 400 000 BP) and Naisiusiu Beds (age 15 000 to 22 000 BP) with the earliest material erupted from Oldoinyo Lengai. Later ashes and tephra from Oldoinyo Lengai (the Namorod ashes of Olduvai) are deposited above calcretes at the top of the Naisiusiu Beds.

Holocene black ash derived from Oldoinyo Lengai forms fixed dunes on the Salei Plain (Guest *et al.* 1961) and also occurs as migrating dunes on the Serengeti Plain (Hay 1976); the ash is abundant on the more northerly Crater Highlands but does not appear to have been deposited further south than Olmoti (Dawson personal observation).

An outlier of the Crater Highlands volcanism is Engelosin, an isolated small plug, 500 m in diameter, and 145 m high, on the Serengeti Plain north of Olduvai [ $2^{\circ}54.5'S$   $35^{\circ}23'E$ ]. It is an anorthoclase–augite–phyric phonolite containing a groundmass of nepheline, anorthoclase, aegirine, a REE silicate and titanite. The age is unknown but its highly eroded nature suggests that it may be Pliocene or older (Hay 1976).

### The Engaruka–Manyara area

*QDS:* 53 Ngorongoro and 54 Monduli.

The main rift escarpment and the escarpments of many minor faults on the Engaruka Block (Fig. 5.8) are notable for the exposure of lava flows forming the lower parts of some of the more easterly Crater Highland volcanoes (Loolmalasin and Ngorongoro). The most common flows are of olivine- and olivine–pyroxene–phyric basalt, but also present are barkevikite trachybasalt and nepheline–phyric olivine nephelinite. In the lower parts of the rift escarpment at Engaruka are flows of limburgite and olivine–phyric basalt (Dawson personal observation). Boulders of the same rock-types are present in outwash in the Engaruka and Engaibataat rivers, and also occur in agglomerate

mounds (possibly resulting from erosion of distal outwash sheets from the main escarpment) on the plain NW and north of Essimigor. Wood (1968) gave an analysis of a high-K basanite boulder from Engaruka (Appendix 2, Dawson 2008).

In the gorge of the Loburu River, cutting eastwards across the northern end of the Engaruka Block, at least one boulder bed is interbedded with the basalts, indicating an erosional break with clastic sedimentation within the lava-dominated sequence (Dawson personal observation).

In the area, are many minor flows or spatter cones that were extruded contemporaneously with, or immediately following, the faulting (Fig. 5.8). These include olivine trachybasalt from Engaruka and Narabala (Engaruka also contains barkevikite). At Kitete [ $3^{\circ}11'S$   $35^{\circ}56.5'E$ ] a number of small flows, ranging from basanite to phonotephrite, were extruded from the main rift fault; these flows have ages of 0.95 to 1.23 Ma (MacIntyre *et al.* 1974). Paslick *et al.* (1995) gave a complete analysis of one of the flows (BD180, an olivine–barkevikite phonotephrite, dated at *c.* 1.0 Ma). In addition, Orkandira hill [ $3^{\circ}11'S$   $36^{\circ}01'E$ ] is an extrusion of analcite in which phlogopite occurs as a poikilitic groundmass phase sometimes protruding into calcite-filled amygdalae.

#### *Essimigor (also known as Losimingori)*

*Type:* stratovolcano; *Lat/Long:*  $3.40^{\circ}S$   $36.10^{\circ}E$ ; *Elevation:* 2165 m; *Relief:* 1000 m; *Volcano diameter:* 16 km; *Eruptive history:* Miocene–Pliocene; *Composition:* nephelinite–phonolite; *QDS:* 54 Monduli.

Essimigor is the oldest volcano in northern Tanzania, with K–Ar ages on poorly-documented lavas of 8.1 Ma on a melane-nephelinite, and of 4.68 and 3.22 Ma on two nephelinites (Appendix 1).

It is a dominantly pyroclastic volcano and, due to deep erosion and thick forest on most of the upper slopes on the eastern, southern and western sides of the mountain, there is no sign of an original crater, the summit area being a series of steep interconnected ridges. A lobe of lavas, possibly flowing from a former, breached crater, extends southwestwards from the main pyroclastic part of the cone (Dawson 1964*b*). The lowest western and southern slopes are blanketed by limestones that were deposited in former extensions of Lake Manyara, and the lower northwestern and northern slopes are partly covered by mounds of poorly-consolidated agglomerate resulting from outwash from the main rift escarpment to the west.

Nephelinitic and phonolitic tuffs and agglomerates, some containing blocks of sodalite-bearing ijolite and nepheline syenite, form the bulk of the volcano. Lavas, both intercalated with the pyroclastics and forming the SW lava lobe, are of three main types: (i) sodalite–anorthoclase–aegirine–augite–phyric phonolites, in which titanite, aenigmatite and magnetite are groundmass phases; (ii) olivine-free nephelinites, in which nepheline, aegirine–augite, melanite and magnetite are the main phenocrysts, and perovskite is a common groundmass mineral; altered melilite is a rare phenocryst phase; and (iii) augite, in which abundant phenocrysts of titanite and rarer perovskite and sodalite, are set in a matrix of nepheline or analcite, perovskite and magnetite; rare olivine grains (? xenocrysts) are surrounded by rims of phlogopite and magnetite. Where analcite is the only groundmass feldspathoid, these rocks would be more correctly described as analcites. Rarer flows are of ankaramite and trachyte. Dykes of monchiquite, ankaramite, analcite, nephelinite and phonolite occur on the southeastern ridge of the mountain and in the summit area. Wood (1968) gave analyses of four nephelinites and Paslick *et al.* (1995) gave complete analyses of olivine augite, melilite nephelinite and augite.



**Fig. 7.6.** The Older Extrusive cone of Tarosero, from the south. The cone shape results from the volcano being composed of viscous trachyte and phonolite lavas.

#### *Tarosero*

*Type:* lava cone; *Lat/Long:*  $3.20^{\circ}S$   $36.36^{\circ}E$ ; *Elevation:* 2242 m; *Relief:* 700 m on north slopes, 500 m on south slopes; *Volcano diameter:* 7 km; *Eruptive history:* Pliocene; *Composition:* alkali olivine basalt, hawaiite, peralkaline trachyte, phonolite and comendite; *QDS:* 54 Monduli.

The gentle cone of Tarosero (Fig. 7.6) stands above a northerly-dipping lava plateau that consists of alkali basalt and benmoreite, the eruptive centre(s) for which is (are) not certain. Early trachyte flows extruded from the volcano, dated at 2.2–2.4 Ma (MacIntyre *et al.* 1974), are faulted like the underlying lava plateau and some are well exposed in the escarpment that forms the western side of the Lembolos graben.

The cone itself consists mainly of younger (2.02 Ma), unfaulted, peralkaline trachytes. There are subsidiary trachyte cones on the lower, northern slopes of the volcano, and a crater (2.5 km in diameter), surrounded by trachytic tuffs, perforates its lower, southern flanks. Peralkaline rhyolites (comendites) occur at Oldoinyo Sambu on the lower northwestern slopes (Dawson 1964*b*).

Principal component analysis of major- and trace-elements in 41 lava samples (Cooper 1972) has established two main lava groups, dominated by trachytes, which are alkaline to peralkaline, characteristically containing Na-rich amphiboles, Na-clinopyroxene and aenigmatite; most are acmite-normative and some are nepheline-normative. Group I ranges from benmoreite through trachytes and quartz trachytes to comendites that can be linked by pyroxene and feldspar fractionation. The more siliceous are peralkaline, and chevkinite  $[(Ce,La,Ca)_4Fe^2(Fe^2Ti)_2Ti_2Si_4O_{22}]$  occurs in one quartz trachyte (Macdonald *et al.* 2002). Within this group are less common phonolites and phonotephrites. Group II comprises quartz trachytes, trachytes and nepheline-normative trachytes containing sodalite, eudyalite and aenigmatite (Dawson 1997). All are peralkaline and, relative to Group I rocks with the same major element concentrations, are enriched in Cl, Ba, Sr, Rb, REE, Nb, Zr and Pb; some have >3000 ppm Zr (Tables 7.2, 7.3).

The trachytes of both groups comprise phenocrysts of zoned anorthoclase (rims higher in  $K_2O$  but lower in BaO than cores), richterite, alkali pyroxene and rare biotite (Table 7.4), the mafic phases being high Na and Fe varieties. The groundmass contains anorthoclase (compositions overlap those of the phenocryst rims), amphibole (containing less  $Na_2O$  and FeO, but higher CaO and MgO than phenocrysts) and aenigmatite, the presence of which coincides with an absence of FeTi oxides in the groundmass. Sodalite is a common phase in the Group II rocks.

**Table 7.2.** Tarosero lavas-selected major element analyses (from Cooper 1972)

Sample	Group I lavas								Group II lavas					
	1	2	3	4	5	6	7	8	9	10	11	12	13	14
SiO <sub>2</sub>	56.87	58.27	60.23	61.49	62.25	63.45	65.7	71.81	59.41	60.72	60.94	61.15	62.12	62.13
TiO <sub>2</sub>	1.65	0.83	0.89	0.52	0.62	0.44	0.41	0.20	0.28	0.48	0.45	0.50	0.30	0.29
Al <sub>2</sub> O <sub>3</sub>	16.29	19.58	20.18	17.60	16.20	17.17	14.16	12.04	15.85	15.09	15.24	15.37	16.15	16.80
Fe <sub>2</sub> O <sub>3</sub>	4.11	1.94	3.69	3.45	3.72	2.70	2.79	4.51	4.99	4.87	4.76	4.89	2.36	3.41
FeO	4.63	2.74	1.07	3.76	2.76	1.18	2.87	0.06	1.27	4.04	4.04	3.85	3.91	2.41
MnO	0.16	0.16	0.10	0.14	0.13	2.87	0.22	0.09	0.25	0.25	0.28	0.27	0.26	0.24
MgO	1.82	0.61	0.49	0.07	0.06	0.19	0.27	0.00	0.38	0.12	0.20	0.18	0.11	0.22
CaO	4.62	2.81	2.24	0.48	0.58	1.08	0.70	0.28	4.22	1.24	1.15	0.69	0.91	1.12
Na <sub>2</sub> O	5.42	7.52	5.56	6.33	6.87	7.55	6.46	5.76	6.38	7.06	6.81	6.92	7.27	6.54
K <sub>2</sub> O	2.85	4.64	4.78	5.31	5.97	5.37	5.66	5.24	6.35	5.30	5.30	5.38	5.72	5.11
P <sub>2</sub> O <sub>5</sub>	0.93	0.23	0.24	0.00	0.06	0.13	0.00	0.00	0.00	0.00	0.00	0.00	0.00	0.00
Sum	99.35	99.33	99.47	99.15	99.22	99.34	99.24	99.99	99.38	99.17	99.17	99.20	99.11	99.31
(Na + K)/Al	0.74	0.88	0.76	1.00	1.17	1.11	1.27	1.35	1.22	1.21	1.17	1.18	1.19	1.16

1. BD329 Benmoreite, N end of Tarosero scarp 3°07.9'S 36°24.75'E; 2. BD509. Phonolite, gorge on lower SW slopes 3°13.5'S 36°18.7'E; 3. BD 513 Qtz-normative trachyte, gorge on lower SW slopes, 3°13.5'S 36°18.7'E; 4. BD488 Qtz-hyp-normative trachyte, east-summit ridge, 3°12'S 36°22.8'E, age 1.94 ± 0.06 Ma.; 5. BD261 Nepheline-normative trachyte, western slopes 3°11.7'S 36°15.4'E; 6. BD255 Nepheline-normative trachyte, Oldoinyo Sambu (small hill on western slopes) 3°08.5'S 36°15'E; 7. BD290 Comenditic trachyte, Oldoinyo Sambu 3°09.5'S 36°17'E; 8. BD289 Comendite, Oldoinyo Sambu 3°09.2'S 36°16.6'E; 9. BD305 Sodalite phonolite, lower north slopes, 3°06'S 36°20.5'E; faulted; age 2.25 ± 0.06 Ma; 10. BD295 Nepheline normative trachyte, gorge on lower SW slopes, 3°13.5'S 36°18.7'E; 11. BD510 Sodalite trachyte, gorge, lower SW slopes, 3°13.5'S 36°18.7'E, age 2.21 ± 0.10 Ma; 12. BD490 Sodalite trachyte, summit of Tarosero, 3°11.1'S 36°21.6'E; dated at 2.10 ± 0.06 Ma; 13. BD306 Sodalite, nepheline-normative trachyte, lower north slopes, 3°06'S 36°20.5'E faulted; age 2.20 ± 0.06 Ma. Major element chemistry is similar to group I sample BD255; 14. BD512 Quartz-normative sodalite trachyte, gorge on lower SW slopes, 3°13.5'S 36°18.7'E. Major element chemistry is similar to Group I sample BD 261.

The range in lava types on this single volcano covers the same compositional spectrum as the regional trachytes in Kenya. The absence of an overall trend in the extrusion sequence (the latest extrusions are of quartz trachyte), together with interbedding of (a) nepheline-normative and quartz-normative lavas, and (b) Group I and Group II lavas, indicates complex evolution and emptying of the sub-volcanic magma chamber or chambers.

In addition to the analyses of Cooper (1972), Paslick *et al.* (1996) gave complete rock analyses of one phonotephrite and one nephelinite. However, it is possible that the nephelinite

sample, from Njanja to the south of Tarosero, may derive from the nearby Burko volcano (Dawson personal observation).

#### Monduli

*Type:* ?stratovolcano; *Lat/Long:* 3.25°S 36.48°E; *Elevation:* 2660 m; *Relief:* 930 m on south and east sides, 600 m on north side; *Volcano diameter:* 6 × 10 km; *Eruptive history:* not known; *Composition:* olivine basalt and trachyte; *QDS:* 54 Monduli.

**Table 7.3.** Tarosero lavas-trace element differences between Group I and Group II rocks of similar silica contents and similar alkalinity (from Cooper 1972)

Sample	Group I BD255	Group II BD306	Group I BD261	Group II BD512	Group II maximum concentrations
SiO <sub>2</sub> (wt%)	63.45	62.12	62.25	62.3	
(Na + K)/Al	1.11	1.19	1.17	1.16	
Ba	640	838	517	1029	1446
Ce	443	992	378	1205	1322
Cl	173	263	172	178	725
Cr	28	7	41	0	13
La	179	476	213	669	868
Nb	131	320	118	454	454
Nd	82	177	104	238	279
Ni	3	4	8	9	9
Pb	21	43	5	49	62
Pr	38	100	46	139	181
Rb	191	360	135	242	391
Sm	32	60	26	78	85
Sr	156	806	22	199	806
Th	62	148	42	192	196
V	53	23	19	9	30
Y	70	173	67	164	295
Zn	87	336	201	340	520
Zr	1145	2611	744	3355	3355

Values in ppm; XRF analyses.

**Table 7.4.** Electron-microprobe analyses of phases in Tarosero trachytes

	In Group I trachyte BD255											In Group II sodalite trachyte BD295					In Group II sodalite trachyte BD512				
	1	2	3	4	5	6	7	8	9	10	11	12	13	14	15	16	17	18	19	20	21
SiO <sub>2</sub>	49.40	50.30	49.60	50.60	49.70	39.60	38.50	65.90	66.50	66.60	66.60	38.70	38.80	38.80	39.90	50.1	45.20	47.60	50.10	49.30	38.50
ZrO <sub>2</sub>	0.16	0.01	0.11	0.06	0.85	0.05	0.07	na	na	na	na	na	na	na	na	11.3	0.07	1.64	0.10	0.49	0.19
TiO <sub>2</sub>	2.03	1.24	1.17	1.23	0.60	2.48	3.07	na	na	na	na	na	na	na	na	0.18	1.85	1.79	0.20	0.69	6.08
Al <sub>2</sub> O <sub>3</sub>	0.57	1.16	2.15	1.43	0.26	11.20	11.60	20.40	18.20	19.00	18.20	26.30	27.80	26.40	26.00	0.20	3.91	0.65	0.46	0.60	1.19
Fe <sub>2</sub> O <sub>3</sub>								0.25	1.40	0.71	1.26	2.99	2.45	3.15	3.97						
FeO	24.90	19.10	19.50	17.70	22.20	12.80	13.30										23.40	23.80	30.70	22.70	41.90
MnO	1.4	1.14	1.15	1.09	1.24	0.42	0.44	na	na	na	na	na	na	na	na	1.24	1.02	1.00	1.41	0.90	1.55
MgO	5.81	10.20	9.69	11.50	4.19	16.90	16.00	na	na	na	na	0.09	0.05	0.20	0.12	na	7.19	1.66	2.72	3.68	0.80
CaO	4.07	6.17	6.03	6.54	15.9	0.02	0.00	1.44	0.15	0.47	0.17	0.05	0.04	0.01	0.02	8.70	7.36	10.70	1.86	16.00	0.62
Na <sub>2</sub> O	7.07	6.26	5.79	6.07	4.01	0.95	0.85	9.21	7.52	8.61	7.81	25.30	24.30	25.30	23.90	12.90	5.00	6.94	8.34	4.92	7.72
K <sub>2</sub> O	1.22	1.24	1.21	1.22	0.00	8.93	8.86	3.07	6.33	4.72	5.57	0.08	0.14	0.09	0.17	0.33	1.30	0.13	1.52	0.00	0.04
Nb <sub>2</sub> O <sub>5</sub>	0.04	0.09	0.06	0.00	0.00	0.06	0.00	na	na	na	na	na	na	na	na	0.55	0.00	0.22	0.02	0.00	0.43
SO <sub>3</sub>	na	na	na	na	na	na	na	na	na	na	na	0.05	0.07	0.04	0.05	na	na	na	na	na	na
Cl	0.02	0.03	0.02	0.03	na	0.02	0.02	na	na	na	na	7.09	6.98	7.15	7.11	2.13	0.00	0.00	0.02	na	na
Sum												100.65	100.63	101.14	101.24	98.05					
Less O≡Cl												1.63	1.60	1.64	1.63	0.48					
Total	96.69	96.94	96.48	97.47	98.95	93.43	92.71	100.27	100.10	100.11	99.61	99.02	99.03	99.30	99.61	97.57	96.30	96.13	97.45	99.28	99.10

Analyst: J. B. Dawson. na, not analysed.

1, Large dark-blue poikilitic ferri-richterite; 2, 3, Green groundmass ferri-richterite; 4, Brown richterite inclusion in feldspar phenocryst; 5, Aegirine phenocryst; 6, Mica phenocryst; 7, Mica included in feldspar phenocryst; 8, Core of anorthoclase phenocryst; total includes 0.25 wt% BaO; Or 16.8, Ab 76.2, An 6.6, Cs 0.4 mol%; 9, Rim of anorthoclase phenocryst; total includes 0.06 wt% BaO; Or 35.5, Ab 63.8, An 0.7, Cs 0.1 mol%; 10, Core of groundmass anorthoclase; BaO below detection; Or 25.9, Ab 71.9, An 2.2 mol%; 11, Rim of groundmass anorthoclase; total includes 0.18 wt% BaO; Or 31.6, Ab 67.3, An 0.8, Cs 0.3 mol%. This specimen also contains zoned chevkinite (Macdonald *et al.* 2002); 12, 13, Core and rim of sodalite phenocryst; 14, 15, Core and rim of sodalite phenocryst; 16, Groundmass eudialyte; total includes 0.57 wt.% La<sub>2</sub>O<sub>3</sub>, 0.94% Ce<sub>2</sub>O<sub>3</sub> and 0.58% Nd<sub>2</sub>O<sub>3</sub>; 17, Dark-brown, partly-absorbed kataphorite xenocryst, mantled by corona of light-brown, unidentified phase and green aegirine; 18, Unidentified light-brown phase, in corona round kataphorite xenocryst; 19, Blue groundmass ardevsonite; 20, Green aegirine in corona around kataphorite xenocryst; 21, Groundmass aenigmatite.

Monduli mountain is an east–west trending structure, with steep southern and eastern slopes, and more gradual northern and western slopes, the northern slopes grading down onto the lava plateau that dips northwards towards Tarosero. The mountain is thickly vegetated, with bamboo forest in the summit area, and also has a thick veneer of tuffs derived from the Meru volcano to the east. Hence much of the structure of Monduli is speculative. The Tarosero escarpment, that forms the eastern boundary of the lava plateau, is obscured by the eastern lower slopes of Monduli, and the steep southern slopes of the mountain may be due in part to faulting. However, the deeply dissected appearance of the eastern and southern slopes suggest that these parts of the structure are formed of poorly consolidated material (? pyroclastics or fault-related volcanic debris) (Dawson 1964*b*). Exposure is poor, and the few patchy outcrops have yielded specimens of olivine basalt and trachyte. A basalt flow on the lower northwestern slopes contains xenoliths of spinel harzburgite that contain primary carbonate (Lee *et al.* 2000).

Paslick *et al.* (1995, 1996) gave complete analyses of one tephrite and two picobasalts, and analyses of olivine and clinopyroxene in the two picobasalts. Roberts (2002) gave analyses

of two basanites and two basalts from the volcano and of a tephri-phonolite dyke which has affinities with similar rocks at Meru immediately to the east.

#### Kilimanjaro

*Type:* line of overlapping shield volcanoes; *Lat/Long:* Kibo cone 3.07°S 37.37°E; *Elevation:* 5895 m; *Relief:* 4400 m; *Diameter:* 85 × 45 km; *Eruptive history:* Pliocene–Recent; *Crater diameter:* Kibo crater 2.5 km (main caldera), 900 m (inner crater); *Composition:* alkali olivine basalt, trachybasalt, peralkaline trachyte and peralkaline phonolite; *QDS:* 42, 56 and 57 Kilimanjaro (Downie *et al.* 1965).

Kilimanjaro is a massive mountain formed by the coalescence of three major volcanoes, Shira, Kibo and Mawenzi (Fig. 7.7). The Kibo summit is the highest point on the African continent and, with the exception of some of the highest Hawaiian Islands which rise from the Pacific Ocean floor, in its relative relief is the highest mountain on Earth. An ascent of the mountain goes from the equatorial luxuriance of the foothills to the Arctic-zone glaciers

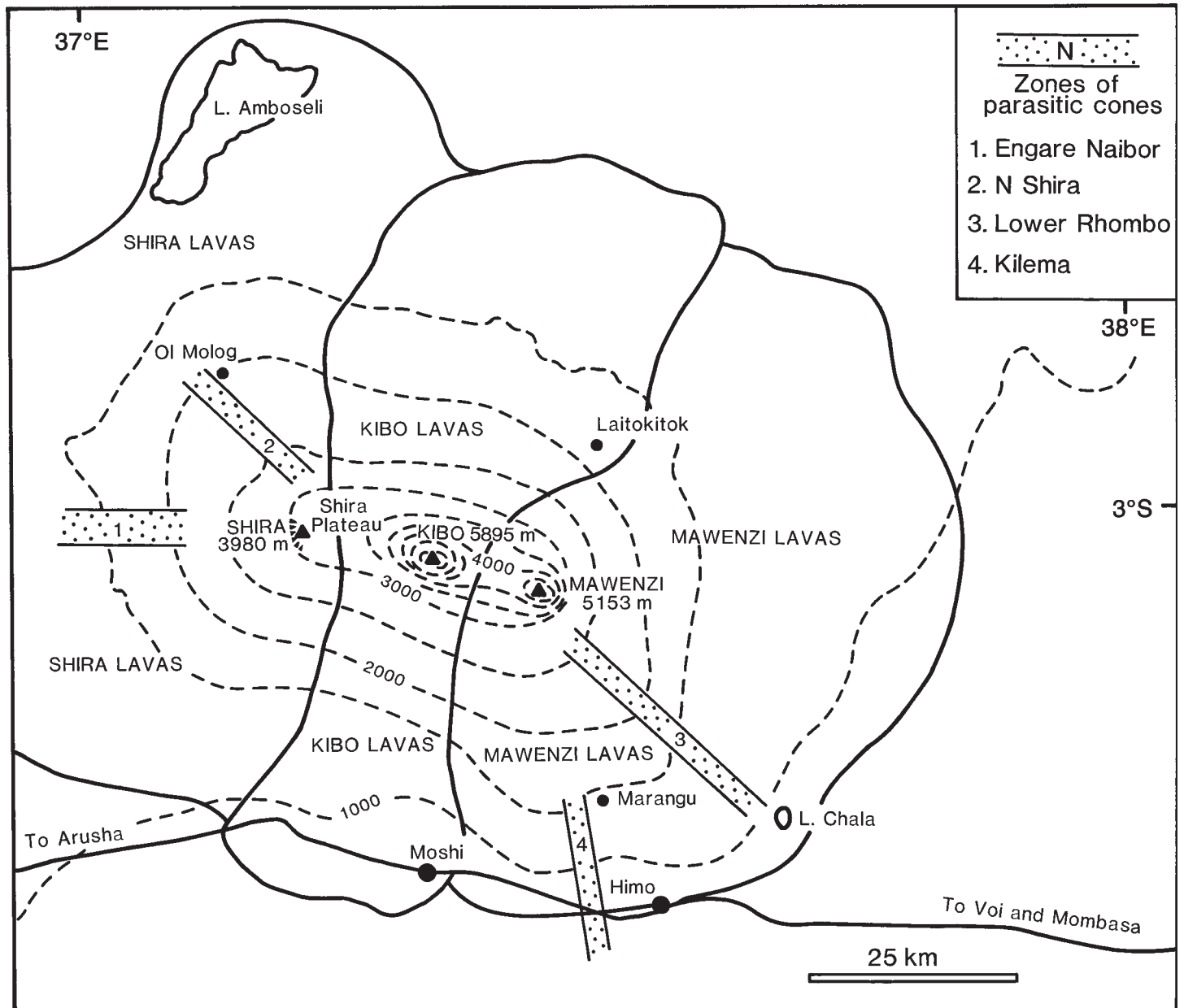


Fig. 7.7. Map of the Kilimanjaro massif showing distribution of lavas from the main centres, and the zones of late parasitic cones.

of the Kibo cone (Plate 4), a traverse of the Earth's vegetation zones on a single mountain. Due to the monsoon and counter-monsoon winds, with their associated high rainfall, there is dense forest on the southwestern, southern and eastern slopes of the massif between around 1500 and 3300 m and, due to the poor exposure, the geology of these lower slopes is poorly-known compared with the upper parts of the volcanoes. However, highly mobile extrusions of basanite and olivine basalt have flowed out onto the plains surrounding the massif, and flat-lying, distal lava flows can be found at considerable distances away from the actual topographic mountain, in the Amboseli area on the western, northern and eastern sides of the massif (Williams 1969).

The most comprehensive account of the geology is that of Downie & Wilkinson (1972). The massif overall is elongated NW-SE, but the WNW-ESE alignment of the three, equally spaced, major eruptive centres is oblique to this major trend.

There are also numerous small parasitic lava cones, often concentrated along elongate zones on the lower and middle slopes of the massif. Two of the larger zones, on the lower north-western slopes of Shira and the lower southeastern slopes of Mawenzi, follow the main NW-SE trend of the massif (Fig. 7.10).

*Shira.* The oldest and most westerly major centre is a relatively simple cone with a large, eroded summit crater, approximately 4 km in diameter. The crater forms a plateau at around 3700 m, but is bounded on its western and southern sides by ridges formed by the old crater rim, the highest point on which is Klute Peak (3970 m). On its northern and eastern sides, the crater is buried by later extrusions from Kibo. A conical hill, Platzkegel, on the southern part of the Shira Plateau, is a major vent infilled with basaltic breccia and cut by dolerite and essexite intrusions. The lower lavas of Shira, exposed on the northwestern

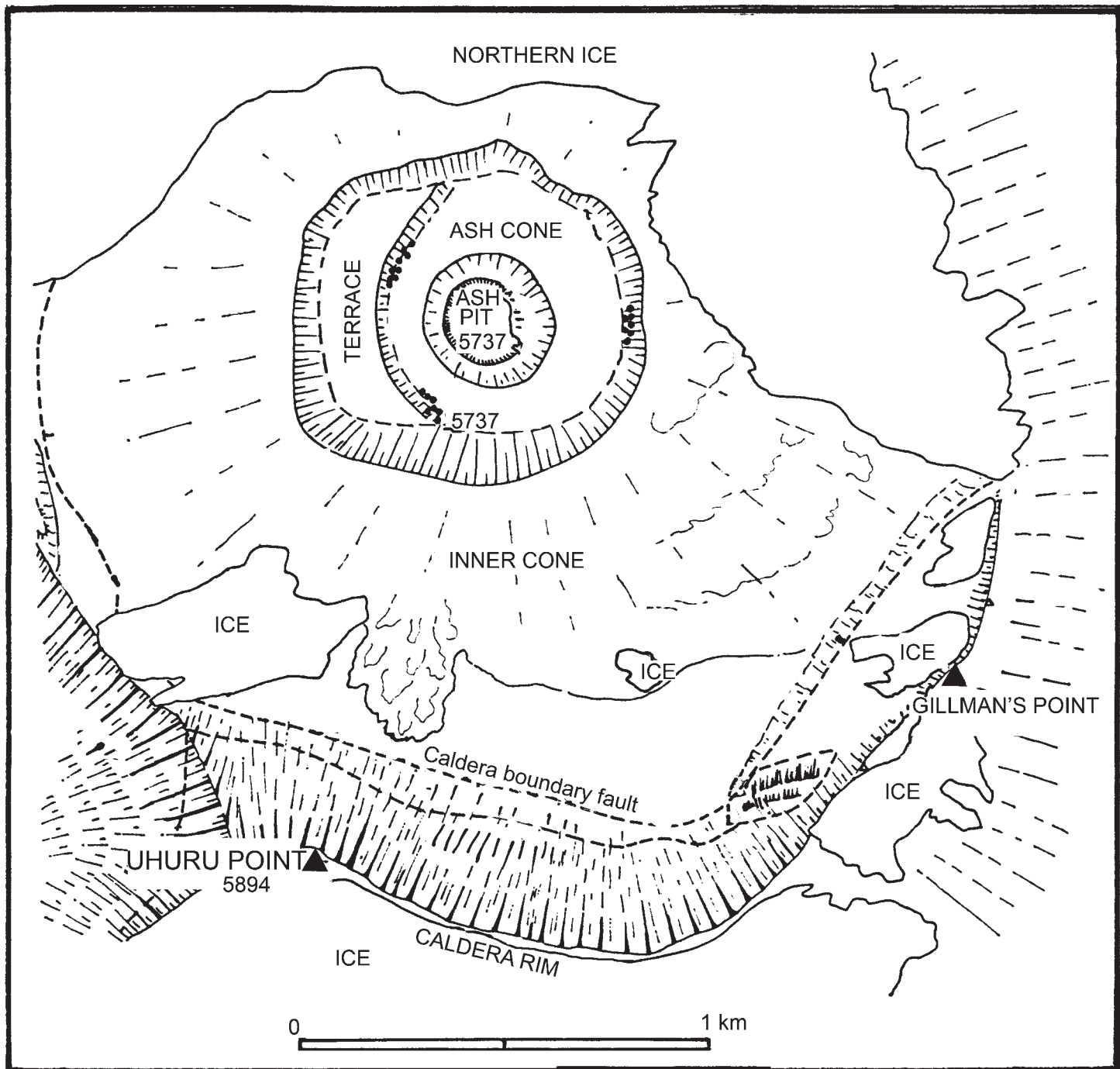


Fig. 7.8. Map of the Kibo crater area (after Downie & Wilkinson 1972).

slopes, are of olivine basalt and trachybasalt. Trachybasalts are common on the plateau, with subordinate amounts of basanite and nephelinite. Exposed in the old crater walls is a radial swarm of dykes of similar composition. Volcanic sediments on the east side of the plateau, overlain by lavas from Kibo, include conglomerates containing pebbles of melanephelinite and trachybasalt derived from Shira, and also ijolite, biotite phonolite and basanite, which do not correspond to any known outcrops. The source of this material was to the NE of Shira, and closer to Kibo.

*Mawenzi.* This most easterly of the volcanoes is lower than Kibo, but much more difficult of access, and parts of its summit area are still unexplored. Allowing for burial beneath the later Kibo lavas, the volcano is around 60 km in diameter. Due to erosion and crater wall collapse, the upper part of the cone has been considerably modified, and it is now a highly eroded precipitous group of arêtes (Plate 5), residual between intersecting cirques. They culminate in Hans Meyer Peak (5153 m), the third highest volcano in Africa (after Kibo and Mt Kenya). The formation of the cirques has modified earlier collapse of the NE crater wall of the original cone that has given rise to an extensive lahar deposit on the plains in Kenya to the NE. The largest of the cirques, on the eastern side, lies at the head of the Great Barranco, a deep gorge that provides the most continuous section through the mountain.

There are two main extrusive centres, Mawenzi itself and Neumann Tower (4425 m), a subsidiary peak 2.5 km east of Mawenzi; both centres have been extinct since the early Pleistocene. At Neumann Tower, ankaramite, olivine basalt and trachybasalt lavas dip outwards from an agglomerate-filled vent. Exposures in the wall of the Great Barranco show them to be overlain by lavas from Mawenzi. The extrusives from Mawenzi are of feldspar-phyric basalt and olivine trachybasalt flows and tuff, that dip steeply away from the centre, except on the west side where the youngest flows are flat-lying beneath the Kibo lavas. Plugs of syenogabbro are exposed in the deeply eroded cirques on the eastern side of the centre. The weathering out of numerous dykes of ankaramitic basalt and olivine trachybasalt has given rise to steep pinnacles and ridges (Plate 5). Most belong to an elongate WNW–ESE swarm that intersects the two centres, but radial swarms also emanate from both the Neumann Tower and Mawenzi centres.

*Kibo.* This is the central cone and highest point of Kilimanjaro. Due to a preponderance of viscous trachytic and phonolitic lavas, it has steep slopes. Those on the western, northern and southern sides are partly coated with ice, and a broad flat summit caldera holds snow for much of the year (Plate 6). At its base, the cone merges with, and laps over, the cones of Shira and Mawenzi. Kibo is the only one of the three to have modern glaciers, though Mawenzi shows evidence of earlier glaciation.

The broad, flat-topped summit is due to the collapse of the original cone to form a caldera 2.5 km wide which itself contains the broad shallow Inner Cone (Fig. 7.8). This in turn contains the Inner Crater, 900 m wide, containing a small ash cone punctured by an ash pit 120 m wide and 130 m deep. Fumaroles and associated sulphur deposits occur in the Inner Crater. The caldera rim is highest on its southern edge and culminates in Uhuru Peak (5895 m), the highest point in Africa. One of the two larger glaciers lies on the southern and western outer slopes of the main cone, and another in the northern part of the caldera overtops the caldera rim to flow down the northwestern upper slopes of the cone. Smaller snowfields occur mainly on the western outer slopes, and also along the southern trough of the caldera.

Activity at Kibo began in the Pleistocene and the earliest lavas are possibly intercalated with the youngest flows from Shira and Mawenzi. However, the earliest known lavas from Kibo erupted from a cone that already matched Mawenzi in height and considerably overtopped Shira. The later activity of Kibo produced flows that, due to the constraints of the other two flanking volcanoes,

flowed mainly to the north and south, lapping over the older flows from the other centres and obscuring the early flows from Kibo itself. The lava extrusion ranges in age from Lower Pleistocene for the earliest flows to the Recent lava flows from the Inner Crater. Because of the fumarole activity, the volcano is classified as still active.

Ten distinct lava groups have been recognized but, in brief, much of the earliest activity was extrusion of mugearite and benmoreite, interspersed with trachyte. Later extrusions are dominantly of trachyte containing large phenocrysts of alkali feldspar (the so-called 'rhomb porphyrys'), whereas the most recent lavas forming the caldera rim and extruded in and from the Inner Crater are of nepheline-phyric aegirine phonolite. Anorthoclase phenocrysts derived from scoriaceous trachyte on the caldera rim yield an age of  $0.21 \pm 0.03$  Ma (Wilkinson *et al.* 1986). Activity was not continuous and the various lava groups were separated by periods of erosion when deep valleys were incised and filled with glacial, fluvio-glacial and alluvial deposits. Despite the relatively high viscosity of the lavas, associated pyroclastics are not abundant, though fine-grained, highly indurated tuffs occur on the upper southern slopes at around 4000 m between the Karanga and South-Eastern valleys (Dawson personal observation). A large lahar deposit, correlated with a huge landslide scar on the upper southwestern slopes (the Kibo Barranco), covers a large area on the plains south and SW of Moshi.

Because of the Recent age of Kibo, exposures of intrusive rocks are scarce. Radial dykes of trachybasalt, trachyte and phonolite crop out in erosion gullies on the upper western slopes, where there is also an outcrop of analcime syenite.

*Parasitic minor cones.* These and associated minor lava flows occur on the lower flanks of the main cones, extending in zones down to the plains, but they also occur on the saddle between Kibo and Mawenzi at 4300 m. The cones are generally only a few hundreds of metres in diameter, but may be up to 1.5 km and up to 200 m high. Most are of scoria or ash, but several have produced extensive lava fields. The cones have apparently been erupted at various periods, as judged by their relationships to extensive lava flows from the three main centres. They have not been systematically studied petrologically, but ankaramite, olivine basalt, trachybasalt, trachyandesite, trachyte and phonolite have been recorded. In the zone of cones on the lower southeastern slopes of Mawenzi (the most accessible, being close to the ascent route from Marangu), the cones above the forest zone are entirely of ankaramite, whereas those lower down in the forest and below are a combination of ankaramite and olivine basalt. At the southeastern extremity of this zone, Lake Chala occupies a caldera 3 km in diameter and 100 m deep. The crater walls expose Mawenzi lavas at their base, overlain by up to 80 m of calcite-cemented grit and agglomerate. It has been suggested that the calcite is of magmatic (carbonatitic) origin.

*Petrochemistry.* Downie & Wilkinson (1972) listed 84 analyses for major and minor oxides, and trace elements (V, Cr, Co, Ni, Cu, Zn, Rb, Sr, Zr, Ba). Of these analyses, eight are of distal basalts and basanites from the Amboseli area, 16 of basalts, trachybasalts ankaramitic basalt and syenogabbro from Mawenzi, nine of basalts, basanite and hawaiite from Shira, 38 of mugearites, benmoreites, trachytes and phonolites from Kibo, and 11 of rocks from parasitic cones and other localities. Recently these data have been supplemented by analyses of 1 basanite, 2 basalts, 1 picrobasalt and 3 trachybasalts from Mawenzi, 2 basanites and a picrobasalt from Shira, and 1 basanite, 3 trachyandesites, 2 tephriphonolites and 5 phonolites from Kibo (Roberts 2002); in addition to the trace elements given in Downie & Wilkinson (1972), these later analyses include values for Ga, Hf, Nb, Pb, Sc, Ta, Th, U and REE.

The three centres are chemically distinct, with Mawenzi being the simplest with most rocks being of hawaiite composition. Kibo is the most silicic and alkaline of the three centres.

The Kilimanjaro rocks have a compatible element range (Cr < 10 to 650 ppm, Ni < 10 to 400 ppm) consistent with olivine and clinopyroxene fractionation. The mafic rocks have concentrations of Rb, Ba, Th, U, Nb and Zr in the order of  $\times 100$  to  $\times 800$  bulk Earth values, and values in the more evolved rocks are one order of magnitude greater than those in the mafic rocks. Further, aegirine phonolites from the latest Inner Crater group on Kibo have high REE concentrations and >3000 ppm Zr and >1500 ppm Nb, suggesting extreme fractional crystallization in the absence of apatite and titanite. Although other evolved rocks can be explained by fractional crystallization of a possible mafic parental magma (Downie & Wilkinson 1972), Roberts (2002) suggests these large increases cannot be due solely to olivine and pyroxene fractionation, and proposes that the high Zr and Nb must result from high concentrations in a melt that was distinct from the parent of the other evolved Kilimanjaro rocks (Roberts 2002). However, Dawson *et al.* (*in press*) find that anorthoclase crystallization in a specimen of Kibo rhomb porphyry results in the residual glass being less silicic, more peralkaline and containing higher Zr (1800 ppm) and Nb (438 ppm) than the bulk trachyte, thus developing a trend that may culminate in the Inner Crater group.

*Glaciation.* Since the first visit to the summit area by H. Meyer and E. Purtscheller in 1889 (Meyer 1900), it has been realized that the ice fields on Kibo are less extensive than in the past; with Meyer recording moraines and glacial striae down to 3500 m. Both Kibo and Mawenzi were glaciated and Downie (1964) records 4 glacial epochs on Kibo. Ice cores taken at six localities on Kibo in 2000 (Thompson *et al.* 2002) have provided a *c.* 12 ka record of Holocene climate variability for the area, including three periods of abrupt climate change at *c.* 8300, *c.* 5200 and *c.* 4000 years ago, the last coinciding with the period of the greatest historically-recorded drought in tropical Africa. Since 1912 the areal extent of the Kibo ice fields has decreased from 12.1 square kilometres to 2.5 in 2003 i.e. by around 80% and Thompson *et al.* (2002) predict they are likely to disappear between 2015 and 2020 if present climate conditions continue. Mote & Kaser (2007) suggested that, although glaciers in mid-latitudes are responding directly to global warming, the disappearance of the Kibo ice fields is more likely to be linked to changes in the surface temperatures of the Indian Ocean. The ensuing changes in the atmospheric circulation lead to lower precipitation; combined with ablation by solar radiation, the effect is retreat of the ice fields

### The Younger Extrusives

Following the Upper Pleistocene faulting at 1.2 Ma, there was another major phase of volcanic activity that, in eruption style (relatively small volume of extruded material, and magma type) contrasts with the relatively quiet, massive extrusions from the earlier basaltic shield volcanoes. Most activity is within the area of the Older Extrusives, but some activity occurred in the Babati–Hanang area, well to the south of the main area of the earlier activity (Fig. 3.1).

The Younger Extrusive activity was highly explosive, giving rise to features varying from major stratovolcanoes dominated by pyroclastic materials (Meru, Oldoinyo Lengai, Kerimasi, Burko, Kwaraha and Hanang) to areas of small tuff cones and explosion craters, many of which occur around the major centres. Tuffs from this phase of activity are widespread throughout the volcanic province. The tuff cone areas often coincide with areas of intense minor faulting, for example at Basotu on the Mbulu Plateau (Downie & Wilkinson 1962) and in the Engaruka–Natron area (Dawson & Powell 1969).

The magma types at most of these later centres are volatile-rich, ultrabasic and high in alkalis, giving rise to olivine-free

nephelinites and phonolites. Blocks of plutonic ijolites, feldspathoidal syenite and metasomites occur in the pyroclastic rocks at several centres. Carbonatite lavas and pyroclastics accompany the nephelinites and phonolites at Oldoinyo Lengai, Kerimasi, Ngurdoto, Kwaraha and Hanang, and numerous minor carbonatite tuff cones are known on the Mbulu plateau (Downie & Wilkinson 1962) and in the Monduli area where they are associated with extrusion of ankaramite and olivine melilitite (Dawson 1964c; Roberts 2002). Alkali carbonatite lava extrusions and ash eruptions have taken place at Oldoinyo Lengai in modern times (Dawson 1989; Dawson *et al.* 1995a), with documented lava extrusion occurring as recently as August 2007 and ash eruption in September 2007 (Mitchell & Dawson 2007). Recent minor flows and tuff cones of olivine nephelinite and olivine melilitite occur on the floor of the rift valley in the Oldoinyo Lengai–Gelai area (Dawson *et al.* 1985; Keller *et al.* 2006), in the Monduli–Arusha area (Dawson *et al.* 1970), and south of Hanang (Dawson *et al.* 1997). Some of the minor tuff cones contain a variety of blocks of upper mantle material that testify to a heterogeneous mantle beneath northern Tanzania.

In addition to these Upper Pleistocene–Holocene centres, activity at some of the older centres persisted after the Middle Pleistocene. At Tarosero, peralkaline trachyte and phonolite flows continued into the Upper Pleistocene. On the Kibo peak of Kilimanjaro (classified as still active), phonolite and trachyte extrusions continued until Recent times, and there is still fumarolic activity in the Inner Crater (Downie & Wilkinson 1972).

### Oldoinyo Lengai

*Type:* stratovolcano; *Lat/Long:* 2.75°S 35.90°E; *Elevation:* 2890 m; *Relief:* 2090 m; *Diameter:* 12 km; *Eruptive history:* around 22 Ka to present; *Crater diameter:* south inactive crater 300  $\times$  200 m; north active crater 400  $\times$  300 m; *Composition:* nephelinite, phonolite, natrocarbonatite; *QDS:* 39 Angata Salei.

Oldoinyo Lengai is the only currently active volcano in northern Tanzania and is unique in being the world's only active carbonatite volcano. A distinctive white capping of weathered carbonatite (Plate 7) on the northern side of the mountain lead to its being identified as a 'Snow Mountain' (together with Kilimanjaro and Mt Kenya) on the 1855 map of the interior of East Africa. Due to its remoteness, the volcano was rarely visited before the 1980s. However, the recognition of the unique natrocarbonatite lavas (Dawson 1962a, b), together with the construction of the Engaruka–Loliondo dirt road in the late 1970s and the boom in geotourism, have resulted in the volcano being visited by many more climbers, both scientists and tourists, in recent years. Since 1983, events at the volcano have been compiled and reported in bulletins published by the Natural History Museum, Smithsonian Institution of Washington, DC 20560, USA. From January 1983 to December 1989, this was the Scientific Event Alert Network (SEAN) Bulletin, and subsequently the eBulletin of the Global Volcanism Network. These bulletins have published reports, diagrams and photographs of activity at the volcano. Many of these reports have been collated by Celia Nyamweru who has also given reviews at various stages of the more recent activity (Nyamweru 1988, 1990, 1997).

*History of activity.* The mountain was first reported as an active volcano in early accounts of the interior of East Africa gleaned from Arab slavers (Wakefield 1870; Farler 1882) and the first eyewitness account of minor ash eruption in 1883 was documented by Gustav Fischer (1884–1885). Before 1960, flows of natrocarbonatite in the active northern crater were recorded in 1904, 1914, and 1954; flows occurred in the period 1960 to 1966, and from 1983 to 2007. Major ash eruptions occurred in 1917, 1926, 1940, 1966–1967 and 2007–2008, with a relatively small ash eruption in

1993. The pre-1960 ash eruptions were interspersed with periods of apparent dormancy (Dawson *et al.* 1995a). The word apparent is used advisedly because, whereas ash eruptions can be seen from a distance and recorded, prior to 1960 the summit was rarely visited; hence, lava extrusion within the crater may well have been underestimated. The activity observed during 1966–1967 and September 2007 was a series of Vesuvian- and Plinian-type eruptions (Dawson *et al.* 1968; Dawson & Mitchell 2007), and the description of the 1940 activity (Richard 1942) also suggests that the eruption was of Plinian type. However, a small ash eruption in 1993 erupted hollow lapilli, interpreted as resulting from explosion of vesiculated foam (Church & Jones 1994), and ash samples from the same eruption had the grain-size distribution characteristics that are typical of the products of basaltic Strombolian eruptions (Dawson *et al.* 1996a).

Following several earth tremors, ranging in magnitude up to 6, in July and August 2007, remote sensing (Hyperion hyperspectral imager on board the NASA Earth-Observing-01 spacecraft) detected two very bright sources in the summit area on August 27, consistent with erupting lava, and another indicating a flow to the NW from the crater (<http://science.jpl.nasa.gov>), and on 4 September the volcano erupted forming a significant Vesuvian-type ash cloud. During September 2007 sporadic eruptions were of the Vesuvian and Plinian types (Dawson & Mitchell 2007) and these have continued until at least April 2008. The crater is now occupied by a major ash cone that has spilled over the outer edges of the original crater.

**Morphology.** Morphologically the volcano is a classic cone that stands close to the Natron Basin boundary fault escarpment, against which its pyroclastic deposits are piled (Plate 7). It is now covered by sparse grass and scrub though, prior to the 1917 ash eruption, the volcano was highly vegetated and access on the lower slopes was by game trails; the former luxuriant vegetation was mainly killed during the eruption and has not recovered to the present day. In late 2007, much grass was ignited and burned as lavas spilled down the outer western and northern slopes.

The cone is incised by deep radial gullies and, on its northeastern upper slopes, by a major landslide scar (the Eastern Chasm) (Plate 7). Debris flows from this landslip occur on the plains to the east and NE, and others originating on the northern slopes occur on the plains north of the volcano, some having a sufficiently long run-out to form low islands in Lake Natron some 16 km north of the volcano. Klaudius & Keller (2006) report a  $^{14}\text{C}$  date of 2500 years BP on plant remains embedded in one of the debris flows. Parasitic craters occur on the western and eastern lower flanks of the cone and a north–south trending line of three small scoria cones occurs on the lower northern flanks (Dawson 1962a).

The summit is occupied by two small craters: the older, inactive southern crater, which is now a shallow, ash-filled bowl, and the active northern crater. The active crater is some 350 m in a north–south direction and 300 m east–west. When first visited in 1904, the active ‘crater’ was little more than a flat lava platform from which rose a number of hornitos; there were no crater walls on the northern, western and eastern sides, thereby allowing lava spill down the outer slopes in these directions, and only a shallow arcuate southern wall below the summit (Uhlig 1905; Reck 1924–25). The changes before 1960 are not well documented, except that the shallow ‘crater’ observed in 1904–1913 was deepened during the 1917 eruption (Reck & Schulze 1921), and the crater was still deep in 1954 (Guest 1956). In 1960, the active crater was a deep (c. 200 m) bowl bounded on its northern, western and eastern sides by cliffs (Fig. 7.9), but on its southern side by collapse terraces. The changes in the profile of the active crater between the early part of the twentieth century and 1983 are given by Dawson *et al.* (1995a) and those between 1960 and 2007 in Figure 7.10. Since 1960, the depth and shape of the



**Fig. 7.9.** The northern crater of Oldoinyo Lengai (1960) looking northwards from the summit. The crater diameter is c. 300 m and the north wall is c. 200 m high. Recent black spatter surrounds several small vents. The crater has subsequently been infilled by ash from the 1966–67 ash eruption and post-1983 lava flows. Photograph by C. Bristow.

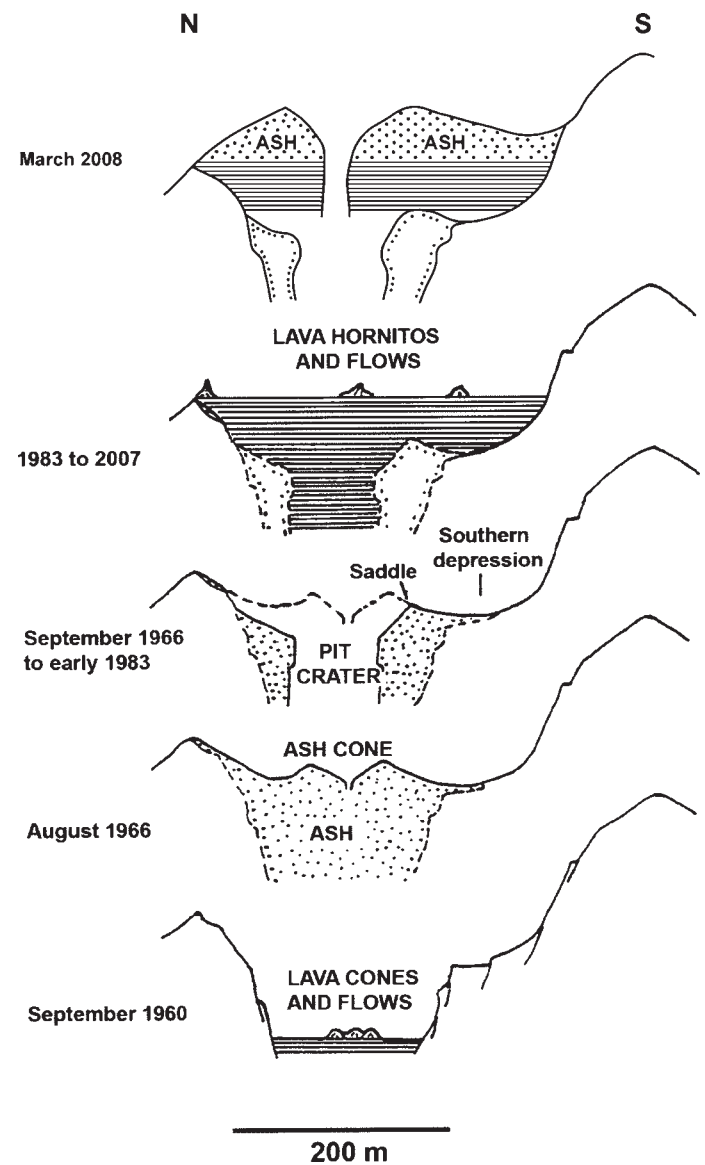


**Fig. 7.10.** Profiles of the northern crater of Oldoinyo Lengai, showing crater changes.

active crater has been modified, first as a result of partial infill by ash during the 1966 ash eruption, followed by partial collapse of this ash cone to form a pit crater. Between 1967 and early 1983, there was no activity but, following the renewal of activity in 1983, the pit crater was gradually filled by lava flows and spatter from a series of small transient cones, hornitos and lava pools (Plate 8). In early 1993, a small ash eruption in which the lapilli were of mixed carbonate–silicate composition accompanied extrusion of exceptionally voluminous and viscous natrocarbonatite lava flows that contained globules of silicate lava (Dawson *et al.* 1994). By November 1998, the crater had become almost infilled by lava, and lava spilled over the lowest northwestern and eastern sectors of the crater rim to flow down the outer slopes (Nyamweru 1999) (Plate 9). Since then, minor lava extrusions and overspill on the northern, northwestern and eastern slopes have continued almost continuously till at least August 2007 including, following a minor ash plume, a major hornito collapse into an underlying lava pool that caused a lava surge that spilled down the western slopes from a low point on the western crater rim on 29 March and 3 April (Bulletin of the Global Volcanism Network 2006; Kervyn *et al.* 2008a). Between late 1998 and September 2007, a crater wall was present only on the south side below the summit, and the ‘crater’ was, as in 1904, a carbonatite lava platform studded with hornitos and lava pools. As a result of the September 2007–April 2008 eruptions, the former crater is (March 2008) occupied by an ash cone with a central ash pit (Bulletin of Global Volcanism Network, **32**, 10–16, 2007).

*Geology.* The volcano was formed in two main stages, separated by a period of quiescence, erosion and instability. The bulk of the volcano (Unit I of Dawson 1962a) consists of yellow, palagonitized and zeolitized nephelinitic and phonolitic tuffs and agglomerates that were extruded from the now inactive southern crater. A maximum age for the onset of the activity is provided by a date of 0.37 Ma on mica-rich tuffs, surrounding the Loolmurwak crater south of the volcano, that are overlain by Oldonyo Lengai yellow tuffs (MacIntyre *et al.* 1974). Hay (1976) correlated the Unit I tuffs with the Nduu and Naisiusiu Beds of the Olduvai Gorge to the west of the volcano, which range in age from 0.4 to 0.15 Ma. Phonolitic nephelinitic and phonolite flows interbedded with the pyroclastics are exposed in the Eastern Chasm and form a flank flow on the lower eastern slopes, and highly viscous, sanidine-phyric phonolite flows occur on the upper southern and southwestern slopes.

A period of dormancy followed during which there was intense erosion and instability, resulting in numerous debris flows, at least one of which had sufficiently long run-out as to form islands in Lake Natron, 15 km north of the volcano. Klaudius & Keller (2006) proposed that much of the northern face of the original cone was destroyed during a major collapse during this interval; the amount of Unit I material in the lahar field to the north and east of the volcano certainly testify to major collapse(s) (Kervyn *et al.* 2008b). The older rock sequence was then penetrated by explosion craters on the western and eastern lower flanks (Unit II pyroclastics of Dawson 1962a), and recently Keller *et al.* (2006) showed these rocks to be olivine melilitite tuffs, mineralogically and chemically similar to tuffs extruded from minor tuff cones and lava flows found to the east and north of the volcano (Dawson *et al.* 1985). Thus, the two major stages in the formation of the volcano are separated by extrusion of a primitive magma type.

The period of intense erosion was followed by a shift of the main extrusion site to the modern, active, northern crater (Dawson 1962a). Klaudius & Keller (2006) suggested that the following activity filled in the breached crater and then built up the northern side of the cone in two separate but related stages. During this period black nephelinitic tuffs and agglomerates, and wollastonite–combeite nephelinite flows (Unit III of Dawson 1962a) were extruded some intercalated with

natrocarbonatite ashes and flows in the summit area. The Namorod Ash of the Olduvai succession, dated at around 1250 BP, has been correlated with the oldest of the Unit III pyroclastic units (Hay 1976). Wollastonite–combeite nephelinite, containing cognate xenoliths of ijolite, was also extruded from the small cones on the northern, lower flanks of the main cone (Dawson 1962a, 1998). Whereas the equivalents of the earlier phonolites and phonolitic nephelinites, and the associated olivine melilitites, occur at other volcanoes (e.g. in the Homa Bay area of Kenya; Le Bas 1977), the wollastonite–combeite nephelinites were thought to be unique to Oldoinyo Lengai. However, a further example has been found recently at the Meru volcano (see below).

Nephelinite and carbonatite activity alternated in this succession, but observations since the beginning of the twentieth century give the impression that extrusion of carbonatite has predominated, with the exception of: (a) extrusion of a combeite nephelinite flow on the western rim possibly just prior to the 1917 ash eruption; (b) the 1966–67 ash eruption when the ashes were a mixture of silicate and natrocarbonatite material (Dawson *et al.* 1968, 1992); (c) the activity in 1993 when highly viscous natrocarbonatite lavas contained globules of silicate material (Dawson *et al.* 1994), and the erupted ash contained spheroids of silicate material exsolving natrocarbonatite (Dawson *et al.* 1996a); and (d) eruption in September 2007 of silicate lapilli rich in combeite, melilite and phosphate (Mitchell & Dawson 2007). There are no records of the nature of the material ejected during the explosive eruptions in 1917, 1926 and 1940.

Extrusions of carbonatite lava have mainly taken place within, and from, the northern crater; exceptions are a small flow that took place from a fracture high on the western slopes in June 1993, and a small flow on the upper eastern slopes, extrusion date unknown (Dawson & Mitchell 2007). Keller & Zaitsev (2006) also record two older, altered natrocarbonatite dykes cutting phonolite lavas high on the upper southern slopes.

*Silicate lavas and plutonic xenoliths.* The phonolites and phonolitic nephelinites of Unit I consist of combinations of nepheline, alkali pyroxene, sanidine, sodalite, vishnevite, melanite garnet, perovskite, apatite, glass and zeolites (Dawson 1962a; Donaldson *et al.* 1987). Wollastonite and combeite (ideal formula  $\text{Na}_2\text{Ca}_2\text{Si}_3\text{O}_9$ ) are common additional phases in the Unit III nephelinites (Dawson 1998; Peterson 1989a, b; Klaudius & Keller 2006) which lack sanidine, and one specimen contains exceptionally Fe-rich nepheline, clinopyroxene and sodalite, and also the rarer phases delhayelite ( $\text{K}_4\text{NaCa}_2[\text{Al}_2\text{Si}_6\text{O}_{19}]\text{F,Cl,H}$ ), barium lamprophyllite and Sr–Ba phosphate (Dawson & Hill 1998). However, wollastonite is often replaced by combeite, so there are two types of combeite: that replacing wollastonite (Plate 10) and magmatic phenocrystic (Plate 11), with the magmatic variety having a higher Na/(Na + Ca) composition (Dawson *et al.* 1989).

These mineralogical differences, together with distinct differences in their Sr and Nd isotope composition (Bell & Dawson 1995a) have led to the nephelinites being referred to as Group I (those from Dawson’s Unit I) and Group II (from Unit III). Compositionally, the Group I nephelinites and associated phonolites are alkaline whereas the Unit II nephelinites are peralkaline, with peralkalinity indices  $([\text{Na} + \text{K}]/\text{Al})$  of up to 2.36. The groundmass glass in one Group II lava is exceptionally peralkaline, with low  $\text{Al}_2\text{O}_3$  (only 2–3 wt%) leading to  $(\text{Na} + \text{K})/\text{Al}$  up to 13, and contains very high concentrations of iron (FeO up to 18.5 wt%),  $\text{SO}_3$  (3–5%), Cl up to 0.4%, and F up to 1%; it is relatively potassic with Na/(Na + K) as low as 0.7 (Dawson & Hill 1998).

All the lavas contain low MgO (<2 wt%), Cr and Ni (<10 ppm), but exceptionally high concentrations of the incompatible elements Rb, Ba, Th, U, Nb, Mo, Sr, Zr, and the REE (Fig. 7.11). Zr/Hf, Zr/Nb, Nb/Ta and Hf/Ta ratios all increase from the Unit I phonolites to the Group II wollastonite–combeite nephelinites (Klaudius & Keller 2006). A Sr v. Nd isotope plot

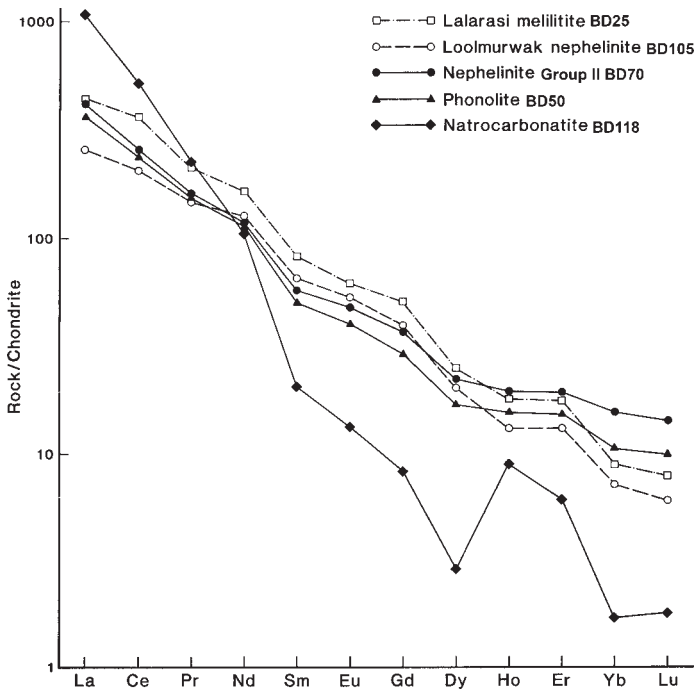


Fig. 7.11. Chondrite-normalized rare earth element plot for selected Oldoinyo Lengai lavas, and primary olivine melilitite and olivine melilitite nephelinite in the Oldoinyo Lengai area. For the location of Oldoinyo Loolmurwak and Lalarasi, see Figure 7.18. Data from Dawson *et al.* (1985) and Donaldson *et al.* (1987).

(Fig. 7.12) shows that the data for the Group II wollastonite–combeite nephelinites overlap those for the natrocarbonatites, and form a group relatively depleted in radiogenic Sr. The Group I nephelinites form a group more enriched in radiogenic Sr and the data for phonolites lie mainly between the two nephelinite groups (Bell & Dawson 1995a).

Plutonic blocks of jacupirangite, ijolite, pyroxenite and nepheline syenite occur in the agglomerates (Plate 12). Mainly cumulates, they comprise combinations of nepheline, hainyite, alkali pyroxene, melanite and schorlomite garnet, apatite, perovskite, titanite, low-Cr–high-Ti spinel, glass, and (in the syenites) sanidine (Dawson *et al.* 1995b); eucolite is a rare phase in nepheline syenite (Dawson & Frisch 1971). Blocks containing wollastonite have been found only in the Unit III black agglomerates and tuffs. Ijolite and pyroxenite blocks ejected during the 1966 ash eruption contain the same phases as those in the agglomerates, together with mica-mantled xenocrystal olivine (Dawson *et al.* 1995b) (Plate 13). Complex zoning of the phases (Plates 14, 15) and mineral disequilibrium is attributed to convective percolation of fluids through permeable cumulates, possibly complicated by magma replenishment during crystallization of individual magma batches. A common feature of the jacupirangites, pyroxenites and ijolites, including those ejected during the 1966 ash eruption, is that the phases are cemented by vesiculated glass from which minor phases such as acicular apatite and skeletal nepheline and vishnevite have precipitated (Donaldson & Dawson 1978) (Plate 16); low analytical totals for the glasses point to significant concentrations of dissolved volatiles in the parent magmas which, in the absence of hydrous phases, is assumed to be largely CO<sub>2</sub>

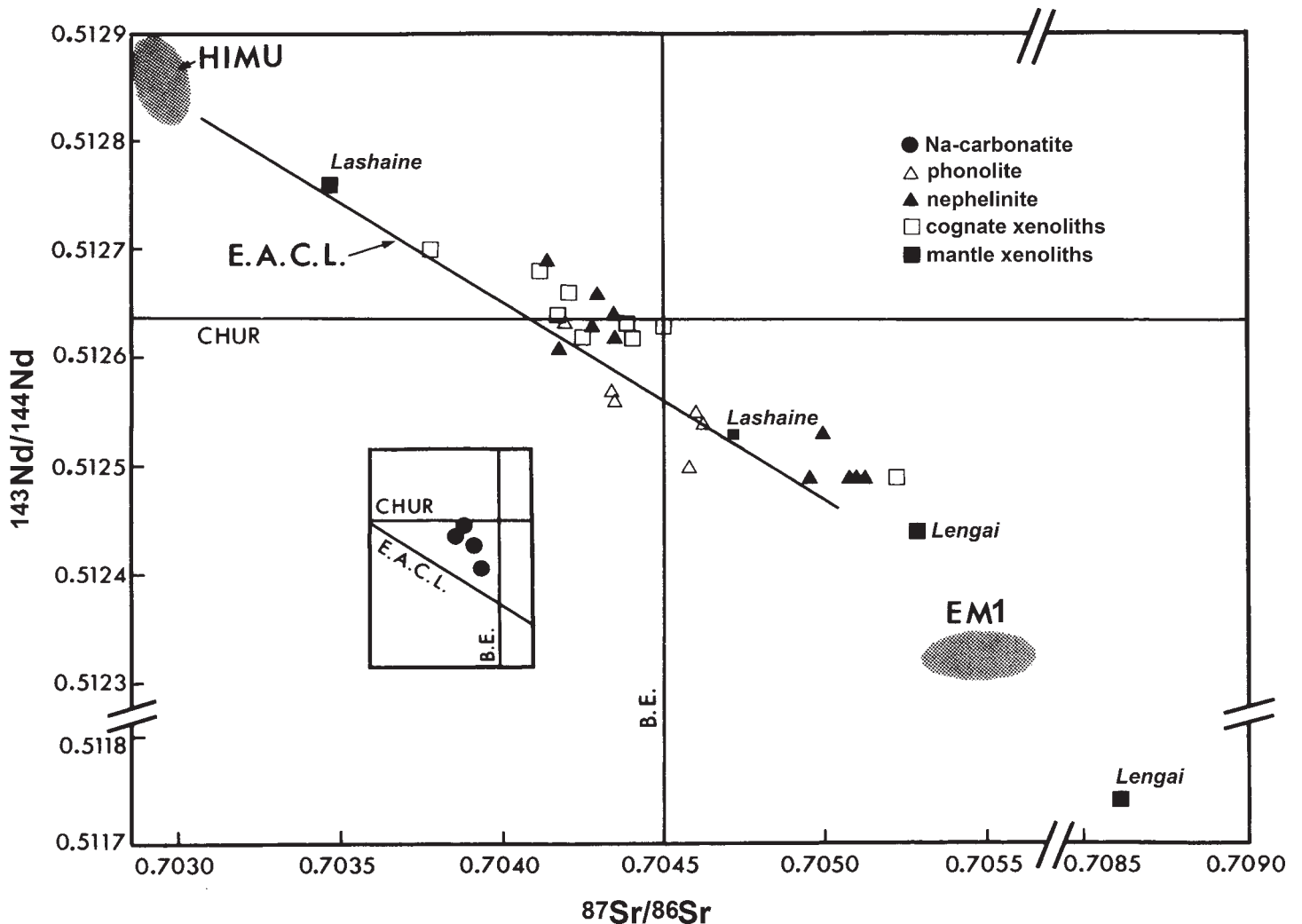


Fig. 7.12. Nd v. Sr isotope plot for lavas, cognate xenoliths (ijolites, jacupirangite and nepheline syenite), and two mantle xenoliths from Oldoinyo Lengai (after Bell & Dawson 1995a). Also shown are two mantle xenoliths from Lashaine (data from Cohen *et al.* 1984). EACL is the East African Carbonatite Line from Bell & Blenkinsop (1987). HIMU and EM1 values in this, and other Nd v. Sr isotope plots (Dawson 2008, figs 8.1 and 8.2) are from Hart (1988).

(Dawson *et al.* 1995b). Blocks of cellular, spinifex-textured wollastonite (Dawson & Sahama 1963) (Plate 17) and titanite pyroxenite possibly derive from dykes within the volcanic pile.

Other deep-seated blocks are of crustal and upper-mantle metasomes, fenites and olivine-mica-pyroxenites, respectively (Morogan & Martin 1985; Dawson & Smith 1992a, b; Kramm & Sindern 1998). In contrast to the other blocks, the metasomatic olivine-mica-pyroxenites (Plate 18): (a) are often mantled by rinds of ijolite, with which they have reacted; and (b) contrasting with the rounded shape of other blocks, are invariably angular, indicating derivation from a well-jointed mantle protolith.

The accretionary lapilli of the 1966 eruption contained euhedral melanite, nepheline and combeite, corroded clinopyroxene and wollastonite, together with larnite, rankinite and cementing natrite (Dawson *et al.* 1992). The lapilli of the September 2007 eruption contain the same phases but are cemented by a NaCa carbonate–phosphate (Mitchell & Dawson 2007). The lapilli from both these eruptions provide evidence for interaction between Ca-silicates (clinopyroxene and wollastonite) and natrocarbonatite to create metasomatic combeite and melilite. The igneous combeite has higher Na / (Na + Ca) ratios than that replacing wollastonite and clinopyroxene, and nepheline embedded in the igneous combeite is richer in Fe<sub>2</sub>O<sub>3</sub> (5.0 wt%) and K<sub>2</sub>O (8.5%) than nepheline in most silicate lavas (0.8–2.1; 4.4–8.1 wt%) (Dawson *et al.* 1989, 1992). An absence of clinopyroxene in the mantling ash indicates they are neither nephelinite nor melilitite, but result from extreme interaction between nephelinite and natrocarbonatite (Mitchell & Dawson 2007). The lapilli from the September 2007 eruption, in contrast to those in the 1966 eruption, are not accretionary, suggesting the ash cloud was not so buoyant.

Ash erupted in 1993 contained spheroids of nepheline- and garnet-phyric nephelinite intermixed with natrocarbonatite. Importantly, rounded globules of natrocarbonatite occurred both within the silicate matrix of the lava and within silicate glass entrapped in the silicate phenocrysts (Dawson *et al.* 1996a).

*The natrocarbonatite lavas.* Natrocarbonatite has not been recognized in the Unit I rocks. The earliest evidence comes from: (i) partly-altered natrocarbonatite lava interbedded with Unit III nephelinitic tuffs and agglomerates in the summit area (Dawson *et al.* 1987); (ii) a natrocarbonatite-nephelinite ash deposit on the lower northern slopes, termed the Footprint Tuff, that was erupted about 600 years ago (Hay 1989); and (iii) an altered block of natrocarbonatite from Unit III agglomerate (Dawson 1993). All historical

reports show that natrocarbonatite has been extruded from the northern crater. Pre-1995 studies on the lavas are reviewed in a collection of papers edited by Bell & Keller (1995).

The lavas are jet-black when first extruded, but become lighter in colour after about 24 hours due to reaction with atmospheric moisture. This is most marked by whitening of the surface of pahoehoe flows, whereas aa flows become grey. These colour contrasts have proved useful for determining, from aerial photographs and observations from the crater rim, when individual lava flows were extruded. In addition to other attributes, the small scale and relatively slow advance of the natrocarbonatite flows have made Oldoinyo Lengai a natural laboratory for the measurement of magma temperatures and rheology. Measured extrusion temperatures range from 544 to 592°C (Krafft & Keller 1989; Dawson *et al.* 1990; Pinkerton *et al.* 1995).

Physically, the lavas have the same basic appearances as basaltic lava flows, varying from aa to pahoehoe morphologies (Figs 7.13–7.15), but most are on a relatively small scale; individual pahoehoe flows may be less than 2 m wide and as little as 20 cm thick (Fig. 7.13). In contrast, a 1960 aa flow was *c.* 1 m thick, and an exceptionally viscous and crystal-rich flow in 1993 was 6 m thick. The length of many flows has been constrained by their ponding against the inner walls of the crater, though recent overspill flows have travelled down the outer slopes for distances of up to 3 km before freezing (Kervyn *et al.* 2008a). Volumes and extrusion rates are variable, from a volume of 900 m<sup>3</sup> and effusion rate of  $8.3 \times 10^{-3} \text{ m}^3 \text{ s}^{-1}$  for an aa flow in 1960, to a volume of 104 000 m<sup>3</sup> and an effusion rate of  $86 \times 10^{-3} \text{ m}^3 \text{ s}^{-1}$ , for a particularly large aa flow in 1993 (Dawson *et al.* 1994). Volumetrically, many of the pahoehoe flows are more comparable to the 1960 flow, though some flows that have spilled down the outer slopes since 1999 must be of considerably greater volume. The least vesicular and crystal-poor flows are the least viscous of any terrestrial magmas, with apparent viscosities as low as 1–5 Pas (Norton & Pinkerton 1997), whereas the viscosity of the exceptionally-thick and crystal-rich aa flow extruded in 1993 is  $3 \times 10^7$  Pas, falling within the range for rhyolites (Dawson *et al.* 1994). There is the tendency for spatter to build up large hornitos, some of which may be up to 20 m high. These become hollow upon magma withdrawal and most collapse shortly afterwards due to weakening by fumarolic activity and weathering, but a few remain intact sufficiently long to develop stalactites on their interior walls (McFarlane *et al.* 2004).



**Fig. 7.13.** A recent natrocarbonatite aa flow in the northern crater of Oldoinyo Lengai, September 1960. Note the black, pre-alteration colour compared with whiteness of older pahoehoe lava in the foreground.



**Fig. 7.14.** Pahoehoe flows in the northern crater, Oldoinyo Lengai, 1988. Compare the texture and thickness of these flows with those of the aa flow illustrated in Figure 7.13.

The natrocarbonatite lavas contain phenocrysts of the Na–K–Ca carbonates nyerereite ( $[\text{Na}_{1.64}\text{K}_{0.38}]_{2.02}[\text{CaSrBa}]_{0.99}(\text{CO}_3)_2$ ) and gregoryite ( $[\text{Na}_{1.74}\text{K}_{0.1}] [\text{CaSrBa}]_{0.16}\text{CO}_3$ ) (Plate 19) in which there is considerable substitution of Sr and Ba for Ca, and  $(\text{SO}_4)^{2-}$ ,  $(\text{PO}_4)^{3-}$ , Cl and F for  $(\text{CO}_3)^{2-}$  (McKie & Frankis 1977; Gittins & McKie 1980; Keller & Krafft 1990). The phases are named after Julius Nyerere, first president of Tanzania and J. W. Gregory, of rift valley fame. These two phenocryst phases are set in a groundmass of smaller grains of nyerereite, apatite, Mn–Fe sulphide, Mn–Fe spinel, phase X (a mixed Ca–Mg–Ba–Na carbonate in which the proportions of the individual cations are variable) and Na-sylvite ( $[\text{KNa}]\text{Cl}$ ) (Plate 20). They are rare solid solutions that result from high-temperature consolidation of the dominantly carbonate liquid (Dawson *et al.* 1995c); phase X may be a variety of khannesite, a member of the burbankite group (Mitchell 1997). The ratio of phenocrysts to groundmass varies considerably, with fewer phenocrysts in the more mobile pahoehoe flows. Other even rarer phases are Fe–Mn–monticellite (Peterson 1990), K-sulphides, Zn-bearing sulphides, spurrite, larnite, and sellaite (Dawson *et al.* 1995c), Sr fluorite and sodic tilleyite (Dawson *et al.* 1996a), neighborite (Mitchell 1997), halite (Genge *et al.* 2001), Mn–F rasvumite (Jago & Gittins 1999), niocalite-cuspidine and galena (Mitchell & Belton 2004), high-Ba nyerereite (Mitchell 2006a) and a sodic phosphate–carbonate (Mitchell 2006b). The magnetization of the lavas is dominated by the small amounts of spinel: a jacob-site ( $\text{MnFe}_2\text{O}_4$ )–magnetite solid solution (Shive *et al.* 1990).

The unusual chemical composition of the natrocarbonatite lavas is shown in extreme concentrations of Na, Ca, K, P, Cl, F, S, Ba, Sr and  $\text{CO}_2$  (Table 7.5); Si and Al are very low and, where present, may be due to xenocrystal contamination. Further, they are most unusual in containing more Mn than Fe. The lavas also contain unusually high concentrations of the light REE (Fig. 7.11), Rb, Br, Mo, W, As, Sb, Pb and U. The La–Yb<sub>CN</sub> (500 to 1000) and U–Th (2 to 3) ratios are the most extreme for terrestrial magmas (Dawson & Gale 1970; papers in Bell & Keller 1995; Simonetti *et al.* 1997; Ohde & Matagario 1999). Li values are also very high (211–294 ppm), though  $\delta^7\text{Li}$  has a narrow range of +3.3 to +5.1 (Halama *et al.* 2007). Halogen contents are F 2.5%, Cl 3.6% and I c. 1 ppm (Dawson & Fuge 1980). Some compositional variation within individual flows is due to: (a) variation in phenocryst/groundmass ratio (the filter-pressed toes of some

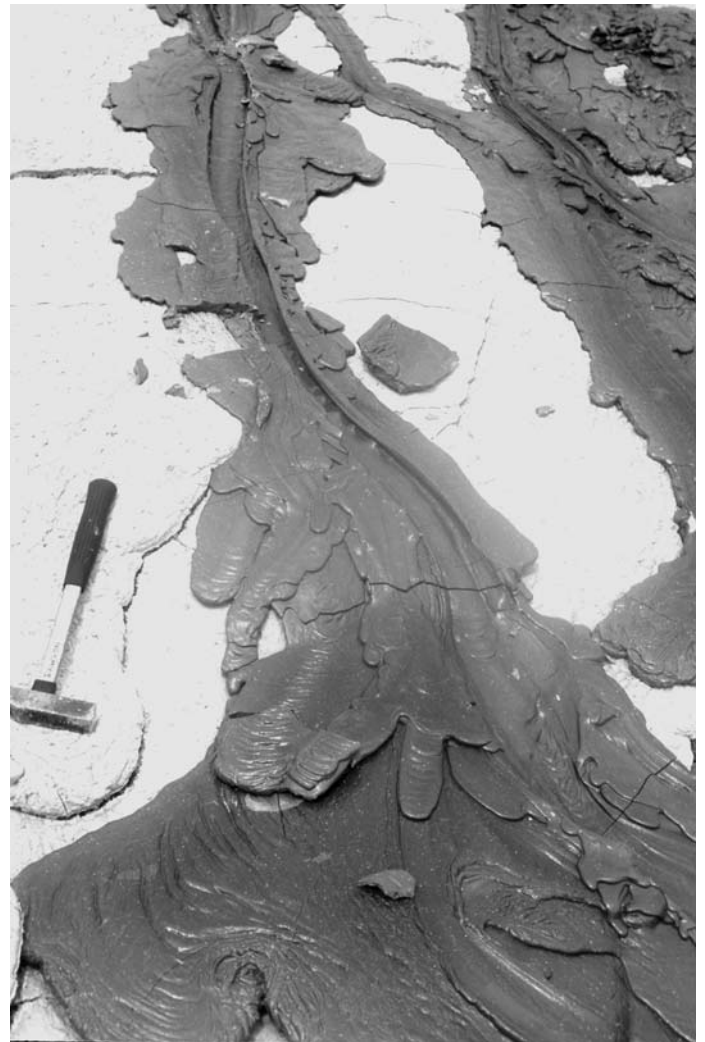


**Fig. 7.15.** Detail of a natrocarbonatite pahoehoe flow, Oldoinyo Lengai, 1988. Despite its very small volume, the low viscosity of the magma has resulted in the flow morphology being similar to that of more voluminous pahoehoe basalt flows.

**Table 7.5.** Representative analyses of natrocarbonatite lavas

	1	2	3	5	6
SiO <sub>2</sub>	0.29	0.14	0.18		
TiO <sub>2</sub>	0.02	0.01	<0.01		
Al <sub>2</sub> O <sub>3</sub>	0.10	0.10	0.10		
Fe <sub>2</sub> O <sub>3</sub>	0.50	0.00	0.21		
FeO	0.24	0.10	0.12		
MnO	0.61	0.24	0.45		
MgO	0.42	0.46	0.22		
CaO	13.36	13.04	14.63		
BaO	1.68	1.92	1.05		
SrO	1.74	1.79	1.63		
Na <sub>2</sub> O	31.06	32.58	32.72		
K <sub>2</sub> O	8.44	8.64	7.27		
H <sub>2</sub> O <sup>+</sup>	0.05	0.23	0.22		
P <sub>2</sub> O <sub>5</sub>	0.73	0.63	1.02		
SO <sub>3</sub>	3.12	3.07	3.18		
CO <sub>2</sub>	32.70	29.20	34.30		
Cl	3.85	4.40	1.80		
F	3.55	5.25	1.35		
Sum	102.47	101.8	100.45		
less O=F + Cl	2.35	2.03	0.97		
Total	100.12	99.77	99.48		
V	232	251	134		
Cu	11	11	7		
Zn	303	43	136		
Rb	259	284	193		
Y	15	<5	<5		
Zr	<20	20	<20		
Nb	74	13	14		
Pb	212	47	108		
Σ REE	1878	1521	1103		
K/Rb	270	251	312		
Ca/Sr	6.5	6.18	7.59		
La/Yb	1127	1911	1657		
Na <sub>2</sub> O/K <sub>2</sub> O	3.68	3.77	4.5		
U				6.73	7.31
Th				2.90	2.8
U/Th				2.32	2.61

1. Phenocryst-poor pahoehoe flow, near extrusion centre
  2. Same phenocryst-poor flow as analysis 1, but distant from extrusion centre (note lower Fe, Mn, Zn, Nb and Pb contents due to sulphide/spinel sedimentation near extrusion centre)
  3. Phenocryst-rich aa-type lava. Compared with analysis 1, note differences in Fe, Mn, Mg, Ca, Sr, K, Cl, F, Zn, Rb, Y, Nb, Pb due to higher phenocryst content.
- Analyses 1–3, lavas extruded in 1988 (Dawson *et al.* 1995c)
5. BD114 Pahoehoe lava
  6. BD118 Aa lava
- Analyses 5 and 6, lavas extruded in 1960 (Dawson & Gale 1970)

flows are almost phenocryst-free resulting in higher Ba, K, Cl, F, V, Cu and Rb than in phenocryst-rich samples); and (b) flowage differentiation, with the distal parts of individual flows being relatively low in Fe, Mn, Zn, Nb, and Pb due to settling out of denser sulphide and spinel grains close to the extrusion site (Dawson *et al.* 1995c). The isotopic compositions of Li, O, C, S, Sr, Nd and Pb (Table 7.6 and considered at greater length in Chapter 8, Dawson 2008) are consistent with a mantle origin for the natrocarbonatites and associated silicate lavas.

Natrocarbonatite lavas are enriched in radon, and have the most extreme disequilibria between U and Th series nuclides yet measured in volcanic rocks. The disequilibria for lavas erupted in 1960 and 1963 suggest gradual formation of the natrocarbonatites (? by separation from a Ra-enriched nephelinite in the

**Table 7.6.** Stable and radiogenic isotope data for natrocarbonatite and trona

Isotope	Range in natrocarbonatite	Trona*	Reference
δ <sup>7</sup> Li	+3.3 to +4.8		1
δ <sup>13</sup> C(PDB)	−5.9 to −6.49	+3.8 to +4.7*	2,3
δ <sup>18</sup> O (SMOW)	+6.1 to +7.03	+38.3 to +40.5*	2,3,4
δ <sup>34</sup> S (CDT)	+2.8 (sulphide), +9.0 (sulphate)		2
<sup>87</sup> Sr/ <sup>86</sup> Sr	0.7037 to 0.70446	0.7056*	5
<sup>143</sup> Nd/ <sup>144</sup> Nd	0.51261 to 0.51268	0.51269*	5
<sup>206</sup> Pb/ <sup>204</sup> Pb	19.24 to 19.26	18.41	5
<sup>207</sup> Pb/ <sup>204</sup> Pb	15.60 to 15.63	15.62	5
<sup>208</sup> Pb/ <sup>204</sup> Pb	39.30 to 39.39	38.25	5

References: 1, Halama *et al.* 2007; 2, Dawson *et al.* 1995c; 3, Keller & Hoefs 1995; 4, Hay 1989; 5, Bell & Simonetti 1996.\*Trona from Lake Magadi: Bell *et al.* 1973; O'Neil & Hay 1973.

sub-volcanic magma chamber) *c.* 15–18 years previously, i.e. shortly after the 1940–41 ash eruption (Williams *et al.* 1986). Similarly, lavas extruded in 1988 formed immediately after the emptying of the magma chamber by the 1966–67 ash eruption (Pyle *et al.* 1991; Pyle 1995). The 1960 Ra–Th disequilibria systematics, together with the other isotopic data (considered at greater length in Dawson 2008, Chapter 8) and major element chemistry, are not consistent with an origin for the natrocarbonatite by mobilization of high-Na evaporites such as those in Lake Natron, as advocated by C. Milton (Bell & Dawson 1995b).

The high Na content of the natrocarbonatites lavas in particular has tended to overshadow other significant geochemical features of the overall Oldoinyo Lengai magmatism. The products of the magmatism are also highly potassic e.g. the natrocarbonatite lavas contain 7–8 wt% K<sub>2</sub>O; and in the silicate lavas and plutonic rocks, sodalites contain 3–4 wt% K<sub>2</sub>O, nepheline contains 20–25% kalsilite molecule, and feldspar is sanidine rather than anorthoclase. The Mn > Fe nature of the natrocarbonatite whole-rock analyses is mentioned above, and some individual phases in both the silicate rocks and the carbonatite have a relatively-high Mn content e.g. wollastonite contains 0.53 wt% MnO, spinels often contain >1 wt%, and one type of carbonatite sulphide contains up to 74 wt% alabandite (MnS) molecule.

*Natrocarbonatite alteration.* Alteration of the pristine, anhydrous natrocarbonatite lavas has given rise to various mineral parageneses depending on the length of exposure to downgrading influences. The whitening of flows, most readily seen on pahoehoe flows, begins shortly after extrusion and is mainly due to interaction with atmospheric moisture, leading to incipient breakdown of the phases in the matrix to form a thin layer of nahcolite (NaHCO<sub>3</sub>) and sylvite (KCl) (Dawson 1962a; Keller & Krafft 1990). Cracks on lava flows can be fringed with thermonatrite (Na<sub>2</sub>CO<sub>3</sub> · H<sub>2</sub>O), apthitalite (NaK<sub>2</sub>SO<sub>4</sub>), halite and sylvite as a result of more intense interaction (Genge *et al.* 2001). More prolonged reaction results in the replacement of nyerereite by pirssonite (Na<sub>2</sub>Ca(CO<sub>3</sub>)<sub>2</sub> · 2H<sub>2</sub>O) and the formation of secondary calcite and kogarkoite (Na<sub>3</sub>SO<sub>4</sub>F), and whole-rock analyses of this type of altered material show loss of K, Rb, P and Cl compared with fresh natrocarbonatite (Dawson *et al.* 1987; Keller & Zaitsev 2006; Zaitsev & Keller 2006). Even more extensive alteration results in a porous texture, replacement of nyerereite and gregoryite by pseudomorphs consisting of aggregates of tiny calcite grains, precipitation of apatite lower in REE but richer in F compared with that in unaltered natrocarbonatite, and formation of an opaque phase akin to romanèchite (BaMn<sub>9</sub>O<sub>16</sub>[OH<sub>4</sub>]). Bulk-rock analyses show considerable loss of Na, K, S, Cl, F, Rb and Sr; REE concentrations are higher, Ba is unaltered, (being fixed in the romanèchite), and δ<sup>18</sup>O is 24.5‰, compared with 5 to 8‰

for unaltered natrocarbonatite (Dawson 1993; Keller & Zaitsev 2006). A study of hornito stalactites formed by weathering of natrocarbonatite show them to be composed mainly of trona, with lesser amounts of nahcolite, thermonatrite, apthitalite, kogarkoite, schairerite ( $\text{Na}_{21}[\text{SO}_4]_7\text{F}_6\text{Cl}$ ), halite and sylvite; the products of subaerial weathering (pirssonite, gaylussite, shortite and calcite) are not found in the stalactites, though retained in the altered rocks forming the roofs of the hornitos, and the stalactites are interpreted as having formed by evaporation of Ca-free brines seeping from the altered roof lavas (Mitchell 2006c).

*Gas species.* Bulk-rock analyses show that fresh lava is anhydrous, leading to the belief that the dominant gas species in the Oldoinyo Lengai magma is  $\text{CO}_2$ . Moreover, during the 1966 and 2007 ash eruptions, despite much lightning and thunder in the ash cloud, no rainfall took place, and lapilli contained anhydrous sodium carbonate (natrite) and NaCa phosphate-carbonate (Dawson *et al.* 1968, 1992; Mitchell & Dawson 2007). However, analyses of gases from fumaroles showed them to be 64–74%  $\text{CO}_2$ , 24–34%  $\text{H}_2\text{O}$ , 0.88–1.0%  $\text{H}_2$ , 0.1–0.4% CO and <0.1%  $\text{H}_2\text{S}$ , HCl, HF and  $\text{CH}_4$ , and the total  $\text{CO}_2$  flux is in the order of  $0.06 \times 10^{12}$  mol  $\text{a}^{-1}$  (Koepenick *et al.* 1996). The gas mixture is similar to that from Nyiragongo, and the  $\text{CO}_2$  flux is second only to that from Mt Etna, although the Etna flux may be enhanced by lava interaction with sedimentary carbonate rocks below the volcano. Another study, which included observations on emissions from a lava pool, found the  $\text{CO}_2$  level to be even lower, and that the  $\text{CO}_2/\text{CO}$  ratio varied rapidly, interpreted as perhaps reflecting the mixing of gases exsolving from shallow and deeper magma chambers (Oppenheimer *et al.* 2002). These gas analysis studies concluded that  $\text{H}_2\text{O}$  may be more important than previously appreciated. However, the natrocarbonatite lava flows readily hydrate on contact with meteoric moisture, so it is not clear whether the measured  $\text{H}_2\text{O}$  content in the gas analyses is truly magmatic or whether it could have resulted from dehydration of the deep pile of hydrated lava within the crater, due to magma heating.

*Natrocarbonatite formation.* The actual formation of natrocarbonatite is still a matter of debate; hypotheses range from its being: (i) a primitive mantle-derived melt; (ii) fractionation of a parental alkali-bearing sövite magma; (iii) fractionation of silicate-bearing natrocarbonatite; or (iv) an immiscible fraction of the associated peralkaline nephelinites. The views of most authors, in a series of papers edited by Bell *et al.* (1998), incline towards liquid immiscibility. Simultaneous ejection of silicate and carbonate material during the 1966, 1993 and 2007 eruptions (Dawson *et al.* 1968, 1992; Church & Jones 1994; Mitchell & Dawson 2007) and the eruption in 1993 of carbonate lavas and tephra containing immiscible globules of silicate magma (within which were immiscible blebs of natrocarbonatite; Plates 21, 22) (Dawson *et al.* 1996a) provides evidence for the coexistence of silicate and carbonate magmas at the volcano (possibly in a compositionally- and density-stratified magma chamber). In the specific context of the well-established relationship between natrocarbonatite and the peralkaline nephelinites, Dawson (1998) suggested that  $\text{CO}_2$  saturation in the sub-volcanic magma chamber resulted in the formation of wollastonite nephelinite plus immiscible natrocarbonatite; interaction of wollastonite nephelinite and natrocarbonatite led to formation of peralkaline combeite nephelinite, with corrosion of wollastonite and clinopyroxene, and the ensuing  $\text{CO}_2$  release by the decarbonation reaction might lead to explosive eruption. An extreme example of this magma hybridization concept is provided by the melilite- and combeite-rich, but pyroxene-free, lapilli from the 20 September 2007 eruption, the origin of which is envisaged as due to mixing of wollastonite nephelinite and extremely large amounts of natrocarbonatite magmas; the result is precipitation of combeite and melilite rather than wollastonite and clinopyroxene (Mitchell & Dawson 2007).

## Kerimasi

*Type:* stratovolcano; *Lat/Long:* 2°51'S 35°5'E; *Elevation:* 2607 m; *Relief:* 1450 m; *Diameter:* 14 km; *Crater diameter:* 1.5 km (outer), 0.75 km (inner); *Eruptive history:* Pleistocene; *Composition:* nephelinite, phonolite, carbonatite; *QDS:* 39 Angata Salei.

Kerimasi post-dates the formation of the the Natron Basin boundary fault at 1.2 Ma, and its lower eastern slopes are penetrated by tuff cones that are dated at 0.37 Ma (MacIntyre *et al.* 1974). It initially erupted up, or very close to the Natron Basin boundary fault, then built up alongside the fault escarpment, and eventually overstepped onto the terrain to the west of the fault, a sector of which is now buried beneath the volcano (Fig. 7.16). Hence, it is steeper and has greater relief on its eastern and northern slopes, but has relatively shallow slopes on its western and southwestern flanks. The summit is occupied by a 100 m deep crater, at the eastern end of which is a smaller, 200 m deep crater (Guest *et al.* 1961). A large debris flow (*c.* 5 km wide and 9 km long) originated from a shallow arcuate feature on the upper eastern slopes of the volcano; this deposit is thickest (8 m) at its toe (Hay 1983; Kervyn *et al.* 2008b). The debris flow is not recent as it is cut by small NW–SE-trending faults and penetrated by tuff cones and explosion craters on the lower northeastern and eastern slopes (Dawson personal observation).

The core of the volcano is of nephelinitic tuffs and agglomerates that are best exposed in deep, radial gullies on the eastern and northern slopes (Fig. 7.17). Guest (1953) listed blocks of garnet gneiss and various volcanic types (olivine basalt, basanite and dolerite) derived from nearby country rocks, but it is the more exotic rock types in the agglomerates that have attracted the attention of numerous petrographers. Rosenbusch (1907) and Erdmannsdorfer (1935) describe ijolite and syenite collected by Uhlig during the German Central Africa Expedition in 1904–5, and Brögger (1921) described and provided an analysis of a melteigite provided by Finckh from the same collection. Guest (1953) described blocks of melanite urtite, melanite ijolite, amphibole melteigite and biotite pyroxenite, providing a whole-rock analysis of the last. James (1966) gave analyses of an ijolite and a nephelinite, and Dawson (personal observation) has found blocks of ijolite, ijolite-mantled mica pyroxenite, perovskite pyroxenite, mica pyroxenite, calcite-cemented pyroxenite and melanite melteigite. Church (1995) provided: (i) descriptions of melilite nephelinite, phonolitic nephelinite and phonolite, afrikandite, uncomphagrite, pyroxenite and ijolite blocks from agglomerates exposed in gullies on the northeastern lower slopes; (ii) microprobe analyses of clinopyroxene, nepheline, melilite, rutile, perovskite, melanite, Ti-magnetite, apatite, K-feldspar and phlogopite in some rocks; and (iii) major, trace and Nd–Sr isotope data on some rocks.

The silicate core is overlain by a carapace of carbonatite tuffs and agglomerates. Carbonatite tuffs containing variable amounts of phases derived from the silicate core (e.g. melanite, pyroxene, titanite, magnetite, phlogopite, nepheline, perovskite) blanket much of the volcano beneath a layer of brown soil. Carbonatite lapilli tuffs, the lapilli cored with either silicate minerals or rock fragments, occur on the lower eastern and upper southwestern slopes (Guest 1953; Mariano & Roeder 1983) and at Miamoja Hill, a small cone on the plain SE of Kerimasi (Dawson personal observation). Blocks of sövite, some with flow-banding and containing apatite, humite, high-Mn forsterite, high-Mn (up to 6 wt%) magnetite, baddeleyite and melanite are present in the carbonate-tuff-cemented agglomerates and as loose blocks in rivers draining the eastern and north-eastern upper slopes (Dawson *et al.* 1996b); some blocks contain zoned calcite phenocrysts (Mariano & Roeder 1983).

Two small plugs of intrusive calcite carbonatite crop out in the northern and eastern walls of the summit crater (James 1966). Abundant blocks of two different types of calcite carbonatite, one consisting of rounded calcite phenocrysts set in a vesicular



Fig. 7.16. Kerimasi from the south. The Natron Basin boundary fault escarpment (left) becomes progressively buried beneath the Kerimasi pyroclastics.

matrix characterized by skeletal parallel-growth calcite, the other of spinifex-textured calcite, occur in debris avalanche deposits on a small fault-bounded ridge [2°55'S 36°03'S] on the lower south-eastern slopes, and on the eastern slopes where the deposits underlie lapilli and blocks from the Deeti cone (Fig. 7.18) (Dawson personal observation). Church (1995) described carbonatite tuffs, together with blocks of sövite and beforsite in gullies on the northeastern slopes of the mountain, and gave whole-rock major, trace and Nd–Sr isotope data on some carbonatites; one distinctive type contains so-called 'corduroy' calcite with closely-spaced, parallel calcite lamellae. She also provided micro-probe analyses of apatites, Fe–Ti magnetites (containing up to 4% TiO<sub>2</sub>, 8.1% MnO and 11.4% MgO), pyrochlore, zirconolite, calzirtite, perovskite, phlogopite, forsterite, periclase, dolomite and monticellite in the sövites.

Additional chemical data (complete analyses for two sövites) were provided by Paslick *et al.* (1995), whole-rock isotope analyses for three sövite specimens by Kalt *et al.* (1997), and by Keller & Spettel (1995) who gave major, minor and trace element analyses for two carbonatites, one from a carbonatite breccia exposed in the walls of Loolmurwak crater, the other a lava from the summit area of the volcano. The lava contains zoned calcite similar that described by Mariano & Roeder (1983).

Church (1995) proposed that the original magma was a primitive melilite nephelinite, (the volcanic equivalent of uncomphagrite) similar to that at Armykon and Oldoinyo Loolmurwak (Dawson *et al.* 1985). This parent magma is proposed to have fractionated melilite and perovskite in a shallow-level magma chamber to give cumulate afrikandite and fractionated ijolite, and the carbonatites formed by immiscible separation from the primary olivine melilitite at low pressures. On isotopic evidence, Church (1995) suggested that the primary Kerimasi magma had exchanged isotopically with metasomatized mantle, as suggested for Oldoinyo Lengai by Bell & Dawson (1995a).

A particular aspect of Kerimasi geology is that Hay (1983) recorded blocks of rock that he interprets as altered natrocarbonatite in the avalanche deposit on the eastern lower slopes. The altered 'natrocarbonatite' contains phenocrysts of elongate primary calcite, and larger porous grains consisting of parallel sheets of calcite, interpreted as pseudomorphs after nyereite. These are texturally the same as the 'corduroy' calcites described by Church (1995) who disagreed with Hay's interpretation, proposing that the 'corduroy' calcite is an exsolution product of former dolomite. However, Church's disagreement does not take into account oxygen and carbon isotope evidence (Hay & O'Neill 1983). The data are: (i) in the primary calcite  $\delta^{18}\text{O}$  is

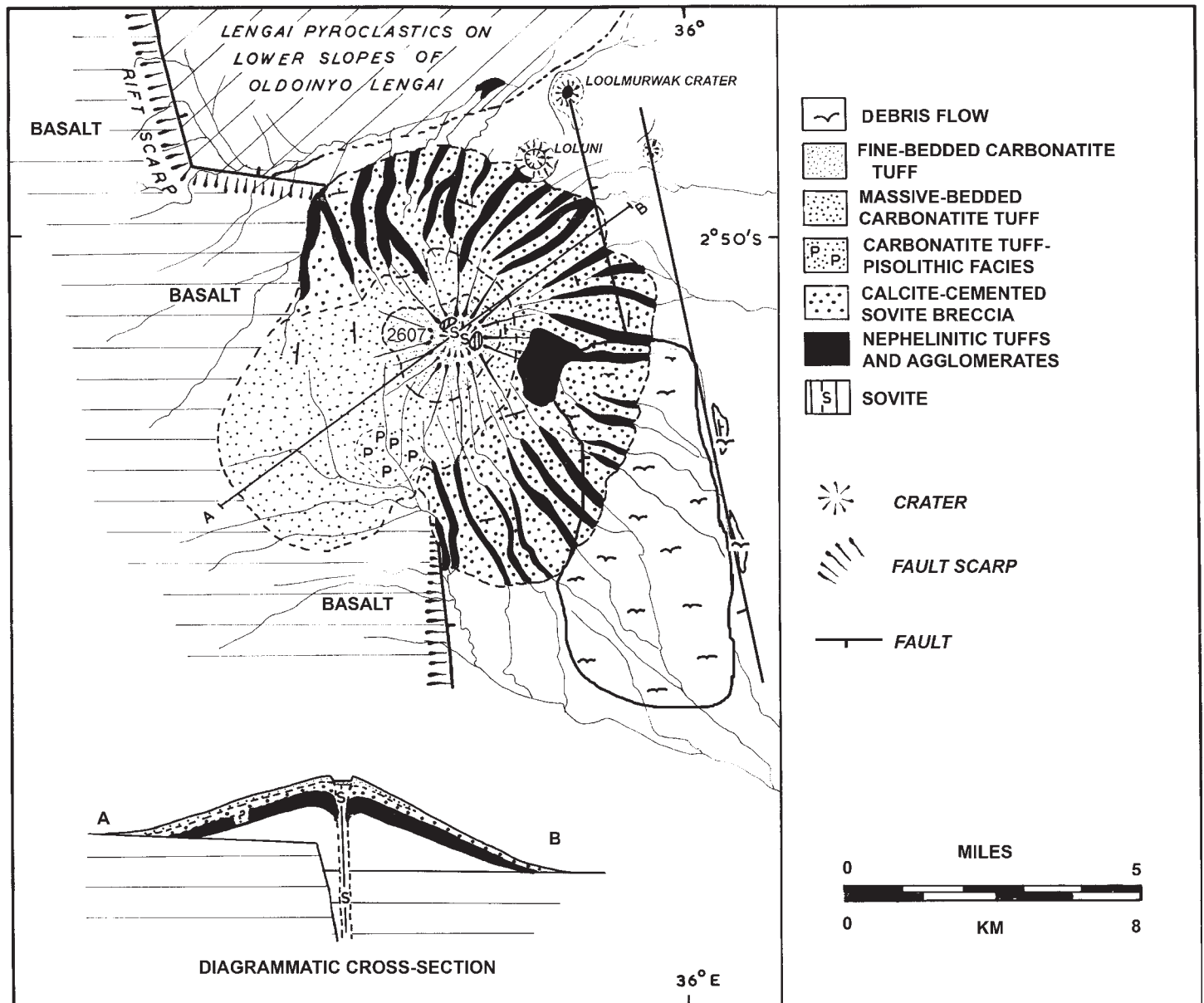


Fig. 7.17. Map and diagrammatic cross-section of Kerimasi. Modified from Dawson (1964b).

+7.2 to 7.3‰, and  $\delta^{13}\text{C}$  -4.2 to -4.3‰ (falling within the parameters for primary igneous carbonatite), compared with (ii)  $\delta^{18}\text{O}$  varying from +21.2 to +25.2‰, and  $\delta^{13}\text{C}$  from -1.4 to -3.3 in the calcite interpreted as pseudomorphing nyerereite. The main significance arising from Hay's interpretation, if correct, is the occurrence of natrocarbonatite at a locality other than Oldoinyo Lengai.

#### Natron-Engaruka tuff-cone area

*Type:* monogenetic tuff-cone/crater volcanic field; *Lat/Long:* centred on 3.40°S 36.00°E; *Elevation:* around 700–800 m; *Relief:* individual features up to 50 m; *Eruptive history:* Pleistocene–Holocene; *Composition:* olivine nephelinite, olivine melilitite; *QDS:* 39 Angata Salei, 40 Gelai and Ketumbeine.

The floor of the rift valley between Lake Natron and Engaruka, flanked on the west by Oldoinyo Lengai and Kerimasi, and on the east by Gelai and Ketumbeine, is covered and punctured by numerous small tuff cones, cratered tuff cones, tuff rings and explosion craters (Fig. 7.18). Some are aligned along minor

faults cutting across the lower slopes of Kerimasi and Gelai. Many are blanketed by tuff from Oldoinyo Lengai, and most between Oldoinyo Lengai and Lake Natron are partially covered or infilled with lahar deposits and outwash sediment from Oldoinyo Lengai. Most features are asymmetric, with maximum ejecta deposition on their northern or northwestern sides. Major craters, up to 1 km wide and 100 m deep, are Kisetey, Loolmurwak (also known as Swallow Crater), Eledoi and Embulu Sabuk. Cross-lamination and dune-bedding in the tuffs around some major craters (Dawson personal observation) are possibly the result of base surges. Megacrysts of kaersutite, mica and augite are common in the ejecta around these craters, and blocks of perovskite-rich pyroxenite, mica-kaersutite pyroxenite and ijolite occur in beds exposed in the walls of Loolmurwak crater (Dawson & Powell 1969).

Within this area are several small flows and scoria cones of olivine melilitite and olivine nephelinite. Although some are partially buried or obscured by debris flows consisting of Unit I pyroclastic materials from Oldoinyo Lengai, others are not, indicating that their extrusion is a very recent phenomenon. These include Armykon Hill on the southern shores of Lake

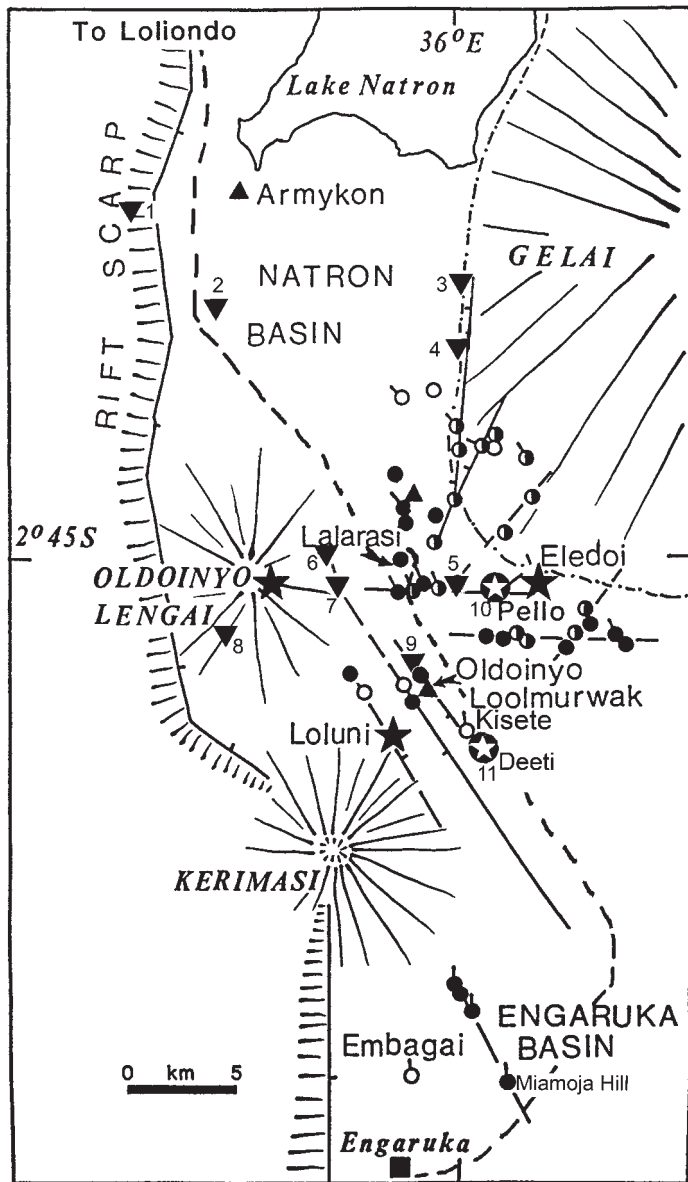


**Fig. 7.18.** The Engaruka–Lake Natron area. Based on Dawson & Powell (1969) with additional data from Keller *et al.* (2006). Explanation of ornaments: solid triangle: melilitite or nephelinite lava flow; inverted solid triangle: melilitite tuff cone; solid star: mantle xenolith locality; open star: mantle xenoliths in melilitite tuff; open circle: crater; half-filled circle: cratered tuff cone; filled circle: tuff cone; tick denotes direction of maximum ejecta deposition. Numbers refer to individual melilitite craters and tuff cones: 1, Sekenge crater; 2, Black Belly crater; 3, Oldoinyo Lolodulal cone; 4, Embululu Sabuk crater; 5, Lalarasi cone; 6, Dorobo cone; 7, Oltawata crater; 8, Kirurum crater; 9, Un-named cone; 10, Pello Hill cratered tuff-cone; 11, Deeti cone.

Natron (a small tholoid with flows of olivine melilitite), a minor flow of olivine melilitite 2 km north of Lalarasi, and an olivine-melilitite nephelinite flow at Oldoinyo Loolmurwak (Dawson *et al.* 1985) Keller *et al.* (2006) recorded other occurrences of olivine melilitite tuffs. Importantly some penetrate the older Unit I agglomerates of Oldoinyo Lengai, but are buried by Unit III combeite-nephelinite ash. Thus olivine melilitite activity occurs both before and after the debris flows that followed the cessation of the Oldoinyo Lengai Unit I activity, and in the interval between the Unit I and Unit III activity. Klaudius & Keller (2006) gave a  $^{14}\text{C}$  date of 2500 years BP on plant remains embedded in one of the debris flows. Agglutinated lapillae of carbonated melilitite occur at Miamoja Hill and at a small hill 2 km north of Loolmurwak crater. In the area immediately south

and SE of Pello Hill, are numerous, small, asymmetric, cratered tuff-cones consisting of melilitite lapilli; exceptionally the crater of one of these cones { $2^{\circ}47.35'S$   $36^{\circ}04'E$ } is partially infilled by a late extrusion of melilitite (Dawson personal observation, September 2007).

The equivalence of olivine melilitite with biotite- and amphibole-pyroxenites, depending upon depth/pressure of crystallization, has been recognized for some time (Tilley & Yoder 1968). Megacrysts of phlogopite, augite and amphibole (together with cumulate rocks of these phases), occur at several of the olivine melilitite localities in the Engaruka–Natron area and can be interpreted as additional pulses of melilitite magma that crystallized at depth/high pressure.

Major and trace element bulk-rock analyses and mineral analyses for the Oldoinyo Loolmurwak nephelinite lava, and melilitites from Lalarasi and Armykon Hill, are given by Dawson *et al.* (1985), James (1995), Keller *et al.* (2006) and Halama *et al.* (2007). Although of ultramafic composition, some of these lavas are unusually alkaline and have high concentrations of the REE (Fig. 7.11).

Xenoliths of peridotite occur at Eledoi crater (Dawson & Powell 1969) and clinopyroxene formation in a vein in one of these peridotites is of very recent age (Cohen *et al.* 1984). Others occur in katungitic scoria at Pello Hill, where there are also xenoliths of basement granulite. Many of the Pello peridotites are metasomatized, in some cases adjacent to olivine–mica–kaersutite–ilmenite veins (Dawson & Smith 1988) (Plate 23). At Deeti Hill, blocks of both olivine–mica pyroxenite (metasomatized upper mantle peridotite) and cumulate-textured kaersutite pyroxenite form the cores of melilitite autoliths (Johnson *et al.* 1997). Also at Deeti are xenoliths of cumulate-textured phlogopite pyroxenite, in which the main phases are cemented by calcite and glass (Dawson personal observation). Olivine–mica pyroxenite xenoliths (metasomatized peridotite) occur at Loluni crater, on the north-eastern slopes of Kerimasi, and also in the pyroclastics of Oldoinyo Lengai (Dawson & Smith 1992a). The metasomatized peridotite xenoliths in this area, some with densities as low as  $3140\text{ kg m}^{-3}$ , provide evidence for anomalously-light upper mantle beneath this sector of the rift (Dawson & Smith 1988).

#### Burko

*Type:* stratovolcano; *Lat/Long:*  $3.31^{\circ}\text{S}$   $36.23^{\circ}\text{E}$ ; *Elevation:* 2136 m; *Relief:* 900 m; *Volcano diameter:*  $7.5 \times 6.0$  km *Eruptive history:* Pleistocene; *Composition:* olivine-free nephelinite; *QDS:* 54 Monduli.

This small, cone sits above the older faulted lava plateau (Fig. 7.19). It is slightly elongate NE–SW, and has its maximum relief on its NW side, where it falls away to the Engaruka Basin. The cone consists of a core of nephelinitic tuffs and agglomerates containing plutonic xenoliths of barkevikite–phlogopite syenite, nepheline syenite and ijolite (Dawson 1964b). The nepheline syenites comprise albite, aegirine-augite and nepheline, and titanite is a constant accessory phase; other minor phases, not present in all specimens, are nosean (Table 7.7), apatite, biotite and an opaque phase. The more abundant ijolites have cumulate textures and comprise mainly zoned nepheline and zoned aegirine-augite; titanite is a common accessory, and other less common phases are nosean, apatite, magnetite and perovskite (in specimens lacking titanite). Astrophyllite occurs in one specimen and another contains primary intergranular calcite.

Nephelinites form blocks in the agglomerates, and also occur as later lava flows. Most are porphyritic with varying amounts of nepheline, aegirine-augite, nosean, melanite and titanite. Common groundmass phases are aegirine, nepheline, perovskite and magnetite in a glassy or devitrified matrix. The nosean and



**Fig. 7.19.** The Younger Extrusives volcano Burko from the south. A sector of the Elunata fault (foreground) represents the older faulted basalt terrain overlain by the volcano.

nepheline phenocrysts are commonly zeolitized. Biotite occurs in a few specimens, but it is corroded and surrounded by an opaque phase reaction rim, suggesting that it is xenocrystal. A nephelinite has given a K–Ar age of 0.97 Ma (Evans *et al.* 1971).

Paslick *et al.* (1995, 1996) give complete rock analyses of four nephelinites and of nepheline, titanite and zoned melanite in one of these specimens; analyses of a zoned nosean are given in Table 7.7.

### Meru

*Type:* stratovolcano; *Lat/Long:* 3°15'S 36°45'E; *Elevation:* 4568 m; *Relief:* *c.* 3100 m; *Volcano diameter:* *c.* 25 km; *Eruptive history:* Pleistocene–Holocene; *Composition:* olivine melilitite, nephelinite, phonolite, carbonatite; *QDS:* 55 Arusha.

Meru (Fig. 7.20) is a major stratovolcano rising to over 3000 m above the surrounding plains. The volcano was first climbed by Jaeger in 1904, and Uhlig (1907) described the recent appearance

**Table 7.7.** *Burko nosean*

	1	2
SiO <sub>2</sub>	33.60	34.90
TiO <sub>2</sub>	0.04	0.01
Al <sub>2</sub> O <sub>3</sub>	31.10	29.10
Fe <sub>2</sub> O <sub>3</sub> *	0.51	0.66
MnO	0.11	0.00
MgO	0.01	0.01
CaO	2.31	1.38
Na <sub>2</sub> O	17.90	17.80
K <sub>2</sub> O	3.53	3.91
P <sub>2</sub> O <sub>5</sub>	0.08	0.02
SO <sub>3</sub>	10.60	10.00
Cl	0.81	0.81
Sum	100.60	98.60
Less O≡Cl	0.18	0.18
Total	100.42	98.42

All iron as Fe<sub>2</sub>O<sub>3</sub>

1, 2. Core and rim of zoned nosean in nephelinite

BD266 Burko. Analyst: D.Steele

of the ash cone during a visit to the crater at that time. The volcano is classified as still active, and last erupted ash within the crater in 1910. Fumarolic activity within the crater was recorded as recently as 1953 (Guest & Leedal 1956). Very recently, Meru has assumed new importance in that it, and its subsidiary centre Ngurdoto, have been shown to have previously unrecognized carbonatitic affinities (Roberts 2002).

From the west, Meru appears a classic cone (Plate 24) but its eastern slopes are dominated by a major horseshoe-shaped collapse crater. Many smaller parasitic cones and craters occur in linear zones on the lower slopes and on the surrounding plains particularly to the west and SW. The volcano overlies a faulted basaltic terrain; on its NW side it buries the NW–SE-trending Lembolos graben, and on the southwestern side blankets the north–south-trending Oljoro graben, in the escarpment of which are basalt and mugearite aged 2.49 to 2.3 Ma (Wilkinson *et al.* 1986).

The earliest extrusives are phonolite and phonolitic nephelinite lavas on the lower western slopes (Meru West), aged around 1.5 Ma (Appendix 1, Dawson 2008). Some minor tholoids of phonolite and trachytic phonolite on the northern and lower western slopes, interbedded with pyroclastic rocks, are between 0.4 and 0.3 Ma. (Wilkinson *et al.* 1983). Little Meru (*c.* 4000 m), a smaller subsidiary monogenetic cone to the NE of the main cone, comprises nephelinite breccia with late nephelinite flows. The bulk of the main cone is dominated by pumice and tephra, interpreted as the products of Plinian eruptions, interbedded with nephelinite and phonolite flows ranging in age from 0.163 to 0.059 Ma, the youngest being in the summit area (Wilkinson *et al.* 1983).

Erosion of the pyroclastic rocks has given rise to deeply incised radial valleys, those on the upper part of the cone perhaps having been glacially initiated, and the cone has been extremely unstable with major lahar deposits, particularly from the northern and eastern slopes, flowing onto the surrounding plains well beyond the main cone. An especially large debris avalanche deposit on the eastern side resulted from a catastrophic collapse of the east side of the cone. The collapse produced a crater, breached on its eastern side, 5 km wide, 8 km long with almost-parallel sidewalls and a 1300 m high western wall (Plate 25). The debris avalanche has a run-out length of 33 km to the east where it eventually came to rest on the lower slopes of Kilimanjaro. Its areal coverage of *c.* 390 km<sup>2</sup> and estimated volume of 28 km<sup>3</sup> (Roberts 2002) make it one of the largest sub-aerial debris avalanches yet recorded, comparable with the collapses at Socompa, Chile (36 km<sup>3</sup>; de Vries *et al.* 2001) and Mt Shasta (26 km<sup>3</sup>; Crandell *et al.* 1984). For comparison, the 1980 avalanche at Mt St Helens had a volume of only 2.8 km<sup>3</sup> (Voight *et al.* 1981). Wilkinson *et al.* (1986) correlated the collapse with the vast ash eruption that spread a pumice mantle over the terrain to the west and NW of the cone, but Roberts (2002) suggested that the collapse was tectonically generated. Prior to this event, the mountain must have been considerably higher than its present-day height and by extrapolating the present slopes to a 1 km wide summit, Roberts (2002) estimated the pre-collapse height to be *c.* 5200 m. Part of the avalanche terrain is now occupied by the Momella Lakes; a study on the limnology of the lakes includes radiocarbon dates on bottom sediments of *c.* 8600 BP (Hecky 1971).

Following this collapse event, a lava dome with small flows of phonolitic nephelinite grew up on the crater floor and this, in turn, was followed by the formation of an ash cone (Plate 25). Xenoliths of fenite and kaersutite-bearing pyroxenite occur in one of the phonolitic-nephelinites flowing eastwards through the breach (Rock 1976).

*Petrography and mineralogy.* The most recent and extensive study of the rocks from Meru (Roberts 2002) shows that most lavas range from nephelinites to phonotephrites and tephriphonolites, whereas the Meru pumice is mainly of a more-evolved phonolite

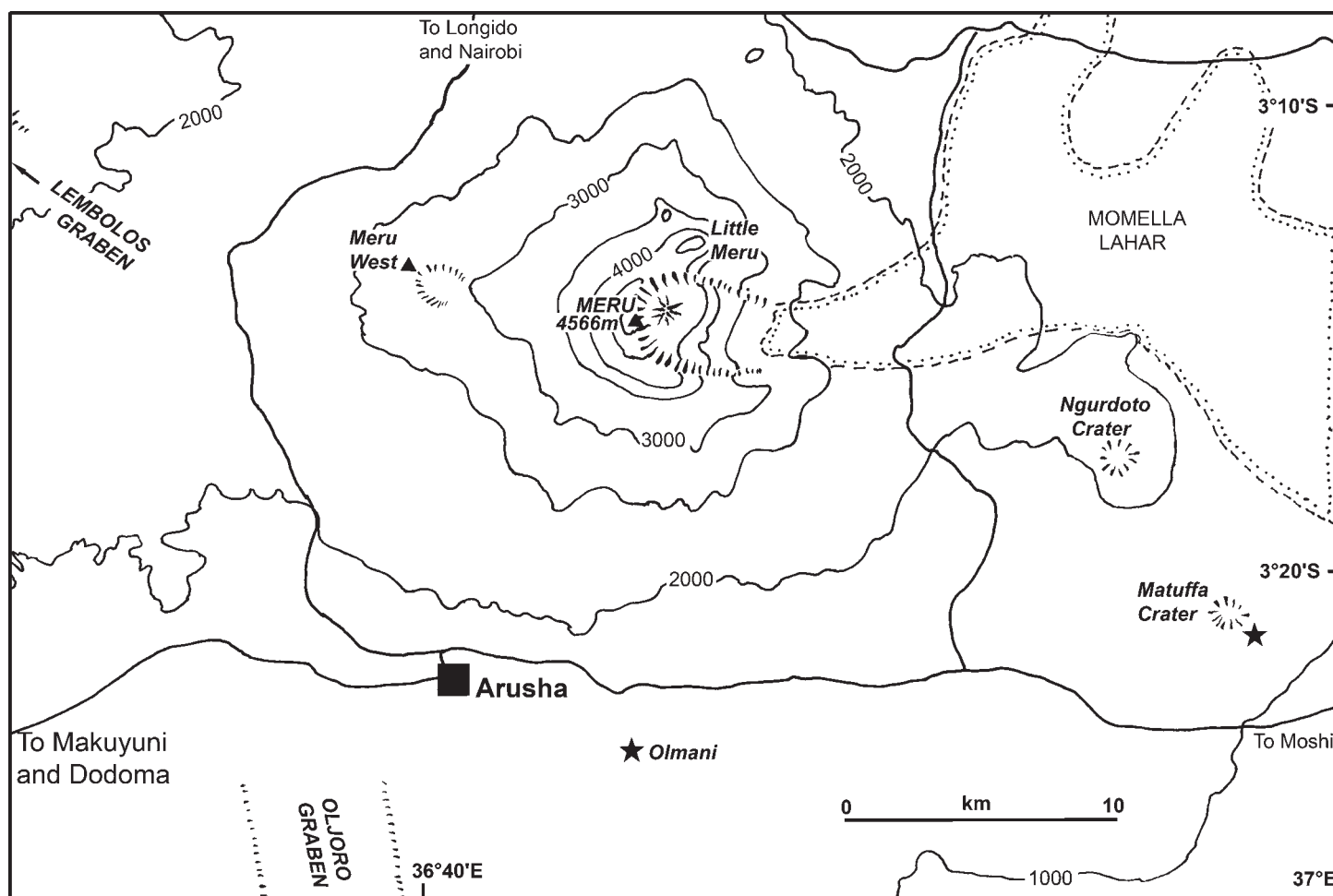


Fig. 7.20. Sketch map of Meru showing localities mentioned in the text. Stars indicate mantle xenolith localities.

composition. Nephelinites, including those in the summit area, the late flows within the crater, and from Little Meru, contain alkali clinopyroxene, nepheline, Ti-magnetite, titanite and kaersutite, often in a glassy matrix; rocks transitional to phonolite contain microphenocrystal sanidine. A distinctive type from Meru West contains schorlomite garnet, sodalite, melilite, a lath-shaped phase resembling delhayelite, and wollastonite, the last being replaced by combeite and apophyllite; this paragenesis is highly unusual, being previously identified only in the late combeite–wollastonite nephelinites from Oldoinyo Lengai.

The tephriphonolites and phonotephrites contain phenocrysts of Ti-augite, kaersutite, and Ti-magnetite in a matrix of plagioclase, Ti-magnetite and interstitial alkali feldspar and nepheline. With a gradation into phonolite, nepheline and anorthoclase become phenocryst phases in addition to clinopyroxene; the glassy matrix contains abundant sanidine, together with apatite and nepheline.

Cumulate amphibole–perovskite pyroxenite blocks, similar to those described in one of the later flows from the crater lava dome by Rock (1976), occur as blocks on the col between Little Meru and the main cone (Roberts 2002).

Roberts (2002) gave many analyses of olivine, clinopyroxene, amphibole and mica and a more limited number of analyses of magnetite, anorthoclase, nepheline, melilite, schorlomite, titanite, apatite, perovskite, sodalite, calcite, combeite, apophyllite and delhayelite. Roberts (2002) also gave major, minor and trace element analyses of 52 rocks, ranging from nephelinite to phonolite. Additionally, Paslick *et al.* (1995, 1996) gave complete rock analyses of one tephrite and two phonolites, and of clinopyroxene and amphibole in one of the phonolites. Wood (1968) provided

analyses of phonolites from the western slopes, and of phonolites described as being from ‘the Kilimanjaro Lakes, 20 miles west of Kilimanjaro’ (Appendix 2, Dawson 2008); this locality appears to be the Momella Lakes where the avalanche deposit contains many lava blocks.

Like the other Younger Extrusive volcanoes, the lower flanks of Meru and the surrounding plains are pockmarked by explosion craters and tuff-cones. Of these, three are noteworthy:

(i) *Ngurdoto* is small stratovolcano [ $3.28^{\circ}\text{S}$   $36.92^{\circ}\text{E}$ ] lying to the SE of Meru; it has a summit crater 360 m deep and measuring  $4 \times 3$  km. Due to material from the Meru debris avalanche on the lower slopes, and thick forest on the upper slopes, exposure is poor. The very few exposures are of tuff containing numerous mica crystals and blocks of pyroxene–phlogopite nephelinite, nephelinite, phonolite, phlogopite–calcite ijolite, melilite and carbonatite. Roberts (2002) provided analyses of a nephelinite, carbonate-rich ijolite and sövite, and of pyroxenes, mica (which in its low  $\text{TiO}_2$  contents is unlike others from the Meru area), kaersutite, schorlomite (in one of the carbonate-rich ijolites), titanite, apatite, perovskite, sodalite, and Sr-calcite (in sövite). Ngurdoto is important in that the overall assemblage indicates that it is a carbonatite-related volcano. Moreover, carbonate–silicate reaction relationships in some of the carbonate-rich blocks are taken by Roberts (2002) to indicate that the original carbonate was natrocarbonatite similar to that of Oldoinyo Lengai. Further, unlike Meru, the rocks at Ngurdoto are potassic, rather than sodic.

(ii) *Matuffa* [ $3^{\circ}22'\text{S}$   $37^{\circ}00'\text{E}$ ] is a heavily forested, small crater to the SE of Ngurdoto. On its lower, southern slopes are several small melilitite scoria cones, one of which contains xenoliths of harzburgite (Roberts 2002).

(iii) *Olmani*, a cinder cone some 8 km east of Arusha, contains blocks of upper mantle dunite, harzburgite and wehrlite, some of which have been partially melted (Jones *et al.* 1983a). The presence of low-Al clinopyroxene, monazite and apatite in some of these otherwise highly-refractory rocks indicates that they have been subject to carbonatite metasomatism (Rudnick *et al.* 1993). The Sr isotope values of the clinopyroxenes ( $^{87}\text{Sr}/^{86}\text{Sr}$  0.70304 to 0.7035) suggest that the metasomatism occurred recently. Originally termed ankaramite, the scoria has more recently been re-classified as olivine melanephelinite (Roberts 2002).

#### Monduli–Arusha–Oljoro volcanic field

*Type:* monogenetic tuff cone field; *Lat/Long:* centred on 3.40°S 36.55°E; *Elevation:* c. 1300 m; *Relief:* individual features up to 100 m; *Eruptive history:* ?Late Pleistocene; *Composition:* olivine basalt, olivine melilitite, ankaramite, carbonatite; *QDS:* 54 Monduli and 55 Meru.

The Ardai Plains SW and south of Monduli, the area between Monduli and the town of Arusha, and the area around the Oljoro valley, comprise a lava plateau. The derivation of the basalts, basanites and mugearites forming the plateau is uncertain, though a possible source is the Monduli volcano. Many minor volcanic features stand up above or penetrate the lava plateau (Fig. 5.8; Dawson 1964a); they consist of lava and scoria cones, asymmetric tuff rings and cratered tuff cones and explosion craters (always with maximum ejecta deposition on the western side of the features).

The morphology of these minor features suggest that they are of Late Pleistocene age, though in the eastern part of the field around Arusha they are partly covered by yellow tuff originating from Meru. Around Monduli the country is covered by a layer of what was formerly believed to be calcrete but which has been re-interpreted as recrystallized carbonatite ash (Dawson 1964c). The lava cones comprise a variety of petrographic types, including phlogopite-bearing basalts, olivine melilitites, and analcites. Roberts (2002) gave analyses of three olivine melilitites and two basanites from the area, and Paslick *et al.* (1995) gave a whole rock analysis of an olivine analcrite from a lava cone on the Ardai Plain.

Of particular interest in the area are:

- the Lashaine asymmetric tuff ring [3°22'S 36°26'E], which lies 8 km south of Monduli township. It comprises a lower unit of olivine melilitite scoria overlain by a mantle of carbonatite tuff; both units contain blocks of upper-mantle peridotite and deep crustal granulite. The peridotites, which comprise garnetiferous- and garnet-free dunite, harzburgite, lherzolite, wehrlite and pyroxenite, are very fresh and retain valuable intra-grain and grain-boundary information that is largely lost in similar peridotite blocks in kimberlite. The numerous studies on the peridotites are summarized by Dawson (2002), and a resumé is given in Chapter 8 (Dawson 2008). The granulite blocks are of basic composition, and contain scapolite. Like some of the peridotites, some retain evidence of a metasomatic event at c. 2 Ga, and others are partly-melted (Reid *et al.* 1975; Dawson 1977, 1987, 2002; Cohen *et al.* 1984; Jones *et al.* 1983b).
- Cameron's Crater, also known as Kisima ya Mungu (the Cauldron of God), on the west side of the Oljoro valley [3.53°E 36.54°S]. The explosion crater is 1.5 km in diameter and 200 m deep. Its thin, surrounding tuff-layer is highly calcareous and contains blocks of crustal granulites and granite, and upper-mantle peridotite.

#### Basotu maars

*Type:* maar field; *Lat/Long:* 4.36°S 36.08°E; *Elevation:* around 2000 m; *Relief:* up to 30 m above the surrounding countryside.

*Eruptive history:* Pleistocene; *Crater diameter:* up to 1 km; *Composition:* nephelinite/carbonatite; *QDS:* 84 Hanang.

30 craters and maars, and their tuff rings, form two NNE–SSW-trending semi-parallel belts around 15 km long on the southern Mbulu Plateau (Fig. 7.21). The elongation of these volcanic zones is controlled by dyke and fault alignment in the Archaean rocks through which the volcanics have erupted (Downie & Wilkinson 1972). The northwestern belt is the more continuous and contains some overlapping features; the other belt, lying some 8 km to the SE, consists of isolated craters and maars. Both fresh- and salt-water lakes occupy maars in both belts. Crater/maar diameters are up to 1 km (many only up to 300 m) and have depths of up to 100 m.

The fragmental material forming the tuff rings consists mainly of fragments of the Precambrian metasediments and volcanics through which the craters erupted, cemented by carbonate suggested by Downie & Wilkinson (1972) to be of igneous (carbonatite) origin.

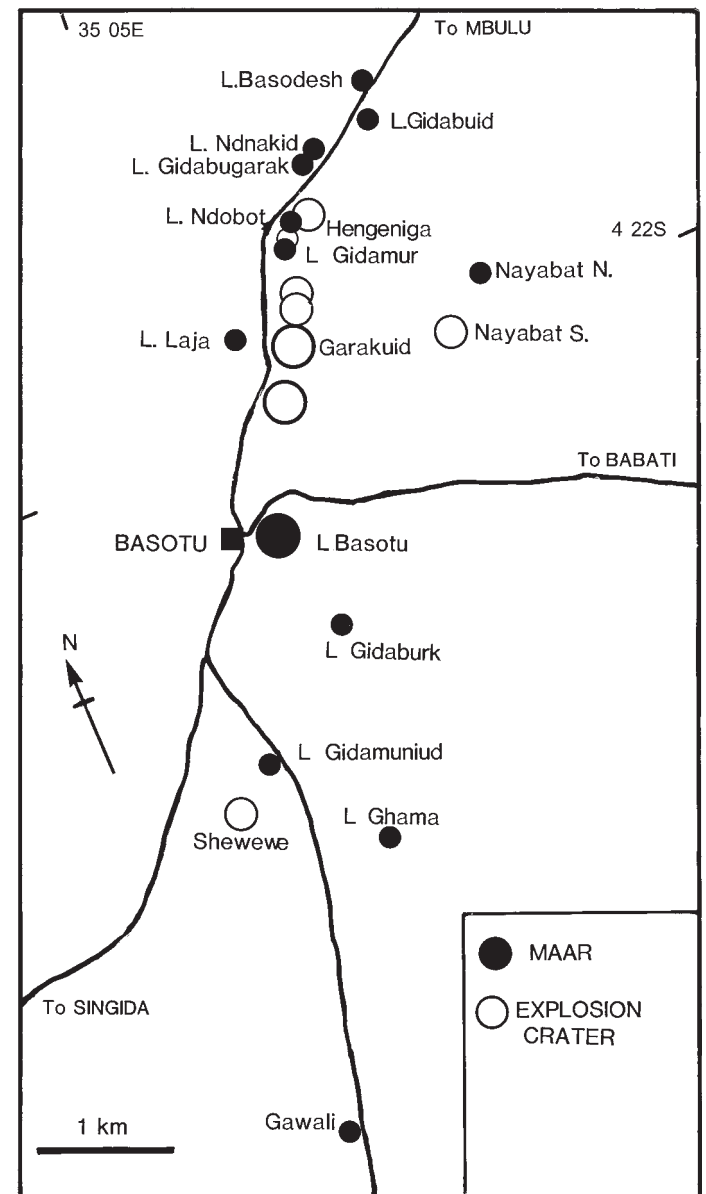


Fig. 7.21. Map of the Basotu maars and craters (after Downie & Wilkinson 1972). The overall NE–SW distribution of the features results from their control by shears and dyke intrusions in the underlying basement.

*Kwaraha (sometimes referred to as Ufiome)*

*Type:* stratovolcano; *Lat/Long:* 4.21°S 35.81°E; *Elevation:* 2225 m; *Relief:* 890 m; *Diameter:* 8 km *Eruptive history:* Pleistocene; *Crater diameter:* ?2 km; *Composition:* nephelinite/carbonatite; *QDS:* 85 Babati.

Kwaraha is one of the smaller Younger Extrusive centres. The southern slopes of the mountain are cut by precipitous, forested ravines, but the relatively gentle western and eastern slopes lead to a flat summit area, where the deep soil cover conceals a shallow crater. The mountain is not entirely volcanic, as north–south-trending ridges of Precambrian metasediments occur on the lower western and eastern slopes (Fig. 7.22).

The volcano consists mainly of nephelinite agglomerates and tuffs that contain a high proportion of fenitized metamorphic xenoliths (gneisses and metasediments) Nephelinite lava and crystal tuff occurs in the summit area. James (1966) provided analyses of melilitite, nephelinite and an augite-magnetite rock (Appendix 2, Dawson 2008). A plug of calcite carbonatite occurs in the breached crater and downslope on the lower south-eastern slopes of the mountain. The flow extends to beyond Galappo mission (M. S. Garson pers. comm. 1992) but is best exposed on the road surface at Galappo school (Dawson personal observation). The flow overlies lahar deposits and itself is overlain by nephelinite lava. The carbonatite contains apatite, Ti-magnetites of unusual stratiform shape (Deans & Seager 1978), and tiny (40–100 microns), yellow octahedra of pyrochlore.

Numerous tuff cones and craters occur within a radius of around 10–12 km on the plains NW, east and west of Kwaraha, and on a ridge of Precambrian metamorphic rocks to the south of the volcano. These are composed mainly of lithic and crystal tuffs consisting of pyroxene, olivine, amphibole, mica and plagioclase with a high amount of carbonatitic cement. Also within the explosion crater areas are numerous small hills of ‘olivine basalt’ (Mudd & Orridge 1966), two of which have proved to be of melilitite. Sora hill [4.17°S 35.88°E] consists of olivine melilitite containing numerous amphibole megacrysts and aggregates, and the prominent hill of Haindadonga [4.15°S 35.9°E], lying within the Tarangire National Park, consists of welded lapilli of phlogopite-phyric melilitite (Dawson *et al.* 1997).

*Hanang*

*Type:* stratovolcano; *Lat/Long:* 4.42°S 35.81°E; *Elevation:* 3420 m; *Diameter:* 10–12 km; *Relief:* 1700 m; *Eruptive history:* Pleistocene; *Crater diameter:* ?2 km; *Composition:* nephelinite/carbonatite; *QDS:* 84 Hanang and 103 Balangida Lelu.

Hanang (Fig. 7.23) is the most southerly of the major volcanoes in northern Tanzania, lying well to the south of the main volcanic area. The adjacent rift escarpment is lower than further north, and Hanang’s relative height makes it an impressive mountain (Fig. 7.24). Overlying updomed basement rocks, it is a steep cone with deep, radial ravines, the largest of which, occupied by

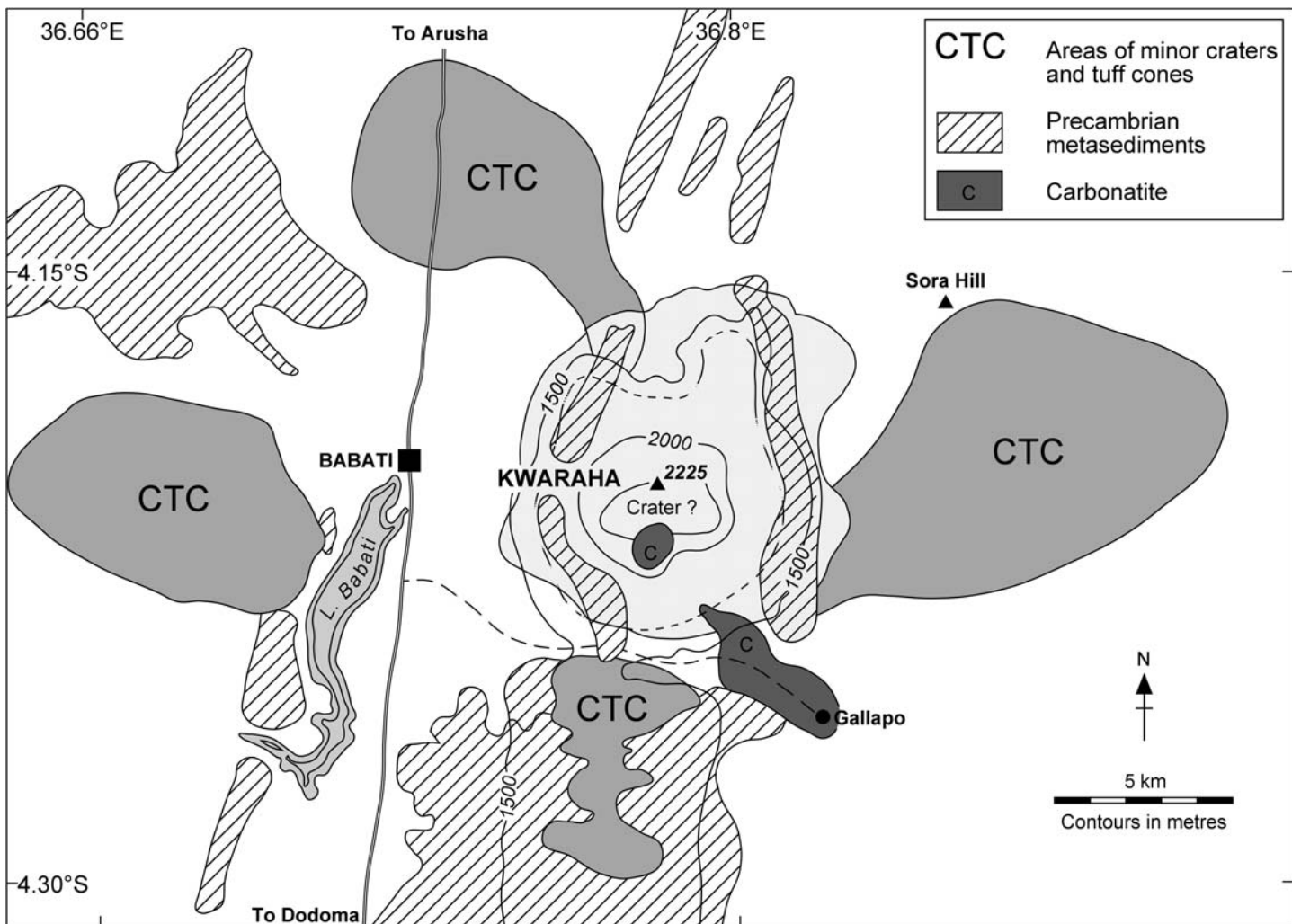


**Fig. 7.22.** Map of the Kwaraha volcano; based on Quarter Degree Sheet 85, information from M. S. Garson, and Dawson (personal observation). Sora Hill is a melilitite cone and is referred to in the text.

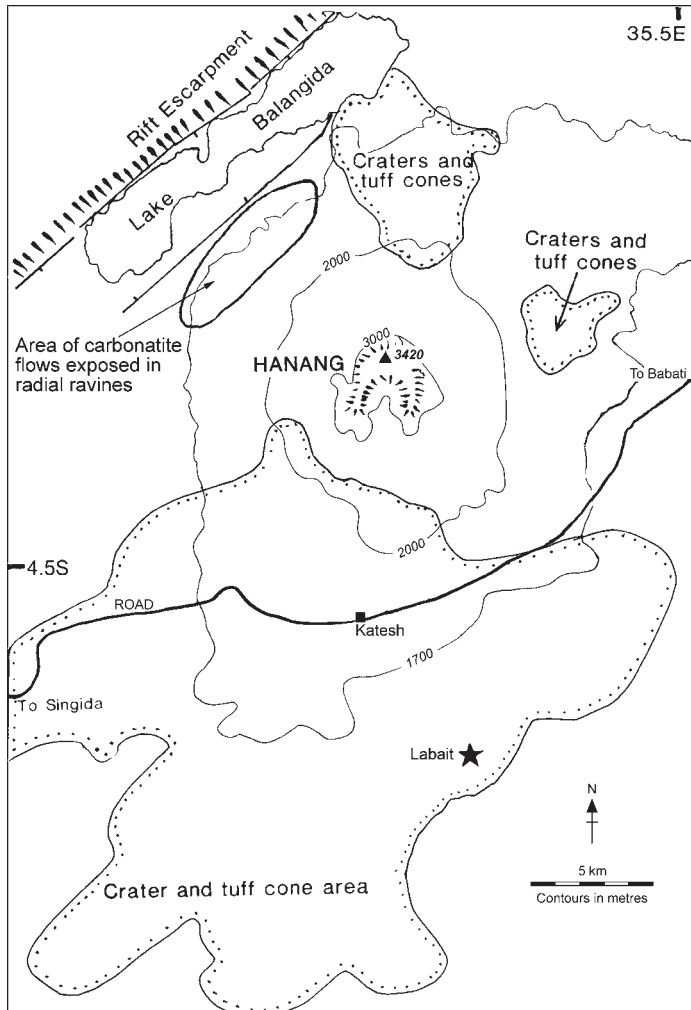


**Fig. 7.23.** Map of Hanang, based on Quarter Degree Sheets 64 and 103, information from M. S. Garson and Dawson (personal observation). Labait is a mantle xenolith locality.

the Hami river, is a major feature on the south side of the volcano. Steep ridges above the Hami gorge, and running SW and SE from the summit, may be the remnants of a breached crater.

Exposure is good only in the summit area and in the radial gorges. The volcano has a core of nephelinitic tuffs and



**Fig. 7.24.** Hanang, looking SE across the dried mud-flats of the Balangida basin.

agglomerates, and a partial cover of nephelinite lavas and carbonatitic tuff. Agglomerates in the summit area contain mainly blocks of nephelinite, and rarer melteigite and ijolite, in a calcareous matrix, together with basement-derived xenoliths of granitic and gabbroic rocks, many of which are fenitized. On the summit ridge are nephelinite dykes. The tuffs and lapilli tuffs forming most of the volcano are carbonate-rich and have outward dips of  $40^\circ$  in the summit area, shallowing off downslope (Thomas 1966). Two nephelinites have given ages of 1.5 and 0.9 Ma (Appendix 1, Dawson 2008).

On the lower northwestern slopes, below the 1700 m contour, three calcite carbonatite flows up to 3 m thick are interbedded with a sequence of nephelinitic flows, tuffs and agglomerates. Both the carbonatite flows and the agglomerates are crowded with boulders of fenitized basement gneiss and contain sporadically-distributed pyrochlore (M. S. Garson pers. comm. 1992). Many of the tuffs and agglomerates are cemented by calcite, probably of carbonatite origin.

Wood (1968) gave major and minor element analyses of seven nephelinites (Appendix 2, Dawson 2008) and Paslick *et al.* (1995, 1996) gave a complete analysis of one nephelinite from the volcano, and an analysis of its clinopyroxene.

Outcrops of nephelinitic tuffs and agglomerates believed to derive from Hanang occur, together with an interbedded sheet of carbonatite, above the escarpment to the west of Lake Balangida. A small dyke of carbonatite crops out in the escarpment. Numerous, small, parasitic tuff cones and craters occur on the lower northern and southern slopes of Hanang, and on the plains up to 25 km around the volcano. The parasitic cones and craters are mainly of calcite-cemented nephelinitic tuffs, but there are some minor scoria cones and flows of olivine nephelinite, olivine melilitite and monchiquite (Selby & Thomas 1966). Olivine melilitite scoria and lava at Labait hill, 7.5 km SE of Katesh, contain xenoliths of upper-mantle garnet lherzolite, chromite harzburgite and dunite (Dawson *et al.* 1997; Dawson 1999; Lee & Rudnick 1999).

#### *Igwisi Hills*

*Type:* monogenetic tuff-cone field; *Lat/Long:*  $4.85^\circ\text{S } 31.92^\circ\text{E}$ ; *Elevation:* c. 1300 m; *Relief:* up to 50 m; *Diameter:* single tuff cones up to 0.9 km; *Eruptive history:* ?Pleistocene; *Crater diameter:* up to 0.4 km; *Composition:* carbonatite-kimberlite.

The volcanism discussed hitherto occurs astride and within the rift valley and on the eastern side of the Tanzania Craton. Tertiary–Recent volcanicity is absent on the central part of the craton (although the site of Mesozoic kimberlite intrusion) but towards the western margin of the craton, three small, cratered tuff-cones stand above the peneplain to form the Igwisi Hills (Fig. 7.25). The youthful morphology of the cones indicates they are young, an inference supported by a poorly-constrained radiometric date (below). The volcanicity is highly unusual, in that the extruded material contains a high proportion of micro-xenoliths of upper mantle garnet peridotite in a carbonatitic matrix (Dawson 1994).

The three asymmetric, cratered tuff cones lie along a 2 km long, NE–SW-trending line. They stand some 70 m high above the surrounding countryside, have maximum ejectamenta deposition on their northwestern sides, and have steep inner walls and flat grassy crater floors. The outer slopes have karst-like solution topography. The SW hill is relatively simple, being an asymmetric, cratered cone highest on its western side (30 m above the crater floor), with the wall of the 0.23 km wide crater being breached on its eastern side. The northeastern hill is elongated NE–SW, and has two craters, a smaller 0.1 km wide SW crater, and a larger 0.35 km wide northeastern crater. The northeastern crater, the rim of which has a maximum height of 40 m, is breached on its northeastern side, and

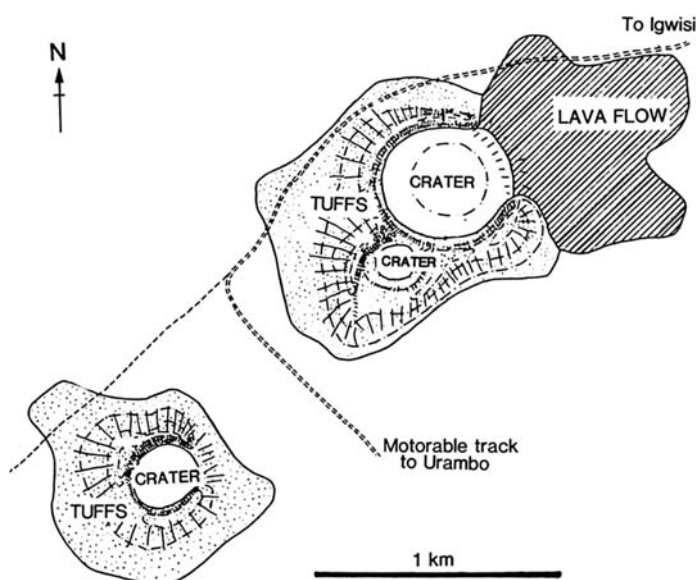


Fig. 7.25. Map of the Igwisi Hills (after Dawson 1994).

through this breach has flowed a viscous lava flow measuring around 0.8 km long and 0.7 km wide.

The tuffs are highly calcitic and contain both rounded nodules and fractured clasts of weathered and fresh olivine, together with blocks of biotite- and hornblende-gneiss. The lava is both flow- and gravity-differentiated and, particularly in its lower part, contains numerous rounded microxenoliths (up to 1 cm) (Plate 26) comprising combinations of strained and recrystallized forsterite, together with enstatite, chrome-diopside, pyrope garnet, phlogopite and calcite which, collectively, make up phlogopite-calcite garnet lherzolite. The matrix consists of smaller forsterite grains (unstrained and containing higher CaO than the nodule olivines), calcite, chlorite, spinel, perovskite and apatite. A U–Pb age on perovskite (poorly constrained due to the fine grain-size of the perovskite) is  $0 \pm 29$  Ma, consistent with a Quaternary age (Batumike *et al.* 2008). This unusual combination of high-temperature, refractory lherzolite micro-xenoliths with a lower-temperature volatile-rich matrix assemblage, is reminiscent of calcite-rich kimberlites (Dawson 1994), though the highly calcitic matrix and high contents of the rare-earth elements, strontium and barium, indicate some affinities with carbonatites. The conditions of equilibration of the phases in the peridotite xenoliths are  $850^\circ\text{C}$  and 35.9 kbar that, together with their mineralogy and the Sr and Nd isotope values of the flow, indicates that the Igwisi Hills magma originated by small degrees of melting of a carbonated peridotite protolith that had isotopic similarities to the source regions for Group I kimberlites and ocean island basalts, at depths of  $>100$  km.

### Hot springs

Hot springs (temperatures  $18\text{--}65^\circ\text{C}$ ) occur sporadically along many of the Pleistocene faults, e.g. on either sides of Lakes Natron, Eyasi and Balangdia, at Lake Manyara and in the relatively unrifted area towards the southern end of the Mponde graben and near Kondoa (James 1967). Most contain high concentrations of Na and K, whilst the brines at Mponde and Kondoa contain gases with high concentrations of nitrogen and helium, typical values (percentage by volume) being in the order of He: 5–7;  $\text{N}_2$ : 89–93; Ar: 1–2;  $\text{CO}_2$ : 1–2;  $\text{H}_2\text{S}$ ,  $\text{H}_2$  and  $\text{CH}_4$ :  $<1\%$  (Harris 1958).

### References

- BAGDASARYAN, G. P., GERASIMOVSKIY, V. I., POLYAKOV, A. I., GUKASYAN, R. K. & VERNADSKIY, V. I. 1973. Age of volcanic rocks in the rift zones of East Africa. *Geochemistry International*, **10**, 66–71.
- BAKER, B. H. 1963. *Geology of the Area South of Magadi*. Geological Survey of Kenya, Report 61.
- BAKER, B. H., MOHR, P. A. & WILLIAMS, L. A. J. 1972. *Geology of the Eastern Rift System of Africa*. Geological Society of America, Special Publications, **36**.
- BATUMIKE, J. M., GRIFFIN, W. L., BELOUSOVA, E. A., PEARSON, N. J., O'REILLY, S. Y. & SHEE, S. R. 2008. Africa's youngest kimberlite? LAM-ICPMS U–Pb dating of kimberlite perovskite from the Kundelungu Plateau, D.R.Congo. *Earth and Planetary Science Letters*, **267**, 609–619.
- BELL, K. & BLENKINSOP, J. 1987. Nd and Sr isotopic compositions of East African carbonatites: implications for mantle heterogeneity. *Geology*, **15**, 99–102.
- BELL, K. & DAWSON, J. B. 1995a. Nd and Sr isotope systematics of the active carbonatite volcano, Oldoinyo Lengai. In: BELL, K. & KELLER, J. (eds) *Carbonatite Volcanism of Oldoinyo Lengai and Petrogenesis of Natrocarbonatite*. Springer Verlag, Berlin, 100–112.
- BELL, K. & DAWSON, J. B. 1995b. An assessment of the alleged role of evaporites and saline brines in the origin of natrocarbonatite. In: BELL, K. & KELLER, J. (eds) *Carbonatite Volcanism of Oldoinyo Lengai and Petrogenesis of Natrocarbonatite*. Springer, Berlin, 137–147.
- BELL, K. & KELLER, J. (eds) 1995. *Carbonatite Volcanism of Oldoinyo Lengai and Petrogenesis of Natrocarbonatite*. Springer, Berlin.
- BELL, K. & PETERSON, T. 1991. Nd and Sr isotope systematics of Shombole volcano, East Africa, and the links between nephelinites, phonolites and carbonatites. *Geology*, **19**, 582–585.
- BELL, K. & SIMONETTI, A. 1996. Carbonatite magmatism and plume activity: implications from the Nd, Pb and Sr isotope systematics of Oldoinyo Lengai. *Journal of Petrology*, **37**, 1321–1339.
- BELL, K., FARQUHAR, R. M. & DAWSON, J. B. 1973. Strontium isotope studies of alkalic rocks: the active carbonatite volcano Oldoinyo Lengai, Tanzania. *Bulletin of the Geological Society of America*, **84**, 1019–1030.
- BELL, K., KJAARSGAARD, B. A. & SIMONETTI, A. (eds) 1998. *Carbonatites – into the Twenty-First Century. A Volume in Honour of John Gittins*. Special Number of *Journal of Petrology*, **39**, 1839–2151.
- BISHOP, W. W., MILLER, J. A. & FITCH, F. H. 1969. New potassium–argon age determinations relevant to the Miocene fossil mammal occurrences in East Africa. *American Journal of Science*, **267**, 669–699.
- BULLETIN OF THE GLOBAL VOLCANISM NETWORK 2006. Oldoinyo Lengai, **31**, Number 3, 13–15, March 2006.
- BRÖGGER, W. C. 1921. Die Eruptivgesteine des Kristianagebietes. IV Das Fengebiet in Telemark, Norwegen. *Videnskapssels kapets Skrifter, I. Matematisk-natur vitenskapelig Klasse No. 9*, Kristiana.
- CHURCH, A. A. 1995. *The Petrology of the Kerimasi Volcano and the Carbonatites of Oldoinyo Lengai with a Review of other Occurrences of Extrusive Carbonatites*. PhD thesis, University College, London.
- CHURCH, A. A. & JONES, A. P. 1994. Hollow natrocarbonatite lapilli from the 1992 eruption of Oldoinyo Lengai, Tanzania. *Journal of the Geological Society, London*, **151**, 59–63.
- COHEN, R. S., O'NIONS, R. K. & DAWSON, J. B. 1984. Isotope geochemistry of xenoliths from East Africa: implications for the development of mantle reservoirs and their interaction. *Earth and Planetary Science Letters*, **68**, 209–220.
- COOPER, J. P. 1972. *Geochemistry of Tarosero volcano, northern Tanzania*. MSc thesis, University of Manchester.
- CRANDELL, D. R., MILLER, C. D., GLICKEN, H. X., CHRISTIANSEN, R. L. & NEWHALL, C. G. 1984. Catastrophic debris avalanche from ancestral Mount Shasta volcano, California. *Geology*, **12**, 143–146.
- CROSSLEY, R. 1979. The Cenozoic stratigraphy and structure of the western part of the rift valley in southern Kenya. *Journal of the Geological Society of London*, **136**, 393–405.
- CURTIS, G. H. & HAY, R. L. 1972. Further geological studies and K–Ar dating at Olduvai Gorge and Ngorongoro crater. In: BISHOP, W. W.

- & MILLER, J. W. (eds). *Calibration of Hominoid Evolution*. Scottish Academic Press, Edinburgh, 107–134.
- DAWSON, J. B. 1962a. The geology of Oldoinyo Lengai. *Bulletin Volcanologique*, **24**, 349–387.
- DAWSON, J. B. 1962b. Sodium carbonate lavas from Oldoinyo Lengai, northern Tanganyika. *Nature*, **196**, 1065–1066.
- DAWSON, J. B. 1964a. Carbonate tuff cones in northern Tanganyika. *Geological Magazine*, **101**, 129–37.
- DAWSON, J. B. 1964b. *Monduli*. Tanzania Geological Survey Quarter Degree Sheet **54**.
- DAWSON, J. B. 1964c. Carbonatitic volcanic ashes in northern Tanganyika. *Bulletin Volcanologique*, **27**, 81–92.
- DAWSON, J. B. 1977. Sub-cratonic and upper mantle models based on xenolith suites in kimberlite and nephelinitic diatremes. *Journal of the Geological Society, London*, **134**, 173–184.
- DAWSON, J. B. 1987. Metasomatized harzburgites in kimberlite and alkaline magmas: enriched restites and ‘flushed’ lherzolites. In: MENZIES, M. A. & HAWKESWORTH, C. J. (eds) *Mantle Metasomatism*. Academic Press, London, 125–144.
- DAWSON, J. B. 1989. Sodium carbonatite extrusions from Oldoinyo Lengai, Tanzania: implications for carbonatite complex genesis. In: BELL, K. (ed) *Carbonatites: genesis and evolution*. Unwin Hyman, London, 255–277.
- DAWSON, J. B. 1993. A supposed sövite from Oldoinyo Lengai, Tanzania: result of extreme alteration of alkali carbonatite lava. *Mineralogical Magazine*, **57**, 93–101.
- DAWSON, J. B. 1994. Quaternary kimberlitic volcanism on the Tanzania craton. *Contributions to Mineralogy and Petrology*, **116**, 473–485.
- DAWSON, J. B. 1997. Neogene–Recent rifting and volcanism in northern Tanzania: relevance for comparisons between the Gardar province and the East African Rift valley. *Mineralogical Magazine*, **61**, 543–548.
- DAWSON, J. B. 1998. Peralkaline nephelinite–natrocarbonatite relationships at Oldoinyo Lengai, Tanzania. *Journal of Petrology*, **39**, 2077–2094.
- DAWSON, J. B. 1999. Melting and metasomatism in spinel peridotite xenoliths from Labait, Tanzania. In: GURNEY, J. J., GURNEY, J. L., PASCOE, M. D. & RICHARDSON, S. H. (eds) *Proceedings of the 7th International Kimberlite Conference, Cape Town, 1998*, **1**, Red Roof Design, Cape Town, 164–173.
- DAWSON, J. B. 2002. Metasomatism and partial melting in upper-mantle peridotite xenoliths from the Lashaine volcano, northern Tanzania. *Journal of Petrology*, **43**, 1749–1777.
- DAWSON, J. B. 2008. *The Gregory Rift Valley and Neogene–Recent Volcanoes of Northern Tanzania*. Geological Society, London, Memoirs, **33**.
- DAWSON, J. B. & FRISCH, T. 1971. Eucolite from Oldoinyo L’engai, Tanzania. *Lithos*, **4**, 297–303.
- DAWSON, J. B. & FUGE, R. 1980. Halogen content of some African carbonatites. *Lithos*, **13**, 139–143.
- DAWSON, J. B. & GALE, N. 1970. Uranium and thorium in alkalic lavas from the active carbonatite volcano Oldoinyo Lengai, northern Tanzania. *Chemical Geology*, **6**, 221–231.
- DAWSON, J. B. & HILL, P. G. 1998. Mineral chemistry of a peralkaline combeite–lamprophyllite nephelinite from Oldoinyo Lengai, Tanzania. *Mineralogical Magazine*, **62**, 179–196.
- DAWSON, J. B. & MITCHELL, R. H. 2007. Oldoinyo Lengai. Contribution to *Bulletin of the Global Volcanism Network*, **32**, November 2007, 14–15.
- DAWSON, J. B. & POWELL, D. G. 1969. The Engaruka–Natron explosion crater area, northern Tanzania. *Bulletin Volcanologique*, **33**, 791–817.
- DAWSON, J. B. & SAHAMA, T. G. 1963. A note on parawollastonite from Oldoinyo Lengai, Tanganyika. *Schweizer Mineralogisches und Petrographisches Mitteilungen*, **43**, 131–133.
- DAWSON, J. B. & SMITH, J. V. 1988. Veined and metasomatized peridotites from Pello Hill, Tanzania: evidence for anomalously-light mantle beneath the Tanzania sector of the eastern Rift Valley. *Contributions to Mineralogy and Petrology*, **100**, 510–527.
- DAWSON, J. B. & SMITH, J. V. 1992a. Olivine–mica–pyroxenite xenoliths from Oldoinyo Lengai, Tanzania: metasomatic products of upper mantle peridotites. *Journal of Volcanology and Geothermal Research*, **50**, 131–142.
- DAWSON, J. B. & SMITH, J. V. 1992b. Potassium loss during metasomatic alteration of mica pyroxenite from Oldoinyo Lengai, northern Tanzania; contrasts with fentization. *Contributions to Mineralogy and Petrology*, **112**, 254–260.
- DAWSON, J. B., BOWDEN, P. & CLARK, G. C. 1968. Activity of the carbonatite volcano Oldoinyo Lengai, 1966. *Geologisches Rundschau*, **57**, 865–879.
- DAWSON, J. B., POWELL, D. G. & REID, A. M. 1970. Ultrabasic xenoliths and lava from the Lashaine volcano, northern Tanzania. *Journal of Petrology*, **11**, 519–548.
- DAWSON, J. B., SMITH, J. V. & JONES, A. P. 1985. A comparative study of bulk rock and mineral chemistry of olivine melilitites and associated rocks from East and South Africa. *Neues Jahrbuch für Mineralogie, Abteilung*, **152**, 143–175.
- DAWSON, J. B., GARSON, M. S. & ROBERTS, B. 1987. Altered former alkalic carbonatite lava from Oldoinyo Lengai, Tanzania: inferences for calcite carbonatite lavas. *Geology*, **15**, 765–768.
- DAWSON, J. B., SMITH, J. V. & STEELE, I. M. 1989. Combeite ( $\text{Na}_{2.33}\text{Ca}_{1.74}\text{others}_{0.12}\text{Si}_3\text{O}_9$ ) from Oldoinyo Lengai, Tanzania. *Journal of Geology*, **97**, 365–372.
- DAWSON, J. B., PINKERTON, H., NORTON, G. E. & PYLE, D. M. 1990. Physico-chemical properties of alkali carbonatite lavas: data from the 1988 eruption of Oldoinyo Lengai, Tanzania. *Geology*, **18**, 260–263.
- DAWSON, J. B., SMITH, J. V. & STEELE, I. M. 1992. 1966 ash eruption of the carbonatite volcano, Oldoinyo Lengai; mineralogy of lapilli, and mixing of silicate and carbonate lava. *Mineralogical Magazine*, **56**, 1–16.
- DAWSON, J. B., PINKERTON, H., PYLE, D. M. & NYAMWERU, C. 1994. June 1993 eruption of Oldoinyo Lengai, Tanzania: Exceptionally viscous and large carbonatite lava flows and evidence for coexisting silicate and carbonate magmas. *Geology*, **22**, 799–802.
- DAWSON, J. B., KELLER, J. & NYAMWERU, C. 1995a. Historic and recent eruptive activity of Oldoinyo Lengai. In: BELL, K. & KELLER, J. (eds) *Carbonatite Volcanism*. Springer, Berlin, 4–22.
- DAWSON, J. B., SMITH, J. V. & STEELE, I. M. 1995b. Petrology and mineral chemistry of plutonic igneous xenoliths from the carbonatite volcano Oldoinyo Lengai, Tanzania. *Journal of Petrology*, **36**, 797–826.
- DAWSON, J. B., PINKERTON, H., NORTON, G. E., PYLE, D. M., BROWNING, P., JACKSON, D. & FALLICK, A. E. 1995c. Petrology and geochemistry of Oldoinyo Lengai lavas extruded in November 1988: magma source, ascent and crystallization. In: BELL, K. & KELLER, J. (eds) *Carbonatite Volcanism*. Springer, Berlin, 47–69.
- DAWSON, J. B., PYLE, D. M. & PINKERTON, H. 1996a. Evolution of natrocarbonatite from a wollastonite nephelinite parent: evidence from the June 1993 eruption of Oldoinyo Lengai, Tanzania. *Journal of Geology*, **104**, 41–54.
- DAWSON, J. B., STEELE, I. M., SMITH, J. V. & RIVERS, M. L. 1996b. Minor and trace element chemistry of carbonates, apatites and magnetites in some African carbonatites. *Mineralogical Magazine*, **60**, 415–425.
- DAWSON, J. B., JAMES, D., PASLICK, C. & HALLIDAY, A. M. 1997. Ultrabasic potassic low-volume magmatism and continental rifting in north-central Tanzania: association with enhanced heat flow. *Russian Geology and Geophysics*, **38**, 69–81.
- DAWSON, J. B., HINTON, R. W. & STEELE, I. M. (in press). The composition of anorthoclase and nepheline in Mount Kenya phonolite and Kilimanjaro trachyte, and crystal-glass partitioning of elements. *Canadian Mineralogist*.
- DE VRIES, B. V., SELF, S., FRANCIS, P. W. & KESZTHELYI, L. 2001. A gravitational spreading origin for the Socompa debris avalanche. *Journal of Volcanological and Geothermal Research*, **105**, 225–247.
- DEANS, T. & SEAGER, A. F. 1978. Stratiform magnetite crystals of abnormal morphology from volcanic carbonatites in Tanzania, Kenya, Greenland and India. *Mineralogical Magazine*, **42**, 463–475.
- DONALDSON, C. H. & DAWSON, J. B. 1978. Skeletal crystallization and residual glass compositions in a cellular alkalic pyroxenite from

- Oldoinyo Lengai: implications for the evolution of the alkalic carbonatite lavas. *Contributions to Petrology and Mineralogy*, **67**, 139–149.
- DONALDSON, C. H., DAWSON, J. B., KANARIS-SOTIRIOU, R., BATCHELOR, R. A. & WALSH, J. N. 1987. The silicate lavas of Oldoinyo Lengai. *Neues Jahrbuch für Mineralogie Abhandlungen*, **156**, 247–279.
- DOWNIE, C. 1964. Glaciations of Mount Kilimanjaro, northeast Tanganyika. *Bulletin of the Geological Society of America*, **75**, 1–16.
- DOWNIE, C. & WILKINSON, P. 1962. The explosion craters of Basotu, Tanganyika Territory. *Bulletin Volcanologique*, **24**, 389–420.
- DOWNIE, C. & WILKINSON, P. 1972. *The Geology of Kilimanjaro*. University of Sheffield, Sheffield.
- DOWNIE, C., HUMPHRIES, D. W., ET AL. 1965. *Kilimanjaro-Moshi (Geological Map of Kilimanjaro)*. Special Sheet covering Tanganyika Geological Survey Quarter Degree Sheets **42**, **56** and **57**.
- DRAKE, P. & CURTIS, G. H. 1987. K–Ar geochronology of the Laetoli fossil localities. In: LEAKEY, M. D. & HARRIS, J. M. (eds) *Laetoli, a Pliocene Site in Northern Tanzania*. Clarendon Press, Oxford, 48–52.
- DUNDAS, D. L. & AWADALLAH, G. W. (unpublished). *Loliondo*. Unpublished report and map of Quarter Degree Sheet 16 and 27, Tanzania Geological Survey. Mapped 1966.
- ERDMANNSDORFER, O. 1935. Über wollastoniturtit und die Entstehungsweisen von alkaligesteiner. *Sitzungsberichte der Heidelberg Akademie für Wissenschaften, Mathematik und Naturgeschichte*, **K 1.2**, 1–23.
- EVANS, A. L., FAIRHEAD, J. D. & MITCHELL, J. G. 1971. Potassium–argon ages from the volcanic province of northern Tanzania. *Nature*, **229**, 19–20.
- FAIRHEAD, J. D., MITCHELL, J. G. & WILLIAMS, L. A. J. 1972. New K/Ar determinations on Rift volcanics of S. Kenya and their bearing on the age of Rift faulting. *Nature*, **238**, 66–9.
- FARLER, J. P. 1882. Native routes in East Africa from Pangani to the Masai country. *Proceedings of the Royal Geographical Society, New Series*, **4**, 730–753.
- FINCKH, L. 1903. Die trachydolerite des Kibo (Kilimandscharo) und die kenyte des Kenya. *Zeitschrift der Deutsches Geologische Gesellschaft*, **55**, Monatsbericht 1–14.
- FISCHER, G. A. 1884–1885. Reise in das Masailand. *Mitteilungen der Geographisches Gesellschaft Hamburg*, Pt 1 (1884), 36–99, Pts 2 and 3 (1885) 189–237 and 238–279.
- GENGE, M. J., BALME, M. & JONES, A. P. 2001. Salt-bearing fumarole deposits in the summit crater of Oldoinyo Lengai, Northern Tanzania: interactions between natrocarbonatite and meteoric water. *Journal of Volcanological and Geothermal Research*, **106**, 111–122.
- GITTINS, J. & MCKIE, D. 1980. Alkalic carbonate magmas: Oldoinyo Lengai and its wider applicability. *Lithos*, **13**, 213–215.
- GROMMÉ, C. S., REILLY, T. A., MUSSETT, A. E. & HAY, R. L. 1970. Palaeomagnetism and potassium–argon ages of volcanic rocks of Ngorongoro caldera, Tanzania. *Geophysical Journal of the Royal Astronomical Society*, **22**, 101–115.
- GUEST, N. J. 1953. *The Geology of Part of Northern Tanganyika Territory*. PhD thesis, University of Sheffield.
- GUEST, N. J. 1956. The volcanic activity of Oldoinyo Lengai 1954. *Records of the Tanganyika Geological Survey*, **4**, 56–59.
- GUEST, N. J. & LEEDAL, G. P. 1956. The volcanic activity of Mount Meru. *Records of the Geological Survey of Tanganyika*, **3**, 40–46.
- GUEST, N. J. & PICKERING, R. 1966a. *Kibangaini*. Tanzania Mineral Resources Division, Quarter Degree Sheet **28**.
- GUEST, N. J. & PICKERING, R. 1966b. *Gelai and Ketumbeine*. Tanzania Mineral Resources Division, Quarter Degree Sheet **40**.
- GUEST, N. J., JAMES, T. C., PICKERING, R. & DAWSON, J. B. 1961. *Angata Salei*. Tanzania Geological Survey Quarter Degree Sheet **39**.
- HALAMA, R., McDONOUGH, W. F., RUDNICK, R. L., KELLER, J. & KLAUDIUS, J. 2007. The Li isotopic composition of Oldoinyo Lengai: Nature of the mantle sources and lack of isotopic fractionation during carbonatite petrogenesis. *Earth and Planetary Science Letters*, **254**, 77–89.
- HARRIS, J. F. 1958. Geological investigations, sampling and diamond drilling at Manyeghi helium-bearing hot springs, Singida District. *Records of the Geological Survey of Tanganyika*, **VIII**, 86–98.
- HART, S. R. 1988. Heterogeneous mantle domains: signatures, genesis and mixing chronologies. *Earth and Planetary Science Letters*, **90**, 273–296.
- HAY, R. L. 1963. Zeolitic weathering in Olduvai Gorge, Tanganyika. *Bulletin of the Geological Society of America*, **74**, 1281–1286.
- HAY, R. L. 1964. Discussion in Dawson (1964b).
- HAY, R. L. 1976. *Geology of the Olduvai Gorge*. University of California Press, Berkeley.
- HAY, R. L. 1983. Natrocarbonatite tephra of Kerimasi volcano. *Geology*, **11**, 599–602.
- HAY, R. L. 1989. Holocene carbonatite–nephelinite tephra deposits of Oldoinyo Lengai, Tanzania. *Journal of Volcanological and Geothermal Research*, **37**, 77–91.
- HAY, R. L. & O'NEILL, J. R. 1983. Carbonatite tuffs in the Laetoli Beds of Tanzania and the Kaiserstuhl in Germany. *Contributions to Mineralogy and Petrology*, **82**, 403–406.
- HECKY, R. E. 1971. *The Palaeolimnology of the Alkaline, Saline Lakes on the Mt Meru Lahar*. PhD thesis, Duke University.
- ISAAC, G. L. & CURTIS, G. H. 1974. Age of the Acheulian industries from the Peninj Group, Tanzania. *Nature*, **249**, 624–627.
- JAGO, B. C. & GITTINS, J. 1999. Mn- and F-bearing rasvumite in natrocarbonatite at Oldoinyo Lengai volcano, Tanzania. *Mineralogical Magazine*, **63**, 53–55.
- JAMES, D. E. 1995. *The Geochemistry of Feldspar-free Volcanic Rocks*. PhD thesis, Open University.
- JAMES, T. C. 1966. *The Carbonatites of Tanganyika: a Phase of Continental-type Volcanism*. DIC thesis, Imperial College, London.
- JAMES, T. C. 1967. Thermal springs in Tanzania. *Transactions of the Institute of Mining and Metallurgy B*, **76**, 1–18.
- JOHNSON, L. H., JONES, A. P., CHURCH, A. A. & TAYLOR, W. R. 1997. Ultramafic xenoliths and megacrysts from a melilitite tuff cone, Deeti, northern Tanzania. *Journal of African Earth Sciences*, **25**, 29–42.
- JONES, A. P., SMITH, J. V. & DAWSON, J. B. 1983a. Glasses in mantle xenoliths from Olmani, Tanzania. *Journal of Geology*, **91**, 167–178.
- JONES, A. P., SMITH, J. V., DAWSON, J. B. & HANSEN, E. C. 1983b. Metamorphism, partial melting and K-metasomatism of garnet–scapolite–kyanite granulite xenoliths from Lashaine, Tanzania. *Journal of Geology*, **91**, 143–165.
- KALT, A., HEGNER, E. & SATIR, M. 1997. Nd, Sr, and Pb isotope evidence for diverse lithospheric mantle sources of East African Rift carbonatites. *Tectonophysics*, **278**, 3145.
- KELLER, J. & KRAFFT, M. 1990. Effusive natrocarbonatite activity at Oldoinyo Lengai, June 1988. *Bulletin Volcanologique*, **52**, 629–645.
- KELLER, J. & SPETTEL, B. 1995. The trace element composition and petrogenesis of natrocarbonatites. In: BELL, K. & KELLER, J. (eds) *Carbonatite Volcanism*. Springer, Berlin, 70–86.
- KELLER, J. & HOEFS, J. 1995. Stable isotope characteristics of recent natrocarbonatites. In: BELL, K. & KELLER, J. (eds) *Carbonatite Volcanism*. Springer, Berlin, 113–123.
- KELLER, J. & ZAITSEV, A. N. 2006. Calciocarbonatite dykes at Oldoinyo Lengai, Tanzania: the fate of natrocarbonatite. *Canadian Mineralogist*, **44**, 857–876.
- KELLER, J., ZAITSEV, A. & WIEDENMANN, D. 2006. Primary magmas at Oldoinyo Lengai: the role of olivine melilitite. *Lithos*, **91**, 150–172.
- KERVYN, M., KLAUDIUS, J., KELLER, J., KERVYN, F., MATTSON, H. B., BELTON, F., MBEDE, E., JACOBS, P. & ERNST, G. J. 2008a. Voluminous lava flows at Oldoinyo Lengai in 2006: chronology of events and insights into the shallow magmatic system. *Bulletin of Volcanology*, **70**, 1069–1086.
- KERVYN, M., KLAUDIUS, J., KELLER, J., MBEDE, E., JACOBS, P. & ERNST, G. J. 2008b. Remote sensing of sector collapse and debris avalanche deposits at Oldoinyo Lengai and Kermasi Volcanoes, Tanzania. *International Journal of Remote Sensing* (in press).
- KJAARSGAARD, B. & PETERSON, T. 1991. Nephelinite–carbonate liquid immiscibility at Shombole volcano, East Africa: petrographic and experimental evidence. *Mineralogy and Petrology*, **43**, 293–314.
- KLAUDIUS, J. & KELLER, J. 2006. Peralkaline silicate lavas at Oldoinyo Lengai, Tanzania. *Lithos*, **91**, 173–190.
- KOEPENICK, K. W., BRANTLEY, S. L., THOMPSON, J. M., ROWE, G. L., NYBLADE, A. A. & MOSHY, C. 1996. Volatile emissions from the crater and flank of Oldoinyo Lengai volcano, Tanzania. *Journal of Geophysical Research*, **101**, 13819–13830.

- KRAFFT, M. & KELLER, J. 1989. Temperature measurements in carbonatite lava lakes and flows from Oldoinyo Lengai, Tanzania. *Science* **245**, 168–170.
- KRAMM, U. & SINDERN, S. 1998. Nd and Sr isotope signature of fenites from Oldoinyo Lengai, Tanzania, and the genetic relationships between nephelinites, phonolites and carbonatites. *Journal of Petrology*, **39**, 1997–2004.
- KRENKEL, E. 1922. *Die Bruchzonen Ostafrikas: Tektonik, Vulkanismus, Erdbeben und Schwereanomalien*. Bornträger, Berlin.
- LE BAS, M. J. L. 1977. *Carbonatite-nephelinite Volcanism. An African Case History*. Wiley, London.
- LE MAITRE, R. W. (ed.) 1989. *A Classification of Igneous Rocks and Glossary of Terms*. Blackwell Scientific Publications, Oxford.
- LEE, C.-T. & RUDNICK, R. L. 1999. Compositionally-stratified cratonic lithosphere: petrology and geochemistry of peridotite xenoliths from the Labait volcano, Tanzania. In: GURNEY, J. J., GURNEY, J. L., PASCOE, M. D. & RICHARDSON, S. H. (eds) *Proceedings of the 7th International Kimberlite Conference, Cape Town, 1998*, Vol. 2, Red Roof Design, Cape Town, 503–521.
- LEE, C.-T., RUDNICK, R. L., MCDONOUGH, W. F. & HORN, I. 2000. Petrologic and geochemical investigation of carbonates in peridotite xenoliths from northeastern Tanzania. *Contributions to Mineralogy and Petrology*, **139**, 470–484.
- MACDONALD, R., MARSHALL, A. S., DAWSON, J. B., HINTON, R. W. & HILL, P. G. 2002. Chevkinite-group minerals from salic volcanic rocks of the East African Rift. *Mineralogical Magazine*, **66**, 287–299.
- McFARLANE, D. A., LUNDBERG, J. & BELTON, F. 2004. An unusual cave from Oldoinyo Lengai, Tanzania. *Journal of Cave and Karst Studies*, **66**, 98–101.
- MACINTYRE, R. M., MITCHELL, J. G. & DAWSON, J. B. 1974. Age of the fault movements in the Tanzanian sector of the East African rift system. *Nature*, **247**, 354–356.
- MCKIE, D. & FRANKIS, E. J. 1977. Nyerereite: a new volcanic carbonate mineral from Oldoinyo Lengai, Tanzania. *Zeitschrift für Kristallographie*, **145**, 73–95.
- MANEGA, P. C. 1993. *Geochronology, Geochemistry and Isotope Study of the Plio-Pleistocene Hominid Sites and the Ngorongoro Volcanic Highlands in Northern Tanzania*. PhD thesis, University of Colorado.
- MARIANO, A. N. & ROEDER, P. L. 1983. Kerimasi: a neglected carbonatite volcano. *Journal of Geology*, **91**, 449–455.
- MEYER, H. 1900. *Der Kilimandjaro*. Reimer, Berlin.
- MITCHELL, R. H. 1997. Carbonate-carbonate immiscibility, neighborite and potassium iron sulphide in Oldoinyo Lengai natrocarbonatite. *Mineralogical Magazine*, **61**, 779–789.
- MITCHELL, R. H. 2006a. Sylvite and fluorite microcrysts, and fluorite-nyerereite intergrowths from natrocarbonatite, Oldoinyo Lengai, Tanzania. *Mineralogical Magazine*, **70**, 103–114.
- MITCHELL, R. H. 2006b. An ephemeral pentasodium phosphate carbonate from natrocarbonatite lapilli, Oldoinyo Lengai, Tanzania. *Mineralogical Magazine*, **70**, 211–218.
- MITCHELL, R. H. 2006c. Mineralogy of stalactites formed by subaerial weathering of natrocarbonatite hornitos at Oldoinyo Lengai, Tanzania. *Mineralogical Magazine*, **70**, 437–444.
- MITCHELL, R. H. & BELTON, F. 2004. Niocalite-cuspidine solid solution and manganese monticellite from natrocarbonatite, Oldoinyo Lengai, Tanzania. *Mineralogical Magazine*, **68**, 787–799.
- MITCHELL, R. H. & DAWSON, J. B. 2007. The September 24th, 2007, ash eruption of the carbonatite volcano, Oldoinyo Lengai, Tanzania: mineralogy of the ash and implications for formation of new hybrid magma type. *Mineralogical Magazine*, **71**, 483–492.
- MOROGAN, V. & MARTIN, R. F. 1985. Mineralogy and partial melting of fenitized crustal xenoliths in the Oldoinyo Lengai carbonatitic volcano, Tanzania. *American Mineralogist*, **70**, 1114–1126.
- MOTE, P. W. & KASER, G. 2007. The shrinking glaciers of Kilimanjaro: can global warming be blamed? *American Scientist*, **95**, 318–325.
- MUDD, G. C. & ORRIDGE, G. R. 1966. *Babati*. Tanzania Mineral Resources Division Quarter Degree Sheet **85**.
- MUZUKA, N. N., RYNER, M. & HOLMGREN, K. 2004. 12,000-year preliminary results of the stable nitrogen and carbon isotope record from the Empakai crater lake sediments, northern Tanzania. *Journal of African Earth Sciences*, **40**, 293–303.
- NORTON, G. & PINKERTON, H. 1997. Rheological properties of natrocarbonatite lavas from Oldoinyo Lengai, Tanzania. *European Journal of Mineralogy*, **9**, 351–364.
- NYAMWERU, C. 1988. Continuing activity of Oldoinyo Lengai volcano, Tanzania: 1983–1985. *Journal of African Earth Sciences*, **7**, 603–610.
- NYAMWERU, C. 1990. Observations on changes in the active crater, Oldoinyo Lengai, from 1960–1988. *Journal of African Earth Sciences*, **11**, 385–390.
- NYAMWERU, C. 1997. Changes in the crater of Oldoinyo Lengai: June 1993–February 1997. *Journal of African Earth Sciences*, **25**, 43–53.
- NYAMWERU, C. 1999. Oldoinyo Lengai. *Bulletin of the Global Volcanism Network*, **24–2**, 12–14.
- OHDE, S. & MATAGARIO, J. P. 1999. Instrumental neutron activation analysis of carbonatites from Panda Hill and Oldoinyo Lengai, Tanzania. *Journal of Radioanalytical and Nuclear Chemistry*, **240**, 325–328.
- O'NEIL, J. R. & HAY, R. L. 1973.  $^{18}\text{O}/^{16}\text{O}$  ratios in cherts associated with the saline lake deposits of East Africa. *Earth and Planetary Science Letters*, **19**, 257–266.
- OPPENHEIMER, C., BURTON, M. R., DURIEUX, J. & PYLE, D. M. 2002. Open-path Fourier transform spectroscopy of gas emissions from Oldoinyo Lengai volcano, Tanzania. *Optics and Lasers in Engineering*, **37**, 203–214.
- ORRIDGE, G. R. 1965. *Mbulu*. Tanzania Mineral Resources Division Quarter Degree Sheet **69**.
- PASLICK, C., HALLIDAY, A., JAMES, D. & DAWSON, J. B. 1995. Enrichment of the continental lithosphere by OIB melts: Isotopic evidence from the volcanic province of northern Tanzania. *Earth and Planetary Science Letters*, **130**, 109–126.
- PASLICK, C., HALLIDAY, A. N., LANGE, R. A., JAMES, D. & DAWSON, J. B. 1996. Indirect crustal contamination: evidence from isotopic and chemical disequilibria in minerals from alkali basalts and nephelinites from northern Tanzania. *Contributions to Mineralogy and Petrology*, **125**, 277–292.
- PETERSON, T. D. 1989a. Peralkaline nephelinites. I Comparative petrology of Shombole and Oldoinyo Lengai. *Contributions to Mineralogy and Petrology*, **101**, 458–478.
- PETERSON, T. D. 1989b. Peralkaline nephelinites. II Low pressure fractionation and the hypersodic lavas of Oldoinyo Lengai. *Contributions to Mineralogy and Petrology*, **102**, 336–346.
- PETERSON, T. D. 1990. Petrology and genesis of natrocarbonatite. *Contributions to Mineralogy and Petrology*, **105**, 143–155.
- PICKERING, R. 1958. *Oldoinyo Ogol*. Tanganyika Geological Quarter Degree Sheet **38**.
- PICKERING, R. 1964. *Endulen*. Tanzania Geological Survey Quarter Degree Sheet **52**.
- PICKERING, R. 1965. *Ngorongoro*. Tanzania Geological Survey Quarter Degree Sheet **53**.
- PINKERTON, H., NORTON, G. E., DAWSON, J. B. & PYLE, D. M. 1995. Field observations and measurement of the physical properties of Oldoinyo Lengai alkali carbonate lavas, November 1988. In: BELL, K. & KELLER, J. (eds) *Carbonatite Volcanism*. Springer, Berlin, 23–46.
- PYLE, D. M. 1995. Decay series evidence for transfer and storage times of natrocarbonatite magma. In: BELL, K. & KELLER, J. (eds) *Carbonatite Volcanism*. Springer, Berlin, 124–136.
- PYLE, D. M., DAWSON, J. B. & IVANOVICH, M. 1991. Short-lived decay series disequilibria in the natrocarbonatite lavas: constraints on the timing of magma genesis. *Earth and Planetary Science Letters*, **105**, 378–396.
- RECK, H. 1924–25. L'Engai Bilder. *Zeitschrift für Vulkanologie*, **8**, 172–174.
- RECK, H. & SCHULZE, G. 1921. Ein Beitrag zur Kenntnis des Baues an der jüngsten Veränderung des l'Engai-Vulkanes im nordlichen Deutsch-Ostafrika. *Zeitschrift für Vulkanologie*, **6**, 47–71.
- REID, A. M., DONALDSON, C. H., BROWN, R. W., RIDLEY, W. I. & DAWSON, J. B. 1975. Mineral chemistry of peridotite xenoliths from the Lashaine volcano, Tanzania. *Physics and Chemistry of the Earth*, **9**, 525–558.
- RICHARD, J. J. 1942. Oldoinyo Lengai – the 1940–41 eruption. Volcanological observations in East Africa. *Journal of the East Africa and Uganda Natural History Society*, **XVI**, 89–108.

- ROBERTS, M. A. 2002. *The Geochemical and Volcanological Evolution of the Mt. Meru Region, Northern Tanzania*. PhD thesis, University of Cambridge.
- ROCK, N. M. S. 1976. Petrogenetic significance of some new xenolithic alkaline rocks from East Africa. *Mineralogical Magazine*, **40**, 611–625.
- ROSENBUSCH, H. 1907. *Mikroskopische Physiographie der Mineralien und Gesteine*, 4th edn. E. Schweizerbart'sche, Stuttgart.
- RUDNICK, R. L., MCDONOUGH, W. F. & CHAPPELL, B. W. 1993. Carbonatite metasomatism in the northern Tanzanian mantle: petrographic and geochemical characteristics. *Earth and Planetary Science Letters*, **114**, 463–475.
- SAGGERSON, E. P. 1966. *Geology of the Loita Hills*. Geological Survey of Kenya, Report **71**.
- SEARLE, R. C. 1971. A gravity survey of Ngorongoro caldera. Tanzania. *Bulletin Volcanologique*, **35**, 350–357.
- SELBY, J. & THOMAS, C. M. 1966. *Balangida Lelu*. Tanzania Mineral Resources Division, Quarter Degree Sheet **103**.
- SHIVE, P. N., NYBLADE, A. A. & WITTKE, J. H. 1990. Magnetic properties of some carbonatites from Tanzania, East Africa. *Geophysical Journal International*, **163**, 103–109.
- SIMONETTI, A., BELL, K. & SHRADY, C. 1997. Trace- and rare-earth geochemistry of the June 1993 natrocarbonatite lavas, Oldoinyo Lengai (Tanzania): Implications for the origin of carbonatite magmas. *Journal of Volcanological and Geothermal Research*, **75**, 89–106.
- THOMAS, C. M. 1966. *Hanang*. Tanzania Mineral Resources Division, Quarter Degree Sheet **84**.
- THOMPSON, L. G., MOSELY-THOMPSON, E., ET AL. 2002. Kilimanjaro ice core record: evidence of Holocene change in tropical Africa. *Science*, **298**, 589–593.
- TILLEY, C. E. & YODER, H. S. 1968. The pyroxenite facies conversion of volcanic and subvolcanic melilite-bearing and other alkali ultramafic assemblages. *Carnegie Institution of Washington Yearbook*, **66**, 457–460.
- UHLIG, C. 1905. Bericht über die Expedition der Otto-Winter Stiftung nach dem Umgebungen des Meru. *Zeitschrift der Gesellschaft für Erdkunde*, **1905**, 120–123.
- UHLIG, C. 1907. Der sogenannte grosse Ostafrikanische Graben zwischen Magad (Natron See) und Lawa ya Mweri (Manyara See). *Geographisches Zeitung*, **15**, 478–505.
- VOIGHT, B., GLICKEN, H., JANDA, R. J. & DOUGLASS, P. M. 1981. Catastrophic rockslide avalanche of May 18. In: LIPMAN, P. W. & MULLINEAUX, D. R. (eds) The 1980 eruption of Mount St Helens, Washington. *United States Geological Survey Professional Paper*, **1250**, 347–377.
- WAKEFIELD, T. 1870. Routes of native caravans from the coast to the interior of East Africa, chiefly from information given by Sadi Bin Ahedi, a native of a district near Gazi, in Udigo, a little north of Zanzaibar. *Journal of the Royal Geographical Society*, **40**, 303–338.
- WILKINSON, P., DOWNIE, C., CATTERMOLLE, P. J. & MITCHELL, J. G. 1983. *Arusha*. Geological Survey of Tanzania, Quarter Degree Sheet **55**.
- WILKINSON, P., MITCHELL, J. G., CATTERMOLLE, P. J. & DOWNIE, C. 1986. Volcanic chronology of the Meru-Kilimanjaro region, Northern Tanzania. *Journal of the Geological Society of London*, **143**, 601–605.
- WILLIAMS, L. A. J. 1969. Geochemistry and petrogenesis of the Kilimanjaro volcanic rocks of the Amboseli area, Kenya. *Bulletin Volcanologique*, **33**, 862–888.
- WILLIAMS, R. W., GILL, J. B. & BRULAND, K. W. 1986. Ra–Th disequilibrium systematics: Timescale of carbonatite magma formation at Oldoinyo Lengai volcano, Tanzania. *Geochimica et Cosmochimica Acta*, **59**, 1249–1259.
- WIRTH, K. R. & ADELSBERGER, K. A. 2002. Mantle source and magmatic evolution of the late Pliocene Ogol lavas of Laetoli, Tanzania. *Geological Society of America, Abstracts with Programs*, **34**, 363.
- WOOD, C. P. 1968. *A Geochemical Study of East African Alkaline Lavas and its Relevance to the Petrogenesis of Nephelinites*. PhD thesis, University of Leeds.
- ZAITSEV, A. N. & KELLER, J. 2006. Mineralogical and chemical transformation of Oldoinyo Lengai natrocarbonatites, Tanzania. *Lithos*, **91**, 191–207.

## Chapter 8

### Regional comparisons, petrochemistry and petrogenesis

In a short review of the structure and volcanism of the southern part of the Gregory Rift, Dawson (1992) drew attention to differences in the contemporaneous volcanism in southern Kenya and northern Tanzania, the differences taking place abruptly at a latitude of *c.* 3°S. In Chapter 3 (Dawson 2008), differences were noted in the relationship of the volcanism to their setting relative to the buried cratonic margin and to the thermal structure of the crust and the upper mantle in the two areas. The composition of the mantle and its effect on the nature of the volcanicity are discussed in greater detail here.

#### Comparative contemporary volcanism in south Kenya and north Tanzania

Table 8.1 summarizes the volcanic stratigraphy of southern Kenya and northern Tanzania, mainly from *c.* 8 Ma, i.e. the age of the oldest known activity in northern Tanzania at Essimangor. The period 8–*c.* 1.3 Ma (the time of the Older Extrusives) is dominated by central-type volcanoes characterized by effusion of basanites, basalts and minor trachytes, the last being reasonably interpreted as fractionates of the more voluminous basic rocks. There were some peralkaline volcanoes such as Essimangor, Sadiman and Mosonik, which, particularly in the case of Essimangor, the oldest of the northern Tanzania volcanoes, are similar to the peralkaline volcanoes (Mt Elgon, Napak, Yelele) that erupted prior to the onset of basaltic activity in Kenya (Baker *et al.* 1972).

In southern Kenya during this period, volcanic rocks were erupted from both major central volcanoes or from fissures and very minor volcanoes, the latter including the rift basalts and the Magadi flood trachytes. The Lengitoto trachytes (6.9–5.0 Ma) and the Kirikiti basalts (3.1–2.5 Ma) are exposed along the western flanks of the rift (Crossley 1979), whereas the faults along the eastern flank expose the Singaraini, Ol Keja Nero and Ol Tepesi basalts and benmoreites (Baker & Mitchell 1976). Within the rift valley itself, these earlier formations are overlain by extensively block-faulted trachytes. The central volcanoes active during this period are Ngong and Ol Esayeti (basalt and basanite: 6.7–3.6 Ma), Ologesaile (trachyte 2.7–2.2 Ma), Lenderut (basanite and tephrite *c.* 2.5–2.2 Ma) and Shombole (peralkaline nephelinite, phonolite carbonatite *c.* 2.0 Ma) (Baker 1958, 1963; Fairhead *et al.* 1972; Baker & Mitchell 1976). The basaltic rocks show some resemblances to those in Tanzania (Appendix 2, Dawson 2008) in terms of the dominance of mildly nepheline-normative basalts with minor quantities of hypersthene-normative basalt (Le Roex *et al.* 2001), but the relatively large amounts of trachyte in Kenya find their equivalents in only minor amounts of trachyte in the Kibangaini trachytes in the very north of Tanzania. Shombole, the most southerly of the Kenya central volcanoes, has more petrological affinities with the almost contemporaneous Mosonik and later carbonatite volcanoes of Tanzania.

In the period *c.* 1.2 Ma to the Holocene, following major faulting, the main activity in the southern part of the Kenya rift valley was fissure eruptions of trachyte and, further north, the formation of the major trachytic caldera volcanoes of Suswa, Longonot and Menengai (Williams *et al.* 1984). In stark petrological contrast, in northern Tanzania, the contemporaneous activity was the formation of peralkaline nephelinite-phonolite-carbonatite volcanoes and the Holocene eruption of small volumes of olivine nephelinite and melilitite, some of katungitic composition.

To the east of the rift valley in southern Kenya, during the late Pleistocene–Holocene a linear NW–SE array of small volcanoes erupted to form the Chyulu Range. The activity started at its north-western end with eruption of nephelinite but then extruded rocks that become less silica-undersaturated as the activity progressed southeastwards, eventually producing hypersthene-normative basalts (Späth *et al.* 2000, 2001). The nearest contemporary volcanism in northern Tanzania is the phonolites and nephelinites of Meru, the olivine melilitite activity in the Meru–Monduli area and the highly evolved trachytes and phonolites of the Kibo centre on Kilimanjaro. As in the rift valley further west, there are again significant differences between the contemporary rocks of the Chyulu Volcanic Province and those only a short distance away in northern Tanzania.

Many of the southern Kenya volcanics are believed to have erupted through the buried margin of the Tanzania craton (Smith & Mosley 1993), and those in northern Tanzania through the craton and/or the craton margin. Hence the differences noted above cannot be attributed solely to differences in tectonic setting.

#### Petrochemistry

Most volcanoes of the northern Tanzania province have been mapped only on a regional scale, and the sampling of most, and the ensuing chemical data (available for only a few volcanoes), are neither extensive nor systematic; further, most lava suites lack isotopic data. The following commentary should be viewed within these constraints.

The composition of igneous rocks is determined by the composition of the source, the degree and depth of melting, any possible effects of fractionation and wall-rock contamination during ascent from the source area, and any magma mixing. The intraplate tectonic setting of the Tanzania volcanic province and the preponderance of mafic lavas strongly suggest that the Tanzanian volcanics are mainly mantle derived.

#### The Northern Tanzania upper mantle

The composition of the upper mantle beneath northern Tanzania has been investigated by: (i) direct observation of the composition of phases in mantle xenoliths brought to the surface, mainly during Younger Extrusive olivine melilitite and olivine nephelinite activity; and (ii) by interpretation of both Older Extrusive and Younger Extrusive lavas.

#### Evidence from mantle xenoliths for mantle heterogeneity

Xenoliths from the Oldoinyo Lengai, Lashaine, Olmani, Monduli, Labait, Pello Hill, Eledoi, Deeti and Igwisi volcanoes provide direct evidence for the make-up of the upper mantle beneath northern Tanzania. However, most have been brought to the surface during the later stages of the Younger Extrusive activity, so caution must be applied to acceptance of the xenoliths as being representative of the upper mantle at the onset of the Older Extrusive magmatism some 8 Ma earlier.

**Table 8.1.** Volcanic stratigraphy of S. Kenya and N. Tanzania

	South Kenya					North Tanzania
	West flank	West rift floor	East rift floor	East flank	Outside rift	
1 Ma		Nyokie ignimbrites (0.65)	Suswa volcanics (0–0.4) Barajai trachytes (0.4)		Chiyulu Hills Nephelinites basanites, basalts	<b>Younger Extrusives</b> Nephelinites, olivine melilitites, phonolites, carbonatites <i>MAJOR FAULTING</i> <b>Older Extrusives</b> Mainly alkali basalts, trachytes, phonolites Some alkaline ultrabasics
		Magadi trachytes (1.4–0.7)	Plateau trachytes (1.9–0.9) Ol Tepesi basalts & trachytes (1.65–1.4) Ol Kejo Nero basalts			
	<i>FAULTING</i>			<i>FAULTING</i>		
2 Ma	Sambu Volcanics	Mosiro trachytes 2,1 Shombole (1.9–2.0) Kordiya basalts	Limuru trachytes (2.0–1.9) Singaraini basalts	Limuru trachytes		Tarosero (2.0–2.2) Shombole (2.0–1.9)
5 Ma	Kirikiti basalts (2.5–3) Lengitoto trachytes (5.1–6.9)  Olivine nephelinites (12–15.2)		Olorgesaille volcanics (2.2–2.7) Ol Esayeiti volcanics (6.7–3.2)	Middle trachytes  Lower trachytes 6.0 Kapiti phonolite (13.4)		Sadiman + Lemagrut (~3–4)  Essimngor 3.2–8.1

The sub-Tanzania upper mantle, as exemplified by the xenoliths, has had a long and complex history. The Lashaine xenoliths were subject to strong depletion at around 3.2 Ga (Burton *et al.* 2000), whereas at Labait chromites in the xenoliths give Re depletion ages of 2.8 and 2.0 Ga (Chesley *et al.* 1999). At Olmani, although not dated, the main peridotite mineralogy is highly refractory. The depletion event, which gave rise to chromite dunite and harzburgite restites in all of the xenolith suites, was followed by at least one episode of metasomatism, with varying degrees of enrichment of the restite protoliths. At Lashaine (for location see Dawson 2008, fig. 5.8) the first enrichment event was at *c.* 2.0 Ga, when K, Fe, Ca, Ti and Rb metasomatism resulted in the formation of diopside and phlogopite (Dawson *et al.* 1970; Ridley & Dawson 1975). Si metasomatism may have caused the formation of enstatite (Rudnick *et al.* 1994), and it is possible that garnet formed at the same time by exsolution from enstatite combined with REE metasomatism, as has been envisaged for garnet formation in Kaapvaal mantle peridotites (Simon *et al.* 2003). A later metasomatic event added K, Fe, Ca, Ti, Nb, Ta, Sr, Ba, the REE and Zr (Dawson 2002); this second pulse of metasomatism, manifest in mantled and unequilibrated minerals, must have been relatively recent in geological terms. Similar two-stage metasomatism events also took place at Labait (Dawson 1999). At other localities there are distinctive trace-element and volatile-component metasomatic signatures to the xenolith suite, particularly with regard to the relative additions of Ba, Ti and K (Dawson 2002). The presence of primary calcite in xenoliths from Lashaine, Monduli and Igwisi, together with the formation of diopside and monazite in xenoliths at Labait, Olmani and Eledoi, give grounds for believing that the metasomatic fluids at these localities were carbonatitic (Dawson 1987; Rudnick *et al.* 1993; Lee *et al.* 2000). In contrast, at Pello Hill the metasomatic fluids also contained water (forming amphibole and mica) and the  $XCO_2/H_2O$  changed during the metasomatism of the wall rock by veins of katungitic composition (Dawson & Smith 1988).

In summary, the sub-Tanzanian upper mantle lithosphere was depleted in the Archaean but has subsequently been subject, at least locally, to variable types and degrees of incompatible-element and volatile enrichment, at different times: one in the Early Proterozoic, the other very recent.

#### *Xenolith isotope variations*

Diopsides in veined and metasomatized xenoliths from Eledoi and Pello Hill have  $^{87}Sr/^{86}Sr$  ratios that range mainly from 0.70344 to 0.70473 (Fig. 8.1), indicating recent metasomatism, as do diopsides from the Olmani peridotites (Rudnick *et al.* 1993). However, other xenoliths from the Oldoinyo Lengai area show considerable isotopic variation. Contrasting with the Pello Hill and Eledoi samples, two blocks of mica pyroxenite (interpreted as metasomatized peridotite, Dawson & Smith 1992) in the agglomerates at nearby Oldoinyo Lengai have  $^{87}Sr/^{86}Sr$  ratios of 0.7086 and 0.70529 and  $^{143}Nd/^{144}Nd$  0.5117 and 0.5124 respectively (Bell & Dawson 1995), indicating an older metasomatism event. On a Sr v. Nd isotope diagram (Fig. 7.12, 8.1), one of these samples plots in a more enriched sector than the EM1 values of Hart (1988). Most peridotite samples from Lashaine mainly have Sr and Nd isotope value close to the Pello and Eledoi samples, but one garnet lherzolite (BD738) contains high amounts of radiogenic Sr, Nd and Pb. Its ratios of  $^{87}Sr/^{86}Sr$  0.83604,  $^{206}Pb/^{204}Pb$  15.39 and  $^{143}Nd/^{144}Nd$  0.51127 are the most extreme for any sample of mantle derivation, indicating old enriched lithosphere (Cohen *et al.* 1984) and, again, emphasizing the variable metasomatic enrichment of the sub-Tanzanian mantle. The important fact is that the timing of the metasomatism was bimodal. Further, whereas the Pello, Eledoi, Olmani and some Lashaine xenoliths indicate young enrichment, the Oldoinyo Lengai and the extreme Lashaine xenoliths were subject to relatively old metasomatism. It is also apparent from Figure 8.1 that the Sr and Nd isotope values of the olivine melilitites in the Oldoinyo Lengai area overlap those of the recently enriched mantle xenoliths from Pello Hill and Eledoi.

Trace element contents in veins, which do not represent primary melts, cutting some of the Pello Hill peridotite xenoliths show high concentrations of Rb, Pb and Ba, but lower Zr and REE relative to ocean island basalt (Table 8.2).

Another example of mantle heterogeneity is shown by the isotope chemistry of carbonatites from Oldoinyo Lengai and Kerimasi. These two volcanoes are only 10 km apart and both are <1 Ma old, yet the carbonatites at these two centres are isotopically different (Fig. 8.1). The  $^{87}Sr/^{86}Sr$  and  $^{143}Nd/^{144}Nd$  ratios for Oldoinyo Lengai carbonatite are 0.70443 to 0.70437 and

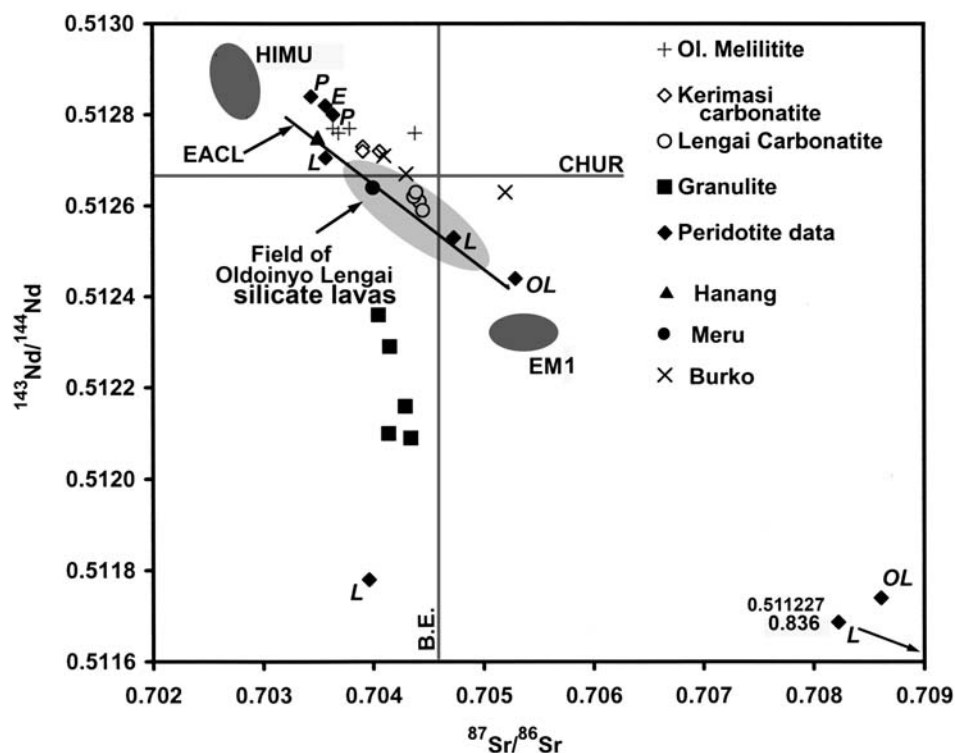


**Fig. 8.1.** Nd v. Sr isotope plot for Younger Extrusive lavas including Oldoinyo Lengai lavas and mantle xenoliths (see Dawson 2008, fig. 7.12), other North Tanzania mantle xenoliths (most data are for peridotite clinopyroxenes) and basic granulites (Cohen *et al.* 1984). Other Younger Extrusive rocks are olivine melilitites (Keller *et al.* 2006, Cohen *et al.* 1984), Kerimasi calcic carbonatites (Paslick *et al.* 1995, Kalt *et al.* 1997) and nephelinites from Hanang, Meru and Burko (Paslick *et al.* 1995). Abbreviations as in Figure 7.12; others P, Pello Hill; E, Eledoi; L, Lashaine; OL, Oldoinyo Lengai. Clinopyroxenes from Olmani peridotite xenoliths (Rudnick *et al.* 1993) plot in the same area as the Pello Hill and Eledoi samples.

0.51263 to 0.51270, respectively (Bell & Dawson 1995), compared with an average of 0.70396 and 0.51273 for five samples from Kerimasi (Paslick *et al.* 1995; Kalt *et al.* 1997). Hence, the underlying lithospheric mantle is isotopically heterogeneous over very small lateral distances.

Some Tanzanian xenoliths analysed for radiogenic isotopes have also been analysed for helium. Apparently contrary to the variability of both the metasomatism and the radiogenic isotopes, the few analysed xenoliths from Lashaine, Eledoi and Pello Hill contain mainly helium with quite constant  $^3\text{He}/^4\text{He}$  ratios, with  $R/R_A$  (the  $^3\text{He}/^4\text{He}$  ratio normalized to that in atmospheric helium) in the range 6.2 to 7.3; separated olivines give slightly higher values than their host bulk rocks (Porcelli *et al.* 1986). In olivines in one sample (BD3847 from Pello Hill), Stuart & Turner (1992) found abundant  $\text{CO}_2$ -rich inclusions that yielded  $R/R_A$  of 8, and also a  $^{40}\text{Ar}-^4\text{He}$  value of 0.7, which is close to the value of 0.55 for these isotopes in the upper mantle. The values for helium  $R/R_A$  are for undoubtedly metasomatized lithosphere, and most are similar to those in some ocean island basalts that are interpreted as being generated from metasomatized oceanic lithosphere e.g. those from La Grille, Grand Comore ( $R/R_A$  6.75–7.08) but higher than in the plume-derived Comore Karthala volcanics with  $R/R_A$  5–5.41 (Class *et al.* 2005). Most Tanzania xenolith data also overlap  $R/R_A$  values of 6.15–6.59 in primitive picrites from Turkana, which are suggested as representing the values of an asthenospheric plume (Furman *et al.* 2006a). The conflicting interpretations of the source regions of the mafic rocks from Comore and Turkana, despite the similarities of their helium isotope values, indicates a lack of agreement on the use of helium isotope values for interpreting plume versus lithosphere derivation of basalts. A departure from the generally relatively narrow range for the Tanzanian xenoliths are  $R/R_A$  ratios of 13.6 to 15.3 found in the exceptional anciently-enriched Lashaine garnet lherzolite BD738 (see above) (Porcelli *et al.* 1986).

#### The Labait Fe-rich peridotites

In addition to metasomatized Mg-rich peridotites, the xenolith suite at Labait contains dunite and wehrlite in which the whole-rock and phase compositions are more iron-rich. On the basis of mineral chemistry, and particularly of spinel, Dawson (1999) suggested that these are cumulates from a ponded picritic melt that crystallized at a depth of c. 60 km, whereas Lee & Rudnick (1999) proposed that they are due to Fe-metasomatism of Mg-peridotites by asthenospheric melts.

#### Lava compositions

The composition of the mantle source can also be assessed by study of primary mantle melts, i.e. those in chemical equilibrium with mantle olivine of around  $\text{Fo}_{90}$ . A  $\text{Mg}/(\text{Mg} + \text{Fe})$  ratio of  $>0.70$  ( $\text{mg}\#$  70) is taken to be an indication of the required composition (Roeder & Emslie 1970), together with high Ni contents ( $>250$  ppm). Table 8.2 lists lavas from northern Tanzania, some of which fulfil these criteria, and other primitive lavas with  $\text{mg}\#$  ( $\text{Mg}/(\text{Mg} + \text{Fe})$ )  $>65$  for comparison with lavas of similar composition from Kenya. The table gives selected major element and trace element data for these lavas, and comparative data for reference samples. Although most of the lavas contain U and Zr values similar to those in the reference ocean island basalt (OIB), the Ba, Nb, La, Ce and Th contents of the Tanzanian lavas are higher than in OIB, particularly those in the Younger Extrusives. Further, although some trace element ratios (Ce/Pb and Nb/U) bracket those in OIB, many Ba/Nb, La/Nb and Rb/Ba ratios are higher, supporting the observation of Paslick *et al.* (1995) that the trace element distribution in the northern Tanzanian lavas requires a mantle source that has a partial, but not exclusively, OIB trace element pattern. Similarly, REE inversion modelling for regional alkali basalts in the Meru–Kilimanjaro

**Table 8.2.** Chemical parameters of Tanzania primary (mg# > 70) and primitive (mg# > 65) lavas, a Tanzania mantle vein, and some standard reference lithologies<sup>‡</sup>

Sample	Rock type	Location	CaO	Al <sub>2</sub> O <sub>3</sub>	CaO/Al <sub>2</sub> O <sub>3</sub>	mg#	Zr	Th	U	Rb	Ba	Nb	La	Ce	Pb	Ba/Nb	La/Nb	Rb/Ba	Ce/Pb	Nb/U	Reference
BD333*	OI basalt	Ketumbeine	8.55	11.19	0.8	68.9	198	4.0	na	23	477	45	45	127	5.0	11		0.05	25.4		1
MD93-4*	Picrobasalt	Monduli	10.04	9.59	1.1	74.4	242	11.0	na	34	677	88	68	130	3.0	7.7	0.8	0.05	43.3		1
MR65*	Basanite	Loljoro	11.06	9.78	1.1	67.4	155	10.9	1.8	18.2	475	41	na	na	14.7	11.6		0.04		22.8	2
MR105*	Basalt	Lembolos	10.78	10.64	1.0	65.4	122	12.2	0.7	14.7	375	33	34	67.1	2.7	11.4	1.03	0.04	24.9	47.1	2
MR110*	Basalt	Oldoinyo Liyu	9.58	11.13	0.9	65.3	175	14.1	1.1	19.8	567	57	53	108.7	3.7	9.9	0.9	0.03	29.4	51.8	2
BD780	OI melilitite	Lashaine	12.24	5.84	2.1	72.8	na	na	na	na	na	na	na	na	na						3
BD105	OI melilitite nephelinite	Loolmurwak	12.97	6.93	1.9	70.9	326	na	na	48	617	97	na	na	na	6.4		0.08			4
BD4200	OI melilitite	Labait	8.87	5.43	1.6	80.4	188	na	na	65.6	695	97	47	82.0	5.5	7.2	0.5	0.09	14.9		5
BD4225	Katungite	Sora Hill	13.70	7.67	1.8	69.3	207	na	na	80.2	1960	107	117	150	6.0	18.3	1.1	0.04	25.0		5
MR281	OI melilitite	Meru	13.27	7.83	1.7	69.2	402	14.0	2.3	57.1	855	147	104	203	5.2	5.8	0.7	0.07	39.3	63.9	2
	Ankaramite	Olmani	11.30	7.72	1.5	75.0	na	na	na	na	na	na	na	na	na						6
OL198	OI melilitite	Oldoinyo Lengai	14.26	7.52	1.9	68.7	370	11.3	3.0	59.6	956	123	na	na	na	7.8		0.06		41.0	7
Mica-pyroxene vein in mantle xenolith <sup>†</sup>		Pello Hill	10.89	6.69	1.6	50.1	164	na	na	81	679	53	5.5	15.3	5	12.8	0.10	0.12			8
Ocean island basalt							280	4.0	1.0	2.31	350	48	37	80.0	3.2	7.3	0.77	0.006	28.1	48.0	9
Lower crust							68	1.2	0.2	11	259	5	8	20	4	51.8	1.6	0.04	5.0	25.0	10
Upper crust							193	10.5	2.7	8.2	628	12	31	63	17	52.3	2.6	0.01	3.7	4.4	10

na, not analysed.

\*Older Extrusive Series; the rest are Younger Extrusives.

<sup>†</sup>BD3834B Mica pyroxenite vein in upper mantle peridotite.References: 1, Paslick *et al.* 1995; 2, Roberts 2002; 3, Dawson *et al.* 1970; 4, Dawson *et al.* 1985; 5, Dawson *et al.* 1997; 6, Jones *et al.* 1983; 7, Keller *et al.* 2006; 8, Dawson & Smith 1988; 9, Sun & McDonough 1989; 10, Rudnick & Gao 2003.<sup>‡</sup>mg#: (Mg/Mg + Fe).

region shows that whereas their HREE patterns can be produced from primitive mantle by *c.* 5% melting over a depth range 85–105 km at a  $T_p$  of *c.* 1500 °C, this type of mantle composition cannot produce the enriched LREE and MREE concentrations in the basalts; hence, an enriched lithospheric source is required for at least the LREE and MREE (Roberts 2002).

A Sr v. Nd isotope plot (Fig. 8.2) for the Tanzanian Older Extrusives (data from Paslick *et al.* 1995) shows that: (i) samples from two of the peralkaline, undersaturated volcanoes (Sadiman and Essimngor) have the most radiogenic Sr and Nd and plot close to EMI. In this they are similar to the sample from Lemagrut which initially erupted peralkaline lavas and also erupted coevally with Sadiman; (ii) other Essimngor samples are quite different, one having similar Sr but lower radiogenic Nd, whilst a third has lower Sr and Nd, resulting in a very wide spread for Essimngor in Sr–Nd isotope space; (iii) basalt and picobasalt samples from the rift wall near Lake Natron fall into two distinct groups, having similar  $^{143}\text{Nd}/^{144}\text{Nd}$ , but distinctly different  $^{87}\text{Sr}/^{86}\text{Sr}$ ; (iv) the rift wall group with the least radiogenic Sr plots, together with most specimens from Ketumbeine and Monduli intermediate along a broad zone extending from EMI to HIMU values though closer to HIMU; and (v) two primitive lavas (*mg#* >65) from Monduli and Ketumbeine are amongst those having the least radiogenic Sr.

In total, the Nd–Sr isotope data for northern Tanzanian lavas, together those for Pb (Paslick *et al.* 1995), converge on a mantle source that, compared with HIMU, has relatively unradiogenic Nd, radiogenic Sr, and very radiogenic Pb. Unlike HIMU sources which need an enrichment in U and Th (or depletion in Pb) without an accompanying enrichment in Rb, the Tanzania mantle source must have been enriched in Rb relative to Sr, U relative to Pb, and also enriched in LREEs.

Paslick *et al.* (1995) explain these parameters as being due to underplating at around 2 Ga of the continental lithosphere by an OIB-like melt that could develop its radiogenic Pb signature before the underplated material was melted to give the Tanzanian lavas. However, this cannot be the sole source as, compared with values for OIB, the concentrations of incompatible elements such as Ba, Th, U, Nb and Zr are enriched in most Tanzanian Older Extrusive primary and primitive lavas, and especially so in the Younger Extrusive primary lavas (Table 8.2). These data, corroborated by the xenolith evidence, indicate an anciently enriched lithospheric component in the source region of the Tanzanian

primary lavas. The even higher concentrations in other lavas can be explained as due to fractionation.

### Effects of crustal contamination and fractional crystallization

In Chapter 3 (Dawson 2008), it was suggested that most of the Tanzanian volcanoes erupted through old cratonic lithosphere overlain by only a thin veneer of mobile-belt rocks. It was further suggested that the potential for crustal contamination of the magmas during ascent must be considered, together with possible compositional variations due to fractional crystallization.

The silica-undersaturated character of the mafic magmas argues against significant assimilation of high-silica crustal material although, from both seismic (see Chapter 4) and xenolith evidence, the Tanzanian lower crust is believed to be of basic composition, the assimilation of which would not show up as high  $\text{SiO}_2$ . To date two studies have been made on Tanzanian volcanic rocks to assess the possibility of contamination, using the AFC (assimilation, fractional crystallization) model of De Paolo (1981). On a range of basalts, Paslick *et al.* (1995) showed that variations in MgO point to some olivine and/or pyroxene fractionation although there is no correlation between  $^{87}\text{Sr}/^{86}\text{Sr}$  and Mg and Sr concentrations. Further, Paslick *et al.* (1995) modelled assimilation and fractional crystallization using Nd and Pb isotope data for a mixture of an uncontaminated magma sample and lower crustal granulite from Lashaine (Cohen *et al.* 1984); the conclusion was that some lavas could, theoretically, have been contaminated with lower crustal material. This was also indicated by disequilibrium between phenocryst and whole-rock Sr, Nd and Pb isotope compositions in a variety of basalts and nephelinites in which some (but not all) ‘phenocrysts’ of olivine, pyroxene, nepheline and plagioclase appear to be xenocrysts. As these xenocrysts might be expected to be of crustal derivation, and the disequilibria cannot be due to mantle variations, it is possible that the xenocrysts were derived from earlier magma that stagnated or crystallized at depth, where they were contaminated by deep crustal material, before later entrainment into batches of magma that erupted at the surface. Although such disequilibrium can have potentially serious implications when using whole-rock isotopic data to identify source reservoirs for volcanic rocks,

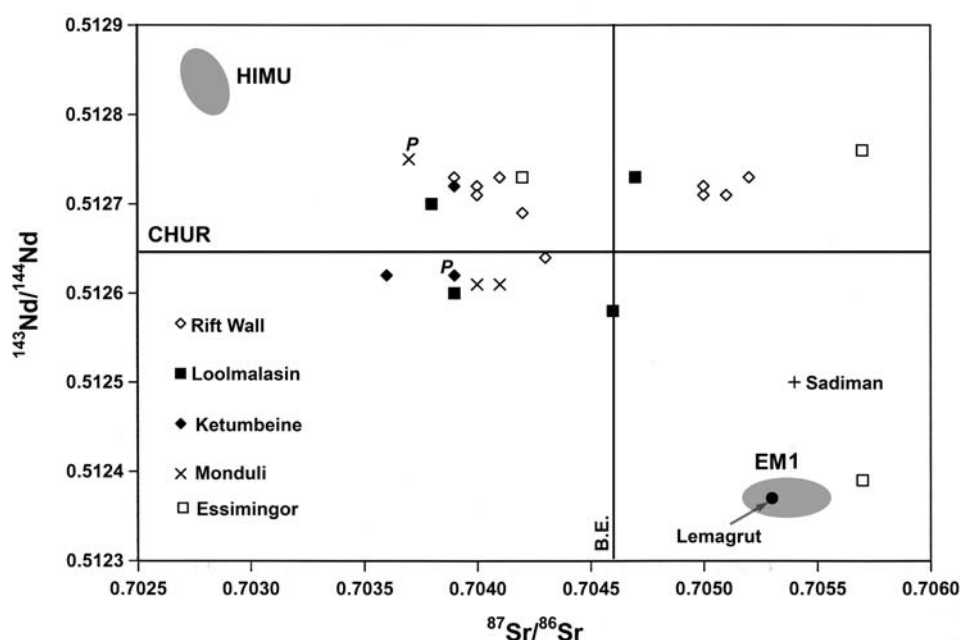


Fig. 8.2. Sr–Nd isotope plot for Older Extrusive lavas (data from Paslick *et al.* 1995). ‘P’ indicates primary or primitive lava (from Table 8.2).

none the less mass balance calculations show that  $^{206}\text{Pb}/^{204}\text{Pb}$  isotope compositions of the Tanzanian lavas would have been changed by only  $<0.25\%$  by this indirect lower crustal contamination (Paslick *et al.* 1996). Some samples, particularly highly silica-undersaturated lavas, contain Pb that is more highly radiogenic than in any known upper crustal rocks in Tanzania which suggests that the Pb is a feature of the mantle source rather than of crustal contamination. In the lavas listed in Table 8.2, Ba, Th, La and U concentrations are similar to, or bracket, those for the upper crust, but values for Nb, Ce, Rb are much higher, giving rise to distinctively high Rb/Ba, Ce/Pb and Nb/U ratios which are more similar to those for OIB; on these parameters, the cited lavas show no evidence of crustal contamination.

In a study using the Sr and Nd isotopic systematics of three lava compositions, one a nephelinite from Oldoinyo Lengai, and various crustal rocks (including Archaean rocks from the Tanzania craton and an average Tanzanian granulite), Bell & Dawson (1995) found that the spread of isotope date for the lavas at Oldoinyo Lengai could theoretically be modelled using a combination of granulite and nephelinite. However, the mafic melt would need to be of extreme peralkalinity and the model was rejected in favour of one involving mixing between a young asthenospheric melt and old enriched lithosphere. This model was reinforced by data from later Pb isotope investigations (Bell & Simonetti 1996; Bell & Tilton 2001).

In summary, the Tanzanian basic lavas show no evidence of upper crustal contamination, but some show theoretical evidence for a very small amount of lower crustal contamination, on the assumption that the contaminating material has the same isotopic characteristics as the Lashaine granulites used in the modelling.

## Petrogenesis

### Basalt-trachyte volcanoes

In northern Tanzania, basalts of the Older Extrusives volcanoes form the greatest volume of extruded material, and the associated

trachytes and phonolites are volumetrically small. Older Extrusive basalts and basanites from Paslick *et al.* (1995, 1996), together with the Kilimanjaro data of Downie & Wilkinson (1972) and other analyses shown in Appendix 2 (Dawson 2008), show a range through nephelinites, nepheline-normative picrobasalts, basanites and basalts. Fractionation can give rise to minor *hy*-normative basalt, hawaiite and benmoreite and, eventually, to both *ne*- and *qz*-normative trachytes (Fig. 8.3).

Although differing in the relative proportions (see above), the erupted basic rock types in Tanzania and southern Kenya show a similar petrological spectrum and the Tanzanian basalts may be viewed within the context of the basaltic rocks erupted within the overall East African rift system. These have been the subject of considerable research and various factors have been considered as relevant to their origin, including the relative input from convecting asthenospheric mantle, lithospheric mantle and continental crust, and possible connections with plume activity (e.g. Rogers *et al.* 2000; Macdonald *et al.* 2001; Macdonald 2003; Rogers 2006; Furman *et al.* 2006a, b).

From trace element evidence, Latin *et al.* (1993) and Macdonald *et al.* (2001) concluded that most Kenyan mafic magmas originated in a mantle melt zone extending across the spinel- to garnet-peridotite boundary. *Ne*-normative lavas with higher Ce/Y and lower Zr/Nb ratios originated at greater depths than *hy*- and *qz*-normative mafic rocks that have lower Ce/Y, higher Zr/Nb ratios and different Sr, Nd and lead isotope values. Moreover, Macdonald *et al.* (2001) recognize a correlation between the silica saturation of the magmas, their depth of origin and their tectonic setting. The least silica-saturated were generated at greater depth and erupted in the section of the rift underlain by the Tanzania Craton and its reworked margin, whereas *hy*-normative basalts formed at shallower depths and erupted in the parts of the rift underlain by the Mozambique Belt. The sequence nephelinite → basanite → alkali basalt → *hy*-normative basalt represents progressively shallower melting (i.e. increased spinel-peridotite component) rather than increased degrees of partial melting. This depth/silica-saturation relationship is shown by major element data, namely the  $\text{Al}_2\text{O}_3$  content and the  $\text{CaO}/\text{Al}_2\text{O}_3$  ratio, both of which are strongly pressure-dependent;

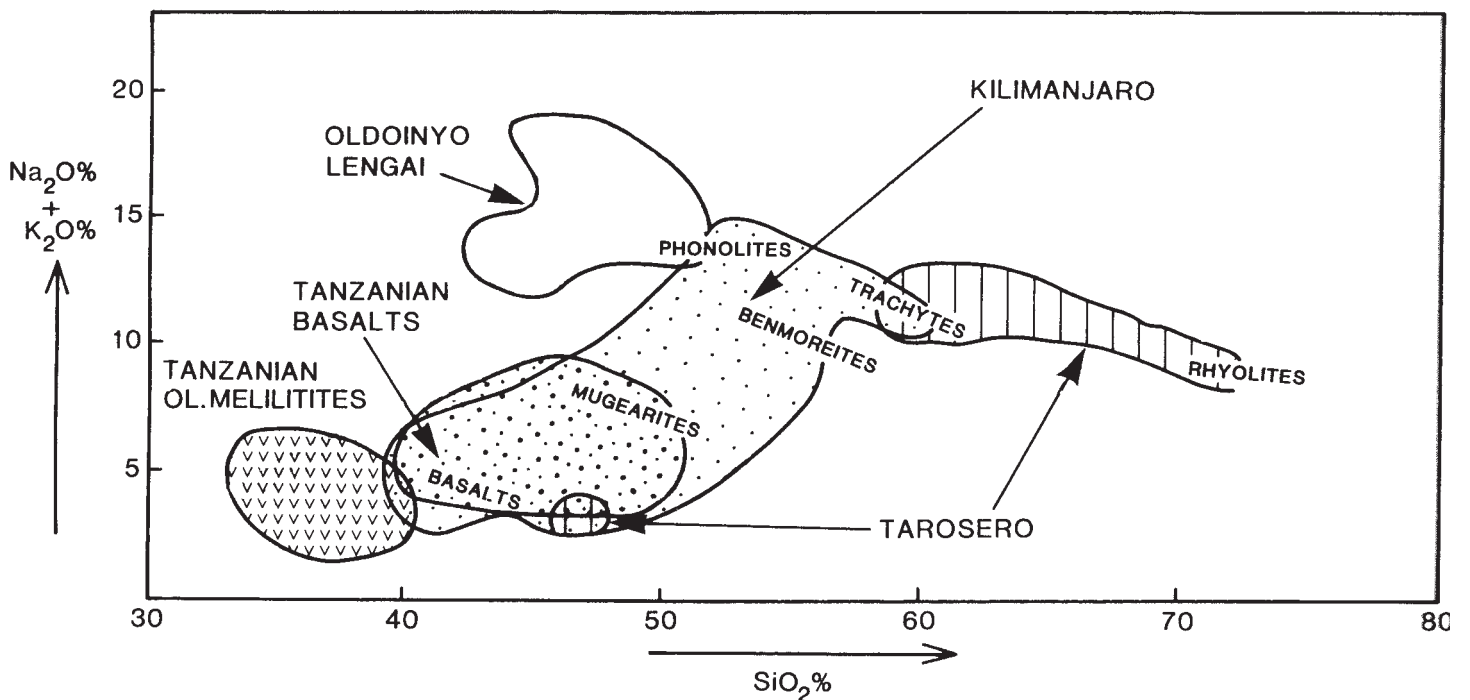


Fig. 8.3. Alkali-silica diagram for lavas from northern Tanzania. Data sources: Downie & Wilkinson (1972), Cooper (1972), Dawson *et al.* (1985), Donaldson *et al.* (1987), Paslick *et al.* (1995) and Appendix 2 (Dawson 2008).

the ratio increases with increasing melting/equilibration pressure, whilst  $\text{Al}_2\text{O}_3$  decreases (Herzberg 1995). Figure 8.4 is an  $\text{Al}_2\text{O}_3$  v.  $\text{CaO}/\text{Al}_2\text{O}_3$  plot, modified after Macdonald *et al.* (2001) for mafic rocks from the axial part of the Kenya rift valley with  $mg\#$  ( $\text{Mg}/\text{Mg} + \text{Fe}$ ) > 65 and therefore potential primary melts. The data set includes some analyses from northern Tanzania (Paslick *et al.* 1995), and additional data for Tanzanian lavas from Table 8.2 are also plotted. As in the case of the Kenyan lavas, the most silica-undersaturated Tanzanian lavas (olivine melilitites and nephelinites) have the highest ratios and lowest  $\text{Al}_2\text{O}_3$  values, and derive from the greatest depth/pressure. The basalts have lower ratios and higher  $\text{Al}_2\text{O}_3$  and are interpreted as being formed at lower pressure/higher levels. The overall trend of the lava types from high to low pressures is immediately apparent, but most data points for the natural rocks do not plot on the line derived for the experimentally derived solidus liquids; most have higher  $\text{CaO}$  for a given  $\text{Al}_2\text{O}_3$  value, a possible explanation for which is that the natural mantle source rocks are more calcic than the fertile peridotite composition used in Herzberg's experiments.

Overall, the Tanzanian rocks, and the olivine melilitites in particular, derive from greater depths than their Kenyan equivalents. This could be equated with their generation beneath the Tanzanian craton, rather than under the thinned craton margin, and hence deeper in the lithosphere.

A model for the Chyulu Hills Volcanic Province (CHVP), where there is a progression from early minor nephelinites through more extensive basalts to the most recent *hy*-normative minor basalts, is that the lavas result from conductive melting of metasomatized lithospheric mantle. In this model, the early nephelinites result from deep, relatively small amounts of melting, whilst a rise of the thermal source higher into the lithosphere results in greater degrees of melting at shallower depths to produce the more extensive, less silica-undersaturated basalts (Späth *et al.* 2001). Such a model might be applicable to certain Tanzanian volcanoes such as Oldoinyo Sambu and Lemagrut, where the dominantly basaltic activity is preceded by minor nephelinitic magmatism, and hence has some analogies with CHVP.

Although this model, at first sight, might not appear to be applicable to the main basaltic-trachytic volcanoes, such as those of the Crater Highlands, Ketumbeine and the Kilimanjaro massif, where there are rocks intermediate in composition between the basic rocks and trachytes, and also trachytes which have no equivalents in the CHVP, other factors may pertain. First, in the case of most of these central volcanoes, the earliest flows are not exposed so whether the first extrusives were nephelinites, or not, is unknown; none the less, they are known as the earliest extrusives at Oldoinyo Sambu and Lemagrut. Second, the CHVP results from fissure eruptions so lacks the large, central sub-volcanic magma chambers that might enable fractionation towards more silicic

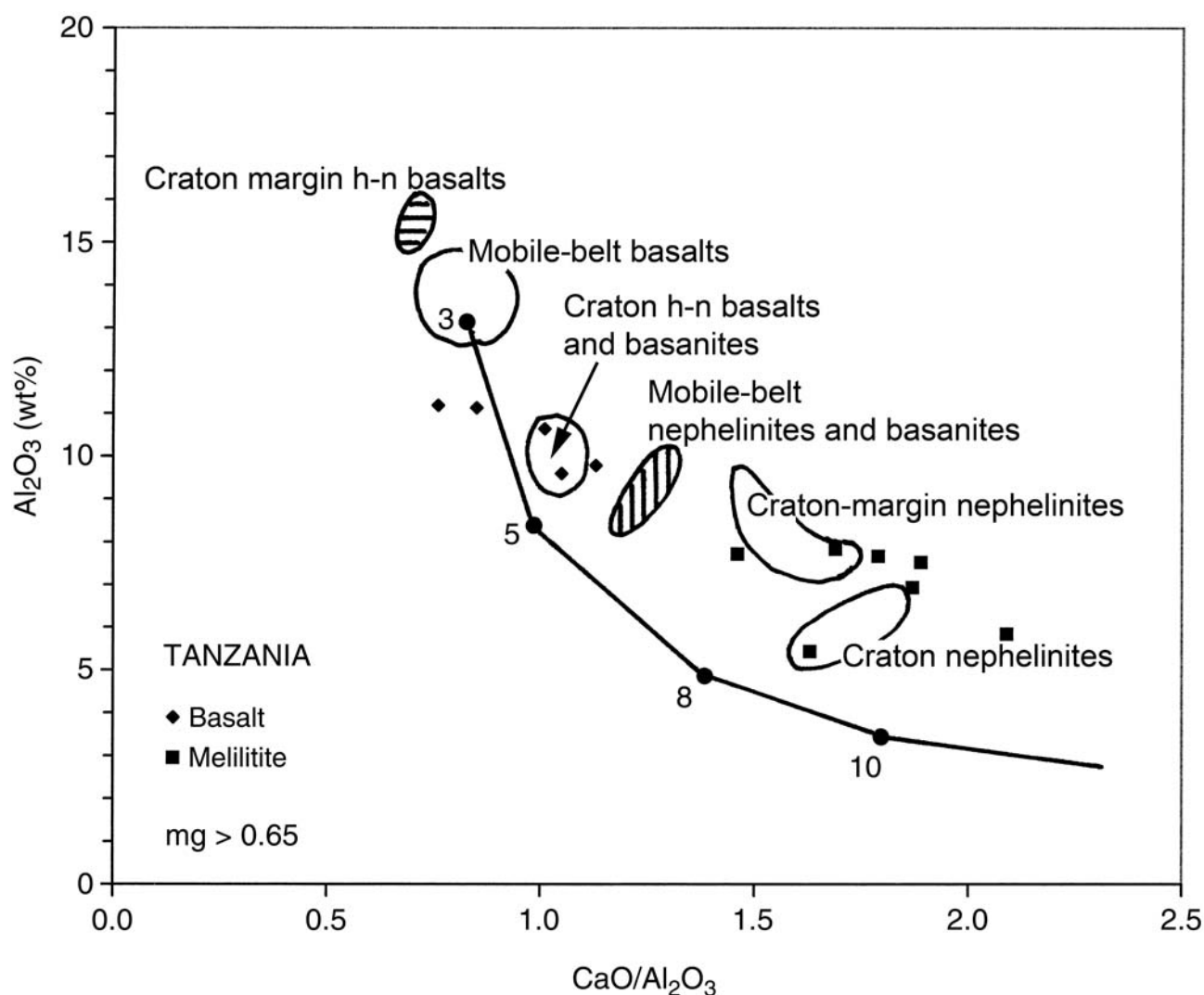


**Fig. 8.4.**  $\text{Al}_2\text{O}_3$  v.  $\text{CaO}/\text{Al}_2\text{O}_3$  plot for northern Tanzania lavas inferred to primary or primitive mantle melts ( $mg > 0.65$ ) (data from Table 8.2), compared with similar lavas from different tectonic regimes in Kenya (Macdonald 2003). The solid line with filled circles represents the composition of liquids formed by partial melting of fertile peridotite, the numbers referring to pressure in GPa along the solidus (Herzberg 1995). h-n basalt, hypersthene-normative basalt.

magmas. Third, the CHVP is very young and whether it will develop trachytic magmas is a question for the future. In short, application of the CHVP model to the main basalt-trachyte volcanoes in Tanzania is constrained by lack of knowledge of the detailed eruption sequence at individual volcanoes. However, if a composite or overlapping eruption sequence such as Oldoinyo Sambu plus Ngorongoro were accepted (nephelinite/melilitite  $\rightarrow$  *ne*-normative basalt  $\rightarrow$  *hy*-normative basalt  $\rightarrow$  mugearite  $\rightarrow$  trachyte), the CHVP model is a plausible starting point, provided that the model is extended to allow fractionation in large magma chambers beneath the central-type volcanoes. Essimngor, Sadiman and Mosonik, among the Older Extrusive centres, can be accommodated within this model if it can be accepted that their highly alkaline rocks are the first products of the initial thermal pulse coming into contact with earlier-enriched lithospheric mantle.

#### *Tarosero trachytes and comendites*

Amongst the Older Extrusives, the alkaline and peralkaline trachytes and comendites of Tarosero are unusual. They erupted from a small isolated cone and, unlike the trachytes at volcanoes such as Ngorongoro, are apparently unconnected with a major basalt centre. To date, Tarosero is the only centre in northern Tanzania known to have erupted such highly silicic lava as comendite and, as noted earlier, the peralkaline members contain unusually high concentrations of incompatible elements (Dawson 2008, table 7.1). Within East Africa, such centres are not common, but Tarosero has some similarities to the Olkaria rhyolitic centre near Lake Naivasha, Kenya. It has been suggested that the Olkaria rhyolites were formed by volatile-induced melting of crustal rocks (Macdonald & Scaillet 2006). Possibly relevant for a similar origin is the very high Cl content in the Tarosero Group II rocks, and the Nd and Pb isotopic evidence for the possible presence of some crustal (granulite) component in other Older Extrusives (Paslick *et al.* 1995). However, to invoke such an origin for the Tarosero comendites, it would be necessary to appeal to some highly selective, and regionally unusual, melting scheme.

#### *The Younger Extrusives: Oldoinyo Lengai as a model*

The Younger Extrusives magmas are silica-undersaturated, alkaline to peralkaline with high concentrations of incompatible elements, and their dominantly pyroclastic eruption style indicates that their magmas were rich in volatiles, a feature emphasized by the presence of carbonatite at most centres.

Sr and Nd isotope data for samples from Younger Extrusive volcanoes are shown on Figure 8.1 which includes data from Oldoinyo Lengai, the best studied of the Younger Extrusive centres. The data show that: (i) whereas lavas from Oldoinyo Lengai form an elongate zone between EM1 and HIMU, data for olivine melilitite, Kerimasi carbonatite, Hanang nephelinite and two Burko nephelinite samples cluster beyond the HIMU-end of the Oldoinyo Lengai grouping, and very close to recently-enriched peridotites; and (ii) a single sample from Meru falls within the Oldoinyo Lengai field and close to the younger Group II nephelinites, reinforcing the Oldoinyo Lengai–Meru mineralogical link mentioned earlier (Dawson 2008, Chapter 7).

In the specific case of Oldoinyo Lengai, although considerable interest has focused on the natrocarbonatite lavas, the principal problem is the genesis of the alkaline nephelinites and phonolites. These lavas have their counterparts at other Younger Extrusive centres, with the exception of the late peralkaline wollastonite–combeite nephelinites that, to date, have been also found only at Meru. Hence any model for Oldoinyo Lengai is probably broadly applicable to other Younger Extrusive volcanoes.

The Oldoinyo Lengai silicate lavas are silica-undersaturated, and contain high concentrations of Na and K, and other incompatible elements. A REE plot (Dawson 2008, fig. 7.11) illustrates high concentrations particularly of the LREE. Although this

pattern is generally believed to be typical of highly-fractionated lavas (and could well be correct in the case of the natrocarbonatite relative to the silicate lavas), this cannot be the sole reason, as similar concentrations exist in the unfractionated primary olivine nephelinite and olivine melilitite from Loolmurwak and Lalarasi (for location see Dawson 2008, fig. 7.18). In terms of their Sr, Nd and Pb isotopes, the Oldoinyo Lengai lavas lie close to a line between HIMU and EM1 mantle sources, which has been interpreted as being due to magma with a primitive mantle signature mixing with enriched lithosphere (Bell & Dawson 1995; Bell & Simonetti 1996). This interpretation finds some support from the presence of enriched peridotite blocks within the ejectamenta from Oldoinyo Lengai itself (Dawson 2008, fig. 7.12). Bearing in mind that the Group II nephelinites at Oldoinyo Lengai are (together with natrocarbonatite) the latest eruptives, a temporal connotation can be placed on the distribution of the Oldoinyo Lengai lavas along the EM1–HIMU line. The earlier Group I nephelinites and phonolites can be interpreted as resulting from greater involvement of the EM1 component during the early stage of the volcano, whereas declining EM1 component and/or a greater HIMU (primitive magma) component is apparent in the latest eruptives. Whereas Bell & Dawson (1995) take the EM1 component to be metasomatized peridotite, Kramm & Sindern (1998) show that Nd and Sr data for Oldoinyo Lengai fenites plot in a more enriched part of the Sr–Nd isotope diagram, and suggested that the interaction between a primitive magma and the  $^{87}\text{Sr}$ -enriched fenites would have had the same effect. However, interaction with fenites would also have the effect of increasing the amount of  $\text{SiO}_2$  in the resulting lavas.

The spread in Nd–Sr space for the Oldoinyo Lengai lavas is mirrored in their  $\delta^7\text{Li}$  Li isotope ratios which, although ranging from  $-0.6$  to  $-1.8$  in phonolite, through  $+2.8$  to  $+3.1$  for nephelinite, to  $+3.3$  to  $+5.1$  for natrocarbonatite, all fall within mantle values as represented by data for OIB and MORB (Halama *et al.* 2007).

Turning to the carbonatite–silicate rock relationship, although the stable and radiogenic isotopes indicate that, like the silicate rocks, the carbonatite is of mantle origin (Dawson *et al.* 1995), the actual formation of natrocarbonatite is still a matter of debate. Hypotheses range from its being: (i) a primitive mantle-derived melt; (ii) a product of fractionation of a parental alkali-bearing sövite magma (Gittins 1989); (iii) due to fractionation of silicate-bearing natrocarbonatite; and (iv) an immiscible fraction of the associated peralkaline nephelinites (papers in Bell *et al.* 1998). Points of fact are that there is no evidence for sövite at Oldoinyo Lengai (Dawson 1993) whereas globules of natrocarbonatite are present in silicate glasses in Group II lavas (Dawson *et al.* 1996).

The controversy at Oldoinyo Lengai reflects the views regarding the origin of carbonatites in general, with some investigators arguing for a direct origin for carbonatite in the mantle (e.g. Harmer & Gittins 1998). The existence of carbonate-rich mantle magmas, such as those of the Benfontein kimberlite sills, South Africa (Dawson & Hawthorne 1973) or the Igwisi Hills (Dawson 1994), is beyond dispute. Others argue for such an origin based on experiments on alkali-enhanced experimental compositions (Wallace & Green 1988; Sweeney *et al.* 1995). In the case of the carbonate-rich rocks that occur as small-volume components in complexes of evolved alkali-rich rocks, other investigators provide good experimental evidence for low-pressure exsolution of the carbonatites from (formerly) carbonated silicate parents (e.g. Wyllie & Lee 1998; Lee & Wyllie 1998).

#### *Parent magma(s) of the Younger Extrusives*

A common feature of most of the Younger Extrusive volcanoes is the presence in their vicinities of tuff cones or lava flows of olivine nephelinite or melilitite; primary and, hence, potential parental magma types. Dawson *et al.* (1985) noted that olivine melilitite

and olivine melilite nephelinite in the Oldoinyo Lengai area are exceptionally alkaline ( $[\text{Na} + \text{K}]/\text{Al}$  1.25 v. 0.75 for South African olivine melilitites) and suggested that the most primitive of these, an olivine melilite nephelinite ( $mg\#$  0.71, Ni 350 ppm) from Oldoinyo Loolmurwak, was a potential parent magma for the Oldoinyo Lengai lavas. Dawson (1998) further suggested a model whereby such a carbonated magma could evolve to the Oldoinyo Lengai nephelinites by olivine, pyroxene and phlogopite fractionation. This model is similar to that of Peterson & Kjaarsgaard (1995) who preferred olivine melilitite to be the parent magma, with eventual peralkaline nephelinite giving rise to natrocarbonatite by immiscible separation, the 'Lengai Trend'. An extension of this model forms calcic carbonatite by immiscibility from nephelinites less alkaline than those at Oldoinyo Lengai, the 'Shombole Trend' (Kjaarsgaard *et al.* 1995).

However, other work has shown that models invoking an olivine melilitite or nephelinite parent magma have certain difficulties, discussed below. But, first, turning to the origin of olivine melilitites, from a series of experiments on a specimen from Tasmania, Brey (1978) concluded that, initially, olivine melilitite could be derived from a 5% melt from a pyrolite composition at *c.* 27 kbar and 1160 °C, with 7–8% H<sub>2</sub>O and 6–7% CO<sub>2</sub> dissolved in the melt; increased pressure and increased XCO<sub>2</sub>/H<sub>2</sub>O resulted in increased silica-undersaturation. Two significant results of the experiments were to demonstrate the importance of the presence of volatiles (consistent with the melilitite/carbonatite association) but also the low degree of melting and consequent low volumes of melt. Of the ultrabasic lavas in the Natron area, in terms of their Si and Al contents the Oldoinyo Loolmurwak olivine melilite nephelinite (Dawson *et al.* 1985) and the Dorobo (Oldoinyo Lengai) olivine melilitite (Keller *et al.* 2006) are most similar to melilitite from Sutherland, South Africa, that Brey inferred to originate at *c.* 5 kbar by melting of a pyrolite mantle containing magnesite. This is consistent with the considerable depth of origin shown earlier for the northern Tanzanian olivine melilitites (Fig. 8.4). The Sr and Nd isotope values of the olivine melilitites in the Oldoinyo Lengai area overlap those of the recently-enriched mantle xenoliths from adjacent Pello Hill and Eledoi (Fig. 8.1).

#### *The Younger Extrusives paradox, and replenishment of the Tanzanian mantle*

That the lavas of Oldoinyo Lengai, an example of Younger Extrusive volcanic centres, might have an olivine melilitite parent (reviewed above) has been proposed earlier on the basis that no other magmas in the immediate vicinity may be regarded as primary mantle-derived magma.

There is an undoubtedly a close field-relationship between carbonatites and olivine melilitite in northern Tanzania (e.g. at Lashaine and in the Oldoinyo Lengai area) but there are problems linking the Oldoinyo Lengai nephelinites directly with a parental olivine melilitite:

1. There is a compositional gap between the rock-types, with no intermediate types that might indicate a fractional crystallization spectrum (Keller *et al.* 2006).
2. Specifically in the case of Oldoinyo Lengai lavas, the nearby olivine melilitites, although having similar  $\delta^7\text{Li}$  values (Halama *et al.* 2007), do not have the same Sr and Nd isotopic characteristics (Dawson 2008, fig. 7.1). The olivine melilitites lie closer to a HIMU source than any of the Oldoinyo Lengai lavas and hence, if olivine melilitite was indeed parental, some mixing with more enriched material is required. Fractional crystallization does not explain these isotope data.
3. For an olivine melilitite parent magma to be parental to other Younger Extrusive volcanoes, the prerequisite would be a very large volume of magma (particularly in the case of Meru) at the onset of the Younger Extrusive activity. The olivine melilitites appear late in the overall Younger

Extrusive activity and, at present, there is field evidence for only limited volumes, consistent with the experimental evidence that olivine melilitite is generated by very small amounts of mantle melting.

4. For olivine melilitite to be parental, repeated or cyclical generation of olivine melilitite magma would be required, both at the beginning and towards the end of the Younger Extrusive activity. Megacrysts of phlogopite, augite and amphibole certainly occur at several of the olivine melilitite localities in the Engaruka–Natron area and can be interpreted as additional pulses of melilitite magma crystallizing at depth but, even so, the volume of material at these occurrences is still very limited compared with the larger Younger Extrusive volcanoes.
5. Experiments and major element composition (Fig. 8.4) indicate that olivine melilitites are formed at considerable depth and the presence of mantle xenoliths in them suggests rapid ascent. This constraint appears at odds with the time necessary for high-level fractionation to form the Younger Extrusives.

If olivine melilitite is not a feasible source material, even allowing for mixing with enriched lithosphere, is there an alternative source for the Younger Extrusives? In many respects, the Younger Extrusives are a petrological repeat of the Older Extrusive volcanoes Essimigor, Sadiman, Shombole and Mosonik. Earlier, it was suggested that the highly alkaline rocks at these volcanoes could be accommodated within a model in which they are the first melting products of enriched lithospheric mantle that was heated by a rising asthenospheric thermal pulse. From the volume constraint, such a model might appear to be more feasible than fractionation of a low-volume olivine melilitite parental magma.

However, like that proposal, to apply such a model to the Younger Extrusives raises a very important question, the necessity for a continued, or re-fertilized, volatile- and incompatibles-enriched mantle source. The earlier Older Extrusive major episode of dominantly basaltic magmatism might be expected to have given rise to depleted mantle beneath northern Tanzania. Yet the Younger Extrusive volcanics are volatile- and incompatibles-enriched and must derive from mantle material that has these very properties. Although, on the timescale available, it might appear unlikely that the largely depleted Tanzanian lithospheric mantle could have been replenished, there is direct evidence from the mantle xenoliths at Pello Hill, Lashaine and Labait for a very young metasomatic event that has resulted in mantle replenishment. Moreover, at Pello Hill, the veined xenoliths provide evidence for an intrusion event. Further, there is seismic evidence for the existence of a mantle plume beneath the Tanzania Craton; a new pulse of upwelling asthenosphere could be the source of the replenishment.

To explain these observations, the following is offered as a tentative, integrated model. First, the Older Extrusives resulted from conductive melting of anciently-enriched lithospheric mantle, with the earliest melts from the deeper parts being peralkaline (e.g. Essimigor) or of limited volume (e.g. earlier nephelinites of Lemagrut and Oldoinyo Sambu). Continuing conductive heating to shallower levels produces larger, less enriched magma batches to produce the Older Extrusive basalt-dominated volcanoes, with high-level fractionation producing derivative benmoreites, mugearites, trachytes and phonolites. Original, enrichment-heterogeneity of the lithospheric mantle can explain contemporaneous alkaline/carbonatitic (Sadiman) and basaltic (Lemagrut) activity during the later part of the conductive heating event. Second, low-volume, enriched asthenospheric melts (the source of the heat for the Older Extrusive magmatism) eventually rise towards the surface, along channels generated during the mid-Pleistocene extension, to produce the Younger Extrusives. There is evidence from xenoliths for the fracturing, veining, injection and metasomatism of the lithospheric mantle

and, from seismicity, for deep, brittle lithosphere fracturing. The asthenosphere melts, although themselves enriched in volatiles and other incompatible components (e.g. CO<sub>2</sub>, Pb, REE), need to interact with residual, anciently-enriched lithosphere to generate the recent metasomatic effects seen in mantle xenoliths and to produce the Younger Extrusives isotope systematics.

An alternative to the above-preferred model is that enriched magma, generated during the Older Extrusive activity, was ponded in the lithosphere and later enabled to migrate upwards following the mid-Pleistocene faulting to form the Younger Extrusives.

## References

- BAKER, B. H. 1958. *Geology of the Magadi Area*. Geological Survey of Kenya, Report **42**.
- BAKER, B. H. 1963. *Geology of the Area South of Magadi*. Geological Survey of Kenya, Report **61**.
- BAKER, B. H. & MITCHELL, J. G. 1976. Volcanic stratigraphy and geochronology of the Kedong–Olorgesale area and the evolution of the South Kenya Rift valley. *Journal of the Geological Society, London*, **132**, 467–84.
- BAKER, B. H., MOHR, P. A. & WILLIAMS, L. A. J. 1972. *Geology of the Eastern Rift System of Africa*. Geological Society of America, Special Publications, **36**.
- BELL, K. & DAWSON, J. B. 1995. Nd and Sr isotope systematics of the active carbonatite volcano, Oldoinyo Lengai. In: BELL, K. & KELLER, J. (eds) *Carbonatite Volcanism of Oldoinyo Lengai and Petrogenesis of Natrocarbonatite*. Springer Verlag, Berlin, 100–112.
- BELL, K. & SIMONETTI, A. 1996. Carbonatite magmatism and plume activity: implications from the Nd, Pb and Sr isotope systematics of Oldoinyo Lengai. *Journal of Petrology*, **37**, 1321–1339.
- BELL, K. & TILTON, G. R. 2001. Nd, Pb and Sr isotopic compositions of East African carbonatites: evidence for mantle mixing and plume inhomogeneity. *Journal of Petrology*, **42**, 1927–1945.
- BELL, K., KJAARSGAARD, B. A. & SIMONETTI, A. (eds) 1998. *Carbonatites – into the Twenty-first Century. A Volume in Honour of John Gittins*. Special Number of Journal of Petrology, **39**, 1839–2151.
- BREY, G. 1978. Origin of olivine melilitites – chemical and experimental constraints. *Journal of Volcanological and Geothermal Research*, **3**, 61–88.
- BURTON, K. W., SCHIANO, P., BIRK, J.-L., ALLÉGRE, C. J., REHKÄMPER, M., HALLIDAY, A. N. & DAWSON, J. B. 2000. The distribution and behaviour of rhenium and osmium amongst mantle minerals and the age of the lithospheric mantle beneath Tanzania. *Earth and Planetary Science Letters*, **183**, 93–106.
- CHESLEY, J. T., RUDNICK, R. L. & LEE, C.-T. 1999. Re–Os systematics of mantle xenoliths from the East African Rift: age, structure and history of the Tanzanian craton. *Geochimica et Cosmochimica Acta*, **63**, 1203–1217.
- CLASS, C., GOLDSTEIN, STUTE, M., KURZ, M. D. & SCHLOSSER, P. 2005. Grand Comore Island: A well-constrained “low <sup>3</sup>He/<sup>4</sup>He” mantle plume. *Earth and Planetary Science Letters*, **231**, 391–409.
- COHEN, R. S., O’NIONS, R. K. & DAWSON, J. B. 1984. Isotope geochemistry of xenoliths from East Africa: implications for the development of mantle reservoirs and their interaction. *Earth and Planetary Science Letters*, **68**, 209–220.
- CROSSLEY, R. 1979. The Cenozoic stratigraphy and structure of the western part of the rift valley in southern Kenya. *Journal of the Geological Society, London*, **136**, 393–405.
- DAWSON, J. B. 1987. Metasomatized harzburgites in kimberlite and alkaline magmas: enriched restites and “flushed” lherzolites. In: MENZIES, M. A. & HAWKESWORTH, C. J. (eds) *Mantle Metasomatism*. Academic Press, London, 125–144.
- DAWSON, J. B. 1992. Neogene tectonics and volcanicity in the North Tanzania sector of the Gregory Rift Valley: contrasts with the Kenya sector. *Tectonophysics*, **204**, 81–92.
- DAWSON, J. B. 1993. A supposed sövite from Oldoinyo Lengai, Tanzania: result of extreme alteration of alkali carbonatite lava. *Mineralogical Magazine*, **57**, 93–101.
- DAWSON, J. B. 1994. Quaternary kimberlitic volcanism on the Tanzania craton. *Contributions to Mineralogy and Petrology*, **116**, 473–485.
- DAWSON, J. B. 1998. Peralkaline nephelinite–natrocarbonatite relationships at Oldoinyo Lengai, Tanzania. *Journal of Petrology*, **39**, 2077–2094.
- DAWSON, J. B. 1999. Melting and metasomatism in spinel peridotite xenoliths from Labait, Tanzania. In: GURNEY, J. J., GURNEY, J. L., PASCOE, M. D. & RICHARDSON, S. H. (eds) *Proceedings of the 7th International Kimberlite Conference, Cape Town, 1998*, Vol. 1, Red Roof Design, Cape Town, 164–173.
- DAWSON, J. B. 2002. Metasomatism and partial melting in upper-mantle peridotite xenoliths from the Lashaine volcano, northern Tanzania. *Journal of Petrology*, **43**, 1749–1777.
- DAWSON, J. B. 2008. *The Gregory Rift Valley and Neogene–Recent Volcanoes of Northern Tanzania*. Geological Society, London, Memoirs, **33**, 9–12.
- DAWSON, J. B. & HAWTHORNE, J. B. 1973. Magmatic sedimentation and carbonatitic differentiation in kimberlite sills at Benfontein, South Africa. *Journal of the Geological Society, London*, **129**, 61–85.
- DAWSON, J. B. & SMITH, J. V. 1988. Veined and metasomatized peridotites from Pello Hill, Tanzania: evidence for anomalously-light mantle beneath the Tanzania sector of the eastern Rift Valley. *Contributions to Mineralogy and Petrology*, **100**, 510–527.
- DAWSON, J. B. & SMITH, J. V. 1992. Olivine–mica–pyroxenite xenoliths from Oldoinyo Lengai, Tanzania. metasomatic products of upper mantle peridotites. *Journal of Volcanology and Geothermal Research*, **50**, 131–142.
- DAWSON, J. B., POWELL, D. G. & REID, A. M. 1970. Ultrabasic xenoliths and lava from the Lashaine volcano, northern Tanzania. *Journal of Petrology*, **11**, 519–548.
- DAWSON, J. B., SMITH, J. V. & JONES, A. P. 1985. A comparative study of bulk rock and mineral chemistry of olivine melilitites and associated rocks from East and South Africa. *Neues Jahrbuch für Mineralogie, Abhandlungen*, **152**, 143–175.
- DAWSON, J. B., PINKERTON, H., NORTON, G. E., PYLE, D. M., BROWNING, P., JACKSON, D. & FALICK, A. E. 1995. Petrology and geochemistry of Oldoinyo Lengai lavas extruded in November 1988: magma source, ascent and crystallization. In: BELL, K. & KELLER, J. (eds) *Carbonatite Volcanism of Oldoinyo Lengai and Petrogenesis of Natrocarbonatite*. Springer, Berlin, 47–69.
- DAWSON, J. B., PYLE, D. M. & PINKERTON, H. 1996. Evolution of natrocarbonatite from a wollastonite nephelinite parent: evidence from the June 1993 eruption of Oldoinyo Lengai, Tanzania. *Journal of Geology*, **104**, 41–54.
- DAWSON, J. B., JAMES, D., PASLICK, C. & HALLIDAY, A. M. 1997. Ultrabasic potassic low-volume magmatism and continental rifting in north-central Tanzania: association with enhanced heat flow. *Russian Geology and Geophysics*, **38**, 69–81.
- DE PAOLO, D. J. 1981. Trace element and isotopic effects of combined wall-rock assimilation and fractional crystallization. *Earth and Planetary Science Letters*, **53**, 189–202.
- DONALDSON, C. H., DAWSON, J. B., KANARIS-SOTIRIOU, R., BATCHELOR, R. A. & WALSH, J. N. 1987. The silicate lavas of Oldoinyo Lengai. *Neues Jahrbuch für Mineralogie Abhandlungen*, **156**, 247–279.
- DOWNIE, C. & WILKINSON, P. 1972. *The Geology of Kilimanjaro*. University of Sheffield, Sheffield.
- FAIRHEAD, J. D., MITCHELL, J. G. & WILLIAMS, L. A. J. 1972. New K/Ar determinations on Rift volcanics of S. Kenya and their bearing on the age of Rift faulting. *Nature*, **238**, 66–69.
- FURMAN, T., KALETA, K. M., BRYCE, J. G. & HANAN, B. B. 2006a. Tertiary mafic lavas of Turkana, Kenya: constraints on East African plume structure and the occurrence of high- $\mu$  volcanism in Africa. *Journal of Petrology*, **46**, 1221–1244.
- FURMAN, T., BRYCE, J., ROONEY, T., HANAN, B., YIRGU, G. & AYELEW, D. 2006b. Heads and tails: 30 million years of the Afar plume. In: YIRGU, G., EBINGER, C. Y. & MAGUIRE, K. H. (eds) *The Afar Volcanic Province within the East African Rift System*. Geological Society, London, Special Publications, **259**, 95–111.

- GITTINS, J. 1989. The origin and evolution of carbonatite magmas. In: BELL, K. (ed.) *Carbonatites: Genesis and Evolution*. Unwin Hyman, London, 580–600.
- HALAMA, R., MCDONOUGH, W. F., RUDNICK, R. L., KELLER, J. & KLAUDIUS, J. 2007. The Li isotopic composition of Oldoinyo Lengai: Nature of the mantle sources and lack of isotopic fractionation during carbonatite petrogenesis. *Earth and Planetary Science Letters*, **254**, 77–89.
- HARMER, R. E. & GITTINS, J. 1998. The case for primary, mantle-derived carbonatite magma. *Journal of Petrology*, **39**, 1895–1903.
- HART, S. R. 1988. Heterogeneous mantle domains: signatures, genesis and mixing chronologies. *Earth and Planetary Science Letters*, **90**, 273–296.
- HERZBERG, C. 1995. Generation of plume magmas through time: an experimental perspective. *Chemical Geology*, **126**, 1–16.
- JONES, A. P., SMITH, J. V. & DAWSON, J. B. 1983. Glasses in mantle xenoliths from Olmani, Tanzania. *Journal of Geology*, **91**, 167–178.
- KALT, A., HEGNER, E. & SATIR, M. 1997. Nd, Sr, and Pb isotope evidence for diverse lithospheric mantle sources of East African Rift carbonatites. *Tectonophysics*, **278**, 31–45.
- KELLER, J., ZAITSEV, A. & WIEDENMANN, D. 2006. Primary magmas at Oldoinyo Lengai: the role of olivine melilitite. *Lithos*, **91**, 150–172.
- KJAARSGAARD, B., HAMILTON, D. L. & PETERSON, T. 1995. Peralkaline nephelinite/carbonatite liquid immiscibility: comparison of phase compositions in experiments and natural lavas from Oldoinyo Lengai. In: BELL, K. & KELLER, J. (eds) *Carbonatite Volcanism of Oldoinyo Lengai and Petrogenesis of Natrocarbonatite*. I.A.V.C.E.I. Proceedings in Volcanology, Vol. 4. Springer, Berlin, 165–190.
- KRAMM, U. & SINDERN, S. 1998. Nd and Sr isotope signature of fenites from Oldoinyo Lengai, Tanzania, and the genetic relationships between nephelinites, phonolites and carbonatites. *Journal of Petrology*, **39**, 1997–2004.
- LATIN, D., NORRY, M. J. & TARZEY, R. J. E. 1993. Magmatism in the Gregory Rift, East Africa: evidence for melt generation by a plume. *Journal of Petrology*, **34**, 1007–1027.
- LE ROEX, A. P., SPÄTH, A. & ZARTMAN, R. E. 2001. Lithospheric thickness beneath the southern Kenya Rift: implications from basalt geochemistry. *Contributions to Mineralogy and Petrology*, **142**, 89–106.
- LEE, C.-T. & RUDNICK, R. L. 1999. Compositionally-stratified cratonic lithosphere: petrology and geochemistry of peridotite xenoliths from the Labait volcano, Tanzania. In: GURNEY, J. J., GURNEY, J. L., PASCOE, M. D. & RICHARDSON, S. H. (eds) *Proceedings of the 7th International Kimberlite Conference, Cape Town, 1998*, Vol. 2, Red Roof Design, Cape Town, 503–521.
- LEE, C.-T., RUDNICK, R. L., MCDONOUGH, W. F. & HORN, I. 2000. Petrologic and geochemical investigation of carbonates in peridotite xenoliths from northeastern Tanzania. *Contributions to Mineralogy and Petrology*, **139**, 470–484.
- LEE, W.-J. & WYLLIE, P. J. 1998. Processes of crustal carbonatite formation by liquid immiscibility and differentiation elucidated by model systems. *Journal of Petrology*, **39**, 2005–2014.
- MACDONALD, R. 2003. Magmatism of the Kenya Rift Valley: a review. *Transactions of the Royal Society of Edinburgh: Earth Sciences*, **95**, 239–253.
- MACDONALD, R. & SCAILLET, B. 2006. The central Kenya peralkaline province: Insights into the evolution of peralkaline salic magmas. *Lithos*, **91**, 59–73.
- MACDONALD, R., ROGERS, N. W., FITTON, J. G., BLACK, S. & SMITH, M. 2001. Plume–lithosphere interactions in the generation of basalts of the Kenya Rift, East Africa. *Journal of Petrology*, **42**, 877–900.
- PASLICK, C., HALLIDAY, A., JAMES, D. & DAWSON, J. B. 1995. Enrichment of the continental lithosphere by OIB melts: Isotopic evidence from the volcanic province of northern Tanzania. *Earth and Planetary Science Letters*, **130**, 109–126.
- PASLICK, C., HALLIDAY, A. N., LANGE, R. A., JAMES, D. & DAWSON, J. B. 1996. Indirect crustal contamination: evidence from isotopic and chemical disequilibria in minerals from alkali basalts and nephelinites from northern Tanzania. *Contributions to Mineralogy and Petrology*, **125**, 277–292.
- PETERSON, T. D. & KJAARSGAARD, B. A. 1995. What are the parental magmas at Oldoinyo Lengai? In: BELL, K. & KELLER, J. (eds) *Carbonatite Volcanism of Oldoinyo Lengai and Petrogenesis of Natrocarbonatite*. I.A.V.C.E.I. Proceedings in Volcanology, Vol. 4. Springer, Berlin, 148–162.
- PORCELLI, D. R., O'NIONS, R. K. & O'REILLY, S. Y. 1986. Helium and strontium isotopes in ultramafic xenoliths. *Chemical Geology*, **54**, 237–249.
- RIDLEY, W. I. & DAWSON, J. B. 1975. Lithophile trace element data bearing on the origin of peridotite, ankaramite and carbonatite from the Lashaine volcano, Tanzania. *Physics and Chemistry of the Earth*, **9**, 559–570.
- ROBERTS, M. A. 2002. *The Geochemical and Volcanological Evolution of the Mt. Meru Region, Northern Tanzania*. PhD thesis, University of Cambridge.
- ROEDER, P. L. & EMSLIE, R. F. 1970. Olivine-liquid equilibrium. *Contributions to Mineralogy and Petrology*, **29**, 275–289.
- ROGERS, N. W. 2006. Basalt magmatism and geodynamics of the East African Rift System. In: YIRGU, G., EBINGER, C. Y. & MAGUIRE, K. H. (eds) *The Afar Volcanic Province within the East African Rift System*. Geological Society, London, Special Publications, **259**, 77–93.
- ROGERS, N. W., MACDONALD, R., FITTON, J. G., GEORGE, R., SMITH, M. & BARREIRO, B. 2000. Two mantle plumes beneath the East African rift system: Sr, Nd and Pb isotope evidence from Kenya Rift basalts. *Earth and Planetary Science Letters*, **176**, 387–400.
- RUDNICK, R. L. & GAO, S. 2003. Composition of the continental crust. In: HOLLAND, H. D. & TUREKIAN, K. K. (eds) *Treatise on Geochemistry: Volume 3. The Crust*. Elsevier, Amsterdam, 1–64.
- RUDNICK, R. L., MCDONOUGH, W. F. & CHAPPELL, B. W. 1993. Carbonatite metasomatism in the northern Tanzanian mantle: petrographic and geochemical characteristics. *Earth and Planetary Science Letters*, **114**, 463–475.
- RUDNICK, R. L., MCDONOUGH, W. F. & ORPIN, A. 1994. Northern Tanzanian peridotite xenoliths: a comparison with Kaapvaal peridotites and inferences on metasomatic interactions. In: MEYER, H. O. A. & LEONARDOS, O. H. (eds) *Proceedings of the 5th International Kimberlite Conference, Araxa 1991*, Companhia de Pesquisa de Recursos Minerais, Brasilia Vol. 1, 336–353.
- SIMON, N. S. C., IRVINE, G. J., DAVIES, G. R., PEARSON, D. G. & CARLSON, R. W. 2003. The origin of garnet and clinopyroxene in “depleted” Kaapvaal peridotites. *Lithos*, **71**, 289–322.
- SMITH, M. & MOSLEY, P. 1993. Crustal heterogeneities and basement influence on the development of the Kenya Rift, East Africa. *Tectonics*, **12**, 591–606.
- SPÄTH, A., LE ROEX, A. P. & OPIYO-AKECK, N. 2000. The petrology of the Chiyulu Hills Volcanic Province, southern Kenya. *Journal of African Earth Sciences*, **31**, 337–358.
- SPÄTH, A., LE ROEX, A. P. & OPIYO-AKECK, N. 2001. Plume–lithosphere interaction and the origin of continental rift-related alkaline volcanism - the Chiyulu Hills Volcanic Province, southern Kenya. *Journal of Petrology*, **42**, 765–787.
- STUART, F. M. & TURNER, G. 1992. The abundance and isotopic composition of noble gases in ancient fluids. *Chemical Geology*, **101**, 98–109.
- SUN, S.-S. & MCDONOUGH, W. F. 1989. Chemical and isotopic systematics of oceanic basalts: implications for mantle compositions and processes. In: SAUNDERS, A. D. & NORRY, M. J. (eds) *Magmatism in the Ocean Basins*. Geological Society, London, Special Publications, **42**, 313–345.
- SWEENEY, R. J., FALLOON, T. J. & GREEN, D. H. 1995. Experimental constraints on the possible origin of natrocarbonatite. In: BELL, K. & KELLER, J. (eds) *Carbonatite Volcanism of Oldoinyo Lengai and Petrogenesis of Natrocarbonatite*. Springer, Berlin, 191–207.
- WALLACE, M. E. & GREEN, D. H. 1988. An experimental determination of primary carbonatite magma composition. *Nature*, **335**, 343–346.
- WILLIAMS, L. A. J., MACDONALD, R. & CHAPMAN, G. R. 1984. Late Quaternary volcanoes of the Kenya Rift Valley. *Journal of Geophysical Research*, **89**, B10, 8553–8570.
- WYLLIE, P. J. & LEE, W. J. 1998. Model system controls on conditions for formation of magnesiocarbonatite and calciocarbonatite magmas from the mantle. *Journal of Petrology*, **39**, 1885–1893.

## Chapter 9

### Future work

This memoir has attempted to give an account of the present knowledge of this part of the Gregory Rift, but should be regarded as an interim report. Like most reviews, it has served to identify areas that would benefit from further research. Some are listed below.

1. The eastern margin of the Tanzania craton is buried to the east of the mapped surface contact between it and the Mozambique fold belt. As noted in Chapter 3, there is now evidence that Archaean and Neoproterozoic rocks exist intermixed with the rocks of the Mozambique Belt, well to the east of the mapped contact. Seismic traverses across the Maasai Block would be highly desirable to determine whether the eastern extent of the craton can be ascertained, and whether there might be any coincidence between its extent and the identified geophysical properties of the Maasai Block suggesting that it might be a discrete terrain.
2. Investigations into the structure and history of the Tanzanian mantle by means of xenolith studies are still at an early stage. Some xenoliths, such as those at Lashaine and Pello Hill, contain micas, whereas others (e.g. at Olmani) contain monazite. Dating these phases could shed new light on the timing of the upper mantle metasomatism. The age and isotopic characteristics of the host rocks of the xenoliths (mainly olivine melilitites and nephelinites) need investigation to find out whether the metasomatism and magmatism are linked. For example, are the helium isotope characteristics of xenoliths imposed by the host magmas during transportation?
3. There is still a dearth of radiogenic isotope data on the Tanzanian volcanic rocks, particularly on systematic collections from individual volcanoes. One such volcano is Tarosero which, within the Tanzanian province, is a unique and atypical locality for peralkaline rhyolites.
4. U-series and diffusion profiling in phenocrysts can determine the timescales of magma replenishment and crystal fractionation in magmatic systems. Currently, there are virtually no data on the strongly silica-undersaturated systems of which the northern Tanzanian volcanoes offer an almost unparalleled selection e.g. Oldoinyo Lengai, Kerimasi and Meru.
5. Although touched upon in the case of plutonic cognate xenoliths from Oldoinyo Lengai (Dawson 2008, Chapter 7), there is considerable scope for studies of melt and fluid inclusions in phenocrysts and xenoliths with the aim of interpreting melt-fluid evolution in strongly alkaline systems.
6. There are uninvestigated sedimentary sequences exposed in gorges on both the western and eastern sides of the Engaruka Basin, which lies geographically between the Natron and Manyara Basins (where mammalian and hominid fossils have been found). Hence, the Engaruka Basin sediments are worthy of a reconnaissance to assess their potential for fossil studies.

## Appendix 1

### Appendix 1A. Radiometric dates from Northern Tanzania

Sample	Lithology and location	Age (Ma)	Refs	Sample	Lithology and location	Age (Ma)	Refs
<i>Lake Natron Area (see also unpublished dates below)</i>				<i>Engaruka-Manyara Area</i>			
572	Phonolitic nephelinite, Shombole	1.96 ± 0.07	3	155	Olivine basalt, south slopes of Ketumbeine	1.54 ± 0.1	6
580	Phonolitic nephelinite, Shombole	2.00 ± 0.05	3		Olivine basalt, south slopes of Ketumbeine	1.66 ± 0.07	6
138	Nephelinite, south slopes of Gelai	0.96 ± 0.03	6	156	Olivine basalt, south slopes of Ketumbeine	1.73 ± 0.08	6
	Nephelinite, south slopes of Gelai	0.99 ± 0.03	6		Olivine basalt, south slopes of Ketumbeine	1.87 ± 0.08	6
	Biotite lava, Mosonik	3.18 ± 0.08	1		Olivine melanephelinite, escarpment base, Engaruka	3.2 ± 0.5	4
KA 1757				11255			
NATM89-07	Nephelinite, Mosonik	3.53 ± 0.06	2	11245	Olivine basalt, escarpment top, Engaruka	1.4 ± 0.5	4
S11/4	Nephelinite, flow from Mosonik	1.28 ± 0.05	11	11247	Trachyandesite, escarpment top, Engaruka	1.8 ± 0.6	4
KA 1755	Basalt, Peninj Gorge	1.90 ± 0.07	1	11	Olivine trachybasalt, flow, small crater, 1 mile south of Engaruka	1.15 ± 0.04	5
KA 1755R	Basalt, Peninj Gorge	1.77 ± 0.04	1		Olivine trachybasalt, flow, small crater, 1 mile south of Engaruka	1.11 ± 0.06	5
KA 2570	Basalt, Malambo Gorge	3.5 ± 0.46	1	139	Olivine trachybasalt, Narabala top of scarp	1.2 ± 0.04	5
KA 1185	Basalt, underlying Peninj Group sediments	2.99 ± 0.09	2		Olivine trachybasalt, Narabala top of scarp	1.18 ± 0.05	5
KA 1754	Basalt, Humbu Formation (Lower Peninj Group)	1.55 ± 0.03	1	137a	Olivine trachybasalt, Narabala, flow from fault	1.21 ± 0.05	5
KA 1754R	Basalt, Humbu Formation	2.27 ± 0.06	1		Olivine trachybasalt, Narabala, flow from fault	1.15 ± 0.04	5
KA 2382	Basalt, Humbu Formation	0.96 ± 0.1	1		Olivine trachybasalt, Narabala, flow from fault	1.09 ± 0.05	5
KA 2382R	Basalt, Humbu Formation	1.21 ± 0.36	1		Olivine trachybasalt, Narabala, flow from fault	1.17 ± 0.04	5
KA 2578	Basalt, Humbu Formation	0.97 ± 0.25	1	S13/2	Olivine basalt, Engaruka Basin escarpment	1.26 ± 0.07	11
KA 2646	Basalt, Humbu Formation	1.21 ± 0.1	1	BD181	Olivine basalt, extruded from main rift fault, Kitete	1.13 ± 0.16	5
	Basal tuff, Humbu Formation	1.70 ± 0.02*	2		Olivine basalt, extruded from main rift fault, Kitete	1.23 ± 0.05	5
KA 2410	Intra-Moinik basalt, Moinik Formation (U. Peninj Group)	1.33 ± 0.05	1	BD180	Olivine basalt, extruded from main rift fault, Kitete	0.95 ± 0.08	5
KA 2589	Intra-Moinik basalt, Moinik Formation	1.38 ± 0.09	1		Olivine basalt, extruded from main rift fault, Kitete	1.08 ± 0.05	5
KA 1186	Intra-Moinik basalt, Moinik Formation	1.41 ± 0.04	2	S13/3	Basalt, extruded from foot of Kitete escarpment	1.0 ± 0.1	11
KA 1187	Intra-Moinik basalt, Moinik Formation	1.13 ± 0.06	2	S14/4	Basalt, top of Kitete escarpment	0.8 ± 0.4	11
S1 1/6	Nephelinite, interbedded with Upper Moinik Formation.	1.31 ± 0.26	11	S14/5	Basalt, foot of Kitete escarpment	1.2 ± 0.06	11
	Bird Print Tuff, Moinik Formation	1.26 ± 0.04*	2	11163	Picritic basalt, escarpment base, north of Lake Manyara	3.8 ± 0.2	4
3	Phlogopite, Kisetey crater tuff	0.57 ± 0.15	5	11170	Basaltic andesite, escarpment top, north of Lake Manyara	2.25 ± 0.1	4
	Phlogopite, Kisetey crater tuff	0.14 ± 0.15	5				
891	Phlogopite, Loolmurwak crater tuff	0.53 ± 0.1	5				
	Phlogopite, Loolmurwak crater tuff	0.41 ± 0.1	5				
105	Phlogopite, Loolmurwak crater tuff	0.19 ± 0.08	5				
	Phlogopite, Loolmurwak crater tuff	0.14 ± 0.12	5				
	Calcrete, on reworked tephra, 3–5 km south of Lake Natron	0.13 Ma	7				
	Calcrete, overlying black tuffs, Loolmurwak crater	0.35 ± 0.01	7				
11031	Phonolite, Oldonyo Lengai	0.15 ± 0.02	4				

(Continued)

(Continued)

Sample	Lithology and location	Age (Ma)	Refs	Sample	Lithology and location	Age (Ma)	Refs
2a	Basalt, interbedded with lacustrine sediments, base of main rift escarpment, Lake Manyara	4.86 ± 0.24	11	20	Trachyte, Ngorongoro	2.45 ± 0.15	9
7b	Basalt, top of rift escarpment, Lake Manyara	1.5 ± 0.1	11		Plagioclase (tuff), Ngorongoro	2.23 ± 0.1	9
<b>Essimngor-Burko-Tarosero-Monduli</b>					Plagioclase (tuff), Ngorongoro	2.28 ± 0.14	9
	Melanephelinite, Essimngor	8.1 ± 1.0	4		Plagioclase (tuff), Ngorongoro	2.45 ± 0.15	9
142	Melanephelinite, Essimngor	7.35 ± 0.65	4		Plagioclase (tuff), Ngorongoro	2.25 ± 0.15	9
	Nephelinite, gully on SE slopes, Essimngor	4.68 ± 0.09	6	11147	Plagioclase (tuff), Ngorongoro	2.81 ± 0.11	9
	Nephelinite, gully on SE slopes, Essimngor	4.89 ± 0.09	6		Olivine basalt, Ngorongoro	3.7 ± 0.8	4
143	Nephelinite, gully on SE slopes, Essimngor	3.23 ± 0.07	6	11124	Phonolite, north of Lemagrut	5.5 ± 0.1	4
	Nephelinite, gully on SE slopes, Essimngor	3.20 ± 0.06	6	11130	Basaltic andesite, Lemagrut	4.3 ± 1.05	4
137b	Nephelinite, gully on SE slopes, Burko	1.03 ± 0.04	6	11115	Silicic andesite, Lemagrut	2.7 ± 0.2	4
	Nephelinite, gully on SE slopes, Burko	0.91 ± 0.03	6	7c	Ankaramite, Lemagrut	3.1 ± 0.3	11
309	Olivine basalt, lower north slopes, Tarosero	2.4 ± 0.62	5		Naibadad beds, Laetoli	2.26 ± 0.06	8
305	Sodalite phonolite, faulted north slopes of Tarosero	2.25 ± 0.06	5		Vogesite lava flow remnant, Ogol lavas, Laetoli area	2.41 ± 0.12	8
306	Sodalite phonolite, faulted north slopes of Tarosero	2.2 ± 0.06	5		Biotite in tuff, upper Laetoli Beds	3.49 ± 0.12	8
510	Phonolite, lower NW slopes of Tarosero	2.21 ± 0.1	5		Biotite in tuff, lower Laetoli Beds (age mean of 2)	3.76 ± 0.03	8
490	Unfaulted trachyte, summit of Tarosero	2.16 ± 0.06	5	LMGT89-02	Ignimbrite, Lemagrut	1.92 ± 0.04	2
	Unfaulted trachyte, summit of Tarosero	2.04 ± 0.04	5	LMGT89-03	Ignimbrite, Lemagrut	1.82 ± 0.03	2
488	Unfaulted trachyte, summit ridge, Tarosero	1.98 ± 0.03	5		Ignimbrite, Lemagrut	1.97 ± 0.01*	2
	Unfaulted trachyte, summit ridge, Tarosero	1.90 ± 0.04	5	NATM89-13	Trachytic lava, Olmoti	1.65 ± 0.03	2
304	Olivine basalt, highest flow on Matunginini fault escarpment	2.00 ± 0.05	5	NATM89-13A	Trachytic lava, Olmoti	1.11 ± 0.09	2
136	Olivine basalt, north slope of Monduli Mtn, near Tarosero escarpment	2.09 ± 0.06	6	NATM89-11A	Ignimbrite, Olmoti	1.23 ± 0.04	2
	Olivine basalt, north slope of Monduli Mtn, near Tarosero escarpment	2.15 ± 0.05	6	NATM89-08	Phonolitic tephrite, Olmoti	1.07 ± 0.05	2
<b>Kwaraha-Hanang</b>				OGMW89-54	Trachyandesite flow, Olduvai, from Olmoti?	1.09 ± 0.03	2
11068	Olivine melanephelinite, Kwaraha	1.5 ± 1.0	4	MW89-17	Nephelinite, Embagai	0.5 ± 0.4	2
11073	Olivine melilite, Kwaraha	1.05 ± 0.15	4	MW89-15A	Nephelinite, Embagai	1.05 ± 0.02	2
11085	Olivine melanephelinite, Kwaraha	1.08 ± 0.18	4	MW89-14A	Nephelinite, Embagai	1.52 ± 0.03	2
11088	Nephelinite, Kwaraha	0.7 ± 0.0	4		Tephros, Embagai	c. 0.6*	2
11001	Nephelinite, Hanang	1.5 ± 0.3	4	<b>Olduvai Gorge</b>			
11030	Nephelinite, Hanang	0.9 ± 0.2	4		Naabi ignimbrite below base of Bed I	2.029 ± 0.005*	13
<b>Crater Highlands</b>					Coarse feldspar crystal tuff (CFCT) above Naabi ignimbrite	2.018 ± 0.019*14	13
	Nephelinite, Sadiman	3.32 ± 0.06	2		Basalt immediately above CFCT, Bed I (?derived from Olmoti (Hay, 1976))	1.96	12
2238	Nephelinite, Sadiman	3.7	7		Basalt immediately above CFCT, Bed I	1.865 ± 0.02	13
Tuff 8	Tephros, Upper Laetolil Beds, ?from Sadiman	3.46 ± 0.12	8		Tuff IB, above basalt, Bed I	1.798 ± 0.004*	13
	Nephelinite, Sadiman	4.5 ± 0.4	4		Tuff IB, above basalt, Bed I	1.786	12
11113	Nephelinite, Sadiman	4.5 ± 0.4	4		Tuff IF top of Bed I	1.749 ± 0.009*	13
NAT90-28	Ignimbrite, Ngorongoro	1.83 ± 10.03	2		Tuff IIA base of Bed II	1.71	12
NAT90-30	Ignimbrite, Ngorongoro	1.98 ± 0.032	2		Ndutu Beds (calcretes and Limicolaria shells)	30-22 Ka BP	7
	Ignimbrite, Ngorongoro	2.02 ± 0.02*	2		Naisiusiu Beds (calcretes, collagen and egg-shell)	20-9 Ka BP	7
					Calcretes overlying Naisiusiu Beds)	6.6-4 Ka BP	7
				<b>Meru Area</b>			
				135	Alkali basalt block, collapsed east wall of caldera, Meru	0.09 ± 0.02	6
					Alkali basalt block, collapsed east wall of caldera, Meru	0.115 ± 0.007	6
				141	Nephelinite block, collapsed east wall of caldera, Meru	0.099 ± 0.005	6
					Nephelinite block, collapsed east wall of caldera, Meru	0.097 ± 0.004	6
				3221	Pumice from mantling ash, Oldonyo Sambu scoria cone	< 0.55	10

(Continued)

(Continued)

Sample	Lithology and location	Age (Ma)	Refs	Sample	Lithology and location	Age (Ma)	Refs
	Pumice from mantling ash, Oldonyo Sambu scoria cone	<0.10	10	4054	Amphibole-rich ankaramitic basalt from Cinderella Cone, Loljoro valley	1.77 ± 0.04	10
3403	Nephelinite, Meru summit	0.059 ± 0.010	10		Amphibole-rich ankaramitic basalt from Cinderella Cone, Loljoro valley	1.67 ± 0.04	10
3655	Nephelinite, Meru summit	0.067 ± 0.008	10		Amphibole-rich ankaramitic basalt from Cinderella Cone, Loljoro valley	1.93 ± 0.04	10
	Nephelinite, SW of Meru West (3885 m)	0.08 ± 0.005	10		Amphibole-rich ankaramitic basalt from Cinderella Cone, Loljoro valley	1.93 ± 0.04	10
3930	Phonolitic nephelinite, summit group, Meru West (2395 m)	0.079 ± 0.004	10	3435	Sanidine phonolite clast from breccia, Meru West scarp	2.03 ± 0.04	10
	Phonolitic nephelinite, summit group, Meru West (2395 m)	0.09 ± 0.004	10		Sanidine phonolite clast from breccia, Meru West scarp	1.99 ± 0.04	10
3114	Phonolitic tephrite, Main Cone group, behind Ash Cone	0.107 ± 0.006	10	3706	Mugearite, Flood lava group, Oljoro valley	2.3 ± 0.06	10
	Phonolitic tephrite, Main Cone group, behind Ash Cone	0.102 ± 0.005	10		Mugearite, Flood lava group, Oljoro valley	2.25 ± 0.04	10
4231	Phonolitic tephrite, Main Cone group, behind Ash Cone	0.107 ± 0.007	10	3705	Alkali basalt, Flood lava group, Oljoro valley	2.44 ± 0.06	10
	Phonolitic tephrite, Main Cone group, behind Ash Cone	0.111 ± 0.007	10		Alkali basalt, Flood lava group, Oljoro valley	2.49 ± 0.06	10
4191	Nephelinite, Main Cone group, NW flanks of Meru	0.163 ± 0.013	10				
	Nephelinite, Main Cone group, NW flanks of Meru	0.148 ± 0.010	10	<b>Kilimanjaro</b>	Lower olivine basalts, Naiperra, Amboseli	0.85 ± 20%	14
3203	Sanidine phonolite, Naigonesoit tholoid, north Meru	0.168 ± 0.009	10		Lower olivine basalts, Naiperra, Amboseli	1.10 ± 15%	14
	Sanidine phonolite, Naigonesoit tholoid, north Meru	0.158 ± 0.010	10		Lower olivine basalts, Ngong Naro, Amboseli	0.420 ± 15%	14
	Sanidine phonolite, Naigonesoit tholoid, north Meru	0.179 ± 0.010	10	KA940	Trachybasalt, Mawenzi	0.514	15,16
3193	Trachytoid phonolite, north of Naigonesoit, north Meru	0.384 ± 0.009	10	KA947	Basalt, Lava Tower series, Shira	0.463	15,16
	Trachytoid phonolite, north of Naigonesoit, north Meru	0.377 ± 0.009	10	KA937	Obsidian, Rhomb Porphyry Series	0.365	15,16
3127	Phonolitic nephelinite clast from breccia, Little Meru	0.273 ± 0.006	10	134	Trachyte, Lent Group, Shira Plateau	0.27 ± 0.02	6
	Phonolitic nephelinite clast from breccia, Little Meru	0.281 ± 0.005	10		Trachyte, Lent Group, Shira Plateau	0.23 ± 0.03	6
3912	Phonolite, Oldonyo Sambu (parasitic cone)	0.311 ± 0.011	10		Trachyte, Lent Group, Shira Plateau	0.23 ± 0.02	6
	Phonolite, Oldonyo Sambu (parasitic cone)	0.3 ± 0.011	10	200	Anorthoclase phenocryst (blocky habit), caldera rim, Kibo	0.22 ± 0.01	10
3303	Phonolitic nephelinite, Oldonyo Sambu	0.313 ± 0.009	10	246	Anorthoclase phenocryst (blocky habit), caldera rim, Kibo	0.19 ± 0.01	10
	Phonolitic nephelinite, Oldonyo Sambu	0.299 ± 0.010	10		Anorthoclase phenocryst (blocky habit), caldera rim, Kibo	0.17 ± 0.01	10
	Phonolitic nephelinite, Oldonyo Sambu	0.303 ± 0.010	10	223	Anorthoclase phenocryst (rhombic habit), caldera rim, Kibo	0.23 ± 0.03	10
3436	Phonolitic nephelinite, Meru West scarp	1.53 ± 0.03	10		Anorthoclase phenocryst (rhombic habit), caldera rim, Kibo	0.26 ± 0.03	10
	Phonolitic nephelinite, Meru West scarp	1.49 ± 0.03	10				
4056	Ankaramitic basalt from Cinderella Cone, Oljoro valley	1.56 ± 0.05	10				
	Ankaramitic basalt from Cinderella Cone, Oljoro valley	1.62 ± 0.05	10				

(Continued)

Dates are by the standard K–Ar, except those asterisked for which the method was single crystal laser fusion on feldspars, and some radiocarbon dates (Ref. 7)

**References:** 1, Isaac & Curtis 1974; 2, Manega 1993; 3, Fairhead *et al.* 1972; 4, Bagdasaryan *et al.* 1973; 5, MacIntyre *et al.* 1974; 6, Evans *et al.* 1971; 7, Hay 1976; 8, Drake & Curtis 1987; 9, Grommé *et al.* 1970; 10, Wilkinson *et al.* 1986; 11, Foster *et al.* 1997; 12, Curtis & Hay 1972; 13, Walter *et al.* 1991; 14, Williams 1969; 15, Evernden & Curtis 1965; 16, Downie *et al.* 1956.

**Appendix 1B.** *Unpublished K–Ar dates on olivine basalts in Lake Natron area*

Sample	Location	Age
DD1248	Foot of main escarpment, north end of L. Natron, 2°4'37"S 35°57'37"E. Early Oldoinyo Sambu activity; overlies Usagaran quartzite.	7.7 ± 0.7
DD1258	Top of main escarpment, 3 km south of summit of Old. Sambu 2°9'47"S 35°56'32"E. Latest Old. Sambu lava: maximum age of the Natron boundary fault	2.5 ± 0.15
DD1298	Top of main escarpment, north of Peninj delta. 2°16'01"S 35°56'21"E. Minimum age of Humbu formation	2.1 ± 1.2
DD1306	West slopes of Peninj valley. 2°16'48"S 35°54'57"E. Maximum age of the Humbu Formation	1.93 ± 0.8
DD1385	East side of Moinik valley. 2°28'33"S 35°52'23"E. Maximum age of the Moinik Formation	0.73 ± 0.3

Samples collected by D.Dundas; analysed by N.J.Snelling. These data, together with the unpublished map (mapped 1966) and report by D. Dundas of Quarter Degree sheets 16 and 27, Loliondo, were made available by courtesy of the Tanzania Department of Mineral Resources in 1966.

**References**

- BAGDASARYAN, G. P., GERASIMOVSKIY, V. I., POLYAKOV, A. I., GUKASYAN, R. K. & VERNADSKIY, V. I. 1973. Age of volcanic rocks in the rift zones of East Africa. *Geochemistry International*, **10**, 66–71.
- BISHOP, W. W., MILLER, J. A. & FITCH, F.H. 1969. New potassium-argon age determinations relevant to the Miocene fossil mammal occurrences in East Africa. *American Journal of Science*, **267**, 669–699.
- CURTIS, G. H. & HAY, R. L. 1972. Further geological studies and K–Ar dating at Olduvai Gorge and Ngorongoro crater. In: BISHOP, W. W. & MILLER, J. W. (eds). *Calibration of Hominoid Evolution*. Scottish Academic Press, Edinburgh, 107–134.
- DRAKE, P. & CURTIS, G. H. 1987. K–Ar geochronology of the Laetoli fossil localities. In: LEAKEY, M. D. & HARRIS, J. M. (eds) *Laetoli, a Pliocene site in northern Tanzania*. Clarendon Press, Oxford, 48–52.
- DOWNIE, C., HUMPHRIES, D. W., WILCOCKSON, W. H. & WILKINSON, P. 1956. Geology of Kilimanjaro. *Nature*, **178**, 828–830.
- EVANS, A. L., FAIRHEAD, J. D. & MITCHELL, J. G. 1971. Potassium-argon ages from the volcanic province of northern Tanzania. *Nature*, **229**, 19–20.
- EVERNDEN, J. F. & CURTIS, G. H. 1965. The potassium-argon dating of Late Cenozoic rocks in East Africa and Italy. *Current Anthropology*, **6**, 343–384.
- FAIRHEAD, J. D., MITCHELL, J. G. & WILLIAMS, L. A. J. 1972. New K/Ar determinations on Rift volcanics of S. Kenya and their bearing on the age of Rift faulting. *Nature*, **238**, 66–69.
- FOSTER, A., EBINGER, C., MBEDE, E. & REX, D. 1997. Tectonic development of the northern sector of the East African Rift System. *Journal of the Geological Society, London*, **154**, 689–700.
- GROMMÉ, C. S., REILLY, T. A., MUSSETT, A. E. & HAY, R. L. 1970. Palaeomagnetism and potassium-argon ages of volcanic rocks of Ngorongoro caldera, Tanzania. *Geophysical Journal of the Royal Astronomical Society*, **22**, 101–115.
- HAY, R. L. 1976. *Geology of the Olduvai Gorge*. University of California Press, Berkeley.
- ISAAC, G. L. & CURTIS, G.H. 1974. Age of the Acheulian industries from the Peninj Group, Tanzania. *Nature*, **249**, 624–627.
- MACINTYRE, R. M., MITCHELL, J. G. & DAWSON, J. B. 1974. Age of the fault movements in the Tanzanian sector of the East African rift system. *Nature*, **247**, 354–356.
- MANEGA, P. C. 1993. *Geochronology, geochemistry and isotope study of the Plio-Pleistocene hominid sites and the Ngorongoro Volcanic Highlands in northern Tanzania*. PhD thesis, University of Colorado.
- Walter, R. C., Manega, P. C., Hay, R. L., Drake, R. E. & Curtis, G. H. 1991. Laser fusion <sup>40</sup>Ar/<sup>39</sup>Ar dating of Bed I, Olduvai Gorge, Tanzania. *Nature*, **354**, 145–149.
- WILKINSON, P., MITCHELL, J.G., CATTERMOLLE, P.J. & DOWNIE, C. 1986. Volcanic chronology of the Meru-Kilimanjaro region, Northern Tanzania. *Journal of the Geological Society of London*, **143**, 601–605.
- WILLIAMS, L. A. J. 1969. Geochemistry and petrogenesis of the Kilimanjaro volcanic rocks of the Amboseli area, Kenya. *Bulletin Volcanologique*, **33**, 862–888.

## Appendix 2

**Appendix 2.** *Unpublished analyses of Northern Tanzania Volcanic rocks*

	1	2	3	4	5	6	7	8	9	10	11	12	13	14	15	16	17
SiO <sub>2</sub>	57.34	62.39	39.26	5.83	1.52	41.35	39.72	48.47	42.2	45.64	44.62	58.65	54.48	51.64	42.06	42.3	43.15
TiO <sub>2</sub>	0.31	0.75	1.66	0.30	0.15	1.26	7.03	2.23	2.61	1.34	0.68	0.64	1.36	3.02	3.28	4.24	1.28
Al <sub>2</sub> O <sub>3</sub>	20.55	14.00	15.75	0.78	0.35	9.31	8.58	15.31	11.32	16.42	20.53	19.17	18.54	15.57	6.93	5.28	15.81
Fe <sub>2</sub> O <sub>3</sub>	1.92	6.26	4.88	11.36	3.24	6.90	8.05	6.69	5.82	4.74	5.7	1.8	2.38	4.83	8.15	4.72	6.87
FeO	3.06	1.77	3.14	1.08	1.13	6.37	7.42	6.36	6.01	2.43	2.22	3.78	6.1	6.87	4.14	12.6	3.9
MnO	0.46	0.15		0.82	0.62	0.41	0.17	tr	0.14	0.14	0.22	0.13	0.12	0.11	0.13	0.13	0.12
MgO	0.78	0.51	3.62	11.70	1.15	12.48	1.44	3.60	7.68	2.13	0.88	0.89	1.96	3.32	14.41	11.62	2.63
CaO	2.23	1.98	16.60	38.01	51.66	18.62	12.92	8.14	16.02	7.92	5.39	1.88	5.18	7.02	12.26	17.86	9.52
Na <sub>2</sub> O	7.39	6.23	7.50	0.12	tr	0.93	2.25	4.49	4.22	6.94	9.04	7.02	5.44	4.13	1.96	0.91	6.98
K <sub>2</sub> O	3.58	4.93	3.03	0.00	tr	1.12	0.98	1.67	2.13	3.94	3.62	3.62	2.64	1.28	1.33	0.16	3.2
H <sub>2</sub> O <sup>+</sup>	1.56	0.38	0.94	0.46	1.12	0.58	1.09	0.00	1.01	3.03	4.24	1.28	0.62	0.92	3.42	0.12	2.4
H <sub>2</sub> O <sup>-</sup>	0.54	0.17		0.02	0.27	0.32	0.46	1.65	0.45	2.48	2.16	0.7	0.29	0.46	1.38	0.08	1.68
CO <sub>2</sub>	Tr	na			35.26	nil	nil	0.26	0.59	2.02	0.43	0.07	0.09			0.07	2.02
P <sub>2</sub> O <sub>5</sub>	tr	0.67	3.28	28.30	3.34	0.43	0.04	0.52	0.40	0.58	0.31	0.15	0.58	0.54	0.46		0.64
Sum	99.72	100.19	99.66	99.92	99.81	100.08	100.15	99.53	100.15	99.77	100.04	99.78	99.78	99.71	99.91	100.09	100.2

	18	19	20	21	22	23	24	25	26	27	28	29	30	31	32	33	34
SiO <sub>2</sub>	44.60	44.66	44.91	54.00	53.30	51.50	40.21	40.42	42.55	40.21	30.07	48.93	43.18	40.52	43.50	48.00	37.30
TiO <sub>2</sub>	2.95	2.79	2.79	2.31	2.31	1.97	3.17	3.98	4.11	3.17	2.15	1.27	3.43	3.27	2.10	3.27	4.06
Al <sub>2</sub> O <sub>3</sub>	11.36	14.20	14.97	14.77	15.08	16.37	12.57	12.42	12.07	12.57	15.40	18.00	10.73	12.51	15.95	14.60	9.30
Fe <sub>2</sub> O <sub>3</sub>	3.93	6.81	2.27	3.28	6.05	4.81	7.63	7.14	6.17	7.83	5.47	3.14	4.92	8.40	5.21	8.21	6.24
FeO	11.13	6.89	10.92	7.87	5.59	6.75	5.13	6.19	7.07	5.13	5.44	5.94	8.93	4.32	5.72	3.00	7.88
MnO	0.15	0.17	0.16	0.13	0.12	0.17	0.20	0.18	0.19	0.20	0.29	0.23	0.17	0.20	0.25	0.19	0.18
MgO	10.35	6.19	5.12	3.53	3.01	2.63	6.55	7.00	6.70	6.55	5.49	2.08	6.80	6.00	2.77	3.44	10.20
CaO	10.98	7.44	7.66	6.75	6.26	5.80	11.41	12.39	11.14	11.41	11.15	3.63	13.79	12.71	7.65	7.02	17.13
Na <sub>2</sub> O	2.73	5.17	5.81	4.59	4.90	5.90	1.26	3.28	3.60	1.26	5.24	7.70	2.72	2.40	6.96	4.28	1.48
K <sub>2</sub> O	0.90	2.82	2.86	1.84	2.00	2.35	2.74	1.38	2.77	2.74	3.63	5.49	0.48	2.29	3.06	3.65	0.62
H <sub>2</sub> O <sup>+</sup>	0.52*	1.23*	1.23*	0.27*	1.08*	0.89*	7.6*	4.15*	3.03*	7.60*	6.19*	2.98*	4.33*	6.02	5.77	3.04	4.45
H <sub>2</sub> O <sup>-</sup>																	
CO <sub>2</sub>	na	na	na	na	na	na	na	na	na	na	na	na	na	na	na	na	na
P <sub>2</sub> O <sub>5</sub>	0.54	0.84	0.78	0.51	0.48	0.70	1.01	1.57	1.50	1.01	0.66	0.18	1.09	1.1	0.53	0.83	na
Sum	100.14	99.15	99.52	99.86	100.18	98.95	99.68	100.10	100.90	99.68	100.18	99.57	100.57	99.74	99.47	99.53	98.84

H<sub>2</sub>O\* is total H<sub>2</sub>O.

	35	36	37	38	39	40	41	42	43	44	45	46	47	48
SiO <sub>2</sub>	48.60	46.08	45.42	44.20	46.00	46.33	47.15	53.50	55.10	55.32	54.50	50.04	53.50	57.78
TiO <sub>2</sub>	1.20	1.23	1.31	1.32	1.24	1.32	1.22	1.57	1.50	1.58	2.30	2.45	2.11	1.13
Al <sub>2</sub> O <sub>3</sub>	12.66	11.38	10.68	12.38	11.40	12.20	15.64	18.91	17.82	17.03	14.89	16.60	16.98	17.04
Fe <sub>2</sub> O <sub>3</sub>	4.64	5.02	4.27	5.39	4.95	6.29	5.78	2.73	2.07	2.42	3.37	3.62	3.41	2.24
FeO	4.21	4.62	5.14	4.37	4.60	4.38	4.20	4.90	5.19	4.51	7.81	5.66	4.93	3.25
MnO	0.22	0.27	0.26	0.28	0.26	0.28	0.27	0.16	0.14	0.16	0.13	0.18	0.17	0.14
MgO	3.55	2.38	2.04	1.97	1.36	1.09	0.87	1.83	1.96	1.65	3.50	3.00	2.31	0.73
CaO	6.90	10.91	15.40	10.68	14.44	10.38	7.20	4.36	4.40	4.09	6.94	6.20	5.14	3.01
Na <sub>2</sub> O	5.28	4.75	4.73	6.51	2.90	7.76	7.86	6.92	6.70	7.05	4.45	7.50	7.10	8.13
K <sub>2</sub> O	4.93	3.73	3.03	3.63	3.23	2.92	4.09	3.58	3.67	4.05	1.83	3.75	3.95	4.75
H <sub>2</sub> O <sup>+</sup>	6.81	7.80	6.22	4.36	7.98	6.63	4.91	0.60	0.78	1.57	0.33	0.23	0.35	2.05
H <sub>2</sub> O <sup>-</sup>														
CO <sub>2</sub>	0.23	0.78	na	3.95	na	na	0.10	na	na	na	na	na	na	na
P <sub>2</sub> O <sub>5</sub>	0.34	0.51	0.95	0.54	0.87	0.44	0.20	0.37	0.42	0.32	0.46	0.59	0.50	0.26
Sum	99.57	99.46	99.45	99.58	99.23	100.02	99.49	99.53	99.75	99.75	100.81	99.82	100.45	100.51

1. Barkevikite phonolite trachyte, Gelai JG923 (Guest 1953).
2. Riebeckite trachyte, Kibangaini JG1145 (Guest, 1953).
3. Melanite melteigite, Kerimasi (Finckh 1911). Total includes 0.29% F.
4. Forsterite–magnetite–apatite carbonatite, Kerimasi JG810 (Guest 1953).
5. Apatite carbonatite, Kerimasi JG828 (Guest 1953).
6. Biotite pyroxenite, Kerimasi JG1254 (Guest 1953).
7. Pyroxene amphibolite, Kisetey Hill JG 818 (Guest 1953).
8. Mugearite, Oldoinyo Sambu (Finck 1903). Total includes 0.14% S.
9. Ijolite, Kerimasi (James 1966).
10. Nephelinite, Kerimasi (James 1966).
11. Nephelinite, “Mlanja” (probably Sadiman) (James 1966).
12. Anorthoclase trachyte, Olmoti (James 1966).
13. Mugearite, Lemagrut (James 1966).
14. Hawaiite, Ngorongoro (James 1966).
15. Augite melilitite, Kwaraha (James 1966).
16. Augite magnetite rock, Kwaraha (James 1966).
17. Nephelinite, Kwaraha (James 1966).
18. Basanite, spur on south side of Ngorongoro crater (Wood 1968).
19. Tephrite, N.E. side of crater floor, Ngorongoro (Wood 1968).
20. Tephrite, spur on south side of Ngorongoro crater (Wood 1968).
21. Mugearite spur on south side of Ngorongoro crater (Wood 1968).
22. Mugearite spur on south side of Ngorongoro crater (Wood 1968).
23. Phono-tephrite spur on south side of Ngorongoro crater (Wood 1968).
24. High-K basanite BD133, boulder in river, Engaruka (Wood 1968).
25. Nephelinite, L. Manyara (Wood 1968).
26. Nephelinite, L. Manyara (Wood 1968).
27. Zeolitised sodalite nephelinite BD441, flow on SE ridge of Burko (Wood 1968).
28. Nephelinite BD371, Elunata escarpment (Essimingor-derived) (Wood 1968).
29. Clinopyroxene-phyric augite BD401, flow, NE slopes of Essimingor (Wood 1968).
30. Melanphelinite BD 364, flow, S.slopes Essimingor (Wood 1968).
31. Augite BD375, flow, SE ridge, Essimingor (Wood 1968).
32. Nephelinite BD400, flow, lower NE slopes, Essimingor (Wood 1968).
33. Nephelinite BD376. N-S dyke, SE ridge, Essimingor (Wood 1968).
34. Analcime ankaramite BD346, Maserani (3°31'S 36°27.7'E) (Wood 1968).
- 35-41. Nephelinites, Hanang (Wood 1968).
42. Tephriphonolite, western slopes of Meru (Wood 1968).
43. Tephriphonolite, western slopes of Meru (Wood 1968).
44. Tephriphonolite, western slopes of Meru (Wood 1968).
45. Mugearite block in lahar, Momella (Meru-derived) (Wood 1968).
46. Tephri-phonolite block in lahar, Momella (Meru-derived) (Wood 1968).
47. Tephri-phonolite block in lahar, Momella (Meru-derived) (Wood 1968).
48. Phonolite block in lahar, Momella (Meru-derived) (Wood 1968).

## References

- FINCKH, L. 1903. Die trachydolerite des Kibo (Kilimandscharo) und die kenye des Kenya. *Zeitschrift der Deutsches Geologische Gesellschaft*, **55**, Monatsbericht 1–14.
- FINCKH, L. 1911. Die von F. Jaeger in Deutsch-Ostafrika gesammelten Gesteine. In: Jaeger, 1911, 71–85.
- GUEST, N. J. 1953. *The geology of part of northern Tanganyika Territory*. PhD thesis, University of Sheffield.
- JAEGER, F. 1911. Das Hochland der Riesenkrater and die umliegender Hochländer Deutsch Ostafrika, Part 1, *Mitteilungen aus den Deutsches Schutzgebieten, Ergänzungsheft*, **4**, 1–133.
- JAMES, D. E. 1995. *The geochemistry of feldspar-free volcanic rocks*. PhD thesis, Open University.
- JAMES, T. C. 1966. *The carbonatites of Tanganyika: a phase of continental-type volcanism*. DIC thesis, Imperial College, London
- WOOD, C. P. 1968. *A geochemical study of East African alkaline lavas and its relevance to the petrogenesis of nephelinites*. PhD thesis, University of Leeds.

# Index

Page numbers in *italic* denote figures. Page numbers in **bold** denote tables.

- aa lava, Oldoinyo Lengai 61, 61  
Afar triple junction 2  
African Plate 1, 18  
African rift valleys, discovery 3, 5  
African Superswell 2, 18  
Amboseli Basin 37  
Amboseli Beds 37  
Angata Salei 50  
Angata Salei Fault 27  
anisotropy, seismic 15  
Archaean, northern Tanzania 9, 12  
  heat flow 17  
Ardai Basin 28, 35  
  faulting 26  
  lava plateau 70  
Armykon Hill 66, 67  
Arusha  
  faulting 28, 30  
  lava plateau 70  
ash  
  Meru 68  
  Oldoinyo Lengai 50, 57–59  
asthenosphere, density 14  
Aswa-Nandi-Loita shear zone 30  
*Australopithecus cf. boisei* 2, 36
- Balangida Basin 34, 35, 72  
  faulting 23, 26  
  magnetic data 17  
Balangida Lelu Basin 35  
  faulting 23, 26  
basalt 39  
  Gelai 41–42  
  Kilimanjaro 54, 56  
  Lemagrut 44  
  Loolmalasin 44  
  Monduli 54  
  Ngorongoro 44  
  Oldeani 50  
  Oldoinyo Sambu 40–41  
  south Kenya 79  
  Tarosero 51  
basalt-trachyte volcanoes, petrogenesis 84–86  
basins, sedimentary 33–37  
Basotu maars and craters 30, 70  
Basso Ebor *see* Lake Stephanie  
Basso Narok *see* Lake Rudolph  
Bast Hills 41  
Bouguer anomalies 13, 14, 23, 35, 44  
Bubu cataclasites 29–30  
Bubu trend 30  
Burko volcano 28, 30, 67–68, 68  
  radiometric data **94**  
Burton, Sir Richard Francis 3
- calcite carbonatite  
  ‘corduroy’, Kerimasi 64–66  
  Hanang 72  
  Kwaraha 71  
calcrete,  
  Olduvai Basin 35, 50  
  Monduli 70  
calderas 39  
  Embagai 42, 45  
  Kibo 45, 56  
  Ngorongoro 44, 45  
  Olmoti 45  
Cameron’s Crater 70  
carbon dioxide, Oldoinyo Lengai 64  
carbonatite  
  Kerimasi 64–66  
  Mosonik 41  
  Oldoinyo Lengai 57, 59  
  Shombole 40  
  *see also* calcite carbonatite; natrocarbonatite  
Chyulu Hills Volcanic Province 79  
  petrogenesis 85–86  
  xenoliths 17  
cirques, Mawenzi 56  
combeite 46, 59, 61, 64, 69  
comendite 86  
conductivity, southern Kenya 17  
contamination, crustal 12, 83–84  
Crater Highlands volcanoes 21, 39, 42–44,  
  43, 50  
  faulting 27, 30  
  lava 26, 27, 42, 50  
  radiometric data **94**  
crust, extension 18  
Crystalline Limestone Series 9  
crystallization, fractional 83–84, 85, 87
- debris flow  
  Eastern Chasm 46, 58, 59  
  Kerimasi 64  
  Meru 68  
  Oldoinyo Lengai 46, 58, 59  
Decken, Count von der, early exploration 3, 5  
Deeti cone 65, 67  
discontinuities, seismic 15  
Dodoman Archaean fold belt 30  
Dodoman Formation 9  
drainage, redirection 23, 33, 36  
dyke injection 13  
dyke swarms  
  Eyasi trend 29  
  Mbulu Plateau 15  
  Shira cone 56
- earthquakes 15–16, 16  
East Africa Plateau 2  
East African Rift system 1, 4  
  discovery 3, 5  
Eastern Rift, extension 18  
Elanairobi volcano 42, 43  
  faulting 27  
Eledoi crater 66, 67  
  xenoliths 80, 81  
Elunata Basin 28, 35  
Elunata fault 68  
Embagai caldera 42, 45  
Embulu Sabuk crater 66  
Engare Nyiro River 33  
Engare Sero River 33  
Engaruka Basin 23, 34, 42  
  faulting 25, 28, 30  
  magnetic data 17  
  *see also* Natron-Engaruka tuff-cone area  
Engaruka Block 50–51  
Engaruka-Manyara area  
  radiometric data **93**  
  volcanoes 50–57  
Engelosin plug 50  
Engitati Hill 44  
Essimngor volcano 21, 28, 51  
  eruption 21  
  lava 51  
  radiometric data **94**  
Ethiopia Afar Geophysical Lithosphere  
  Experiment 13  
Ethiopia Dome 1, 2  
Euler deconvolution technique 17, 35
- exploration, early European 3, 5  
extension, crustal 18  
Extrusives *see* Older Extrusives;  
  Younger Extrusives  
Eyasi Basin 23, 34, 35  
  faulting 30  
  magnetic data 17, 35  
Eyasi fault *see* Sonjo-Eyasi fault  
Eyasi half-graben 9, 21  
  faulting 29  
Eyasi trend 29, 30
- faulting  
  early, northern Tanzania 21  
  Neogene-Recent 10–11  
  southern extension 29  
  Olduvai Basin 35  
  Plio-Pleistocene 23–29  
  Upper Pleistocene-Recent 29–30  
faults  
  listric 29  
  relationship with basement 29–30  
Fischer, Gustav, early exploration 5, 57  
Fischer’s Tower 5  
Footprint Tuff 61  
fossils  
  Laetoli 35–37  
  Lake Manyara 35  
  Olduvai Gorge 6, 35, 36
- Gallapo 71  
Gelai volcano 41–42  
geophysics 13–18  
  modelling 14  
glaciation  
  Kibo cone 56, 57  
  Kilimanjaro 56, 57  
gravity studies 13–14  
Gregory, John Walter, work on rift valleys 5  
Gregory Rift Valley 2, 9  
  earthquakes 15  
  southern extension 29  
gregoryite 62, 63  
grid-faulting, Kibangaini 29, 41–42
- halite 33, 35  
Hami River 72  
Hanang volcano 35, 71–72  
  radiometric data **94**  
Hans Meyer Peak 56  
heat flow 9, 12, 16–17  
helium ratio, xenoliths 81  
High Natron Beds 33  
Höhnel, Ludwig von, early exploration 5  
hominids 2, 36–37  
*Homo erectus* 36  
*Homo habilis* 36  
hornitos, Oldoinyo Lengai 46, 58, 59, 61, 64  
Humbu Formation 33
- Igwisi Hills 73  
  tuff-cones 72–73  
  xenoliths 15, 17, 49, 80  
isotope variation, xenoliths 80–81
- Kavironidian Formation 9  
Kenya  
  early exploration 3  
  early rift structure 21

- Kenya (*Continued*)  
 faulting 21  
 southern  
 conductivity 17  
 petrogenesis 84–85  
 volcanism 79, **80**
- Kenya Dome 1, 2  
 Bouguer anomaly 13
- Kenya Rift International Seismic Project 13, 30
- Kerimasi volcano 25, 64–66, 65, 66, 67  
 faulting 29  
 magma 65  
 tephra 36
- Ketumbeine volcano 42, 42  
 faulting 26
- Kibangaini  
 grid-faulting 29, 41–42  
 trachytes 79
- Kibo cone 39, 45, 54, 55, 56  
 glaciation 57  
 lava 56, 79
- Kilimanjaro 30, 45, 54–57, 54  
 early exploration 3, 5  
 eruption 37  
 geological survey 6  
 Great Barranco 56  
 glaciation 57  
 Kibo cone 39, 45, 54, 55, 56, 79  
 lava 39  
 Mawenzi cone 54, 56  
 parasitic minor cones 56  
 petrochemistry 56–57  
 radiometric data **95**  
 Shira cone 54, 55–56
- Kilimanjaro Depression 21, 22, 23
- Kilimatinde, faulting 29
- Kilombero rift zone 29  
 kimberlite 49
- Kirikiti-Lengitoto faulting 23, 79
- Kisetey crater 66
- Kisima ya Mungu 70
- Kitingiri Basin, gravity anomaly 13
- Klute Peak 55
- Kondoa, earthquakes 15, 16, 29
- Kondoan trend 30
- KRISP *see* Kenya Rift International Seismic Project
- Kwaraha volcano 71  
 radiometric data **94**
- Labait volcano, xenoliths 15, 17,  
 80, 81, 87
- Laetoli Basin 34
- Laetoli Beds 36–37, 50  
 first mapping 6  
 fossils 36–37
- lahar  
 Kibo 56  
 Meru 68  
 Oldoinyo Lengai 66
- Laikipia Plateau 5
- Lake Albert, discovery 3
- Lake Babati, seismicity 15
- Lake Baringo 4, 5
- Lake Burungi 35
- Lake Eyasi 35
- Lake Magad 43, 44, 45
- Lake Magadi 9, 33  
 gravity anomaly 14
- Lake Malawi 3, 4
- Lake Manyara 4, 5, 35  
 magnetic data 17  
 seismicity 15, 16
- Lake Naivasha 4, 5
- Lake Natron 4, 5, 27, 33  
 olivine basalt dates **96**  
 proto-lake 23, 25, 33  
 radiometric data **93**
- salts 33, 40
- Lake Nyanza 4  
 discovery 3
- Lake Nyasa, discovery 3
- Lake Rudolph 4, 5
- Lake Stephanie 5
- Lake Tanganyika 4  
 discovery 3
- Lake Turkana, gravity anomaly 14
- Lake Victoria, discovery 3
- Lalarasi Hill 67
- Lashaine tuff cone 70
- Lashaine volcano, xenoliths 9, 15, 17, 80, 87
- lava, mantle composition, northern  
 Tanzania 81, **82**, 83
- lead, isotope variation 83, 84
- Leakey, Louis Seymour Bazett  
 Laetoli fossils 37  
 Olduvai Gorge fossils 6, 35
- Leakey, Mary 36, 37
- Leletema Hills 9
- Lemagrut volcano 22, 43, 44, 50  
 lava 37
- Lembolos graben 23, 24, 26, 68
- Lenderut volcano 79
- Lengai Trend 87
- Lengitoto trachytes 79
- lithosphere, strength 17–18
- Livingstone, David 3
- Loliondo 9
- Loluni crater 67
- Longido 9
- Longonot volcano 5, 79
- Loolmalasin volcano 42, 43–44
- Loolmurwak crater 59, 66, 67
- Lorngabolo River 42
- Losimingori *see* Essimigor volcano
- maars, Basotu 30, 70
- Maasai Block  
 early rift structure 21  
 faulting 26–27, 30  
 magnetic data 17
- Maasailand, exploration by Joseph Thomson 3, 5
- Magadi Basin 33
- magma  
 crustal contamination 83–84  
 parent, Younger Extrusives 86–87  
 paradox 87–88
- magmatism 2, 9, 15, 39, 57
- magnesite 33
- magnetic anomaly data 17
- magnetotelluric data, southern Kenya 17
- mantle  
 anomalous 14, 67  
 density 13–14  
 plume 1–2, 15, 18, 87  
 replenishment 60, 87–88  
 seismic data 13–14  
 upper, northern Tanzania 79–83  
 heterogeneity 79–81  
 lava composition 81, **82**, 83
- Manyara Basin 34–35  
 boundary fault system 23, 25, 26, 27, 28, 30  
 fossils 35  
 gravity anomaly 13  
 magnetic data 17  
 seismicity 15, 16
- Manyara Group 21, 34
- Masasi Series 9
- Masek Beds 36
- Matisiwi fault 26
- Matuffa crater 69
- Matunginini fault escarpment 24, 26, 28
- Mautia Hill 9
- Mawenzi cone 45, 54  
 glaciation 57  
 lava 56
- Mbulu Plateau  
 dyke swarms 15, 16  
 faulting 26–27, 30  
 maars and craters 70  
 magnetic data 17  
 melilitite 39, 84–85, 86–87  
 Meru 68–69, 79  
 Monduli 70  
 Natron-Engaruka 66–67  
 Oldoinyo Lengai 59  
 Sadiman 50
- Menengai volcano 79
- Meru area, radiometric data **94–95**
- Meru volcano 28, 30, 49, 68–70, 69, 79  
 gravity anomaly 13  
 petrography and mineralogy 68–69
- metamorphism, Usagaran 9
- metasomatism 14, 80–81, 87
- Miamoja Hill 64, 67
- Moho depth 13, 14
- Moinik Formation 33
- Moinik River 33
- Momella Lakes 68, 69
- Monduli area basins 35  
 lava plateau 70
- Monduli volcano 28, 30, 52, 54  
 faulting 26  
 radiometric data **94**  
 xenoliths 80
- Mosonik volcano 41, 79
- Mozambique Belt 2, 9  
 heat flow 17  
 Tertiary–Recent rift fractures 29–30  
 seismic data 13, 14, 15
- Mozambique orogenic fold belt 9
- Mponde graben 26, 29  
 gravity anomaly 13
- Msasa River Gorge 26
- Mt Kenya, first sighting 3
- Naisiusiu Beds 36, 50, 59
- Namorod Ash 59
- natrocarbonatite 33  
 Oldoinyo Lengai 46, 48, 57, 59, 61–64, 63  
 alteration 63–64  
 formation 64  
 gas species 64  
 Olduvai Basin 35
- Natron Basin 23, 33, 34  
 boundary fault system 23, 25–26, 27,  
 30, 41, 64, 65  
 gravity anomaly 13  
 magnetic data 17  
 structure 33
- Natron-Engaruka tuff-cone area 66–67, 67
- Ndonyo Engai, first sighting 3
- Ndutu Beds 36, 50, 59
- neodymium isotope variation 80–81, 83
- Neogene–Recent  
 faults, northern Tanzania 10–11  
 volcanic rocks 39–73  
 nomenclature 39, **40**
- nephelinite 39, 46  
 Burko 67–68  
 Essimigor 51  
 Hanang 72  
 Kerimasi 64–65  
 Kibo cone 56  
 Kwaraha 71  
 Lemagrut 44, 50  
 Meru 68–69, 79  
 Mosonik 41  
 Natron-Engaruka area 66–67  
 Older Extrusives 84–85  
 Oldoinyo Lengai 46, 59–61, 86–87  
 Oldoinyo Sambu 41  
 Sadiman 50  
 Shombole 40

- Neumann Tower 56  
 Ngaloba Beds 37  
 Ngong volcano 79  
 Ngong-Turoka fault 23  
 Ngorongoro caldera 43, 44, 45  
   faulting 27  
   seismicity 15  
 Ngurdoto crater 69  
 Nguruman fault 21  
 Nile, source of 3  
 niobium 83, 84  
 Njorowa Gorge 5  
 North Tanzania Divergence 1, 2, 21, 29, 30  
 Nubian Plate 1, 2, 18  
 Nutcracker Man 2, 36  
 Nyangea-Athi-Ikutha shear zone 30  
 Nyanzian Formation 9  
 nyerereite 62, 63
- Ogol Hills 22  
 Ogol lava 50  
 Ol Esayeti volcano 79  
 Ol Keja Nero basalt 79  
 Ol Tepesi basalt 79  
 Olbalbal Depression 22, 27, 36  
 Oldeani volcano 43, 50  
   faulting 27  
 Older Extrusives 23, 24, 39, 40–42  
   petrogenesis 84–86  
 Oldoinyo Lengai volcano 46, 57–64, 58  
   activity 57–58  
   ash 57–59  
   early exploration 3, 5, 6, 57  
   Eastern Chasm 46, 58, 59  
   geology 59  
   lava 59–64, 86  
   minerals 46, 47, 48, 59–61  
   morphology 58–59  
   parent magma 87  
   petrogenesis 86  
   seismicity 15  
   tephra 36  
   xenoliths 80  
 Oldoinyo Sambu volcano 39, 40–41, 40  
   lava 23  
 Olduvai Basin 22, 34, 35–37  
   drainage reversal 23, 36  
 Olduvai Beds 36  
 Olduvai Gorge  
   faulting 29  
   fossils 2, 6, 36  
   radiometric data **94**  
   sediments 36  
 Oljoro graben 26, 68  
   lava plateau 70  
 Olkaria rhyolites 86  
 Olmani cinder cone 69, 70  
   xenoliths 80  
 Olmoti volcano 43, 45  
   faulting 27  
 Olorgesaille Formation 29  
 Olorgesaille volcano 79  
 Olsirwa volcano 43, 44  
 Orkandira Hill 51
- P-waves, low velocity layer 9, 13  
 pahoehoe lava, Oldoinyo Lengai 61, 61, 62  
 Pan-African orogenic event 9  
 Pangani graben 9, 13, 21  
   boundary faults 30  
   seismicity 16  
 Parangan trend 30  
 Pare Mountains 9  
   folding 30  
   seismicity 16  
 Pello Hill tuff cone 67  
   xenoliths 14, 49, 80, 81, 87
- Peninj Group sediments 23, 33  
 Peninj River 33  
   delta 40  
 peridotite 49, 67, 70  
   mantle 14, 72  
 petrochemistry, Kilimanjaro 56–57  
 petrogenesis 84–88  
   basalt-trachyte volcanoes 84–86  
   Older Extrusives 84–86  
   Tarosero trachytes and comendites 86  
   Younger Extrusives 86–88  
 phonolite  
   Elanairobi 42  
   Essimngor 51  
   Kilimanjaro 54, 56  
   Meru 68–69, 79  
   Mosonik 41  
   Oldoinyo Lengai 59, 86  
   Sadiman 50  
   Tarosero 51, **52**  
 phosphates 35  
 plate tectonics  
   development 21–30  
   modelling 18  
 Pleistocene  
   Lower, faulting 23–29  
   Upper–Recent, faulting 29–30  
 Pliocene–Pleistocene, faulting 23–29  
 plume, mantle 18  
   Tanzania Craton 1–2, 15, 87  
 Project EAGLE *see* Ethiopia Afar Geophysical  
   Lithosphere Experiment
- Recent, faulting 29  
 Reck, Hans 6, 35  
 replenishment, mantle 60, 87–88  
 rhyolite  
   Olkaria 86  
   peralkaline 5  
 rifting 18  
 rubidium isotope variation 83, 84  
 Ruhuhu graben 29  
 Rungwe volcanics, work of Joseph  
   Thomson 3
- S-wave velocity variation 15  
 Sadiman volcano 43, 50  
 Salei Plain 50  
 salts, Lake Natron 33  
 Sambu volcanics 33  
 Sanjan Fault 25, 41  
 Sea of Nyamwezi *see* Lake Nyanza  
 sedimentary basins 33–37  
 seismic experiments 13, 14–15  
 seismicity 15–16, 16  
 Serengeti Plain 21, 22, 50  
 shear zones 29–30  
 Shira cone 54, 55–56  
 Shombole Trend 87  
 Shombole volcano 40, 40, 79  
 Singaraini basalt 79  
 Somali Plate 1, 2  
   rifting 18  
 Sonjo-Eyasi fault 13, 21–22, 27, 30  
 Speke, John Hanning 3  
 springs  
   freshwater 44  
   hot 73  
 stromatolites, Lake Manyara 35  
 strontium isotope variation 80–81, 83  
 Suess, Eduard, early work on rift valleys 3, 5  
 Suswa volcano 79
- Tanganyika Geological Survey  
   mapping 6, 22  
   *see also* Tanzanian Geological Survey
- Tanganyika-Rukwa-Malawi rift 29  
 Tanzania, early exploration 5–6  
 Tanzania Broadband Seismic Experiment 13, 15  
 Tanzania Craton 1, 2, 9  
   heat flow 17  
   plume 15  
   relationship to Tertiary–Recent rift  
     fractures 29–30  
   seismic anisotropy 15  
   seismic data 13, 14, 15  
   thermal anomaly 15  
 Tanzania, northern 2  
   early faulting 21  
   early rift structure 21  
   late Tertiary depression 21–23  
   petrogenesis 84–85  
   regional geology 9–12  
   rock analyses **97–98**  
   upper mantle composition 79–83  
   volcanism 79, **80**  
 Tanzanian Geological Survey, mapping 9, 39  
 tanzanite 9  
 Tarosero volcano 23, 26, 51–52, 51  
   lava 51–52, **53**  
   radiometric data **94**  
   trachytes and comendites, petrogenesis 86  
 Tarosero fault 26  
 TBSE *see* Tanzania Broadband Seismic Experiment  
 tectonics *see* plate tectonics  
 Teleki, Count, early exploration 5  
 teleseismic experiments 14–15  
 Tertiary, late, depression 21–23, 39  
 thermal anomaly 15  
 thermonatrite 33  
 Thomson, Joseph, early exploration 3, 5  
 trachybasalt 42, 43, 54, 55, 56  
 trachyte  
   Gelai 41, 42  
   Ketumbeine 42  
   Kibangaini 79  
   Kibo cone 56  
   Kilimanjaro 54, 56  
   Lengitoto 79  
   Loolmalasin 44  
   Monduli 54  
   Ngorongoro 44  
   Oldeani 50  
   Olmoti 43  
   petrogenesis 84–86  
   Tarosero 51, 52, **53**  
 trona 33, 35, 40, **63**, 64  
 tuff  
   Laetoli Basin 37  
   Oldoinyo Lengai 59  
   Olduvai Basin 35  
   Salei and Serengeti plains 50  
 tuff cones  
   Hanang 72  
   Igwisi Hills 72–73  
   Kwaraha 71  
   Natron-Engaruka area 66–67, 67  
   Younger Extrusives 57  
 tuff rings  
   Basotu maars 70  
   Lashaine 70  
 Turkwell Fault 21
- Ufiome 71  
 Uhlig, Carl, Manyara-Natron sector 5–6  
 Uhuru Peak 45, 55, 56  
 uplift, domal 18, 21  
 uranium 83, 84  
 Usagara Mountains 9  
 Usagaran metamorphic event 9
- volcanism 2  
 early 21, 39

- volcanism (*Continued*)  
 northern Tanzania 10–11, 79, **80**  
 Older Extrusives 23, 24, 39, 40–42  
 Oldoinyo Lengai 57–59  
 south Kenya 79, **80**  
 Younger Extrusives 25, 39,  
 57–73
- volcanoes  
 linearity 30  
 peralkaline 39, 59, 79  
 shield 39, 40, 41, 42–44, 50, 54
- water 64, 80  
 Wembere Basin 35  
 Western Rift
- earthquakes 15  
 extension 18  
 wollastonite 46, 47, 59, 60, 64, 69
- xenoliths  
 Burko 67  
 Chyulu Hills 17  
 Eledoi 67, 80, 81  
 Igwisi Hills 15, 17, 49, 80  
 isotope variation 80–81  
 Labait 15, 17, 80, 81, 87  
 Lashaine tuff 9, 15, 17, 80, 81, 87  
 mantle composition 79–80  
 Meru 68  
 Monduli 80  
 Oldoinyo Lengai 60, 67, 80
- Olmani 80  
 Pello Hill 14, 49, 67, 80, 81, 87
- Yaida Basin 34, 35  
 Yaida graben 21  
 faulting 30  
 Yayai Basin 28, 35  
 Younger Extrusives 25, 39, 57–73  
 parent magma 86–87  
 paradox 87–88  
 petrogenesis 86–88
- zeolite, Olduvai Basin 36  
*Zinjanthropus boisei* see *Australopithecus*  
*cf. boisei*